

**Next generation conjugate vaccines;
development from lab bench
towards clinical trials**

Robert Marinus François van der Put

Colofon

@ Robert Marinus François van der Put, 2024. All rights reserved. No parts of this thesis may be reproduced or transmitted in any form or by any means without written permission of the author.

ISBN: 978-94-6506-125-2

DOI: 10.33540/2392

Layout & cover: Robert Marinus François van der Put.

The printing of this thesis was financially supported by Intravacc.

About the cover: Abstract representation of intricate repeating and connected structures similar like sugars and or peptides and their carrier proteins for vaccine applications.

Printed by: Ridderprint

Next generation conjugate vaccines; development from lab bench towards clinical trials

De volgende generatie conjugaat vaccins;
ontwikkelingen van het laboratorium tot klinische trials
(Met een samenvatting in het Nederlands)

Proefschrift

ter verkrijging van de graad van doctor aan de
Universiteit Utrecht
op gezag van de
rector magnificus, prof. dr. H.R.B.M. Kummeling,
ingevolge het besluit van het College voor Promoties
in het openbaar te verdedigen op

woensdag 10 juli 2024 te 12:15 uur

door

Robert Marinus François van der Put

geboren op 26 december 1975
te Etten-Leur

Promotor: Prof. dr. R.J. Pieters

Copromotor: Dr. B. Metz

Beoordelingscommissie: Prof. dr. G.J.P.H. Boons
Prof. dr. J.C.M. Van Hest
Prof. dr. E. Mastrobattista
Dr. F. Micoli
Prof. dr. S.H.M. Rooijackers

Table of Contents

1	Chapter 1	General introduction	p. 9
3	Chapter 3	HPAEC-PAD quantification of <i>Haemophilus influenzae</i> type b polysaccharide in upstream and downstream samples	p. 59
5	Chapter 5	The first-in-human synthetic glycan-based conjugate vaccine candidate against <i>Shigella</i>	p. 111
7	Chapter 7	A modular vaccine platform for prophylactic and therapeutic vaccines: exogeneous decoration of bacterial outer membrane vesicles with synthetic peptide antigens	p. 189
A	Appendices	Dankwoord Curriculum Vitae List of Publications	p. 231

Chapter 2 Carriers and antigens: new developments in glycoconjugate vaccines p. 21

2

Chapter 4 A synthetic carbohydrate conjugate vaccine candidate against shigellosis: improved bioconjugation and impact of alum on immunogenicity p. 75

4

Chapter 6 Validation and application of an FFF-MALS method to characterize the production and functionalization of outer membrane vesicles for conjugate vaccines p. 149

6

Chapter 8 Summary and Perspectives
Nederlandse Samenvatting p. 217

8



The page features decorative geometric patterns in the top-left and bottom-left corners. These patterns consist of interconnected lines and circles of varying sizes, creating a network-like structure. The colors are shades of blue, ranging from light to dark, set against a dark blue background.

Chapter 1

General introduction

Vaccines and vaccination

1 Society relies heavily on vaccination to prevent and protect against infectious diseases. To counter the threat of infectious diseases caused by bacteria and viruses, we count on our immune systems' abilities. Vaccines are very effective in providing the necessary protection and prevention of disease. Ideally a vaccine is a stable product that can be produced efficiently in large quantities and administered easily. Furthermore, the antigens present in the vaccine should preferably elicit a life-long immune response. The development of new vaccines is key in the battle against multi-resistant bacteria [1, 2]. More importantly, the progressive antigenic variation of viruses and bacteria including waning immunity after vaccination emphasizes the need for the improvement of existing vaccines [3, 4]. The protective immune response, or efficacy of a vaccine, is not the key denominator to success. This accomplishment relies also heavily on 1) the public's commitment to get vaccinated and 2) the availability or equity of vaccines.

The history of vaccine development

The first strategies to battle infectious diseases have already been implemented more than 5 centuries ago [5]. Global efforts in immunization already took place in the Middle East, China, Africa, Asia, and India [6]. It wasn't until the originally conceived strategy by Jenner to battle smallpox using live attenuated virus, this really came to life. In 1796 this approach got the term vaccination (derived from *Vacca*, the Latin word for cow). Jenner observed that milkmaids had acquired immunity to smallpox after being infected with cowpox. Jenner went on and injected a young boy with the pus from a cowpox patient before challenging him with smallpox. This led to the observation that the child, and others that were subjected to the same routine, survived [5]. Smallpox was eventually eradicated, and vaccination has been halted in 1979.

It then took until the 1880s before Pasteur developed a successor to Jenner's cowpox vaccine in the form of a live-attenuated vaccine protecting against rabies. Vaccine development then came to life in the early 20th century with the development of toxoid vaccines (tetanus & diphtheria) and the ability to propagate viruses on the chorioallantoic membranes of chicken embryos (influenza). However, the introduction of cell culture had an ever-bigger effect, leading to the development of vaccines preventing measles, mumps, rubella, and polio. The first introduction of a polysaccharide-based vaccine was around 1985, directed against *Haemophilus influenzae* type b. This conjugate vaccine showed to be more effective in inducing immunity in children compared to the non-conjugated PS vaccines [7, 8].

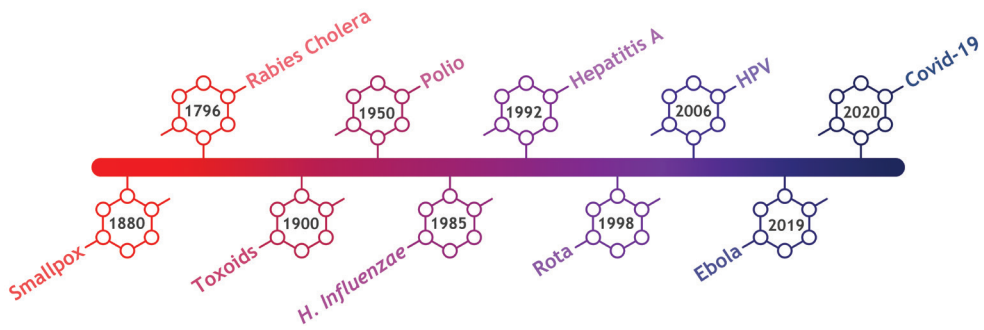


Figure 1: Historic timeline of vaccine development

Vaccination is one of the most successful ways to battle infectious diseases preventing death and morbidity and has saved millions of lives. When looking at vaccines protecting against diseases like hepatitis A, measles, mumps, rubella, and chickenpox, these have saved in excess of 10 million lives alone since the 1960s [9]. A diseases like smallpox has been eradicated 40 years ago. The animal borne virus rinderpest was exterminated more recently (2011). Both diseases disappeared as a direct effect of vaccination. Poliomyelitis will hopefully follow soon [10, 11]. Other vaccines directed against infectious diseases contribute to a decrease in morbidity of more than 90% [9]. Nevertheless, children under the age of 5 are still heavily affected by vaccine preventable diseases. The bias in vaccine equity and the widening gap in poverty are primarily at the basis of the death of more than 2-3 million people, of which 1.5 million children, annually [12, 13].

Vaccine platforms

New vaccines have a long way to go in development. The current situation has moved far away from the somewhat coarse and in retrospect seemingly unethical experiments conducted by Jenner. Current vaccines are much safer and induce fewer adverse events. Through modern screening techniques, such as reversed vaccinology, vaccines can increasingly be tailored to target specific epitopes derived from the pathogen of interest. Additionally, components have been added to vaccines to increase their stability and efficacy, such as stabilizers, preservatives, excipients and adjuvants. After Jenner's and Pasteur's live-attenuated vaccines, new vaccine platform strategies have come into play to develop safe and effective vaccines. The type of vaccines can be categorized based on their production platform. Different vaccine platforms are discussed separately in the next sections.

Live-attenuated vaccines

1 Live-attenuated vaccines contain the pathogen, which can still cause a natural infection. The vaccine holds its ability to infect and replicate in the host. However, these pathogens are attenuated which leads to a considerable reduction in its virulence. Attenuation can be attained by several methods. Incapacitating disease potential by inducing mutations can be obtained by either cultivating at less favorable temperatures [14, 15] and or serial passing at suboptimal conditions [16]. This requires substantial efforts and the need for elaborate quality control tests. For this platform, it cannot be stressed enough that the pathogens' ability to reverse its virulence and replicate without causing illness are key check points.

Inactivated vaccines

Inactivated vaccines are generally considered safer, which is mainly due to the absence of potential reversion. These types of vaccines are based on fully inactivated virulent pathogens, such as viruses and bacteria. The method of inactivation can be achieved either through physical and or chemical treatment. Physical inactivation is predominantly obtained by subjection to pH [17] or exposure to heat [18]. When looking at chemical inactivation, actively used compounds among others, include β -propiolactone, hydrogen peroxide, glutaraldehyde, and formaldehyde [19-21].

Virus-like particle vaccines

Virus-like particles are mimics of viruses built from viral structural proteins. These particles can be produced by transfection of a construct into mammalian cells. These particles are created by self-assembly, but they are unable to replicate in the host because of the lack of genetic material [22, 23]. Their repetitive antigenic structure induces both a cellular and humoral immune response [24, 25]. Moreover, their size (20-200 nm) aids in being processed and presented efficiently by the immune system [26]. At the moment, human papillomavirus vaccine is the only example of a marketed vaccine using virus-like particles.

Toxoid vaccines

Toxins can cause serious disease of which tetanus and diphtheria are most known. These toxins secreted by bacteria are very harmful, but when inactivated, forming toxoids, they can very well be used as vaccines. The inactivation of toxoids is generally done by formaldehyde treatment, which, when performed under mild conditions, can preserve the physicochemical properties and immunogenicity [27].

Bacterial and viral vector-based vaccines

The antigen of choice is genetically inserted into engineered viruses, which can express one or several antigens in the host when infecting the host's cells. These antigens are then at the basis to elicit a memory-immune response and induce protection. Most viral vectors used are usually replication deficient non-pathogenic viral vectors. The main advantage here is the omission and use of the whole pathogenic virus. A prime example is the FDA approved vesicular stomatitis virus derived Ebola vaccine, which is a replicate competent vector. Here, the vector uses the cell's protein production machinery to express the surface glycoprotein from Ebola. Adeno-associated viruses, in this case a replicate incompetent vectors, and as such generally considered safer, are another example [28]. Similar attempts are also made to use bacteria as a vector-based vaccine, with a major potential in mucosal administration. However, there are substantial risks for infection in the immunocompromised, elderly and children. Other potential issues would be an immune response of the host towards the vector, which can interfere with the therapeutic efficacy when vaccinating with the same vector multiple times [29].

mRNA vaccines

These vaccines are based on the transcription of mRNA by ribosomes in the human cell resulting in the expression of specific antigens, which in their turn activate the immune system. The introduction of mRNA vaccines has taken a flight during the recent Covid-19 pandemic. However, efforts in development go back more than three decades [30]. The major limitations at that time entailed inflammation and the short half-life of mRNA. The introduction of loading mRNA into liposomes overcame these shortcomings with improved immunological response [31]. More recently optimization of lipid nanoparticles and introduction of modified nucleosides and codon optimization significantly improved the mRNA vaccine concept followed quickly by human trials and introduction to the market.

Synthetic peptide vaccines

Peptide vaccines can be designed based on the synthesis of specific epitopes, mimicking fragments of protein antigen sequences, originating from pathogens that are subsequently recognized by the immune system. The design of these peptides is done either by *in-silico* screening [32, 33] or genome analysis and subsequent selection of potential targets. These peptides can be produced fast and at large scale. Since peptides are fairly small, in most cases they must be conjugated to a carrier or presented together with an adjuvant to induce the correct immune response. One downside is that, for a sufficient immune response, multiple T-cell epitopes are needed to overcome antigenic diversity and variations in MHC in the population [32, 34].

Nanoparticles and OMVs

1

Nanoparticles (NP) are particles in the range of approximately 100 nm and can be used to either deliver or contain vaccine antigens. There are several types of NP, of which carbon polymers, dendrimers, liposomes, immune stimulating complexes (ISCOM) and outer membrane vesicles (OMV) are key examples. NPs can be used to induce a particular immune response, improve the efficacy, and improve vaccine antigen uptake [35]. One major advantage is that they can directly be processed by the immune system through accessing the lymphatic drainage system. Additionally, NP have the ability to present the antigen and to act as an adjuvant at the same time. Other important characteristics are hydrophobicity, surface charge and their size. For NP vaccine design to be effective there has to be a fundamental understanding on the *in-vivo* distribution, delivery and immunostimulatory capabilities [36]. In general NP can be used to either encapsulate or adsorb the antigen on their surface (ISCOM and polymers). However, the application of OMV takes it a step further, where either homologues or heterologous vaccine antigens can be expressed. Furthermore, the introduction of detoxified lipopolysaccharide (LPS) decreases toxicity without losing the adjuvanting properties [37, 38]. Lastly OMV are excellent and versatile carriers, where vaccine antigens can be conjugated (covalently coupled) to induce specific immune responses toward *e.g.* peptides, proteins, and oligosaccharides.

Polysaccharide and polysaccharide conjugate vaccines

With regards to polysaccharide (PS) vaccines, there are vaccines that only consist of the extracted and purified PS or where the PS is covalently attached (conjugated) to a carrier protein. While both extracted and purified PS vaccines do work, there are certain advantages towards conjugating the PS to a carrier. The current carriers that are mainly used entail tetanus toxoid, diphtheria toxoid including CRM197, *Neisseria meningitidis* outer membrane protein, cholera toxin subunit b and recombinant mutant *Pseudomonas aeruginosa* exoprotein A. The immunogenicity responses towards the PS originating from the capsular structures from *Haemophilus influenzae* type b (Hib), *Streptococcus pneumoniae*, *Neisseria meningitidis* and *Salmonella* Typhi have all been improved significantly through conjugation to carrier proteins [39, 40]. PS-protein conjugates really excel in children under the age of two, where an immature immune system restricts an adequate immune response towards PS vaccines alone to induce a memory response. The addition of a carrier protein helps the immune system to trigger a T-cell dependent immune response, inducing long-lasting immunity. Current innovations with respect to conjugate vaccines are directed towards the development of synthetic oligosaccharides [41], omitting the need for tedious purification procedures and the use of new carriers [42, 43].

Vaccine perspective

With the outbreak of the SARS-CoV-2 pandemic [44] it has become even more apparent that fast and reactive vaccine development is required [45]. Future pandemics will require global efforts and collaborations to save lives. On other fronts the development of new - and improvement of existing - vaccines are also key, not only with the rise in antibiotic resistance for bacterial infections [1, 2] but also with observed antigenic variation and waning immunity with the introduction of additional serotypes in single- or multi-valent vaccines [3, 4].

Current developments also show a trend towards other applications and routes of immunization for vaccination strategies. Vaccines have found their way in the therapeutic domain, aiding in promoting the immune response to battle premalignant conditions, chronic infections, or diseases as cancer. Other examples of current therapeutic vaccines are *e.g.* to prevent diseases like cervical cancer caused by human papilloma virus [46]. Currently a plethora of other therapeutic vaccines are in development of which a Coxsackievirus B vaccine linked to type 1 diabetes [47, 48] and a vaccine potentially delaying the onset of disease for amyotrophic lateral sclerosis (ALS) and/or frontotemporal dementia (FTD) [49] are prime examples. Additionally, one would preferably add other routes of immunization, such as intranasal vaccination, towards inducing mucosal immunity and potentially preventing transmission, especially considering the Covid-19 pandemic [38, 50-52]. In the field of vaccine development ideally a platform-based approach is applied which are scalable and make use of well-known validated processes that would aid in the speed of development and could be tailored to target new emerging diseases and improve existing vaccines as well [53].

Thesis outline

1 This thesis provides insight into the development of conjugate vaccines. The focus is on the evaluation and optimization of production process steps. To optimize such production processes and to warrant shorter development times design of experiments was introduced. Evaluation was done by the introduction of new and existing analytical methods. The introduction of innovative antigens in the form of synthetic oligosaccharides and peptides, linked to new carrier proteins, like outer membrane vesicles, prove to be effective successors of the traditional extracted polysaccharides coupled to protein antigens.

In **Chapter 2**, we review the recent advancements in available and applied carrier proteins and vaccine antigens in the development of conjugate vaccines. We emphasize the fact that progression in conjugate vaccine development is radical and moving fast from the traditional carriers and extracted saccharides towards (synthetically) designed carriers and antigens.

Chapter 3 is based on previous work done on the development and production of a traditional *Haemophilus influenzae* type b (Hib) conjugate vaccine. Here, we utilized a new analytical method; high performance anion exchange chromatography coupled to pulsed amperometric detection (HPAEC-PAD) and compared this to traditional methods like colorimetric assays and size exclusion chromatography to provide an in-depth assessment of the production and purification of polyribosylribitol phosphate (PRP).

Chapter 4 introduces a new and innovative vaccine antigen, in the form of a synthetically designed oligosaccharide, mimicking part of the lipopolysaccharide (LPS) O-antigen of *Shigella flexneri* type 2a. Where traditional vaccine preparation, like for Hib, still used random activation and lattice-type conjugation, the transition here was towards site selective, or sun-type, conjugation. The production process was optimized by using design of experiments, resulting in a more consistent production process with controllable process parameters. Four different vaccine preparations showed in immunogenicity studies that there is a distinct optimum of oligosaccharide conjugated to the carrier protein.

In **Chapter 5**, the optimized small-scale production parameters defined in chapter 4, were applied in a scale-up study. During scale-up the full production process was characterized on the removal of impurities. The GMP-grade carrier protein (tetanus toxoid) and synthetic oligosaccharide were introduced in the scaled-up process. This led to the production of

both a non-clinical and clinical batch complying to ICH-guidelines. The non-clinical batch passed all toxicity-related criteria and showed to be immunogenic in rabbits and mice. The clinical product was successfully tested in humans and showed to be safe. Moreover, this vaccine was subject to a stability study and proved to be stable for a total period of at least six years.

In **Chapter 6**, the validation of a field-flow-fractionation coupled to multi-angle light scattering (FFF-MALS) analysis of outer membrane vesicles (OMVs) was described. OMVs are versatile vaccine constituents and excellent candidates for a new type of carrier for conjugate vaccines. After initial development, the method was successfully validated according to ICH-guidelines to provide verification of the quality and reliability of the assay. The validated method was effectively used to evaluate both the production process of OMVs originating from different bacterial origin and GMBS-functionalized, or conjugation-ready-OMVs.

In **Chapter 7**, the development of an outer membrane vesicle peptide-based conjugate vaccine is summarized. The FFF-MALS method was key in the characterization and development of this vaccine. Firstly, the initial functionalization reaction of the OMV using GMBS (linker) was investigated. This was followed by a design of experiment studying the conjugation reaction efficiency and optimization the coupling of a synthetic peptide to these functionalized OMVs. Here, we showed that the quantity of peptide conjugated to the OMV could be increased significantly. Finally, we provide the scientific data for a GMP-ready scaled-up process and stability tests for the vaccine candidate.

Finally, **Chapter 8** discusses the major findings in this thesis and provides a perspective on the future of conjugate vaccine development.

References

1. Cohen, M.L., Epidemiology of drug resistance: implications for a post-antimicrobial era. *Science*, 1992. 257(5073): p. 1050-5.
2. Dadgostar, P., Antimicrobial Resistance: Implications and Costs. *Infect Drug Resist*, 2019. 12: p. 3903-3910.
3. Gao, H., E.H.Y. Lau, and B.J. Cowling, Waning Immunity After Receipt of Pertussis, Diphtheria, Tetanus, and Polio-Related Vaccines: A Systematic Review and Meta-analysis. *J Infect Dis*, 2022. 225(4): p. 557-566.
4. Shu, S.N., [Challenge and consideration of emerging and re-emerging infectious diseases in children]. *Zhonghua Er Ke Za Zhi*, 2021. 59(8): p. 624-626.
5. Control, C.f.D. History of Smallpox. September 29th 2022]; Available from: <https://www.cdc.gov/smallpox/history/history.html>.
6. Plotkin, S., History of vaccination. *Proc Natl Acad Sci U S A*, 2014. 111(34): p. 12283-7.
7. Schneerson, R., et al., Quantitative and qualitative analyses of serum antibodies elicited in adults by Haemophilus influenzae type b and pneumococcus type 6A capsular polysaccharide-tetanus toxoid conjugates. *Infect Immun*, 1986. 52(2): p. 519-28.
8. Schneerson, R., et al., Haemophilus influenzae type B polysaccharide-protein conjugates: model for a new generation of capsular polysaccharide vaccines. *Prog Clin Biol Res*, 1980. 47: p. 77-94.
9. Orenstein, W.A. and R. Ahmed, Simply put: Vaccination saves lives. *Proc Natl Acad Sci U S A*, 2017. 114(16): p. 4031-4033.
10. Henderson, D.A., The eradication of smallpox--an overview of the past, present, and future. *Vaccine*, 2011. 29 Suppl 4: p. D7-9.
11. Kew, O. and M. Pallansch, Breaking the Last Chains of Poliovirus Transmission: Progress and Challenges in Global Polio Eradication. *Annu Rev Virol*, 2018. 5(1): p. 427-451.
12. Desai, S.N. and D. Kamat, Closing the global immunization gap: delivery of lifesaving vaccines through innovation and technology. *Pediatr Rev*, 2014. 35(7): p. e32-40.
13. Dr Jean-Marie Okwo-Bele, D.o.t.D.o.I., Vaccines and Biologicals. Together we can close the immunization gap. September 28th 2022]; Available from: <https://apps.who.int/mediacentre/commentaries/vaccine-preventable-diseases/en/index.html>.
14. Glezen, W.P., Cold-adapted, live attenuated influenza vaccine. *Expert Rev Vaccines*, 2004. 3(2): p. 131-9.
15. Resch, T.K., et al., Serial Passaging of the Human Rotavirus CDC-9 Strain in Cell Culture Leads to Attenuation: Characterization from In Vitro and In Vivo Studies. *J Virol*, 2020. 94(15).
16. Folorunso, O.S. and O.M. Sebolai, Overview of the Development, Impacts, and Challenges of Live-Attenuated Oral Rotavirus Vaccines. *Vaccines (Basel)*, 2020. 8(3).
17. Durno, L. and O. Tounekti, Viral Inactivation: Low pH and Detergent. *PDA J Pharm Sci Technol*, 2015. 69(1): p. 163-72.
18. Jonges, M., et al., Influenza virus inactivation for studies of antigenicity and phenotypic neuraminidase inhibitor resistance profiling. *J Clin Microbiol*, 2010. 48(3): p. 928-40.
19. McGucken, P.V. and W. Woodside, Studies on the mode of action of glutaraldehyde on Escherichia coli. *J Appl Bacteriol*, 1973. 36(3): p. 419-26.
20. Dembinski, J.L., et al., Hydrogen peroxide inactivation of influenza virus preserves antigenic structure and immunogenicity. *J Virol Methods*, 2014. 207: p. 232-7.
21. Uittenbogaard, J.P., et al., Reactions of beta-propiolactone with nucleobase analogues, nucleosides, and peptides: implications for the inactivation of viruses. *J Biol Chem*, 2011. 286(42): p. 36198-214.
22. Ding, X., et al., Virus-Like Particle Engineering: From Rational Design to Versatile Applications. *Biotechnol J*, 2018. 13(5): p. e1700324.
23. Roldao, A., et al., Virus-like particles in vaccine development. *Expert Rev Vaccines*, 2010. 9(10): p. 1149-76.
24. Roy, P. and R. Noad, Virus-like particles as a vaccine delivery system: myths and facts. *Hum Vaccin*, 2008. 4(1): p. 5-12.
25. Bolhassani, A., S. Safaiyan, and S. Rafati, Improvement of different vaccine delivery systems for cancer therapy. *Mol Cancer*, 2011. 10: p. 3.
26. Harding, C.V. and R. Song, Phagocytic processing of exogenous particulate antigens by macrophages for presentation by class I MHC molecules. *J Immunol*, 1994. 153(11): p. 4925-33.

27. Bizzini, B., et al., Chemical characterization of tetanus toxin and toxoid. Amino acid composition, number of SH and S-S groups and N-terminal amino acid. *Eur J Biochem*, 1970. 17(1): p. 100-5.
28. Ertl, H.C., Viral vectors as vaccine carriers. *Curr Opin Virol*, 2016. 21: p. 1-8.
29. Mingozzi, F. and K.A. High, Immune responses to AAV vectors: overcoming barriers to successful gene therapy. *Blood*, 2013. 122(1): p. 23-36.
30. Hoerr, I., et al., In vivo application of RNA leads to induction of specific cytotoxic T lymphocytes and antibodies. *Eur J Immunol*, 2000. 30(1): p. 1-7.
31. Conry, R.M., et al., Characterization of a messenger RNA polynucleotide vaccine vector. *Cancer Res*, 1995. 55(7): p. 1397-400.
32. Li, W., et al., Peptide Vaccine: Progress and Challenges. *Vaccines (Basel)*, 2014. 2(3): p. 515-36.
33. Meyers, L.M., et al., Highly conserved, non-human-like, and cross-reactive SARS-CoV-2 T cell epitopes for COVID-19 vaccine design and validation. *NPJ Vaccines*, 2021. 6(1): p. 71.
34. Singh, A., et al., Designing a multi-epitope peptide based vaccine against SARS-CoV-2. *Sci Rep*, 2020. 10(1): p. 16219.
35. Lugade, A.A., et al., Single low-dose un-adjuvanted HBsAg nanoparticle vaccine elicits robust, durable immunity. *Nanomedicine*, 2013. 9(7): p. 923-34.
36. Zhao, L., et al., Nanoparticle vaccines. *Vaccine*, 2014. 32(3): p. 327-37.
37. Zariri, A., et al., Modulating endotoxin activity by combinatorial bioengineering of meningococcal lipopolysaccharide. *Sci Rep*, 2016. 6: p. 36575.
38. van der Ley, P.A., et al., An Intranasal OMV-Based Vaccine Induces High Mucosal and Systemic Protecting Immunity Against a SARS-CoV-2 Infection. *Front Immunol*, 2021. 12: p. 781280.
39. Frasch, C.E., Preparation of bacterial polysaccharide-protein conjugates: analytical and manufacturing challenges. *Vaccine*, 2009. 27(46): p. 6468-70.
40. Knuf, M., F. Kowalzik, and D. Kieninger, Comparative effects of carrier proteins on vaccine-induced immune response. *Vaccine*, 2011. 29(31): p. 4881-90.
41. van der Put, R.M., et al., A Synthetic Carbohydrate Conjugate Vaccine Candidate against Shigellosis: Improved Bioconjugation and Impact of Alum on Immunogenicity. *Bioconjug Chem*, 2016. 27(4): p. 883-92.
42. Palmieri, E., et al., GMMA as an Alternative Carrier for a Glycoconjugate Vaccine against Group A Streptococcus. *Vaccines (Basel)*, 2022. 10(7).
43. Tontini, M., et al., Preclinical studies on new proteins as carrier for glycoconjugate vaccines. *Vaccine*, 2016. 34(35): p. 4235-4242.
44. Zhu, N., et al., A Novel Coronavirus from Patients with Pneumonia in China, 2019. *N Engl J Med*, 2020. 382(8): p. 727-733.
45. Shang, W., et al., The outbreak of SARS-CoV-2 pneumonia calls for viral vaccines. *NPJ Vaccines*, 2020. 5(1): p. 18.
46. Tabibi, T., et al., Human Papillomavirus Vaccination and Trends in Cervical Cancer Incidence and Mortality in the US. *JAMA Pediatr*, 2022. 176(3): p. 313-316.
47. Stone, V.M., et al., A hexavalent Coxsackievirus B vaccine is highly immunogenic and has a strong protective capacity in mice and nonhuman primates. *Sci Adv*, 2020. 6(19): p. eaaz2433.
48. Stone, V.M., et al., Coxsackievirus B Vaccines Prevent Infection-Accelerated Diabetes in NOD Mice and Have No Disease-Inducing Effect. *Diabetes*, 2021. 70(12): p. 2871-2878.
49. Zhou, Q., et al., Active poly-GA vaccination prevents microglia activation and motor deficits in a C9orf72 mouse model. *EMBO Mol Med*, 2020. 12(2): p. e10919.
50. Poletti, P., et al., Association of Age With Likelihood of Developing Symptoms and Critical Disease Among Close Contacts Exposed to Patients With Confirmed SARS-CoV-2 Infection in Italy. *JAMA Netw Open*, 2021. 4(3): p. e211085.
51. Huang, C., et al., Clinical features of patients infected with 2019 novel coronavirus in Wuhan, China. *Lancet*, 2020. 395(10223): p. 497-506.
52. Zhou, F., et al., Clinical course and risk factors for mortality of adult inpatients with COVID-19 in Wuhan, China: a retrospective cohort study. *Lancet*, 2020. 395(10229): p. 1054-1062.
53. Monrad, J.T., J.B. Sandbrink, and N.G. Cherian, Promoting versatile vaccine development for emerging pandemics. *NPJ Vaccines*, 2021. 6(1): p. 26.



Chapter 2

Carriers and antigens: new developments in glycoconjugate vaccines

Robert M. F. van der Put,^{a,b} Bernard Metz,^a and Roland Pieters^b

^a Intravacc, P.O. Box 450, 3720 AL Bilthoven, the Netherlands, ^b Department of Chemical Biology & Drug Discovery, Utrecht Institute for Pharmaceutical Sciences, Utrecht University, P.O. Box 80082, NL-3508 TB Utrecht, The Netherlands,

Abstract

Glycoconjugate vaccines have proven their worth in the protection and prevention of infectious diseases. The introduction of the *Haemophilus influenzae* type b vaccine is the prime example, followed by other glycoconjugate vaccines. Glycoconjugate vaccines consist of two components: the carrier protein and the carbohydrate antigen. Current carrier proteins are tetanus toxoid, diphtheria toxoid, CRM197, *Haemophilus* protein D and the outer membrane protein complex of serogroup B meningococcus. Carbohydrate antigens have been produced mainly by extraction and purification from the original host. However, current efforts show great advances in the development of synthetically produced oligosaccharides and bioconjugation. This review evaluates the advances of glycoconjugate vaccines in the last five years. We focus on developments regarding both new carriers and antigens. Innovative developments regarding carriers are outer membrane vesicles, glycoengineered proteins, new carrier proteins, virus-like particles, protein nanocages and peptides. With regard to conjugated antigens, we describe recent developments in the field of antimicrobial resistance (AMR) and ESKAPE pathogens..

Keywords

Anti-Microbial Resistance, Carbohydrates, Carrier proteins, ESKAPE Pathogens, Glycoconjugate vaccines, Glycoengineered proteins, Outer membrane vesicles, Protein nanocages, Virus like particles.

Introduction

Vaccines have proven to be one of the most effective applications to prevent and protect against infectious diseases. As such, society relies heavily on existing vaccines, but also on the development of new vaccines and vaccine platforms. It has already been more than five centuries since the first strategies to battle infectious diseases were implemented [1]. However, it was not until the late 18th century that Jenner came up with his strategy to battle smallpox, utilizing live-attenuated viruses [1]. In the 19th century, Pasteur developed a successor in the form of a live-attenuated vaccine protecting against rabies. New and more efficient production platforms were established when viruses, such as influenza, mumps, measles, rubella, and polio, were propagated on cells and bacteria, such as *Clostridium tetani* and *Corynebacterium diphtheriae*, were isolated and grown in a culture medium for the production of toxoid vaccines (tetanus and diphtheria). The very first concepts for glycoconjugates were already evaluated in the early 1930s by Avery and Goebel [2]. However, the first conjugate vaccine targeting *Haemophilus influenzae* type b (Hib) was

developed around 1985 [3, 4], based on extracted polysaccharides (PS). Glycoconjugate vaccines appeared to be an important vaccine technology platform. Utilizing the PS is important since they aid bacteria in their ability to infect individuals and to evade the immune system and trigger an inflammatory response. Glycoconjugate vaccines consist of the extracted and purified PS alone or covalent attachment (conjugate) of these PS to carrier proteins. Vaccines containing purified PS alone do work, but they can only stimulate B-cells to produce antibodies and no immunological memory response. There are certain benefits in using a carrier protein with the PS conjugated to a carrier. Conjugation to a carrier protein significantly improves the immunogenicity towards a T-cell-dependent response to the PS [5, 6]. This has been shown for PS originating from the capsular structures of Hib, *Streptococcus pneumoniae*, *Neisseria meningitidis* and *Salmonella* Typhi [7, 8]. For children under the age of two, these conjugate vaccines are extremely effective, which is fortunate since the disease burden of encapsulated bacteria at that age is high [9, 10]. Long-lasting immunity is induced by the conjugation to a carrier protein, triggering the immune system towards a T-cell-dependent immune response [11].

The use of conjugate vaccines has had some undesirable effects. Pichichero (2013) [12] and Broker (2017) [13] describe the interference of immunogenicity thoroughly and refer to two underlying mechanisms: antigen competition and carrier-induced epitope suppression (CIES). Antigen competition is caused by the processing of antigens in combination vaccines. On these specific occasions, a protein (*e.g.*, tetanus toxoid) is co-administered as an independent vaccine constituent (against tetanus) in combination with a conjugate vaccine using the same protein, but now as a carrier (*e.g.*, DaKTP-Hib-HepB). CIES is attributed to a pre-existing vaccination using the carrier protein as the single vaccine component as well as the carrier for the conjugate vaccine or simply co-administration. It became apparent that there was a diminished immune response observed towards the conjugated polysaccharide antigen [14-17]. CIES is difficult to predict for any particular glycoconjugate vaccine. Based on immunological data from preclinical animal studies, it is still difficult to estimate the outcome of a clinical study. The introduction of new and different carriers originating from the same species as the immunogen could potentially circumvent poor immunogenicity. It could also induce a broader application for targeting multiple serotypes [18] and would at least have the potential to partially solve these issues attributed to antigen competition and CIES. The selection and development of carriers and PS have led to exciting combinations and innovative approaches. In this review article, we provide an overview of recent innovations in the development of novel conjugate vaccines. The vaccine carriers include new proteins, virus-like particles (VLP), (glycoengineered) Outer Membrane Vesicles (OMVs) and proteins nanocages and peptides. Furthermore, this review discusses the latest development of the antigenic parts of a conjugate vaccine, aimed to protect against AMR-designated ESKAPE pathogens.

Conjugate vaccine carriers

2

The choice of a carrier for conjugate vaccines has to take certain criteria into account, of which a proven track and safety record is the most important. The first traditional carrier proteins utilized were, in fact, toxoids produced from tetanus and diphtheria toxins. Even though chemical detoxification of these toxins can lead to potential heterogeneity and unwanted modifications, they have proven to be safe and efficacious. A second selection criterium was that these carriers could be produced at a large scale under GMP conditions. Several other additional criteria cannot be disregarded. New carriers will also have to be evaluated for their immunogenicity after conjugation, reproducible manufacturing and sufficient surface exposure of reactive amino acids for conjugation, solubility, and stability. Extensive physicochemical and immunological characterization is important for the selection of a carrier. Moreover, immunological responses of new carrier proteins have to be evaluated.

This information will be assessed by regulatory agencies, such as WHO, EMA or FDA. Additionally, when the carrier is also used as an antigen itself, it is key to evaluate at which site conjugation is performed. Here, the conjugation of antigens to potential B-cell epitopes can interfere with or reduce the immune response towards the carrier antigen. With the previously described CIES, the selection and development of new carrier proteins beyond the traditional currently licensed carriers seems inevitable. In the next sections, we discuss the traditional carrier proteins for glycoconjugate vaccines followed by a detailed evaluation of new carrier proteins.

Traditional protein carriers

The currently used carrier proteins in licensed vaccines are tetanus toxoid (TT), diphtheria toxoid (DT), CRM197, *Haemophilus* protein D (PD) and the outer membrane protein complex of serogroup B meningococcus (OMPC). TT and DT are the first protein carriers used for Hib conjugate vaccines due to their safety profile. The Hib conjugate vaccines were administered as stand-alone vaccines. They are derived from the chemical detoxification of bacterial toxins. CRM197 is a non-toxic mutant due to the detoxification of diphtheria toxin by means of genetic mutation. A single glycine to glutamic amino acid substitution at position 52 resulted in a non-toxic mutant [19]. There are multiple licensed vaccines using CRM197, of which Hib, multivalent meningococcal and pneumococcal conjugate vaccines are prime examples [20, 21]. PD (cell-surface protein) are applied in a multivalent pneumococcal vaccine [22, 23] and in an OMPC-based vaccine for both Hib and pneumococcal vaccines [24, 25].

Other protein carriers

The groups of Broker et al. (2017) [13] and Micoli et al. (2018) [26] have given an overview of investigated carrier proteins actively applied in the field including analytical characterization criteria. A prime example was the recombinant non-toxic form of *Pseudomonas aeruginosa* exotoxin A (rEPA) used as a carrier for *Escherichia coli* [27,28], *Shigella* O-antigens, *Staphylococcus aureus* type 5 and 8 capsular PS and the *S. Typhi* Vi antigen [29-32]. Other examples included the pneumococcal recombinant proteins spr96/2021 and spr1875 [33]; proteins originating from the extra-intestinal pathogenic *E. coli*-derived Upec-5211 and Orf3526 [33]; a recombinant protein comprising of filaments of promiscuous human CD4+ T-cell epitopes [34, 35]; and the recombinant tetanus toxin HC fragment [36]. Furthermore, they discuss several examples of synthetic peptide-based carriers, including the best-known example, a 13 amino acids non-natural pan DR (PADRE) universal helper T-lymphocyte epitope [37-43]. Lastly, they provide data on the use of proteins with the dual role of both carrier and antigen (detoxified pneumococcal-based pneumolysin [44], *S. aureus*-derived recombinant proteins [45], *Clostridioides difficile* toxin fragments [46], Group B *Streptococcus* pili proteins GBS80 and GBS67 [47, 48] and flagellin as the carrier protein for *Salmonella enteritidis* O-antigen [49]) and the application of nanoparticles (KLH [50], Q β virus-like particles [51] and glycoengineered outer membrane vesicles [52]).

Recent developments regarding protein carriers

In this section, we provide an overview of developments with respect to the application of different carrier proteins in the field of prophylactic vaccines in the last five years. A multitude of different proteins and other types of carriers have been investigated. Even though the traditional carrier proteins and other potential carriers (liposomes, polymers, inorganic gold particles, dendrimers and nanodiscs) are still very much applicable in the development of conjugate vaccines, here we have focused on six new and different types of carriers including: (1) Outer membrane vesicles (OMV) and generalized modules for membrane antigens (GMMA), (2) glycoengineered proteins and OMVs, (3) proteins, (4) virus-like particles (VLP), (5) protein nanocages and (6) peptides (Figure 1).

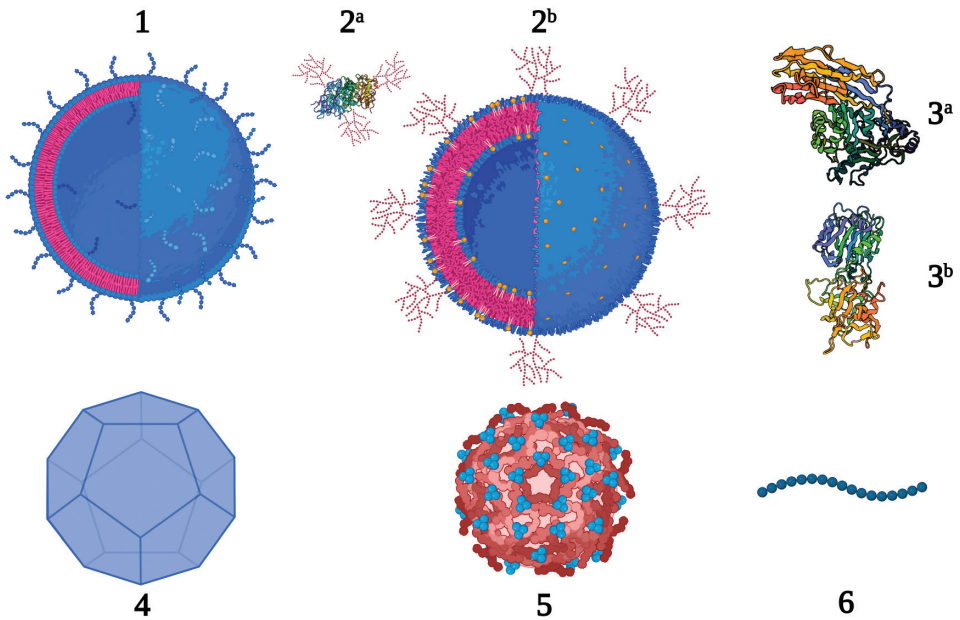


Figure 1: New carrier proteins for conjugate vaccines; OMV and GMMA (1), glycoengineered proteins (2^a *Pseudomonas aeruginosa* exotoxin A, PDB 1IKQ) and OMV (2^b), proteins (3^a *Streptococcus pyogenes* streptolysin O and 3^b, receptor binding fragment HC of tetanus neurotoxin, PDB 1AF9), VLP (4), protein nanocages (5) and peptides (6).

Outer membrane vesicles / Generalized modules for membrane antigens

The use of outer membrane vesicles (OMV) or generalized modules for membrane antigens (GMMA) provides a versatile and flexible platform for the development of monovalent or multivalent conjugate vaccines [53]. This platform is an excellent basis as a carrier and can be produced from a multitude of different bacteria [54]. The safety profiles of OMVs and GMMAs have been studied in several clinical studies [55-57]. Additionally, they are of particular interest for their self-adjuvant properties, governed by the presence of pathogen-associated molecular patterns (PAMPs), such as lipooligosaccharide (LOS) and lipoproteins [58-60]. Due to these characteristics, there is less need for the addition of adjuvants, *e.g.*, aluminum hydroxide. In comparison to smaller carriers, the sheer size of OMVs and GMMAs (50–200 nm) with their large surface area bearing a variety of properties, such as hydrophobicity, charge and the potential for receptor interaction, provide a significant constructive effect on the uptake by APCs [61]. Finally, a major benefit is that they can be efficiently manufactured using high-yielding production platforms [62, 63]. Several groups provide ample data on the successful application of OMV, and GMMA as a carrier (Table 1). The group of Micoli *et al.* has reported extensively on their GMMA carriers

originating from different pathogens and conjugating various polysaccharide and protein antigens [53, 64]. Palmieri et al. have investigated conjugates using GMMAs originating from *S. enterica* and conjugating Group A *Streptococcus* cell wall oligosaccharide [65], whereas Scaria et al. describe the application of OMV, a membrane vesicle derived from *N. meningitidis* as the carrier for a malaria transmission-blocking antigen.

Table 1: OMV/GMMA conjugation strategies

Carrier type	Carrier	Antigen	Chemistry	References
OMV	<i>S. Typhimurium</i>	SARS-CoV-2 spike receptor-binding domain (RBD)	SpyCatcher-Spy-Tag ^[1]	Jiang et al. 2022 [66]
GMMA	<i>S. Typhimurium</i>	Group A <i>Streptococcus</i> cell wall carbohydrate	Reductive amination	Palmieri et al. 2022 [65]
GMMA	<i>S. Typhimurium</i>	Malaria transmission-blocking protein Pfs25	Oxidation / reductive amination	Di Benedetto et al. 2021 [67]
GMMA	<i>S. typhimurium</i>	<i>P. falciparum</i> circumsporozoite protein	Thiol-maleimide	Micoli et al. 2020 [53]
	<i>Shigella sonnei</i>	<i>E. coli</i> SsIE	Reductive amination	
	<i>N. meningitidis</i> type B / <i>S. typhimurium</i>	<i>N. meningitidis</i> serogroups A and C oligosaccharides	SIDEA	
OMV	<i>N. meningitidis</i> type B	Malaria transmission blocking antigen Pfs230	Thiol-maleimide	Scaria et al. 2019 [68]

^[1] See protein nanocages for a detailed description of the SpyCatcher-SpyTag ligation.

Glycoengineered OMVs and proteins

Where traditional glycoconjugate vaccines rely on the extracted or synthetically designed saccharides being chemically conjugated to a carrier protein, *in vivo* protein glycan coupling technology (PGCT) is achieved through recombinant enzymatic construction of a glycoconjugate directly in bacteria [69]. These glycoconjugates consist of a carrier protein and a carbohydrate moiety originating from the bacterial capsule or the O-antigen polysaccharide (O-PS) [70]. A prerequisite here is that the O-PS structure has been identified, including the gene cluster responsible for its production. PGCT is based on the *Campylobacter jejuni* N-linked glycosylation system, which can be expressed in *E. coli*. Moreover, the *E. coli* mutant is capable of producing heterologous polysaccharides

on its glycosyl carrier lipid [71]. The final construction of the glycoconjugate requires the presence of genome clusters of the bacterial polysaccharide, which is achieved by a plasmid encoding for the carrier protein, including oligosaccharyl transferase (OTase); characteristically originating from PglB from *C. jejuni* [71]. Bioconjugation in general leads to heterogeneously expressed glycoproteins. The polysaccharides themselves show polydispersity, and the number of carbohydrate repeat units can vary significantly. Additionally, the conjugation rate, or quantity of polysaccharides conjugated to one single carrier protein, varies as well. For these reasons, the structure elucidation of the conjugate is not evident and requires several methods [72, 73]. Next to this, there are some other challenges, such as OTases, that are not fully compatible with most bacterial O-SP, resulting in even more heterogeneous bioconjugates. Nevertheless, PGCT does not need intermediate steps, such as glycan synthesis, purification, conjugation, and process controls. As such, PGCT is potentially more cost-effective. This new and exciting field of conjugate vaccines is already well studied (Table 2). Nicolardi et al. describe the development of a protein-based glycoengineered vaccine using the exotoxin A from *P. aeruginosa* as a carrier targeting *E. coli* serotypes O2, O6A and O25B [72]. Harding et al. report (1) on a polyvalent pneumococcal bioconjugate vaccine using the natural acceptor protein ComP as a vaccine carrier decorated with *S. pneumoniae* CPSs [74] and (2) *K. pneumoniae* K1 and K2 serotypes produced in glycoengineered *E. coli*.

Table 2: Glycoengineered conjugation strategies

Carrier type	Carrier	Antigen	Chemistry	References
Protein / Bi-valent	<i>P. aeruginosa</i> exotoxin A	<i>E. coli</i> O2, O6A and O25B	Bioconjugation	Nicolardi et al. [72]
Polysaccharide / Quadrivalent	<i>P. aeruginosa</i> exotoxin A	<i>S. dysenteriae</i> type O1, O antigen from <i>S. flexneri</i> 2a, 3a and 6	Bioconjugation	Martin et al. 2022 [75]
Polysaccharide / monovalent	<i>P. aeruginosa</i> exotoxin A	<i>Shigella flexneri</i> 2a O-polysaccharide	Bioconjugation	Ravenscroft et al. 2019 [76]
Polysaccharide / protein Bi-valent	<i>P. aeruginosa</i> exotoxin A	<i>K. pneumoniae</i> K1 and K2 CPSs	Bioconjugation	Feldman et al. 2019 [77]
Oligosaccharide / mono- bi- and trivalent	<i>E. coli</i> Acceptor protein ComP	<i>S. pneumoniae</i> CPS	Bioconjugation	Harding et al. 2019 [74]
Polysaccharide / monovalent	<i>S. pneumoniae</i> NanA, PiuA, and Sp0148	<i>S. pneumoniae</i> serotype 4 CPS	Bioconjugation	Reglinksy et al. 2018 [78]

Carrier type	Carrier	Antigen	Chemistry	References
OMV	<i>E. coli</i> OMV	Poly- <i>N</i> -acetyl-d-glucosamine (rPNAG)	Bioconjugation	Stevenson et al. 2018 [79]
Polysaccharide / monovalent	<i>S. Paratyphi</i> A antigenic peptide (P2)	<i>S. enterica</i> serovar Paratyphi A O-polysaccharide	Bioconjugation	Sun et al. 2018 [80]
Polysaccharide / monovalent	<i>P. aeruginosa</i> exotoxin A	<i>F. tularensis</i> O-antigen	Bioconjugation	Marshall et al. 2018 [81]

Protein-based carriers

Antigen competition and CIES pose a problem for the inclusion of antigens with respect to their use of vaccines. For this reason, the introduction of new protein carriers that improve upon the traditional carriers is much needed. Recent developments in conjugate vaccine design include proteins from both homologues and heterologous origin as carriers of conjugated antigens. From this, either a monovalent or bivalent (combining two target antigens) approach is used to target specific pathogens (Table 3). Wang et al. targeted *S. pyogenes* (Group A *Streptococcus*, GAS) cell wall oligosaccharides (GAC) conjugated to the streptococcal C5a peptidase carrier as a bivalent conjugate vaccine [82, 83]. Furthermore, Kapoor et al. also target the GAC oligosaccharides from GAS. However, they found an application in the use of the secreted toxin antigen streptolysin O (SLO) as the protein carrier [84]. Additionally, Romero-Saavedra et al. described the use of two enterococcal proteins (secreted antigen A and the peptidyl-prolyl cis-trans isomerase) as a carrier for the *Enterococcus faecalis* polysaccharide di-heteroglycan [85].

Table 3: Protein-based conjugation strategies

Carrier type	Carrier	Antigen	Chemistry	References
Bivalent	Genetically detoxified tetanus toxin (8MTT)	Cattle tick fever peptide P0, <i>H. influenzae</i> type b (PRP)	Thiol-maleimide, CDAP	Chang et al. 2022 [86]
Bivalent	<i>S. pneumoniae</i> serotype type 14 CPS	recombinant SARS-CoV-2 RBD	Reductive amination	Deng et al. 2022 [87]
Monovalent	Group A <i>Streptococcus</i> Streptolysin O	Group A <i>Streptococcus</i> cell-wall oligosaccharides	Click chemistry	Kapoor et al. 2022 [84]
Bivalent	Rotavirus recombinant ΔVP8 protein	<i>S. Typhi</i> capsular polysaccharide (Vi)	EDAC-ADH	Park et al. 2021 [88]

Carrier type	Carrier	Antigen	Chemistry	References
Bivalent	<i>Streptococcus</i> C5a peptidase ScpA193, Fn and Fn2	Group A <i>Streptococcus</i> cell-wall trisaccharide	di(<i>N</i> -succinimidyl) glutarate	Wang et al. 2021 [83]
Monovalent	<i>S. aureus</i> fusion protein (Hla-MntC-ACOL0723)	<i>S. aureus</i> 5 (CP5, Reynolds strain) and 8 (CP8, Becker strain)	Carbodiimide	Ahmadi et al. 2020 [89]
Monovalent	<i>S. Typhimurium</i> flagellin	<i>S. Typhimurium</i> lipid-A free lipopolysaccharide	Decarboxylative amidation	Chiu et al. 2020 [90]
Monovalent	Recombinant tetanus toxoid heavy chain fragment	HIV-1 fusion peptide (FP8)	Sulfo-SIAB	Ou et al. 2020 [91]
Bivalent	Hepatitis B virus surface antigen	Pneumococcal type 33 F-capsular polysaccharide	Carbodiimide	Qian et al. 2020 [92]
Bivalent	Recombinant Tetanus Toxoid Heavy Chain Fragment C	HIV-1 fusion peptide (FP) with eight amino acid residues (FP8)	Amine-to-sulphydryl, Thiol-maleimide	Yang et al. 2020 [93]
Monovalent	<i>Enterococcus</i> secreted antigen A and the peptidyl-prolyl cis-trans isomerase	<i>E. faecalis</i> polysaccharide di-heteroglycan	CDAP	Romero-Saavedra et al. 2019 [85]
Bivalent	<i>Plasmodium falciparum</i> Pfs25	<i>S. Typhi</i> Vi capsular polysaccharide	Carbodiimide	An et al. 2018 [94]
Monovalent	<i>S. enteritidis</i> homologous serovar phase 1 flagellin protein	<i>S. enteritidis</i> core and O-polysaccharide (COPS)	CDAP	Baliban et al. 2018 [95]
Monovalent	Recombinant tetanus toxoid heavy chain fragment C	Oxycodone-based hapten	Carbodiimide	Baruffaldi et al. 2018 [96]
Monovalent, bivalent, and trivalent	EPEC adhesins CFA/I and CS6	<i>C. jejuni</i> and <i>Shigella</i> polysaccharides and <i>Shigella flexneri</i> LPS	TEMPO-mediated oxidation and carbodiimide	Laird et al. 2018 [97]

Virus like particles

Virus-like particles (VLPs) are part of the family of subunit vaccines. VLPs are formed by means of viral capsid protein self-assembly. The formed particles mimic the original virus but cannot replicate or induce an infection. This is an advantage with respect to the risks associated with live-attenuated vaccines [98]. Next to serving as a vaccine component themselves, VLPs also provide a platform as a carrier. Similar to chemical conjugation, glycoengineered proteins and OMVs, protein display can be used for VLPs to present heterologous protein antigens (Table 4). An example is reported by Basu et al., who in one study, conjugated two Zika virus proteins (MS2 and PP7) and, in another study, coupled multiple synthetic peptides mimicking Chikungunya virus B-cell epitopes to a canonical ssRNA phage Q β VLP (Q β) [99,100]. Warner et al. used the same strategy but conjugated synthetic peptides originating from the Dengue virus to the Q β VLP carrier [101]. More recently, Zha et al. demonstrated that a recombinantly expressed SARS-Cov-2 receptor-binding domain (RBD) can be conjugated to VLPs, derived from the cucumber mosaic virus [102]. Carbral-Miranda et al. used the cucumber mosaic virus VLP carrier to successfully conjugate a Zika virus E-DIII protein [103].

Table 4: VLP conjugation strategies

Carrier type	Carrier	Antigen	Chemistry	References
Protein display	Q β	Dengue virus synthetic peptides	Protein display	Warner et al. 2021 [101]
Protein display	Cucumber mosaic virus	Recombinantly expressed SARS-Cov-2 receptor-binding domain	Protein display	Zha et al. 2021 [102]
Protein display	Cucumber mosaic virus	Zika virus E-DIII protein	Protein display	Cabral-Miranda et al. 2019 [103]
Protein display	Q β	Zika virus MS2 and PP7 / Chikungunya virus B-cell synthetic peptides	Protein display	Basu et al. 2018, 2020 [99,100]
Chemical conjugation	Q β	Thomsen-nouveau antigen, GD2 protein, SARS-CoV-2 peptides	di-NHS ester adipate	Sungsuwan et al. 2022 [104]
Chemical conjugation	Recombinant adenoviral type 3 dodecahedron	<i>S. pneumoniae</i> serotype 14 CPS trisaccharide	Glutaraldehyde	Prasanna et al. 2021 [105]

Carrier type	Carrier	Antigen	Chemistry	References
Chemical conjugation	Q β	HIV-1 V1V2 glycopeptide	Click chemistry	Zong et al. 2021 [106]
Chemical conjugation	Q β	Synthetic pertussis LPS-like pentasaccharide	diNHS ester adipate	Wang et al. 2020 [107]
Chemical conjugation	Full-length hepatitis B core antigen virus-like particles	Meningococcal group C polysaccharides	Amine-PEG-maleimide	Xu et al. 2019 [108]

Protein nanocages

A comprehensive overview of the application of nanocages is given by Curley et al. [109]. Nanocages are constructed from non-viral protein subunits and have similarities to VLPs. A number of these subunits can self-assemble into nanocages. They form symmetrical structures that differ from VLPs in terms of shape and size [110]. Nanocages contain repetitive structures recognized by B-cell receptors. One specific example where nanocages are utilized as a carrier for vaccine development is ferritin-based nanocages. These ferritin modules derived from *Helicobacter pylori* assemble into a 12 nm diameter spherical cage and are composed of 24 subunits with a hollow core [111]. An interesting aspect here is the application of the innovative SpyCatcher-SpyTag conjugation approach as described by Chen et al. [112] and Wang et al. [113]. This method of protein ligation is based on the modified domain of the *S. pyogenes* surface protein (SpyCatcher) that specifically recognizes a 13-amino-acid peptide (SpyTag). A covalent isopeptide bond is formed between the side chain of lysine in the SpyCatcher and aspartate in the SpyTag. This results in covalently linked protein complexes [114]. Several vaccine targets have been investigated that use protein carrier nanocages (Table 5), including hemagglutinin from the influenza virus [115] and the pre-S1 protein from hepatitis B [113].

Table 5: Protein nanocages conjugation strategies

Carrier type	Carrier	Antigen	Chemistry	References
Tri-valent	<i>E. coli</i> Sd-ferritin	SARS-Cov-2 RBD B.1.617.2, D614G and B.1.351	SpyCatcher-Spy-Tag	Chen et al. 2022 [112]
Monovalent	Horse spleen apoFerritin	Influenza virus PR8 H1N1 hemagglutinin and M2e peptide	Thiol-maleimide	Sheng et al. 2022 [116]
Monovalent	<i>E. coli</i> SpyTag-ferritin	Δ N SpyCatcher-fused preS1	SpyCatcher-Spy-Tag	Wang et al. 2020 [113]
Bivalent	Horse spleen apoFerritin	Influenza virus hemagglutinin	Thiol-maleimide	Wei et al. 2020 [115]

Peptides

Peptide-based vaccines are a type of subunit vaccine predominantly comprised of short (single-epitope) sequences that can be produced synthetically. These types of vaccines have several advantages, such as their good safety profile, fast and simple manufacturability at a large-scale and high purity [117]. Additionally, designing peptide vaccines combining multiple single epitopes and creating synthetic long peptides into recombinant overlapping peptide vaccines could broaden their applications and effectiveness [118, 119]. In most cases, the antigenic peptide has to be equipped with an adjuvant, e.g., the universal T-cell epitope PADRE, and also with poly-leucine as a hydrophobic solubilizing moiety in order for them to be useable. Several exemplary applications are described in Table 6.

Table 6: Peptides conjugation strategies

Carrier type	Carrier	Antigen	Chemistry	References
Semi-synthetic	IC28 peptide from bacterial flagellin	Recombinant SARS-Cov-2 RBD	Thiol-maleimide	He et al. 2022 [120]
Synthetic	PADRE and poly-leucine	<i>S. pyogenes</i> (GAS) M-protein-derived B-cell epitopes J8, PL1, and 88/30	Click-chemistry	Azuar et al. 2021 [121]
Synthetic	T-helper cell epitope P25 and poly-leucine	Hookworm APR-1 B-cell epitope (p3)	Click-chemistry	Shalash et al. 2021 [122]
Semi-synthetic	<i>S. Typhi</i> OmpC synthetic peptide	<i>S. Typhi</i> Vi poly-saccharide	ADH-EDC	Haque et al. 2019 [123]

Conjugate vaccine antigens

Since the introduction of the first carbohydrate conjugate vaccine targeting *H. influenzae* type b [4], conjugate vaccines have been developed for many different applications in the prophylactic domain to prevent infectious diseases, such as pneumonia, meningitis and sepsis. Currently, there are close to twenty conjugate vaccines on the market, licensed by the FDA, EMA and WHO. These vaccines are all based on the chemical conjugation of capsular polysaccharides targeted against Hib, *N. meningitidis* serogroup ACWY, *S. pneumoniae* or *S. Typhi*. Recent developments show conjugate vaccines targeting other pathogens such as a multivalent extraintestinal pathogenic *E. coli* bioconjugate (ExPEC), *Klebsiella* O-antigen based, Group B *Streptococcus*, other serotypes of *S. pneumoniae*, PNAG (*N. meningitidis*, *S. aureus*, *Neisseria gonorrhoea*, *Klebsiella pneumoniae*, *E. coli* and *S. pneumoniae*), *Shigella flexneri* 2a and others [124, 125].

Next to the area of infectious diseases, carbohydrate-based conjugate vaccines find their application in the therapeutic domain targeting different forms of cancer. Often these vaccines are based on synthetic moieties mimicking tumor-associated carbohydrate antigens (TACAs) [126] including protein-linked Tn, Sialyl-Tn (STn) and TF (conjugated to the -OH group of serine) and glycolipid-based gangliosides GM2, GD2, GD3, fucosyl-GM1, Globo-H and Lewis^x. The advantages of vaccination and targeting these TACAs include the significant reduction in toxicity and invasiveness compared to cytotoxic therapies such as radio- and chemotherapy [127]. Soriaul et al., Shivatare et al. and Hossain et al. gave an excellent overview of the current field of carbohydrate-based cancer vaccines. This included potential carrier proteins, adjuvants, and modifications of TACA antigens to improve stability, reduce hydrolytic cleavage and the cost of large-scale chemical or enzymatical synthesis [128-130]. Another area where carbohydrate-based conjugate vaccines find their application is the field of neurodegenerative diseases such as Alzheimer's disease [131]. Overall, it cannot be denied that conjugate vaccines find their use in the broadest sense stretching multiple disease areas.

Despite the broad potential, the importance of the battle against antimicrobial resistance pathogens (AMR) cannot be overstated. Resistance to antibiotics can occur naturally in bacteria. However, the main reason for AMR is related to incompliance with respect to dosage and in adherence with the duration of the treatment. If antibiotic resistance would confine itself to a single pathogenic species or antibiotic, it would potentially still be manageable. At this moment, several bacteria show multidrug resistance (MDR), meaning they are resistant to multiple antibiotics. MDR is even more problematic specifically due to bacteria's abilities to transfer AMR-related genes between different species (Table 7).

Table 7: AMR for each of the ESKAPE pathogens

Species	AMR
<i>Enterococcus faecium</i>	Vancomycin
<i>Staphylococcus aureus</i>	Methicillin and Vancomycin
<i>Klebsiella pneumoniae</i>	Carbapenem, ESBL ^[a]
<i>Acinetobacter baumannii</i>	Carbapenem
<i>Pseudomonas aeruginosa</i>	Carbapenem
<i>Escherichia coli</i>	Carbapenem, ESBL ^[a]

^[a] Extended-spectrum beta-lactamases

The so-called ESKAPE pathogens (*Enterococcus faecium*, *Staphylococcus aureus*, *Klebsiella pneumoniae*, *Acinetobacter baumannii*, *Pseudomonas aeruginosa* and *Enterobacter spp.*) have developed MDR against macrolides, lipopeptides, fluoroquinolones, oxazolidinones, β -lactams, tetracyclines, β -lactam- β -lactamase inhibitor combinations and against the

last line of defense antibiotics such as glycopeptides, carbapenems and polymyxins [132]. Murray et al. (2019) estimated that the global burden of AMR included 23 pathogens and 88 pathogen–drug combinations spreading across 204 territories and countries. They attributed 1.27 million deaths directly to AMR and even a staggering 4.95 million deaths associated with AMR. This makes AMR the third largest global killer due to an infectious agent after COVID-19 and tuberculosis [133]. Now, looking past the COVID-19 pandemic, AMR can be classified as the new overlooked pandemic [134,135]. WHO and CDC have produced priority lists on which AMR targets have been classified (Figure 2 [136, 137]).

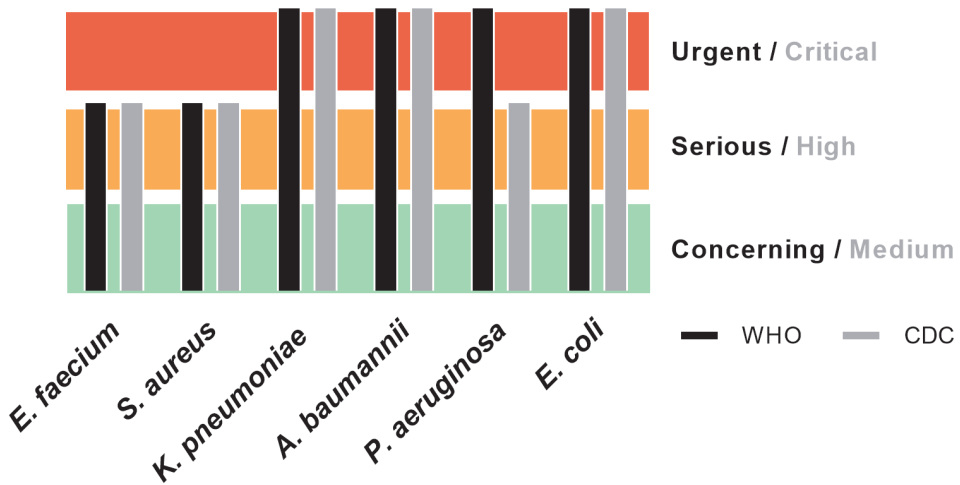


Figure 2: Priority list scaling for the ESKAPE pathogens according to both CDC and WHO.

A collaborative study performed in 2019 (European Antimicrobial Resistance Collaborators, EARC) provided confirmational data that six of the ESKAPE pathogens that are at the top of AMR list, are each responsible for more than 25,000 associated deaths in Europe in 2019 alone (Figure 3 [138]). While the list extends much further than the six ESKAPE pathogens alone, both agencies rate all the ESKAPE pathogens at the top of their priority list.

EARC AMR related deaths in Europe 2019

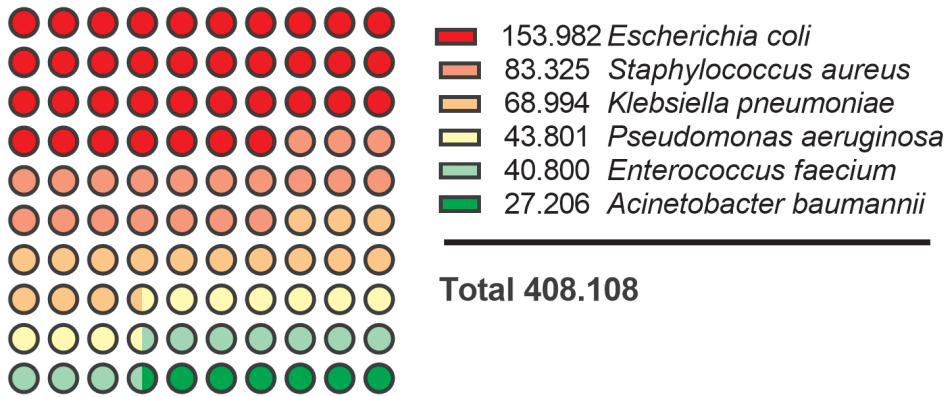


Figure 3: EARC nr. of deaths caused by ESKAPE pathogens in 2019 [136]

Glycoconjugate vaccines have proven to be successful in the battle against infectious diseases and potential AMR targets. Current developments show that substantial progress is made in the development of conjugate vaccines applying complex glycans obtained by either extraction, chemical synthesis or through bioconjugation. Here, we provide an overview of the individual AMR challenges for each of the ESKAPE pathogens and the recent applications of carbohydrate conjugate vaccines targeting AMR in the last five years.

Enterococcus faecium

E. faecium is a Gram-positive commensal bacterium that is associated with severe infections in immunocompromised populations. Infections are persistent in the hospital environment with common hospital-acquired infections (bloodstream and urinary tract infections) in patients suffering from other underlying conditions. Up to 30% of all healthcare-related enterococcal infections are resistant to vancomycin, with increasing resistance towards other antibiotics [136, 137]. Primary targets for vaccine development include capsular polysaccharide, cell wall teichoic acid and lipoteichoic acid. Another polysaccharide which is anchored to the peptidoglycan layer with possible immunogenic properties is the enterococcal polysaccharide antigen [139].

Kalfopoulou et al. provided data on two highly specific antibodies directed against the polysaccharide and carrier protein. Both antibodies showed good opsonic killing against target bacterial strains in upwards of 40% for *E. faecium* and 90% for *E. faecalis*

respectively [140]. Romero-Saavedra et al. showed similar results with antibodies against the corresponding conjugate, as well as against the respective protein and carbohydrate antigens. This included effective opsonophagocytic killing against different *E. faecalis* and *E. faecium* strains and recognition of 22 enterococcal strains [85]. Zhou et al. took a different approach with a synthetic cell wall teichoic acid (Figure 4), and also demonstrated a robust immune response and high antibody titers [141]. All three described examples provided successful data and are promising vaccine candidates against *E. faecium* targeting different antigens. They also included homologues carrier proteins, thus providing potential broader protection among multiple serotypes (Table 8).

Table 8: Carbohydrate conjugate vaccines targeting *Enterococcus faecium*

Carrier type	Carrier	Antigen	Chemistry	References
Traditional extracted	<i>Enterococcus</i> secreted antigen A	Di-heteroglycan	CDAP	Kalfopoulou et al. 2019 [140]
Traditional extracted	<i>Enterococcus</i> secreted antigen A and peptidyl-prolyl cis-trans isomerase	Di-heteroglycan	CDAP	Romero-Saavedra et al. 2019 [85]
Semi synthetic	KLH and HSA	Cell wall teichoic acid	Disuccinimidyl glutarate	Zhou et al. 2017 [141]

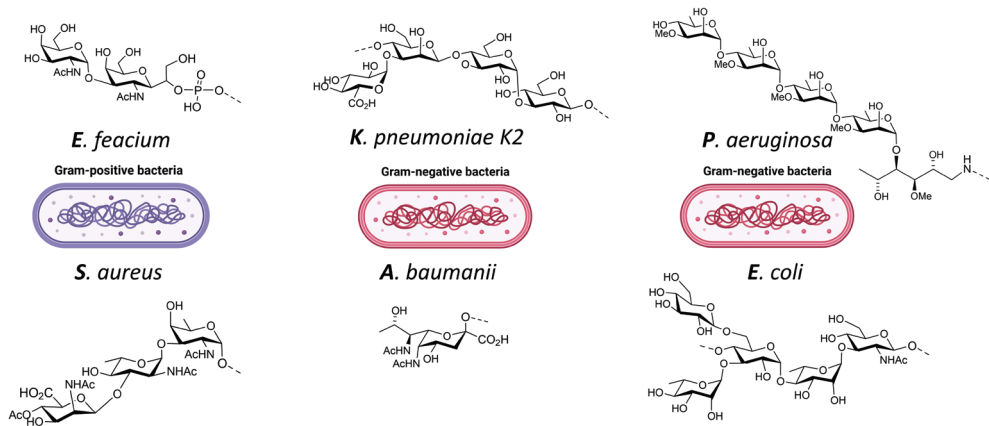


Figure 4: ESKAPE pathogens and examples of target antigens: *E. faecium*: cell wall teichoic acid [141]; *S. aureus*: trisaccharide type 8 capsular polysaccharide [142]; *K. pneumoniae*: capsular polysaccharide K2 [143]; *A. baumannii*: pseudaminic-acid [144]; *P. aeruginosa*: methyl Rhamnan pentasaccharide [145]; *E. coli*: serotype O25B [146].

Staphylococcus aureus

S. aureus is a commensal Gram-positive bacterium associated with methicillin resistance (MRSA) and not only hospital-acquired infections in patients suffering from other underlying conditions, but also as a communal acquired infection of the skin and soft tissue. MRSA results in increased morbidity, mortality, length of hospitalization of patients and incurred costs [136, 137]. Vancomycin is the first line antibiotic in the treatment of MRSA infections [147]. However, both intermediate and complete resistance to vancomycin has developed among clinical isolates within the past decades [148]. While the incidence of vancomycin resistance is still rare, it has become a serious public health concern [149]. The capsular polysaccharide from *S. aureus* has 13 different serotypes identified from clinical isolates of which types 5 and 8 are the most abundant [150]. Furthermore, the broadly associated poly-(1->6)-*N*-acetyl-D-glucosamine exopolysaccharide (PNAG) is also a potential target for vaccine development.

Gening et al. describe the successful development of a PNAG glycoconjugate including passive and active protection against different pathogens. Their conjugate 5GlcNH₂-TT is being produced under GMP conditions and has entered safety and effectiveness testing in humans and economically important animals [151]. Zhao et al. provide data on the successful development of a synthetic capsular polysaccharide type 8 trisaccharide (Figure 4) conjugated to CRM197. They report a robust immune response including monoclonal antibodies recognizing the *S. aureus* strain [142]. While the prior two groups employ more traditional conjugation using carriers and antigens, the group of Stevenson et al. provided data on an OMV bioconjugate. They first showed the successful decoration of the *E. coli* OMV with PNAG followed by the introduction of an *S. aureus* enzyme responsible for PNAG deacetylation. Antibodies that were generated by vaccinating with this candidate provided efficient *in vitro* killing of *S. aureus* and *Francisella tularensis* as well [79]. All three described groups provided results that reveal the potential for effective vaccines targeting *S. aureus* utilizing different platforms (Table 9).

Table 9: Carbohydrate conjugate vaccines targeting *Staphylococcus aureus*

Carrier type	Carrier	Antigen	Chemistry	References
Semi synthetic	Tetanus toxoid, Shiga toxin 1b subunit (Stx1b) and <i>S. aureus</i> alpha-hemolysin	Synthetic penta- and nona-β-(1->6)-d-glucosamine (PNAG)	Thiol-maleimide	Gening et al. 2021 [151]
Semi-synthetic	CRM197	Capsular polysaccharide type 8 trisaccharide	Bis(p-nitrophenyl adipate)	Zhao et al. 2020 [142]

Carrier type	Carrier	Antigen	Chemistry	References
Bioconjugate	<i>E. coli</i> OMV	Poly-N-ace-tyl-d-glucosamine (rPNAG)	Bioconjugation	Stevenson et al. 2018 [79]

Klebsiella pneumoniae

K. pneumoniae is a commensal Gram-negative bacterium. It is associated with persistent urinary tract, soft tissue, and ventilator-associated pneumonia infections. Furthermore, it affects the elderly and immunocompromised patients causing pneumonia and sepsis. Infections can also be found in communal settings and are widespread. Resistance is found for third generation cephalosporins and carbapenems. This resistance is conferred through extended-spectrum beta-lactamase (ESBL) or Amp-C beta-lactamase production. Last resort options to treat ESBL-producing Enterobacteriaceae infections are limited and can include the use of intravenous (IV) carbapenem antibiotics [136, 137]. *K. pneumoniae* polysaccharides offer a wide array of targets for vaccine development, of which the capsular polysaccharide-derived K-antigen (77 serotypes) and lipopolysaccharide-derived O-antigen are the most promising [152]. Early developments of a 24-valent vaccine (1990s) have been shown to be effective in humans, but further development has been stopped due to overly complicated manufacturing [153].

Lin et al. suggest that traditional depolymerization of the CPS results in the loss of immunogenicity. They circumvent this by first extracting the polysaccharides from *K. pneumoniae* before applying CPS depolymerases identified from phages to cleave K1 and K2 (Figure 4) CPS, resulting in intact structural units of oligosaccharides without modifications. Conjugate vaccines employing TT as a carrier and using both K1 and K2 oligosaccharides were successful in protecting mice in a challenging study post-vaccination [143]. Feldman et al. reported on the recombinant production of a bioconjugate vaccine produced in glycoengineered *E. coli* targeting serotypes K1 and K2. The bioconjugates proved to be immunogenic and provided protection in mice when subjected to a lethal infection using two hypervirulent *K. pneumoniae* strains [77]. Ravinder et al. designed synthetic saccharides mimicking the K2 oligosaccharide. After investigating different quantities in repeat units, they concluded that there was an optimum at five repeat units of the saccharide. Their glycoconjugate vaccine equipped with the heptasaccharide exhibited good bactericidal activity [154]. There are multiple strategies being investigated in the field to design new vaccines targeting *K. pneumoniae* that include traditionally extracted polysaccharides, synthetic strategies and bioconjugates. This will yield multiple vaccine candidates with great potential (Table 10).

Table 10: Carbohydrate conjugate vaccines targeting *Klebsiella pneumoniae*

Carrier type	Carrier	Antigen	Chemistry	References
Traditional extracted	Poly(lactic-co-glycolic acid) (PLGA)	<i>K. pneumoniae</i> K2O1 capsule antigen	W/O/W emulsion	Ghaderinia et al. 2022 [155]
Traditional extracted	CRM197	Capsular polysaccharide K1 and K2	Thiol-maleimide	Lin et al. 2022 [143]
Bioconjugate	<i>E. coli</i>	<i>K. pneumoniae</i> serotype O2 polysaccharide	Bioconjugation	Peng et al. 2021 [156]
Semi-synthetic	CRM197	K2 hexa-, hepta-, and octa-saccharide	Thiol-maleimide	Ravinder et al. 2020 [154]
Bioconjugate	<i>P. aeruginosa</i> exotoxin A	Capsular polysaccharide K1 and K2	Bioconjugation	Feldman et al. 2019 [77]
Traditional extracted	<i>P. aeruginosa</i> rFlaA and rFlaB	O-polysaccharide O1, O2, O3 and O5	Thiol-maleimide	Hegerle et al. 2018 [157]
Semi synthetic	CRM197	Synthetic hexasaccharide	p-nitrophenyl adipate ester	Seeberger et al. 2017 [158]

Acinetobacter baumannii

A. baumannii is a commensal Gram-negative bacterium with great capability to spread in hospital settings. A particular challenge lies in the fact that it is frequently found at healthcare facilities. It is the leading cause of ventilator-associated pneumonia, and bloodstream, wound and urinary tract infections while being inherently resistant to various classes of antibiotics and easily acquiring resistance. It shows high mortality rates for invasive infections, particularly in carbapenem-resistant strains. Some *Acinetobacter* strains have built resistance to practically all antibiotics. Therefore, they are designated at the top of all AMR priority lists. While overall carbapenem-resistant *Acinetobacter* rates have decreased, gene transfer between other species, making them carbapenemases competent, is an increasing problem [136, 137]. *A. baumannii* shows great biodiversity in polysaccharide structures, of which more than 40 different serotypes are described [159].

Rudenko et al. provided data on glycoconjugates using extracted K9 CPS fragments. They report on a substantial cross-reactive antibody response, including protective effectiveness demonstrated by a challenge of immunized mice with a lethal dose of *A. baumannii* K9 [160]. Li et al. demonstrated that their bioconjugate vaccine candidate elicited an efficient immune response and provided protection against an *A. baumannii*

infection in a murine sepsis model [161]. Wei et al. employed a synthetically produced pseudaminic acid (Figure 4) conjugated to CRM197. Antibodies raised to their vaccine candidate were able to recognize pseudaminic acid [144]. Among the different research groups, the three different conjugation strategies all provided the ability to come up with effective vaccine designs targeting *A. baumannii* yielding multiple vaccine candidates that show great potential (Table 11).

Table 11: Carbohydrate conjugate vaccines targeting *Acinetobacter baumannii*

Carrier type	Carrier	Antigen	Chemistry	References
Traditional extracted	BSA, OVA, KLH	CPS K9 di- and trimers	Reductive amination, squaric acid	Rudenko et al. 2022 [160]
Bioconjugate	Cholera toxin B subunit	O-linked PglS	Bioconjugation	Li et al. 2022 [161]
Semi synthetic	CRM197	Pseudaminic acid	OPA (ortho-phthalaldehyde)	Wei et al. 2021 [144]
Semi-synthetic	CRM197	Pseudaminic acid	Thiol-maleimide	Lee et al. 2018 [162]

Pseudomonas aeruginosa

P. aeruginosa is a Gram-negative bacterium and primarily opportunistic nosocomial pathogen. It is rated as one of the most common causes of pneumonia in immunocompromised patients, including those with lung disease. Typically, cystic fibrosis, HIV-1 and cancer patients often suffer from opportunistic *P. aeruginosa* infections in conjunction with chronic lung infections [163]. Between 2% and 3% of *P. aeruginosa* strains carry the carbapenemase enzyme making them carbapenem-resistant. This resistance particularly increases the risk of mortality among patients with bloodstream infections and leaves very few treatment options [136, 137]. *P. aeruginosa* carries O-polysaccharide, part of the LPS, as an important variable region and virulence factor. Further characterization of serotyping can be done by applying the International Antigenic Scheme. *P. aeruginosa* can be subdivided into 20 standard O serotypes (O1–O20) based on the structure of O-polysaccharide [164]. Serotypes O5, O6 and O11 are most prevalent in burn wound infections [165], whereas serotypes O6 and O11 are most common in pneumonia [166].

Jamshidi et al. reported on the successful development of a pentasaccharide conjugate from *P. aeruginosa*'s A-Band polysaccharide (Figure 4). Evaluation of the immunogenicity showed that antibodies were able to recognize *P. aeruginosa* LPS [145]. Hegerle et al. investigated a dual-use conjugate vaccine targeting both *P. aeruginosa* (rFlaA and rFlaB, carrier protein) and *K. pneumoniae* (O-polysaccharide O1, O2, O3 and O5, antigens).

A quadrivalent conjugate vaccine formulation for the four antigens provided passive protection in both rabbits and mice when challenged [157]. Taken together, these vaccine candidates provide promising preclinical results and provide proof-of-concept for *P. aeruginosa* vaccines (Table 12).

Table 12: Carbohydrate conjugate vaccines targeting *Pseudomonas aeruginosa*

Carrier type	Carrier	Antigen	Chemistry	References
Semi synthetic	PLGA	<i>P. aeruginosa</i> LPS and OPS	Carbodiimide	Maleki et al. 2022 [167]
Semi synthetic	HSA	Methyl Rhamnan Pentasaccharide	Reductive amination	Jamshidi et al. 2022 [145]
Traditional extracted	<i>P. aeruginosa</i> rFlaA and rFlaB	O-polysaccharide O1, O2, O3 and O5	Thiol-maleimide	Hegerle et al. 2018 [157]

Escherichia coli

Part of the group of *Enterobacter* spp, *E. coli* is a Gram-negative commensal bacterium. It is associated with increasing reports of resistance in most countries and high mortality rates. Resistance has been observed towards third generation cephalosporins through ESBL or Amp-C beta-lactamase production. *E. coli* is widespread and responsible for community-acquired and hospital-acquired urinary tract infections and bloodstream infections, ventilator-associated pneumonia infections and diarrheal disease as well. Resistance leaves very limited treatment options [136, 137]. Serotyping of *E. coli* is based on the capsular polysaccharides, part of the protective structure on their surface. There is significant diversity where more than 180 different O-antigens and approximately 80 K-antigens have been reported [168].

Both Nicolardi et al. and Kowarik et al. (Figure 4) successfully constructed their bioconjugate via the traditional pathways and provide extensive data on the characterization. However, no immunogenicity data was provided making it impossible to assess the effectiveness [72,146]. Both Stevenson et al. and Gening et al. have provided successful immunogenicity data which was discussed for *S. aureus* already regarding the PNAG antigen and which could be applied towards *E. coli* as well [79,151] (Table 13).

Table 13: Carbohydrate conjugate vaccines targeting *Escherichia coli*

Carrier type	Carrier	Antigen	Chemistry	References
Semi synthetic	Tetanus toxoid, Shiga toxin 1b subunit (Stx1b) and <i>S. aureus</i> alpha-hemolysin (Hla H35L)	Synthetic penta- and nona-β-(1->6)-d-glucosamine (PNAG)	Thiol-maleimide	Gening et al. 2021 [151]
Bioconjugate	<i>P. aeruginosa</i> exotoxin A	<i>E. coli</i> O25B	Bioconjugation	Kowarik et al. 2021 [146]
Bioconjugate	<i>P. aeruginosa</i> exotoxin A	O1, O2, O4, O6, O8, O15, O16, O18, O25 and O75	Bioconjugation	Saade et al. 2020 [169]
Bioconjugate	<i>P. aeruginosa</i> exotoxin A	<i>E. coli</i> O2, O6A and O25B	Bioconjugation	Nicolardi et al. [72]
Bioconjugate	<i>E. coli</i> OMV	Poly-N-acyl-d-glucosamine (rPNAG)	Bioconjugation	Stevenson et al. 2018 [79]

Discussion

Recent developments regarding six selected carriers and their applications are described in the field of conjugate vaccines. OMVs provide a very diverse and flexible platform for the construction of new conjugate vaccines (Table 1). For OMV specifically, we find that there are only a few pathogens used in current approaches for the extraction of OMVs; *Salmonella*, *Shigella* and *Neisseria*. For the future, it is important, with respect to CIES, to include the plethora of other pathogens from which OMVs can be produced [62]: e.g., *A. baumannii* [170], *Bordetella pertussis* [171], *Borrelia burgdorferi* [172], *H. pylori* [173], *K. pneumoniae* [174] and *P. aeruginosa* [175]. Glycoengineered OMVs and proteins go beyond the traditionally extracted OMVs as a carrier. The *in vivo* conjugation of specific antigens elaborates more on combinations of different pathogens and targets for vaccination (Table 2). The well-known PGCT and OTase-combined expression systems have great potential for new conjugate vaccine development. Whereas less unit operations are required for processing and conjugation of carrier and antigen, heterogeneity of these bioconjugates remains a challenge [72,73]. One direct solution for preventing such heterogeneity would be the more elaborate production of conjugates from individual carrier proteins and synthetically produced oligosaccharides (Table 3). In the field, a lot of progress is made towards synthetically designed oligosaccharides as a replacement for extracted oligosaccharides, aiding in better-controlled production processes [176]. The trade-off between bioconjugation and synthetic oligosaccharide

conjugation lies between bioconjugation-related heterogeneity and sometimes longer development times for synthetic oligosaccharides. Other nanoparticles, such as VLPs and protein nanocages, are also studied in the field (Tables 4 and 5). VLPs can be decorated with different antigens in the form of peptides, proteins, or CPS either through protein display or chemical conjugation. There is a clear advantage for VLPs with the absence of infectivity compared to traditional inactivated viruses and associated risks. Both the full potential of VLPs and protein nanocages as carriers are not yet obvious, with limited variation in the carrier–antigen combinations actively pursued in the field at this time. Synthetically manufactured peptides are finding their application in the cancer field, but also for infectious diseases (Table 6). The main advantage of peptides is that they can be easily designed and manufactured at a large scale and at very high purities with conjugation-ready reactive groups. Additionally, they can be employed both as a carrier and an antigen, used as an adjuvant and provide a specific B- or T-cell-mediated immune response. Peptides might be considered one of the highest potentials in fast vaccine design which could aid in new developments.

With the exciting developments in new carrier proteins, we looked further into the field of vaccination and current and future challenges. With increasing multi-drug-resistant strains in the field of AMR, it cannot be overstated that this can be classified as the new (silent) pandemic [134, 135]. With the WHO- and CDC-listed ESKAPE pathogens (Table 7), one would urge the development of new vaccines for each of these specific bacteria. Concentrating on recent developments it shows that more examples of the design of synthetic oligosaccharides against the ESKAPE pathogens are found than conjugate vaccines as a whole. Nevertheless, there are, however limited, multiple examples for each of the six pathogens (Tables 8–13). While other new carrier proteins are described in this review, their application in the field of ESKAPE pathogens is not obvious. The bioconjugates excluded, it is striking to see that most of the carriers still consist of CRM197 and also TT, which will not be beneficial towards CIES and the effectiveness of newly designed vaccines. When looking at those examples provided, it can be concluded that there are multiple promising vaccine candidates that show favorable preclinical results and provide proof-of-concept for all six ESKAPE pathogens.

Conclusion

A large influx of new vaccines has been achieved through the use of conjugation strategies. Many conjugate vaccines are developed to prevent infections and diseases. Because of carrier-induced epitope suppression and many AMR targets, traditional carrier proteins, such as TT, DT, CRM197, PD and OMPC, cannot always be used [177]. New carriers

will help the development of conjugate vaccines. These carriers can be derived from many different organisms or be produced synthetically and contribute to increased protection against diseases. These carriers will have to be evaluated extensively by physicochemical and immunological methods in combination with the antigen. Looking at recent developments and the data provided in this review, we conclude that all six types of carriers have promising potential. With respect to conjugate vaccines, it was not surprising to find a wide array of new carriers and vaccine candidates to battle different diseases including ESKAPE pathogens. With the lessons learned from Covid-19 and the introduction of mRNA vaccines, we would expect that both vaccine platforms (conjugate and mRNA vaccines) co-exist with conjugate vaccines in the developments to battle ESKAPE pathogens. New vaccine candidates are needed soon to combat infectious diseases.

2

Perspective

Conjugate vaccines have proven their application in preventing disease and providing protection through eliciting functional antibodies against infectious diseases. The introduction of new carriers is crucial to provide ample versatility and choice to target particular diseases and AMR targets specifically. It can be expected that the new carriers currently under investigation find their way to clinical trials. Reliable and large-scale production processes of these carriers will be developed within the coming years.

Improvements in the availability and quality of existing polysaccharide antigens for vaccination will largely depend on two platforms. Both bioconjugation and synthetically manufactured polysaccharides show the most potential. Bioconjugation and synthetic routes have their downsides but both platforms eliminate the need for tedious extraction and purification of polysaccharides. As such more reliable and consistently produced bioconjugates will become available. Additionally, new routes for the large-scale production of synthetic oligosaccharides will become available but will have to be financially evaluated in terms of cost-effectiveness. Recent advances in carbohydrate-based antigens and new carriers are currently available. They will enable the swift design of new glycoconjugates targeting AMR and other vaccine-preventable diseases. Lastly, we expect the development of conjugate vaccines in the fight against cancer and neurodegenerative diseases.

Acknowledgments

Figure 1 and 4 were created using Biorender.com, accessed on 05 December 2022.

Author Contributions

Conceptualization, R.M.F.v.d.P., B.M. and R.J.P.; investigation, R.M.F.v.d.P.; writing—original draft preparation, R.M.F.v.d.P.; writing—review and editing, R.M.F.v.d.P., B.M. and R.J.P.; supervision, B.M. and R.J.P. All authors have read and agreed to the published version of the manuscript.

Funding

This research received no external funding.

Conflicts of Interest

The authors declare no conflicts of interest.

References

1. CDC. History of Smallpox. Available online: <https://www.cdc.gov/smallpox/history/history.html> (accessed on September 29th 2022).
2. Avery, O.T.; Goebel, W.F. Chemo-Immunological Studies on Conjugated Carbohydrate-Proteins : Ii. Immunological Specificity of Synthetic Sugar-Protein Antigens. *J Exp Med* 1929, 50, 533-550, doi:10.1084/jem.50.4.533.
3. Schneerson, R.; Robbins, J.B.; Parke, J.C., Jr.; Bell, C.; Schlesselman, J.J.; Sutton, A.; Wang, Z.; Schiffman, G.; Karpas, A.; Shiloach, J. Quantitative and qualitative analyses of serum antibodies elicited in adults by Haemophilus influenzae type b and pneumococcus type 6A capsular polysaccharide-tetanus toxoid conjugates. *Infect Immun* 1986, 52, 519-528.
4. Schneerson, R.; Robbins, J.B.; Barrera, O.; Sutton, A.; Habig, W.B.; Hardegree, M.C.; Chaimovich, J. Haemophilus influenzae type B polysaccharide-protein conjugates: model for a new generation of capsular polysaccharide vaccines. *Prog Clin Biol Res* 1980, 47, 77-94.
5. Pollard, A.J.; Perrett, K.P.; Beverley, P.C. Maintaining protection against invasive bacteria with protein-polysaccharide conjugate vaccines. *Nat Rev Immunol* 2009, 9, 213-220, doi:10.1038/nri2494.
6. Kelly, D.F.; Pollard, A.J.; Moxon, E.R. Immunological memory: the role of B cells in long-term protection against invasive bacterial pathogens. *JAMA* 2005, 294, 3019-3023, doi:10.1001/jama.294.23.3019.
7. Frasch, C.E. Preparation of bacterial polysaccharide-protein conjugates: analytical and manufacturing challenges. *Vaccine* 2009, 27, 6468-6470, doi:10.1016/j.vaccine.2009.06.013.
8. Knuf, M.; Kowalzik, F.; Kieninger, D. Comparative effects of carrier proteins on vaccine-induced immune response. *Vaccine* 2011, 29, 4881-4890, doi:10.1016/j.vaccine.2011.04.053.
9. Peltola, H.; Kayhty, H.; Sivonen, A.; Makela, H. Haemophilus influenzae type b capsular polysaccharide vaccine in children: a double-blind field study of 100,000 vaccinees 3 months to 5 years of age in Finland. *Pediatrics* 1977, 60, 730-737.
10. Koskela, M.; Leinonen, M.; Haiva, V.M.; Timonen, M.; Makela, P.H. First and second dose antibody responses to pneumococcal polysaccharide vaccine in infants. *Pediatr Infect Dis* 1986, 5, 45-50, doi:10.1097/00006454-198601000-00009.
11. Costantino, P.; Rappuoli, R.; Berti, F. The design of semi-synthetic and synthetic glycoconjugate vaccines.

- Expert Opin Drug Discov 2011, 6, 1045-1066, doi:10.1517/17460441.2011.609554.
12. Pichichero, M.E. Protein carriers of conjugate vaccines: characteristics, development, and clinical trials. *Hum Vaccin Immunother* 2013, 9, 2505-2523, doi:10.4161/hv.26109.
 13. Broker, M.; Berti, F.; Schneider, J.; Vojtek, I. Polysaccharide conjugate vaccine protein carriers as a "neglected valency" - Potential and limitations. *Vaccine* 2017, 35, 3286-3294, doi:10.1016/j.vaccine.2017.04.078.
 14. Schutze, M.P.; Leclerc, C.; Vogel, F.R.; Chedid, L. Epitopic suppression in synthetic vaccine models: analysis of the effector mechanisms. *Cell Immunol* 1987, 104, 79-90, doi:10.1016/0008-8749(87)90008-6.
 15. Herzenberg, L.A.; Tokuhisa, T.; Herzenberg, L.A. Carrier-priming leads to hapten-specific suppression. *Nature* 1980, 285, 664-667, doi:10.1038/285664a0.
 16. Barington, T.; Kristensen, K.; Henriksen, J.; Heilmann, C. Influence of prevaccination immunity on the human B-lymphocyte response to a *Haemophilus influenzae* type b conjugate vaccine. *Infect Immun* 1991, 59, 1057-1064, doi:10.1128/iai.59.3.1057-1064.1991.
 17. Dagan, R.; Eskola, J.; Leclerc, C.; Leroy, O. Reduced response to multiple vaccines sharing common protein epitopes that are administered simultaneously to infants. *Infect Immun* 1998, 66, 2093-2098, doi:10.1128/IAI.66.5.2093-2098.1998.
 18. Dagan, R.; Poolman, J.; Siegrist, C.A. Glycoconjugate vaccines and immune interference: A review. *Vaccine* 2010, 28, 5513-5523, doi:10.1016/j.vaccine.2010.06.026.
 19. Giannini, G.; Rappuoli, R.; Ratti, G. The amino-acid sequence of two non-toxic mutants of diphtheria toxin: CRM45 and CRM197. *Nucleic Acids Res* 1984, 12, 4063-4069, doi:10.1093/nar/12.10.4063.
 20. Broker, M.; Costantino, P.; DeTora, L.; McIntosh, E.D.; Rappuoli, R. Biochemical and biological characteristics of cross-reacting material 197 CRM197, a non-toxic mutant of diphtheria toxin: use as a conjugation protein in vaccines and other potential clinical applications. *Biologicals* 2011, 39, 195-204, doi:10.1016/j.biologicals.2011.05.004.
 21. Shinefield, H.R. Overview of the development and current use of CRM(197) conjugate vaccines for pediatric use. *Vaccine* 2010, 28, 4335-4339, doi:10.1016/j.vaccine.2010.04.072.
 22. Forsgren, A.; Riesbeck, K.; Janson, H. Protein D of *Haemophilus influenzae*: a protective nontypeable *H. influenzae* antigen and a carrier for pneumococcal conjugate vaccines. *Clin Infect Dis* 2008, 46, 726-731, doi:10.1086/527396.
 23. Prymula, R.; Peeters, P.; Chrobok, V.; Kriz, P.; Novakova, E.; Kaliskova, E.; Kohl, I.; Lommel, P.; Poolman, J.; Prieels, J.P.; et al. Pneumococcal capsular polysaccharides conjugated to protein D for prevention of acute otitis media caused by both *Streptococcus pneumoniae* and non-typable *Haemophilus influenzae*: a randomised double-blind efficacy study. *Lancet* 2006, 367, 740-748, doi:10.1016/S0140-6736(06)68304-9.
 24. Donnelly, J.J.; Deck, R.R.; Liu, M.A. Immunogenicity of a *Haemophilus influenzae* polysaccharide-*Neisseria meningitidis* outer membrane protein complex conjugate vaccine. *J Immunol* 1990, 145, 3071-3079.
 25. Kilpi, T.; Ahman, H.; Jokinen, J.; Lankinen, K.S.; Palmu, A.; Savolainen, H.; Gronholm, M.; Leinonen, M.; Hovi, T.; Eskola, J.; et al. Protective efficacy of a second pneumococcal conjugate vaccine against pneumococcal acute otitis media in infants and children: randomized, controlled trial of a 7-valent pneumococcal polysaccharide-meningococcal outer membrane protein complex conjugate vaccine in 1666 children. *Clin Infect Dis* 2003, 37, 1155-1164, doi:10.1086/378744.
 26. Micoli, F.; Adamo, R.; Costantino, P. Protein Carriers for Glycoconjugate Vaccines: History, Selection Criteria, Characterization and New Trends. *Molecules* 2018, 23, doi:10.3390/molecules23061451.
 27. Cryz, S.J., Jr.; Cross, A.S.; Sadoff, J.C.; Wegmann, A.; Que, J.U.; Furer, E. Safety and immunogenicity of *Escherichia coli* O18 O-specific polysaccharide (O-PS)-toxin A and O-PS-cholera toxin conjugate vaccines in humans. *J Infect Dis* 1991, 163, 1040-1045, doi:10.1093/infdis/163.5.1040.
 28. Cross, A.; Artenstein, A.; Que, J.; Fredeking, T.; Furer, E.; Sadoff, J.C.; Cryz, S.J., Jr. Safety and immunogenicity of a polyvalent *Escherichia coli* vaccine in human volunteers. *J Infect Dis* 1994, 170, 834-840, doi:10.1093/infdis/170.4.834.
 29. Kossaczka, Z.; Lin, F.Y.; Ho, V.A.; Thuy, N.T.; Van Bay, P.; Thanh, T.C.; Khiem, H.B.; Trach, D.D.; Karpas, A.; Hunt, S.; et al. Safety and immunogenicity of Vi conjugate vaccines for typhoid fever in adults, teenagers, and 2- to 4-year-old children in Vietnam. *Infect Immun* 1999, 67, 5806-5810, doi:10.1128/IAI.67.11.5806-5810.1999.

- 2
30. Fattom, A.; Schneerson, R.; Watson, D.C.; Karakawa, W.W.; Fitzgerald, D.; Pastan, I.; Li, X.; Shiloach, J.; Bryla, D.A.; Robbins, J.B. Laboratory and clinical evaluation of conjugate vaccines composed of *Staphylococcus aureus* type 5 and type 8 capsular polysaccharides bound to *Pseudomonas aeruginosa* recombinant exoprotein A. *Infect Immun* 1993, 61, 1023-1032, doi:10.1128/iai.61.3.1023-1032.1993.
 31. Cohen, D.; Ashkenazi, S.; Green, M.S.; Gdalevich, M.; Robin, G.; Slepion, R.; Yavzori, M.; Orr, N.; Block, C.; Ashkenazi, I.; et al. Double-blind vaccine-controlled randomised efficacy trial of an investigational *Shigella sonnei* conjugate vaccine in young adults. *Lancet* 1997, 349, 155-159, doi:10.1016/S0140-6736(96)06255-1.
 32. Szu, S.C.; Stone, A.L.; Robbins, J.D.; Schneerson, R.; Robbins, J.B. Vi capsular polysaccharide-protein conjugates for prevention of typhoid fever. Preparation, characterization, and immunogenicity in laboratory animals. *J Exp Med* 1987, 166, 1510-1524, doi:10.1084/jem.166.5.1510.
 33. Tontini, M.; Romano, M.R.; Proietti, D.; Balducci, E.; Micoli, F.; Balocchi, C.; Santini, L.; Massignani, V.; Berti, F.; Costantino, P. Preclinical studies on new proteins as carrier for glycoconjugate vaccines. *Vaccine* 2016, 34, 4235-4242, doi:10.1016/j.vaccine.2016.06.039.
 34. Falugi, F.; Petracca, R.; Mariani, M.; Luzzi, E.; Mancianti, S.; Carinci, V.; Melli, M.L.; Finco, O.; Wack, A.; Di Tommaso, A.; et al. Rationally designed strings of promiscuous CD4(+) T cell epitopes provide help to *Haemophilus influenzae* type b oligosaccharide: a model for new conjugate vaccines. *Eur J Immunol* 2001, 31, 3816-3824, doi:10.1002/1521-4141(200112)31:12<3816::AID-IMMU3816>3.0.CO;2-K.
 35. Baraldo, K.; Mori, E.; Bartoloni, A.; Norelli, F.; Grandi, G.; Rappuoli, R.; Finco, O.; Del Giudice, G. Combined conjugate vaccines: enhanced immunogenicity with the N19 polyepitope as a carrier protein. *Infect Immun* 2005, 73, 5835-5841, doi:10.1128/IAI.73.9.5835-5841.2005.
 36. Bongat, A.F.; Saksena, R.; Adamo, R.; Fujimoto, Y.; Shiokawa, Z.; Peterson, D.C.; Fukase, K.; Vann, W.F.; Kovac, P. Multimeric bivalent immunogens from recombinant tetanus toxin HC fragment, synthetic hexasaccharides, and a glycopeptide adjuvant. *Glycoconj J* 2010, 27, 69-77, doi:10.1007/s10719-009-9259-4.
 37. Xin, H.; Dziadek, S.; Bundle, D.R.; Cutler, J.E. Synthetic glycopeptide vaccines combining beta-mannan and peptide epitopes induce protection against candidiasis. *Proc Natl Acad Sci U S A* 2008, 105, 13526-13531, doi:10.1073/pnas.0803195105.
 38. Rothbard, J.B.; Taylor, W.R. A sequence pattern common to T cell epitopes. *EMBO J* 1988, 7, 93-100, doi:10.1002/j.1460-2075.1988.tb02787.x.
 39. Ingale, S.; Wolfert, M.A.; Gaekwad, J.; Buskas, T.; Boons, G.J. Robust immune responses elicited by a fully synthetic three-component vaccine. *Nat Chem Biol* 2007, 3, 663-667, doi:10.1038/nchembio.2007.25.
 40. Bixler, G.S., Jr.; Eby, R.; Dermody, K.M.; Woods, R.M.; Seid, R.C.; Pillai, S. Synthetic peptide representing a T-cell epitope of CRM197 substitutes as carrier molecule in a *Haemophilus influenzae* type B (Hib) conjugate vaccine. *Adv Exp Med Biol* 1989, 251, 175-180, doi:10.1007/978-1-4757-2046-4_15.
 41. Belot, F.; Guerreiro, C.; Baleux, F.; Mulard, L.A. Synthesis of two linear PADRE conjugates bearing a deca- or pentadecasaccharide B epitope as potential synthetic vaccines against *Shigella flexneri* serotype 2a infection. *Chemistry* 2005, 11, 1625-1635, doi:10.1002/chem.200400903.
 42. Alexander, J.; del Guercio, M.F.; Maewal, A.; Qiao, L.; Fikes, J.; Chesnut, R.W.; Paulson, J.; Bundle, D.R.; DeFrees, S.; Sette, A. Linear PADRE T helper epitope and carbohydrate B cell epitope conjugates induce specific high titer IgG antibody responses. *J Immunol* 2000, 164, 1625-1633, doi:10.4049/jimmunol.164.3.1625.
 43. Alexander, J.; del Guercio, M.F.; Frame, B.; Maewal, A.; Sette, A.; Nahm, M.H.; Newman, M.J. Development of experimental carbohydrate-conjugate vaccines composed of *Streptococcus pneumoniae* capsular polysaccharides and the universal helper T-lymphocyte epitope (PADRE). *Vaccine* 2004, 22, 2362-2367, doi:10.1016/j.vaccine.2003.11.061.
 44. Michon, F.; Fusco, P.C.; Minetti, C.A.; Laude-Sharp, M.; Uitz, C.; Huang, C.H.; D'Ambra, A.J.; Moore, S.; Remeta, D.P.; Heron, I.; et al. Multivalent pneumococcal capsular polysaccharide conjugate vaccines employing genetically detoxified pneumolysin as a carrier protein. *Vaccine* 1998, 16, 1732-1741, doi:10.1016/s0264-410x(98)00225-4.
 45. Pozzi, C.; Wilk, K.; Lee, J.C.; Gening, M.; Nifantiev, N.; Pier, G.B. Opsonic and protective properties of antibodies raised to conjugate vaccines targeting six *Staphylococcus aureus* antigens. *PLoS One* 2012, 7,

- e46648, doi:10.1371/journal.pone.0046648.
46. Romano, M.R.; Leuzzi, R.; Cappelletti, E.; Tontini, M.; Nilo, A.; Proietti, D.; Berti, F.; Costantino, P.; Adamo, R.; Scarselli, M. Recombinant *Clostridium difficile* toxin fragments as carrier protein for PSII surface polysaccharide preserve their neutralizing activity. *Toxins (Basel)* 2014, 6, 1385-1396, doi:10.3390/toxins6041385.
 47. Nilo, A.; Morelli, L.; Passalacqua, I.; Brogioni, B.; Allan, M.; Carboni, F.; Pezzicoli, A.; Zerbini, F.; Maione, D.; Fabbrini, M.; et al. Anti-Group B *Streptococcus* Glycan-Conjugate Vaccines Using Pilus Protein GBS80 As Carrier and Antigen: Comparing Lysine and Tyrosine-directed Conjugation. *ACS Chem Biol* 2015, 10, 1737-1746, doi:10.1021/acschembio.5b00247.
 48. Nilo, A.; Passalacqua, I.; Fabbrini, M.; Allan, M.; Usera, A.; Carboni, F.; Brogioni, B.; Pezzicoli, A.; Cobb, J.; Romano, M.R.; et al. Exploring the Effect of Conjugation Site and Chemistry on the Immunogenicity of an anti-Group B *Streptococcus* Glycoconjugate Vaccine Based on GBS67 Pilus Protein and Type V Polysaccharide. *Bioconjug Chem* 2015, 26, 1839-1849, doi:10.1021/acs.bioconjchem.5b00365.
 49. Simon, R.; Tennant, S.M.; Wang, J.Y.; Schmidlein, P.J.; Lees, A.; Ernst, R.K.; Pasetti, M.F.; Galen, J.E.; Levine, M.M. *Salmonella enterica* serovar enteritidis core O polysaccharide conjugated to H:g,m flagellin as a candidate vaccine for protection against invasive infection with *S. enteritidis*. *Infect Immun* 2011, 79, 4240-4249, doi:10.1128/IAI.05484-11.
 50. Wang, L.X. Synthetic carbohydrate antigens for HIV vaccine design. *Curr Opin Chem Biol* 2013, 17, 997-1005, doi:10.1016/j.cbpa.2013.10.001.
 51. Polonskaya, Z.; Deng, S.; Sarkar, A.; Kain, L.; Comellas-Aragones, M.; McKay, C.S.; Kaczanowska, K.; Holt, M.; McBride, R.; Palomo, V.; et al. T cells control the generation of nanomolar-affinity anti-glycan antibodies. *J Clin Invest* 2017, 127, 1491-1504, doi:10.1172/JCI91192.
 52. Valguarnera, E.; Feldman, M.F. Glycoengineered Outer Membrane Vesicles as a Platform for Vaccine Development. *Methods Enzymol* 2017, 597, 285-310, doi:10.1016/bs.mie.2017.06.032.
 53. Micoli, F.; Alfini, R.; Di Benedetto, R.; Necchi, F.; Schiavo, F.; Mancini, F.; Carducci, M.; Palmieri, E.; Balocchi, C.; Gasperini, G.; et al. GMMMA Is a Versatile Platform to Design Effective Multivalent Combination Vaccines. *Vaccines (Basel)* 2020, 8, doi:10.3390/vaccines8030540.
 54. Jan, A.T. Outer Membrane Vesicles (OMVs) of Gram-negative Bacteria: A Perspective Update. *Front Microbiol* 2017, 8, 1053, doi:10.3389/fmicb.2017.01053.
 55. Launay, O.; Lewis, D.J.M.; Anemona, A.; Loulergue, P.; Leahy, J.; Scire, A.S.; Maugard, A.; Marchetti, E.; Zancan, S.; Huo, Z.; et al. Safety Profile and Immunologic Responses of a Novel Vaccine Against *Shigella sonnei* Administered Intramuscularly, Intradermally and Intranasally: Results From Two Parallel Randomized Phase 1 Clinical Studies in Healthy Adult Volunteers in Europe. *EBioMedicine* 2017, 22, 164-172, doi:10.1016/j.ebiom.2017.07.013.
 56. de Kleijn, E.D.; de Groot, R.; Labadie, J.; Lafeber, A.B.; van den Dobbelaars, G.; van Alphen, L.; van Dijken, H.; Kuipers, B.; van Omme, G.W.; Wala, M.; et al. Immunogenicity and safety of a hexavalent meningococcal outer-membrane-vesicle vaccine in children of 2-3 and 7-8 years of age. *Vaccine* 2000, 18, 1456-1466, doi:10.1016/s0264-410x(99)00423-5.
 57. Cartwright, K.; Morris, R.; Rumke, H.; Fox, A.; Borrow, R.; Begg, N.; Richmond, P.; Poolman, J. Immunogenicity and reactogenicity in UK infants of a novel meningococcal vesicle vaccine containing multiple class 1 (PorA) outer membrane proteins. *Vaccine* 1999, 17, 2612-2619, doi:10.1016/s0264-410x(99)00044-4.
 58. Skidmore, B.J.; Chiller, J.M.; Morrison, D.C.; Weigle, W.O. Immunologic properties of bacterial lipopolysaccharide (LPS): correlation between the mitogenic, adjuvant, and immunogenic activities. *J Immunol* 1975, 114, 770-775.
 59. Liu, Y.; Hammer, L.A.; Liu, W.; Hobbs, M.M.; Zielke, R.A.; Sikora, A.E.; Jerse, A.E.; Egilmez, N.K.; Russell, M.W. Experimental vaccine induces Th1-driven immune responses and resistance to *Neisseria gonorrhoeae* infection in a murine model. *Mucosal Immunol* 2017, 10, 1594-1608, doi:10.1038/mi.2017.11.
 60. Lehmann, A.K.; Halstensen, A.; Aaberge, I.S.; Holst, J.; Michaelsen, T.E.; Sornes, S.; Wetzler, L.M.; Guttormsen, H. Human opsonins induced during meningococcal disease recognize outer membrane proteins PorA and PorB. *Infect Immun* 1999, 67, 2552-2560, doi:10.1128/IAI.67.5.2552-2560.1999.

61. Bachmann, M.F.; Jennings, G.T. Vaccine delivery: a matter of size, geometry, kinetics and molecular patterns. *Nat Rev Immunol* 2010, 10, 787-796, doi:10.1038/nri2868.
62. van der Pol, L.; Stork, M.; van der Ley, P. Outer membrane vesicles as platform vaccine technology. *Biotechnol J* 2015, 10, 1689-1706, doi:10.1002/biot.201400395.
63. Gerritzen, M.J.H.; Salverda, M.L.M.; Martens, D.E.; Wijffels, R.H.; Stork, M. Spontaneously released *Neisseria meningitidis* outer membrane vesicles as vaccine platform: production and purification. *Vaccine* 2019, 37, 6978-6986, doi:10.1016/j.vaccine.2019.01.076.
64. Micoli, F.; Alfini, R.; Di Benedetto, R.; Necchi, F.; Schiavo, F.; Mancini, F.; Carducci, M.; Oldrini, D.; Pitirollo, O.; Gasperini, G.; et al. Generalized Modules for Membrane Antigens as Carrier for Polysaccharides: Impact of Sugar Length, Density, and Attachment Site on the Immune Response Elicited in Animal Models. *Front Immunol* 2021, 12, 719315, doi:10.3389/fimmu.2021.719315.
65. Palmieri, E.; Kis, Z.; Ozanne, J.; Di Benedetto, R.; Ricchetti, B.; Massai, L.; Carducci, M.; Oldrini, D.; Gasperini, G.; Aruta, M.G.; et al. GMMA as an Alternative Carrier for a Glycoconjugate Vaccine against Group A *Streptococcus*. *Vaccines (Basel)* 2022, 10, doi:10.3390/vaccines10071034.
66. Jiang, L.; Driedonks, T.A.P.; Jong, W.S.P.; Dhakal, S.; Bart van den Berg van Saparoea, H.; Sitaras, I.; Zhou, R.; Caputo, C.; Littlefield, K.; Lowman, M.; et al. A bacterial extracellular vesicle-based intranasal vaccine against SARS-CoV-2 protects against disease and elicits neutralizing antibodies to wild-type and Delta variants. *J Extracell Vesicles* 2022, 11, e12192, doi:10.1002/jev2.12192.
67. Di Benedetto, R.; Alfini, R.; Carducci, M.; Aruta, M.G.; Lanzilao, L.; Acquaviva, A.; Palmieri, E.; Giannelli, C.; Necchi, F.; Saul, A.; et al. Novel Simple Conjugation Chemistries for Decoration of GMMA with Heterologous Antigens. *Int J Mol Sci* 2021, 22, doi:10.3390/ijms221910180.
68. Scaria, P.V.; Rowe, C.G.; Chen, B.B.; Muratova, O.V.; Fischer, E.R.; Barnafo, E.K.; Anderson, C.F.; Zaidi, I.U.; Lambert, L.E.; Lucas, B.J.; et al. Outer membrane protein complex as a carrier for malaria transmission blocking antigen Pfs230. *NPJ Vaccines* 2019, 4, 24, doi:10.1038/s41541-019-0121-9.
69. Langdon, R.H.; Cuccui, J.; Wren, B.W. N-linked glycosylation in bacteria: an unexpected application. *Future Microbiol* 2009, 4, 401-412, doi:10.2217/fmb.09.10.
70. Kay, E.; Cuccui, J.; Wren, B.W. Recent advances in the production of recombinant glycoconjugate vaccines. *NPJ Vaccines* 2019, 4, 16, doi:10.1038/s41541-019-0110-z.
71. Wacker, M.; Linton, D.; Hitchen, P.G.; Nita-Lazar, M.; Haslam, S.M.; North, S.J.; Panico, M.; Morris, H.R.; Dell, A.; Wren, B.W.; et al. N-linked glycosylation in *Campylobacter jejuni* and its functional transfer into *E. coli*. *Science* 2002, 298, 1790-1793, doi:10.1126/science.298.5599.1790.
72. Nicolardi, S.; Danuser, R.; Dotz, V.; Dominguez-Vega, E.; Al Kaabi, A.; Beurret, M.; Anish, C.; Wuhrer, M. Glycan and Protein Analysis of Glycoengineered Bacterial *E. coli* Vaccines by MALDI-in-Source Decay FT-ICR Mass Spectrometry. *Anal Chem* 2022, 94, 4979-4987, doi:10.1021/acs.analchem.1c04690.
73. MacCalman, T.E.; Phillips-Jones, M.K.; Harding, S.E. Glycoconjugate vaccines: some observations on carrier and production methods. *Biotechnol Genet Eng Rev* 2019, 35, 93-125, doi:10.1080/02648725.2019.1703614.
74. Harding, C.M.; Nasr, M.A.; Scott, N.E.; Goyette-Desjardins, G.; Nothaft, H.; Mayer, A.E.; Chavez, S.M.; Huynh, J.P.; Kinsella, R.L.; Szymanski, C.M.; et al. A platform for glycoengineering a polyvalent pneumococcal bioconjugate vaccine using *E. coli* as a host. *Nat Commun* 2019, 10, 891, doi:10.1038/s41467-019-08869-9.
75. Martin, P.; Alaimo, C. The Ongoing Journey of a *Shigella* Bioconjugate Vaccine. *Vaccines (Basel)* 2022, 10, doi:10.3390/vaccines10020212.
76. Ravenscroft, N.; Braun, M.; Schneider, J.; Dreyer, A.M.; Wetter, M.; Haeuptle, M.A.; Kemmler, S.; Steffen, M.; Sirena, D.; Herwig, S.; et al. Characterization and immunogenicity of a *Shigella flexneri* 2a O-antigen bioconjugate vaccine candidate. *Glycobiology* 2019, 29, 669-680, doi:10.1093/glycob/cwz044.
77. Feldman, M.F.; Mayer Bridwell, A.E.; Scott, N.E.; Vinogradov, E.; McKee, S.R.; Chavez, S.M.; Twentyman, J.; Stallings, C.L.; Rosen, D.A.; Harding, C.M. A promising bioconjugate vaccine against hypervirulent *Klebsiella pneumoniae*. *Proc Natl Acad Sci U S A* 2019, 116, 18655-18663, doi:10.1073/pnas.1907833116.
78. Reglinski, M.; Ercoli, G.; Plumptre, C.; Kay, E.; Petersen, F.C.; Paton, J.C.; Wren, B.W.; Brown, J.S. A recombinant conjugated pneumococcal vaccine that protects against murine infections with a similar efficacy to

- Prevnar-13. *NPJ Vaccines* 2018, 3, 53, doi:10.1038/s41541-018-0090-4.
79. Stevenson, T.C.; Cywes-Bentley, C.; Moeller, T.D.; Weyant, K.B.; Putnam, D.; Chang, Y.F.; Jones, B.D.; Pier, G.B.; DeLisa, M.P. Immunization with outer membrane vesicles displaying conserved surface polysaccharide antigen elicits broadly antimicrobial antibodies. *Proc Natl Acad Sci U S A* 2018, 115, E3106-E3115, doi:10.1073/pnas.1718341115.
80. Sun, P.; Pan, C.; Zeng, M.; Liu, B.; Liang, H.; Wang, D.; Liu, X.; Wang, B.; Lyu, Y.; Wu, J.; et al. Design and production of conjugate vaccines against *S. Paratyphi A* using an O-linked glycosylation system in vivo. *NPJ Vaccines* 2018, 3, 4, doi:10.1038/s41541-017-0037-1.
81. Marshall, L.E.; Nelson, M.; Davies, C.H.; Whelan, A.O.; Jenner, D.C.; Moule, M.G.; Denman, C.; Cuccui, J.; Atkins, T.P.; Wren, B.W.; et al. An O-Antigen Glycoconjugate Vaccine Produced Using Protein Glycan Coupling Technology Is Protective in an Inhalational Rat Model of Tularemia. *J Immunol Res* 2018, 2018, 8087916, doi:10.1155/2018/8087916.
82. Wang, S.; Zhao, Y.; Wang, G.; Feng, S.; Guo, Z.; Gu, G. Group A Streptococcus Cell Wall Oligosaccharide-Streptococcal C5a Peptidase Conjugates as Effective Antibacterial Vaccines. *ACS Infect Dis* 2020, 6, 281-290, doi:10.1021/acsinfectdis.9b00347.
83. Wang, G.; Zhao, J.; Zhao, Y.; Wang, S.; Feng, S.; Gu, G. Immunogenicity Assessment of Different Segments and Domains of Group A Streptococcal C5a Peptidase and Their Application Potential as Carrier Protein for Glycoconjugate Vaccine Development. *Vaccines (Basel)* 2021, 9, doi:10.3390/vaccines9020139.
84. Kapoor, N.; Uchiyama, S.; Pill, L.; Bautista, L.; Sedra, A.; Yin, L.; Regan, M.; Chu, E.; Rabara, T.; Wong, M.; et al. Non-Native Amino Acid Click Chemistry-Based Technology for Site-Specific Polysaccharide Conjugation to a Bacterial Protein Serving as Both Carrier and Vaccine Antigen. *ACS Omega* 2022, 7, 24111-24120, doi:10.1021/acsomega.1c07360.
85. Romero-Saavedra, F.; Laverde, D.; Kalfopoulou, E.; Martini, C.; Torelli, R.; Martinez-Matamoros, D.; Sanguinetti, M.; Huebner, J. Conjugation of Different Immunogenic Enterococcal Vaccine Target Antigens Leads to Extended Strain Coverage. *J Infect Dis* 2019, 220, 1589-1598, doi:10.1093/infdis/jiz357.
86. Chang, M.J.; Ollivault-Shiflett, M.; Schuman, R.; Ngoc Nguyen, S.; Kaltashov, I.A.; Bobst, C.; Rajagopal, S.P.; Przedpelski, A.; Barbieri, J.T.; Lees, A. Genetically detoxified tetanus toxin as a vaccine and conjugate carrier protein. *Vaccine* 2022, 40, 5103-5113, doi:10.1016/j.vaccine.2022.07.011.
87. Deng, Y.; Li, J.; Sun, C.; Chi, H.; Luo, D.; Wang, R.; Qiu, H.; Zhang, Y.; Wu, M.; Zhang, X.; et al. Rational Development of a Polysaccharide-Protein-Conjugated Nanoparticle Vaccine Against SARS-CoV-2 Variants and Streptococcus pneumoniae. *Adv Mater* 2022, 34, e2200443, doi:10.1002/adma.202200443.
88. Park, W.J.; Yoon, Y.K.; Park, J.S.; Pansuriya, R.; Seok, Y.J.; Ganapathy, R. Rotavirus spike protein DeltaVP8* as a novel carrier protein for conjugate vaccine platform with demonstrated antigenic potential for use as bivalent vaccine. *Sci Rep* 2021, 11, 22037, doi:10.1038/s41598-021-01549-z.
89. Ahmadi, K.; Aslani, M.M.; Pouladfar, G.; Faezi, S.; Kalani, M.; Pourmand, M.R.; Ghaedi, T.; Havaei, S.A.; Mahdavi, M. Preparation and preclinical evaluation of two novel Staphylococcus aureus capsular polysaccharide 5 and 8-fusion protein (Hla-MntC-SACOL0723) immunoconjugates. *IUBMB Life* 2020, 72, 226-236, doi:10.1002/iub.2159.
90. Chiu, T.W.; Peng, C.J.; Chen, M.C.; Hsu, M.H.; Liang, Y.H.; Chiu, C.H.; Fang, J.M.; Lee, Y.C. Constructing conjugate vaccine against Salmonella Typhimurium using lipid-A free lipopolysaccharide. *J Biomed Sci* 2020, 27, 89, doi:10.1186/s12929-020-00681-8.
91. Ou, L.; Kong, W.P.; Chuang, G.Y.; Ghosh, M.; Gulla, K.; O'Dell, S.; Varriale, J.; Barefoot, N.; Changela, A.; Chao, C.W.; et al. Preclinical Development of a Fusion Peptide Conjugate as an HIV Vaccine Immunogen. *Sci Rep* 2020, 10, 3032, doi:10.1038/s41598-020-59711-y.
92. Qian, W.; Huang, Z.; Chen, Y.; Yang, J.; Wang, L.; Wu, K.; Chen, M.; Chen, N.; Duan, Y.; Shi, J.; et al. Elicitation of integrated immunity in mice by a novel pneumococcal polysaccharide vaccine conjugated with HBV surface antigen. *Sci Rep* 2020, 10, 6470, doi:10.1038/s41598-020-62185-7.
93. Yang, G.J.; Yang, Y.; Shaddeau, A.; Cai, C.X.; Li, Y.; Gulla, K.; Zhang, Y.; Ou, L.; Cooper, J.W.; Lei, Q.P. A unique algorithm for the determination of peptide-carrier protein conjugation ratio by amino acid analysis using intrinsic internal standard. *Vaccine* 2020, 38, 4507-4511, doi:10.1016/j.vaccine.2020.04.080.

94. An, S.J.; Scaria, P.V.; Chen, B.; Barnafo, E.; Muratova, O.; Anderson, C.; Lambert, L.; Chae, M.H.; Yang, J.S.; Duffy, P.E. Development of a bivalent conjugate vaccine candidate against malaria transmission and typhoid fever. *Vaccine* 2018, 36, 2978-2984, doi:10.1016/j.vaccine.2018.04.035.
95. Baliban, S.M.; Curtis, B.; Toema, D.; Tennant, S.M.; Levine, M.M.; Pasetti, M.F.; Simon, R. Immunogenicity and efficacy following sequential parenterally-administered doses of Salmonella Enteritidis COPS:FlIC glycoconjugates in infant and adult mice. *PLoS Negl Trop Dis* 2018, 12, e0006522, doi:10.1371/journal.pntd.0006522.
96. Baruffaldi, F.; Kelcher, A.H.; Laudenschlager, M.; Gradinati, V.; Limkar, A.; Roslawski, M.; Birnbaum, A.; Lees, A.; Hassler, C.; Runyon, S.; et al. Preclinical Efficacy and Characterization of Candidate Vaccines for Treatment of Opioid Use Disorders Using Clinically Viable Carrier Proteins. *Mol Pharm* 2018, 15, 4947-4962, doi:10.1021/acs.molpharmaceut.8b00592.
97. Laird, R.M.; Ma, Z.; Dorabawila, N.; Pequegnat, B.; Omari, E.; Liu, Y.; Maue, A.C.; Poole, S.T.; Maciel, M.; Satish, K.; et al. Evaluation of a conjugate vaccine platform against enterotoxigenic Escherichia coli (ETEC), Campylobacter jejuni and Shigella. *Vaccine* 2018, 36, 6695-6702, doi:10.1016/j.vaccine.2018.09.052.
98. Fries, C.N.; Curvino, E.J.; Chen, J.L.; Permar, S.R.; Fouda, G.G.; Collier, J.H. Advances in nanomaterial vaccine strategies to address infectious diseases impacting global health. *Nat Nanotechnol* 2021, 16, 1-14, doi:10.1038/s41565-020-0739-9.
99. Basu, R.; Zhai, L.; Contreras, A.; Tumban, E. Immunization with phage virus-like particles displaying Zika virus potential B-cell epitopes neutralizes Zika virus infection of monkey kidney cells. *Vaccine* 2018, 36, 1256-1264, doi:10.1016/j.vaccine.2018.01.056.
100. Basu, R.; Zhai, L.; Rosso, B.; Tumban, E. Bacteriophage Qbeta virus-like particles displaying Chikungunya virus B-cell epitopes elicit high-titer E2 protein antibodies but fail to neutralize a Thailand strain of Chikungunya virus. *Vaccine* 2020, 38, 2542-2550, doi:10.1016/j.vaccine.2020.01.091.
101. Warner, N.L.; Fritze, K.M. Development of Bacteriophage Virus-Like Particle Vaccines Displaying Conserved Epitopes of Dengue Virus Non-Structural Protein 1. *Vaccines (Basel)* 2021, 9, doi:10.3390/vaccines9070726.
102. Zha, L.; Chang, X.; Zhao, H.; Mohsen, M.O.; Hong, L.; Zhou, Y.; Chen, H.; Liu, X.; Zhang, J.; Li, D.; et al. Development of a Vaccine against SARS-CoV-2 Based on the Receptor-Binding Domain Displayed on Virus-Like Particles. *Vaccines (Basel)* 2021, 9, doi:10.3390/vaccines9040395.
103. Cabral-Miranda, G.; Lim, S.M.; Mohsen, M.O.; Pobelov, I.V.; Roesti, E.S.; Heath, M.D.; Skinner, M.A.; Kramer, M.F.; Martina, B.E.E.; Bachmann, M.F. Zika Virus-Derived E-DIII Protein Displayed on Immunologically Optimized VLPs Induces Neutralizing Antibodies without Causing Enhancement of Dengue Virus Infection. *Vaccines (Basel)* 2019, 7, doi:10.3390/vaccines7030072.
104. Sungsuwan, S.; Wu, X.; Shaw, V.; Kavunja, H.; McFall-Boegeman, H.; Rashidjahanabad, Z.; Tan, Z.; Lang, S.; Tahmasebi Nick, S.; Lin, P.H.; et al. Structure Guided Design of Bacteriophage Qbeta Mutants as Next Generation Carriers for Conjugate Vaccines. *ACS Chem Biol* 2022, doi:10.1021/acscchembio.1c00906.
105. Prasanna, M.; Podsiadla-Bialoskorska, M.; Mielecki, D.; Ruffier, N.; Fateh, A.; Lambert, A.; Fanuel, M.; Camberlein, E.; Szolajska, E.; Grandjean, C. On the use of adenovirus dodecahedron as a carrier for glycoconjugate vaccines. *Glycoconj J* 2021, 38, 437-446, doi:10.1007/s10719-021-09999-3.
106. Zong, G.; Toonstra, C.; Yang, Q.; Zhang, R.; Wang, L.X. Chemoenzymatic Synthesis and Antibody Binding of HIV-1 V1/V2 Glycopeptide-Bacteriophage Qbeta Conjugates as a Vaccine Candidate. *Int J Mol Sci* 2021, 22, doi:10.3390/ijms222212538.
107. Wang, P.; Huo, C.X.; Lang, S.; Caution, K.; Nick, S.T.; Dubey, P.; Deora, R.; Huang, X. Chemical Synthesis and Immunological Evaluation of a Pentasaccharide Bearing Multiple Rare Sugars as a Potential Anti-pertussis Vaccine. *Angew Chem Int Ed Engl* 2020, 59, 6451-6458, doi:10.1002/anie.201915913.
108. Xu, L.; Li, Z.; Su, Z.; Yang, Y.; Ma, G.; Yu, R.; Zhang, S. Development of meningococcal polysaccharide conjugate vaccine that can elicit long-lasting and strong cellular immune response with hepatitis B core antigen virus-like particles as a novel carrier protein. *Vaccine* 2019, 37, 956-964, doi:10.1016/j.vaccine.2018.12.073.
109. Curley, S.M.; Putnam, D. Biological Nanoparticles in Vaccine Development. *Front Bioeng Biotechnol* 2022, 10, 867119, doi:10.3389/fbioe.2022.867119.
110. Flenniken, M.L.; Uchida, M.; Liepold, L.O.; Kang, S.; Young, M.J.; Douglas, T. A library of protein cage

- architectures as nanomaterials. *Curr Top Microbiol Immunol* 2009, 327, 71-93, doi:10.1007/978-3-540-69379-6_4.
111. Chakraborti, S.; Chakrabarti, P. Self-Assembly of Ferritin: Structure, Biological Function and Potential Applications in Nanotechnology. *Adv Exp Med Biol* 2019, 1174, 313-329, doi:10.1007/978-981-13-9791-2_10.
 112. Chen, R.R.R. Development of Receptor Binding Domain (RBD)-Conjugated Nanoparticle Vaccines with Broad Neutralization against SARS-CoV-2 Delta and Other Variants. *Advanced Science* 2022, 9.
 113. Wang, W.; Zhou, X.; Bian, Y.; Wang, S.; Chai, Q.; Guo, Z.; Wang, Z.; Zhu, P.; Peng, H.; Yan, X.; et al. Dual-targeting nanoparticle vaccine elicits a therapeutic antibody response against chronic hepatitis B. *Nat Nanotechnol* 2020, 15, 406-416, doi:10.1038/s41565-020-0648-y.
 114. Zakeri, B.; Fierer, J.O.; Celik, E.; Chittock, E.C.; Schwarz-Linek, U.; Moy, V.T.; Howarth, M. Peptide tag forming a rapid covalent bond to a protein, through engineering a bacterial adhesin. *Proc Natl Acad Sci U S A* 2012, 109, E690-697, doi:10.1073/pnas.1115485109.
 115. Wei, J.; Li, Z.; Yang, Y.; Ma, G.; Su, Z.; Zhang, S. An Apoferritin-Hemagglutinin Conjugate Vaccine with Encapsulated Nucleoprotein Antigen Peptide from Influenza Virus Confers Enhanced Cross Protection. *Bioconjug Chem* 2020, 31, 1948-1959, doi:10.1021/acs.bioconjchem.0c00308.
 116. Sheng, Y.Y. Apoferritin nanoparticle based dual-antigen influenza conjugate vaccine with potential cross-protective efficacy against heterosubtypic influenza virus. *Particuology* 2022, 64, 56-64.
 117. Skwarczynski, M.; Toth, I. Peptide-based synthetic vaccines. *Chem Sci* 2016, 7, 842-854, doi:10.1039/c5sc03892h.
 118. Jiang, S.; Song, R.; Popov, S.; Mirshahidi, S.; Ruprecht, R.M. Overlapping synthetic peptides as vaccines. *Vaccine* 2006, 24, 6356-6365, doi:10.1016/j.vaccine.2006.04.070.
 119. Zhang, H.; Hong, H.; Li, D.; Ma, S.; Di, Y.; Stoten, A.; Haig, N.; Di Gleria, K.; Yu, Z.; Xu, X.N.; et al. Comparing pooled peptides with intact protein for accessing cross-presentation pathways for protective CD8+ and CD4+ T cells. *J Biol Chem* 2009, 284, 9184-9191, doi:10.1074/jbc.M809456200.
 120. He, Y.; Yu, W.; Shen, L.; Yan, W.; Xiao, L.; Qi, J.; Hu, T. A SARS-CoV-2 vaccine based on conjugation of SARS-CoV-2 RBD with IC28 peptide and mannan. *Int J Biol Macromol* 2022, 222, 661-670, doi:10.1016/j.ijbiomac.2022.09.180.
 121. Azuar, A.; Shibu, M.A.; Adilbish, N.; Marasini, N.; Hung, H.; Yang, J.; Luo, Y.; Khalil, Z.G.; Capon, R.J.; Hussein, W.M.; et al. Poly(hydrophobic amino acid) Conjugates for the Delivery of Multi-epitope Vaccine against Group A Streptococcus. *Bioconjug Chem* 2021, 32, 2307-2317, doi:10.1021/acs.bioconjchem.1c00333.
 122. Shalash, A.O.; Becker, L.; Yang, J.; Giacomini, P.; Pearson, M.; Hussein, W.M.; Loukas, A.; Skwarczynski, M.; Toth, I. Oral Peptide Vaccine against Hookworm Infection: Correlation of Antibody Titers with Protective Efficacy. *Vaccines (Basel)* 2021, 9, doi:10.3390/vaccines9091034.
 123. Haque, S.; Sengupta, S.; Gupta, D.; Bhan, M.K.; Kumar, R.; Khan, A.; Jailkhani, B. S.Typhi derived OmpC peptide conjugated with Vi-polysaccharide evokes better immune response than free Vi-polysaccharide in mice. *Biologicals* 2019, 62, 50-56, doi:10.1016/j.biologicals.2019.10.001.
 124. Micoli, F.; Costantino, P.; Adamo, R. Potential targets for next generation antimicrobial glycoconjugate vaccines. *FEMS Microbiol Rev* 2018, 42, 388-423, doi:10.1093/femsre/fuy011.
 125. Del Bino, L.; Osterlid, K.E.; Wu, D.Y.; Nonne, F.; Romano, M.R.; Codee, J.; Adamo, R. Synthetic Glycans to Improve Current Glycoconjugate Vaccines and Fight Antimicrobial Resistance. *Chem Rev* 2022, 122, 15672-15716, doi:10.1021/acs.chemrev.2c00021.
 126. Feng, D.; Shaikh, A.S.; Wang, F. Recent Advance in Tumor-associated Carbohydrate Antigens (TACAs)-based Antitumor Vaccines. *ACS Chem Biol* 2016, 11, 850-863, doi:10.1021/acschembio.6b00084.
 127. Guo, C.; Manjili, M.H.; Subjeck, J.R.; Sarkar, D.; Fisher, P.B.; Wang, X.Y. Therapeutic cancer vaccines: past, present, and future. *Adv Cancer Res* 2013, 119, 421-475, doi:10.1016/B978-0-12-407190-2.00007-1.
 128. Sorieul, C.; Papi, F.; Carboni, F.; Pecetta, S.; Phogat, S.; Adamo, R. Recent advances and future perspectives on carbohydrate-based cancer vaccines and therapeutics. *Pharmacol Ther* 2022, 235, 108158, doi:10.1016/j.pharmthera.2022.108158.
 129. Shivatare, S.S.; Shivatare, V.S.; Wong, C.H. Glycoconjugates: Synthesis, Functional Studies, and Therapeutic

- Developments. *Chem Rev* 2022, 122, 15603-15671, doi:10.1021/acs.chemrev.1c01032.
130. Hossain, F.; Andreana, P.R. Developments in Carbohydrate-Based Cancer Therapeutics. *Pharmaceuticals (Basel)* 2019, 12, doi:10.3390/ph12020084.
131. Bajad, N.G.; Swetha, R.; Gutti, G.; Singh, M.; Kumar, A.; Singh, S.K. A systematic review of carbohydrate-based bioactive molecules for Alzheimer's disease. *Future Med Chem* 2021, 13, 1695-1711, doi:10.4155/fmc-2021-0109.
132. De Oliveira, D.M.P.; Forde, B.M.; Kidd, T.J.; Harris, P.N.A.; Schembri, M.A.; Beatson, S.A.; Paterson, D.L.; Walker, M.J. Antimicrobial Resistance in ESKAPE Pathogens. *Clin Microbiol Rev* 2020, 33, doi:10.1128/CMR.00181-19.
133. Antimicrobial Resistance, C. Global burden of bacterial antimicrobial resistance in 2019: a systematic analysis. *Lancet* 2022, 399, 629-655, doi:10.1016/S0140-6736(21)02724-0.
134. Laxminarayan, R. The overlooked pandemic of antimicrobial resistance. *Lancet* 2022, 399, 606-607, doi:10.1016/S0140-6736(22)00087-3.
135. Gautam, A. Antimicrobial Resistance: The Next Probable Pandemic. *JNMA J Nepal Med Assoc* 2022, 60, 225-228, doi:10.31729/jnma.7174.
136. WHO. Prioritization of pathogens to guide discovery, research and development of new antibiotics for drug-resistant bacterial infections, including tuberculosis. Available online: <https://www.who.int/publications/i/item/WHO-EMP-IAU-2017.12> (accessed on 11-11-2022).
137. CDC. 2019 AR Threats Report. Available online: <https://www.cdc.gov/drugresistance/biggest-threats.html#carp> (accessed on 11-11-2022).
138. European Antimicrobial Resistance, C. The burden of bacterial antimicrobial resistance in the WHO European region in 2019: a cross-country systematic analysis. *Lancet Public Health* 2022, 7, e897-e913, doi:10.1016/S2468-2667(22)00225-0.
139. Teng, F.; Singh, K.V.; Bourgogne, A.; Zeng, J.; Murray, B.E. Further characterization of the epa gene cluster and Epa polysaccharides of *Enterococcus faecalis*. *Infect Immun* 2009, 77, 3759-3767, doi:10.1128/IAI.00149-09.
140. Kalfopoulou, E.; Laverde, D.; Miklic, K.; Romero-Saavedra, F.; Malic, S.; Carboni, F.; Adamo, R.; Lenac Rovis, T.; Jonjic, S.; Huebner, J. Development of Opsonic Mouse Monoclonal Antibodies against Multidrug-Resistant Enterococci. *Infect Immun* 2019, 87, doi:10.1128/IAI.00276-19.
141. Zhou, Z.; Ding, W.; Li, C.; Wu, Z. Synthesis and immunological study of a wall teichoic acid-based vaccine against *E. faecium* U0317. *Journal of Carbohydrate Chemistry* 2017, 36, 205-219, doi:10.1080/07328303.2017.1390576.
142. Zhao, M.; Qin, C.; Li, L.; Xie, H.; Ma, B.; Zhou, Z.; Yin, J.; Hu, J. Conjugation of Synthetic Trisaccharide of *Staphylococcus aureus* Type 8 Capsular Polysaccharide Elicits Antibodies Recognizing Intact Bacterium. *Front Chem* 2020, 8, 258, doi:10.3389/fchem.2020.00258.
143. Lin, T.L.; Yang, F.L.; Ren, C.T.; Pan, Y.J.; Liao, K.S.; Tu, I.F.; Chang, Y.P.; Cheng, Y.Y.; Wu, C.Y.; Wu, S.H.; et al. Development of *Klebsiella pneumoniae* Capsule Polysaccharide-Conjugated Vaccine Candidates Using Phage Depolymerases. *Front Immunol* 2022, 13, 843183, doi:10.3389/fimmu.2022.843183.
144. Wei, R.; Yang, X.; Liu, H.; Wei, T.; Chen, S.; Li, X. Synthetic Pseudaminic-Acid-Based Antibacterial Vaccine Confers Effective Protection against *Acinetobacter baumannii* Infection. *ACS Cent Sci* 2021, 7, 1535-1542, doi:10.1021/acscentsci.1c00656.
145. Jamshidi, M.P.; Cairns, C.; Chong, S.; St Michael, F.; Vinogradov, E.V.; Cox, A.D.; Sauvageau, J. Synthesis and Immunogenicity of a Methyl Rhamnan Pentasaccharide Conjugate from *Pseudomonas aeruginosa* A-Band Polysaccharide. *ACS Infect Dis* 2022, 8, 1347-1355, doi:10.1021/acsinfectdis.2c00184.
146. Kowarik, M.; Wetter, M.; Haauptle, M.A.; Braun, M.; Steffen, M.; Kemmler, S.; Ravenscroft, N.; De Benedetto, G.; Zuppiger, M.; Sirena, D.; et al. The development and characterization of an *E. coli* O25B bioconjugate vaccine. *Glycoconjug J* 2021, 38, 421-435, doi:10.1007/s10719-021-09985-9.
147. Sorrell, T.C.; Packham, D.R.; Shanker, S.; Foldes, M.; Munro, R. Vancomycin therapy for methicillin-resistant *Staphylococcus aureus*. *Ann Intern Med* 1982, 97, 344-350, doi:10.7326/0003-4819-97-3-344.
148. Chang, S.; Sievert, D.M.; Hageman, J.C.; Boulton, M.L.; Tenover, F.C.; Downes, F.P.; Shah, S.; Rudrik, J.T.; Pupp,

- G.R.; Brown, W.J.; et al. Infection with vancomycin-resistant *Staphylococcus aureus* containing the *vanA* resistance gene. *N Engl J Med* 2003, 348, 1342-1347, doi:10.1056/NEJMoa025025.
149. McGuinness, W.A.; Malachowa, N.; DeLeo, F.R. Vancomycin Resistance in *Staphylococcus aureus*. *Yale J Biol Med* 2017, 90, 269-281.
150. O'Riordan, K.; Lee, J.C. *Staphylococcus aureus* capsular polysaccharides. *Clin Microbiol Rev* 2004, 17, 218-234, doi:10.1128/CMR.17.1.218-234.2004.
151. Gening, M.L.; Pier, G.B.; Nifantiev, N.E. Broadly protective semi-synthetic glycoconjugate vaccine against pathogens capable of producing poly-beta-(1-->6)-N-acetyl-d-glucosamine exopolysaccharide. *Drug Discov Today Technol* 2020, 35-36, 13-21, doi:10.1016/j.ddtec.2020.09.002.
152. Choi, M.; Hegerle, N.; Nkeze, J.; Sen, S.; Jamindar, S.; Nasrin, S.; Sen, S.; Permala-Booth, J.; Sinclair, J.; Tapia, M.D.; et al. The Diversity of Lipopolysaccharide (O) and Capsular Polysaccharide (K) Antigens of Invasive *Klebsiella pneumoniae* in a Multi-Country Collection. *Front Microbiol* 2020, 11, 1249, doi:10.3389/fmicb.2020.01249.
153. Cryz, S.J. Progress in immunization against *Klebsiella* infections. *Eur J Clin Microbiol* 1983, 2, 523-528, doi:10.1007/BF02016559.
154. Ravinder, M.; Liao, K.S.; Cheng, Y.Y.; Pawar, S.; Lin, T.L.; Wang, J.T.; Wu, C.Y. A Synthetic Carbohydrate-Protein Conjugate Vaccine Candidate against *Klebsiella pneumoniae* Serotype K2. *J Org Chem* 2020, 85, 15964-15997, doi:10.1021/acs.joc.0c01404.
155. Ghaderinia, P.; Shapouri, R.; Rostamizadeh, K.; Khodavandi, A.; Mahdavi, M. Capsular K-antigen-PLGA Nano conjugated Vaccine against *Klebsiella pneumoniae pneumoniae* K2O1 Infection. *Journal of Advances in Medical and Biomedical Research* 2022, 30, 73-74, doi:10.30699/jams.30.e57891.
156. Peng, Z.; Wu, J.; Wang, K.; Li, X.; Sun, P.; Zhang, L.; Huang, J.; Liu, Y.; Hua, X.; Yu, Y.; et al. Production of a Promising Biosynthetic Self-Assembled Nanoconjugate Vaccine against *Klebsiella Pneumoniae* Serotype O2 in a General *Escherichia Coli* Host. *Adv Sci (Weinh)* 2021, 8, e2100549, doi:10.1002/adv.202100549.
157. Hegerle, N.; Choi, M.; Sinclair, J.; Amin, M.N.; Ollivault-Shiflett, M.; Curtis, B.; Laufer, R.S.; Shridhar, S.; Brammer, J.; Toapanta, F.R.; et al. Development of a broad spectrum glycoconjugate vaccine to prevent wound and disseminated infections with *Klebsiella pneumoniae* and *Pseudomonas aeruginosa*. *PLoS One* 2018, 13, e0203143, doi:10.1371/journal.pone.0203143.
158. Seeberger, P.H.; Pereira, C.L.; Khan, N.; Xiao, G.; Diago-Navarro, E.; Reppe, K.; Opitz, B.; Fries, B.C.; Witzenrath, M. A Semi-Synthetic Glycoconjugate Vaccine Candidate for Carbapenem-Resistant *Klebsiella pneumoniae*. *Angew Chem Int Ed Engl* 2017, 56, 13973-13978, doi:10.1002/anie.201700964.
159. Giguere, D. Surface polysaccharides from *Acinetobacter baumannii*: Structures and syntheses. *Carbohydr Res* 2015, 418, 29-43, doi:10.1016/j.carres.2015.10.001.
160. Rudenko, N.; Karatovskaya, A.; Zamyatina, A.; Shepelyakovskaya, A.; Semushina, S.; Brovko, F.; Shpirt, A.; Torgov, V.; Kolotyrykina, N.; Zinin, A.; et al. Immune Response to Conjugates of Fragments of the Type K9 Capsular Polysaccharide of *Acinetobacter baumannii* with Carrier Proteins. *Microbiol Spectr* 2022, 10, e0167422, doi:10.1128/spectrum.01674-22.
161. Li, X.; Pan, C.; Liu, Z.; Sun, P.; Hua, X.; Feng, E.; Yu, Y.; Wu, J.; Zhu, L.; Wang, H. Safety and immunogenicity of a new glycoengineered vaccine against *Acinetobacter baumannii* in mice. *Microb Biotechnol* 2022, 15, 703-716, doi:10.1111/1751-7915.13770.
162. Lee, I.M.; Yang, F.L.; Chen, T.L.; Liao, K.S.; Ren, C.T.; Lin, N.T.; Chang, Y.P.; Wu, C.Y.; Wu, S.H. Pseudaminic Acid on Exopolysaccharide of *Acinetobacter baumannii* Plays a Critical Role in Phage-Assisted Preparation of Glycoconjugate Vaccine with High Antigenicity. *J Am Chem Soc* 2018, 140, 8639-8643, doi:10.1021/jacs.8b04078.
163. Pier, G.B. The challenges and promises of new therapies for cystic fibrosis. *J Exp Med* 2012, 209, 1235-1239, doi:10.1084/jem.20121248.
164. Liu, P.V. Comparison of the Chinese schema and the International Antigenic Typing System for serotyping *Pseudomonas aeruginosa*. *J Clin Microbiol* 1987, 25, 824-826, doi:10.1128/jcm.25.5.824-826.1987.
165. Estahbanati, H.K.; Kashani, P.P.; Ghanaatpisheh, F. Frequency of *Pseudomonas aeruginosa* serotypes in burn wound infections and their resistance to antibiotics. *Burns* 2002, 28, 340-348, doi:10.1016/s0305-

- 4179(02)00024-4.
166. Lu, Q.; Eggimann, P.; Luyt, C.E.; Wolff, M.; Tamm, M.; Francois, B.; Mercier, E.; Garbino, J.; Laterre, P.F.; Koch, H.; et al. *Pseudomonas aeruginosa* serotypes in nosocomial pneumonia: prevalence and clinical outcomes. *Crit Care* 2014, 18, R17, doi:10.1186/cc13697.
 167. Maleki, M.; Azimi, S.; Salouti, M. Protective effect of two new nanovaccines against *Pseudomonas aeruginosa* based on LPS and OPS: A comparison study. *Immunobiology* 2022, 227, 152278, doi:10.1016/j.imbio.2022.152278.
 168. Whitfield, C. Biosynthesis and assembly of capsular polysaccharides in *Escherichia coli*. *Annu Rev Biochem* 2006, 75, 39-68, doi:10.1146/annurev.biochem.75.103004.142545.
 169. Saade, E.; Gravenstein, S.; Donskey, C.J.; Wilson, B.; Spiessens, B.; Abbanat, D.; Poolman, J.; de Palacios, P.I.; Hermans, P. Characterization of *Escherichia coli* isolates potentially covered by ExPEC4V and ExPEC10V, that were collected from post-transrectal ultrasound-guided prostate needle biopsy invasive urinary tract and bloodstream infections. *Vaccine* 2020, 38, 5100-5104, doi:10.1016/j.vaccine.2020.06.024.
 170. McConnell, M.J.; Rumbo, C.; Bou, G.; Pachon, J. Outer membrane vesicles as an acellular vaccine against *Acinetobacter baumannii*. *Vaccine* 2011, 29, 5705-5710, doi:10.1016/j.vaccine.2011.06.001.
 171. Roberts, R.; Moreno, G.; Bottero, D.; Gaillard, M.E.; Fingerhann, M.; Graieb, A.; Rumbo, M.; Hozbor, D. Outer membrane vesicles as acellular vaccine against pertussis. *Vaccine* 2008, 26, 4639-4646, doi:10.1016/j.vaccine.2008.07.004.
 172. Shang, E.S.; Champion, C.I.; Wu, X.Y.; Skare, J.T.; Blanco, D.R.; Miller, J.N.; Lovett, M.A. Comparison of protection in rabbits against host-adapted and cultivated *Borrelia burgdorferi* following infection-derived immunity or immunization with outer membrane vesicles or outer surface protein A. *Infect Immun* 2000, 68, 4189-4199, doi:10.1128/IAI.68.7.4189-4199.2000.
 173. Keenan, J.; Day, T.; Neal, S.; Cook, B.; Perez-Perez, G.; Allardyce, R.; Bagshaw, P. A role for the bacterial outer membrane in the pathogenesis of *Helicobacter pylori* infection. *FEMS Microbiol Lett* 2000, 182, 259-264, doi:10.1111/j.1574-6968.2000.tb08905.x.
 174. Lee, J.C.; Lee, E.J.; Lee, J.H.; Jun, S.H.; Choi, C.W.; Kim, S.I.; Kang, S.S.; Hyun, S. *Klebsiella pneumoniae* secretes outer membrane vesicles that induce the innate immune response. *FEMS Microbiol Lett* 2012, 331, 17-24, doi:10.1111/j.1574-6968.2012.02549.x.
 175. Ellis, T.N.; Leiman, S.A.; Kuehn, M.J. Naturally produced outer membrane vesicles from *Pseudomonas aeruginosa* elicit a potent innate immune response via combined sensing of both lipopolysaccharide and protein components. *Infect Immun* 2010, 78, 3822-3831, doi:10.1128/IAI.00433-10.
 176. van der Put, R.M.F.; Smitsman, C.; de Haan, A.; Hamzink, M.; Timmermans, H.; Uittenbogaard, J.; Westdijk, J.; Stork, M.; Ophorst, O.; Thouron, F.; et al. The First-in-Human Synthetic Glycan-Based Conjugate Vaccine Candidate against *Shigella*. *ACS Cent Sci* 2022, 8, 449-460, doi:10.1021/acscentsci.1c01479.
 177. FDA. Vaccines Licensed for Use in the United States. Available online: <https://www.fda.gov/vaccines-blood-biologics/vaccines/vaccines-licensed-use-united-states> (accessed on 17-11-2022).



Chapter 3

HPAEC-PAD quantification of *Haemophilus influenzae* type b polysaccharide in upstream and downstream samples

Robert M.F. van der Put,^a Alex de Haan,^a Jan G.M. van den IJssel,^a Ahd Hamidi,^a and Michel Beurret^b

^a Unit Product Development, Institute for Translational Vaccinology (Intravacc), P.O. Box 450, 3720 AL Bilthoven, The Netherlands, ^b Unit Vaccinology, Centre for Infectious Disease Control (CIb), National Institute for Public Health and the Environment (RIVM), Bilthoven, The Netherlands

Abstract

Due to the rapidly increasing introduction of *Haemophilus influenzae* type b (Hib) and other conjugate vaccines worldwide during the last decade, reliable and robust analytical methods are needed for the quantitative monitoring of intermediate samples generated during fermentation (upstream processing, USP) and purification (downstream processing, DSP) of polysaccharide vaccine components. This study describes the quantitative characterization of in-process control (IPC) samples generated during the fermentation and purification of the capsular polysaccharide (CPS), polyribosyl-ribitol-phosphate (PRP), derived from Hib. Reliable quantitative methods are necessary for all stages of production; otherwise, accurate process monitoring and validation is not possible. Prior to the availability of high-performance anion exchange chromatography methods, this polysaccharide was predominantly quantified either with immunochemical methods, or with the colorimetric orcinol method, which shows interference from fermentation medium components and reagents used during purification. Next to an improved high-performance anion exchange chromatography-pulsed amperometric detection (HPAEC-PAD) method, using a modified gradient elution, both the orcinol assay and high performance size exclusion chromatography (HPSEC) analyses were evaluated. For DSP samples, it was found that the correlation between the results obtained by HPAEC-PAD specific quantification of the PRP monomeric repeat unit released by alkaline hydrolysis, and those from the orcinol method was high ($R^2= 0.8762$), and that it was lower between HPAEC-PAD and HPSEC results. Additionally, HPSEC analysis of USP samples yielded surprisingly comparable results to those obtained by HPAEC-PAD. In the early part of the fermentation, medium components interfered with the different types of analysis, but quantitative HPSEC data could still be obtained, although lacking the specificity of the HPAEC-PAD method. Thus, the HPAEC-PAD method has the advantage of giving a specific response compared to the orcinol assay and HPSEC and does not show interference from various components that can be present in intermediate and purified PRP samples.

Keywords

Anion exchange chromatography, Bacterial polysaccharides analysis, Downstream processing, High pressure liquid chromatography, Polysaccharide, Upstream processing.

Abbreviations

CPS, capsular polysaccharide; DSP, downstream processing; ESTD, external standard; Glc, glucose; Glc-6-P, d-glucose-6-phosphate; Hib, *Haemophilus influenzae* type b; HPAEC-PAD, high performance anion exchange chromatography with pulsed amperometric detection; HPSEC, high performance size exclusion chromatography; IPC, in process control; kDa, kilo Dalton; μ RIU, micro-refractive index unit; Mw, absolute weight-average molecular mass; MWCO, molecular weight cut-off; NA, nucleic acids; NaAc, sodium acetate; NaOH, sodium hydroxide; OD, optical density; PBS, phosphate buffered saline; PRP, polyribosyl-ribitol-phosphate (Hib CPS); Rib, d(-)-ribose; RI, refractive index; RIVM, National Institute for Public Health and the Environment; RU, repeating unit(s) of the polysaccharide; tR, retention time; USP, upstream processing; WFI, water for injection; WHO, World Health Organization.

Introduction

Due to the need in recent years for a more rapid introduction of *Haemophilus influenzae* type b (Hib) conjugate vaccines world-wide [1–3], an improved production process, based on publicly available data [4] has been developed at the National Institute for Public Health and the Environment (RIVM) of the Netherlands [5]. This process has been transferred to different vaccine producers belonging to the Developing Countries Vaccine Manufacturers Network (DCVMN) [6]. The RIVM and Intravacc in the Netherlands had already been involved in technology transfer of various other vaccine production processes for several decades [7]. The Hib bacterium was cultivated in a rich yeast-based medium, and the Hib capsular polysaccharide (CPS), polyribosyl ribitol phosphate (PRP) [8, 9], was purified by differential precipitation using detergents and alcohol [5]. In order to evaluate the process steps during fermentation (upstream processing, USP) and purification (downstream processing, DSP), several quality control (QC) tests, both immunochemical (e.g. ELISA), physicochemical (e.g. high performance size exclusion chromatography, HPSEC) (both developed in-house) and colorimetric (orcinol), have originally been used. However, these tests can be influenced by matrix components (e.g. fermentation medium, detergents and alcohol) and are consequently not unconditionally applicable as in-process controls (IPC). Preferably, more specific methods should be used [10–14], fit for real-time monitoring. In order to meet these needs, a high-performance anion exchange chromatography method with pulsed amperometric detection (HPAEC-PAD) has been developed [15], and evaluated, for its potential to overcome the aforementioned matrix effects. Correlation between the results obtained by HPAEC-PAD quantification of the PRP monomeric repeat unit (RU) released by alkaline hydrolysis [10–13, 16], and those from the orcinol colorimetric assay (method adapted from Ashwell [17]) was expected to be high for DSP samples. USP

samples which cannot be analyzed directly by the orcinol method due to interference by fermentation medium components (e.g. glucose), have so far been tested by a PRP-specific ELISA developed in-house. This ELISA has never been fully validated at RIVM, and therefore was not evaluated in this study. In addition, an HPSEC method that affords more complete information (i.e. multiple UV wavelength and refractive index detection [6]) than simple immunological and physicochemical tests has been used for the real-time monitoring of both USP and DSP. In this manuscript, these three different analytical methods (orcinol, HPAEC-PAD and HPSEC) have been evaluated for their potential to allow monitoring of the Hib vaccine production processes.

Materials and methods

Chemicals

All chemicals were of the highest possible grade: d-glucose-6-phosphate, sodium salt (Glc-6-P, MW 282.12; Sigma nr. G7879); d(-)-ribose (Rib, MW150.13; Acros Chimica nr. 13236); ferric chloride hexahydrate (Acros Organics nr. 21709); hexadecyl-trimethylammoniumbromide (Cetavlon, Merck nr. 8.14119); hydrochloric acid (Merck nr. 1.00317); orcinol (Acros Organics nr.12955); sodium acetate (NaAc; Fluka nr. 71183); sodium deoxycholate (DOC, Merck nr. 1.06504); sodium hydroxide (NaOH, 50% solution; Baker nr. 61007067); Phosphate-buffered saline pH 7.2(PBS, 10 mM sodium phosphate, 150 mM sodium chloride); PRP reference material (RIVM lot 00Hib350-1/2-7.1 [5]; 0.552 mg/mL (orcinol assay [17])).

Hib fermentation

Batch fermentation took place in a 5 L bioreactor (Applikon, BL90) with a working volume of 3.5 L. The process as described before was followed [5]. Fermentation samples were collected hourly and more often at critical points (i.e. maximum OD, pH set point 7.5 and after cooling overnight). Optical density (OD_{590}) was measured using a standard 6300 (Jenway) spectrophotometer.

PRP purification

PRP purification took place at 100 mL scale. The process as described before was followed [5]. Diafiltration was performed using a standard Millipore, Pellicon XL filter on a Labscale (Millipore) system. All samples generated during each purification step (see Fig. 1) were collected and analyzed.

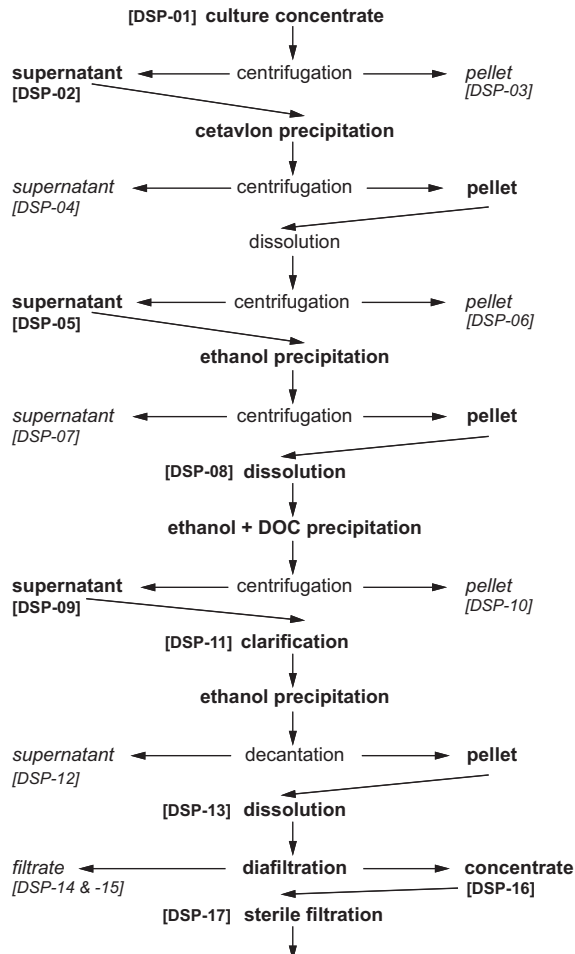


Figure 1: Purification (DSP) of PRP by differential fractionation [5]. In **bold**: product fractions; in *italic*: waste fractions.

Orcinol assay

Performed as described by Ashwell [17]. Essentially PRP was quantified using d(–)-ribose (Rib) as the standard (5–60 nmol). All samples, and the PRP reference material (RIVM) used as positive control, were pre-diluted in triplicate to contain ~30 nmol of PRP (middle of the calibration curve for most accurate measurement). PRP concentrations were derived from the calculated mass of the RU of PRP bearing a sodium counter-ion (PRP RU[Na⁺]; Mw 368.21), each RU containing one Rib equivalent [8, 9].

HPAEC-PAD conditions

Alkaline conditions

This was carried out essentially as described by Tsai et al [10–12]. In short, Hib USP and some specific DSP supernatants were 0.22 μm filtered to remove cell debris. Aliquots were diluted to 250 μL with WFI, followed by addition of 250 μL hydrolysis reagent (200mM NaOH). After 16 h at 20–25°C on a continuous rolling mixer, 50 μL of 200 μM Glc-6-P (external standard, ESTD), was added, followed by 10 kDa MWCO ultrafiltration (Millipore, Microcon YM-10, 0.5 mL). PRP reference material (RIVM) was put through the same hydrolysis treatment to construct a calibration curve (0.25–10 μg), as was the fermentation medium as a negative control. A volume of 20 μL was injected using a 25 μL loop [15].

Equipment

An ICS-3000 (Thermo Fisher Scientific) metal-free ion chromatography system was used, where the autosampler was set at 6°C, and column and detector compartments both at 30°C. The pulse amperometric detector unit (integrated amperometry mode) was equipped with a disposable gold electrode (Thermo Fisher Scientific nr. 060216), and a reference pH electrode (Ag/AgCl; Thermo Fisher Scientific nr. 061879). The recommended four-potential carbohydrate PAD waveform (Thermo Fisher Scientific) was used: 0.00 s (+0.1 V), 0.20 s (+0.1 V; start data acquisition), 0.40 s (+0.1 V; stop data acquisition), 0.41 s (–2.0 V), 0.42 s (–2.0 V), 0.43 s (+0.6 V), 0.44 s (–0.1 V), 0.50 s (–0.1 V).

HPAEC-PAD column

A CarboPac PA10 column (4mm \times 250mm; Thermo Fisher Scientific nr. 046110) protected by an Amino Trap column(4mm \times 50mm; Thermo Fisher Scientific nr. 046122) was used.

HPAEC-PAD elution programs

Eluents E1 (water) and E2 (1M NaAc with 250mM NaOH) were prepared using pure water, degassed for 30 min by means of sonication, and protected by a helium headspace (0.2 bar). Elution was performed at 1 mL/min (average back pressure 150 bar). The elution HPAEC-PAD programs were performed as previously described [15].

HPSEC conditions

HPSEC equipment

An UltiMate-3000 (Thermo Fisher Scientific) HPLC system was used, where the autosampler was set at 6°C, and column and detector compartment both at 35°C. Detection was done using a multi-wavelength UV detector (set at 215, 260, and 280 nm), and a refractive index (RI) RI-101 detector (Shodex; set at 35°C).

HPSEC columns

A set consisting of Shodex OHpak SB-G guard column, and SB-805 HQ plus SB-804 HQ columns mounted in series (in this order) was used. Column performance was evaluated using pullulan standards of known absolute weight-average molecular mass (M_w) (Shodex nr. P-82, or Polymer Standards Service nr. PSS-pulkit). The elution volumes (V^e) were plotted against the $\log(M_w)$ of the standards, to construct a molecular size calibration curve. Purified PRP (RIVM) was used as a positive control and allowed relative PRP quantification based on the RI signal.

HPSEC elution programs

Eluent E3 (PBS 10mM, pH 7.2) was prepared using pure water, and filtered using a 0.2 μm filtration unit (FastCap PES filters 298, Nalgene 298-9020) before use. Isocratic elution was performed at 1 mL/min (average back pressure 20 bar) for 30 min.

3

Calculations

Chromatographic data was acquired, integrated and processed using the Chromeleon software (v. 6.70, SP 10; Thermo Fisher Scientific), which was also used to control the instrument. The PRP (HPAEC-PAD), Rib (orcinol) and molecular size (HPSEC) calibration equations were determined with Excel (Microsoft), using the LINEST linear regression function.

Results and discussion

USP

USP fractions, the orcinol test could not be used, due to strong interference from the media components (e.g. glucose, Glc), with pretreatment of samples considered too time-consuming and introducing bias. The HPAEC-PAD analysis gave a specific peak profile after alkaline hydrolysis of PRP to its monomeric RU, as shown before [15]. Before USP-04 it was difficult to quantify PRP because of unreliable Glc-6-P external standard (ESTD) areas (overlapping contaminants peaks). Most importantly, the PRP RU peak was visible from start of growth, after the lag phase ($t \sim 4.4$ h) and did not show any interference by matrix effects when reaching maximum OD, set point pH 7.5, and more importantly, after overnight cooling, inducing cell lysis and subsequent release of PRP (see Fig. 2). HPSEC analysis of the non-hydrolyzed fermentation supernatants showed striking similarity to HPAEC-PAD (hydrolyzed) analyses, where both results overlap for almost the entire log phase. For both HPSEC and HPAEC-PAD analyses, there was a slight offset (~ 2 h) compared

to the OD_{590} measurement (see Fig. 3). Possibly due to the fact that either PRP was not released yet or quantities of PRP (Q_{PRP}) were below detection levels. In conclusion similar process characteristics could be observed for the lag and log phases ($n = 3$, see Fig. 3). Up until reaching maximum OD_{590} , a steady and comparable increase in OD_{590} , HPSEC (RI signal) and Q_{PRP} measured by HPAEC-PAD was observed. After initial lag and log phases, three specific process points were assigned: maximum OD_{590} , OD_{590} at set point pH 7.5, and OD_{590} after cooling overnight (see Table 1). As shown by HPAEC-PAD analysis, Q_{PRP} in the culture supernatant still increased even after maximum OD_{590} was reached ($38.3 \pm 8.3\%$ - $69.3 \pm 10.6\%$). It is suggested that PRP was released from the bacteria due to lysis or induced stress, which was shown by the inverse proportional relationship between Q_{PRP} and OD_{590} after reaching maximum OD_{590} (see Fig. 3). After reaching set point pH 7.5, the culture was cooled to prevent further extensive lysis of the bacteria and prevent unfavorable process dynamics during DSP (release of high quantities of DNA and protein). During this step, an increase in Q_{PRP} was noticeable ($69.3 \pm 10.6\%$ - $100.0 \pm 15.9\%$), as was a continuous decrease in OD_{590} [5]. During USP the quantity of crude PRP obtained, determined using HPAEC-PAD was very comparable. Yield reproducibility was within about 15% ($n = 3$). When evaluating the USP samples in total, a good correlation ($R^2: 0.744$, data not shown) between HPSEC and HPAEC-PAD was observed. Both methods showed that release of PRP continued during the cooling phase ($t > 10.8$ h). However, PRP quantities estimated by HPSEC became significantly higher from ~ 11 h on and after overnight cooling, compared to HPAEC-PAD analysis (see Fig. 3 and Table 1). This was confirmed by comparing the RI and UV traces of the HPSEC analyses of USP samples (data not shown), where UV showed an increase with time of both protein and nucleic acids (NA) co-eluting with the PRP peak, detected by RI. Even though the HPSEC method overestimates PRP quantities it still is a rapid, direct and simple method suitable for real-time monitoring, but not accurate quantification.

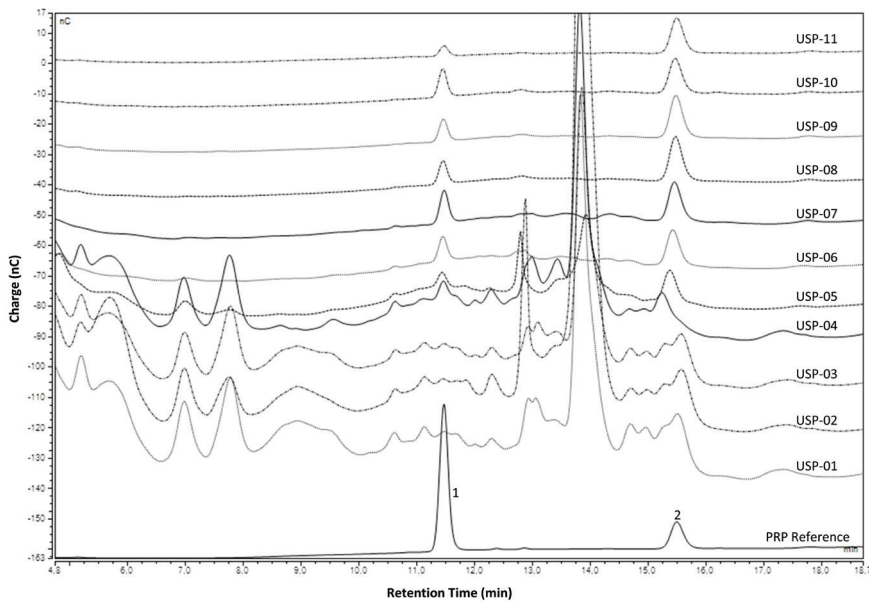


Figure 2: USP samples analyzed by high performance anion exchange chromatography with pulsed amperometric detection (HPAEC-PAD) after alkaline hydrolysis. USP samples: nr. 1, $t = 0$ h; nr. 2, $t = 1.2$ h; nr. 3, $t = 2.8$ h; nr. 4, $t = 4.4$ h (start log phase); nr. 5, $t = 6.3$ h; nr. 6, $t = 7.4$ h; nr. 7, $t = 8.6$ h; nr. 8, $t = 9.5$ h (max OD); nr. 9, $t = 11.6$ h; nr. 10, $t = 12.6$ h (pH set point 7.5); and nr. 11 ($t = 29.2$ h, after overnight cooling). PRP RU [1] (t_R 11.46 min) appeared at the beginning of the log phase (USP-04, $t \sim 4.4$ h), nevertheless the Glc-6-P ESTD [2] (t_R 15.48 min) was still poorly resolved from hydrolyzed medium components at this time. Also at this point, the Glc peak (t_R 2.19 min, not shown) started to steadily decrease (at ~ 9 h it was barely detectable).

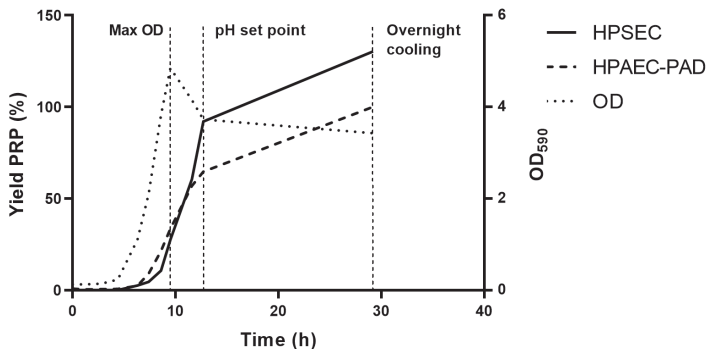


Figure 3: Hib fermentation (USP), monitored with three different methods ($n = 1$ fermentation). PRP yield has been normalized relative to the Q_{PRP} after overnight cooling as determined by HPAEC-PAD set to 100%. Result only reflects one experiment: due to different timing in sample points, no average was calculated.

Table 1: Normalized quantity of PRP (Q_{PRP}) for the different upstream process (USP) set points, with standard deviation (n = 3 fermentations).

	Time (h)	OD ₅₉₀	Q_{PRP} orcinol (%)	Q_{PRP} HPAEC-PAD (%)	Q_{PRP} HPSEC (RI) (%) ^{b, c}
Maximum OD ₅₉₀	8.3 ± 1.0	5.0 ± 0.3	n.a.	38.3 ± 8.3	42.3 ± 13.3
At set point pH 7.5	10.8 ± 1.7	4.4 ± 0.3	n.a.	69.3 ± 10.6	90.4 ± 22.0
After overnight cooling	25.8 ± 3.0	4.0 ± 0.6	n.a.	100.0 ± 15.9	148.3 ± 5.8
DSP-01 ^e	n.a.	n.a.	93.4	100	147.9
DSP-17	n.a.	n.a.	55.5 ± 21.2	55.8 ± 8.2	55.4 ± 18.1
Yield (%) ^f	n.a.	n.a.	59	56	37

^a HPAEC-PAD results have been normalized to final HPAEC-PAD yield after overnight cooling, set to 100 %.

^b HPSEC RI peak areas ($\mu\text{RIU} \cdot \text{min}$) were first converted to mg, relative to a standard injection of PRP reference material [5], after which they were normalized to final HPAEC-PAD yield after overnight cooling, which was set to 100 %.

^c HPSEC RI peak areas ($\mu\text{RIU} \cdot \text{min}$) were first converted to mg, relative to a standard injection of PRP reference material [5], after which they were normalized to HPAEC-PAD yield for DSP-01, which was set to 100 % [5].

^d HPAEC-PAD results have been normalized to final HPAEC-PAD yield for DPS-01, which was set to 100 %.

^e DSP-01 is final USP sample after storage at -20 °C (n = 1).

^f Yield (in %): (DSP-01 / DSP-17) * 100

DSP

After the USP, the fermentation broth was clarified by batch centrifugation and the supernatant was inactivated by formaldehyde treatment, after which it was concentrated to a final volume of 100 ml using membrane filtration. This final concentrate was buffer exchanged using PBS, after which it was ready for DSP. The DSP process consists of several differential precipitations using ethanol and detergents (see Fig. 1). For all intermediate process steps, product and waste fractions have been analyzed by HPSEC, HPAEC-PAD and the orcinol assay. When evaluating DSP samples, the three different analysis methods gave rather similar results (see Fig. 4). However, the HPSEC response for DSP-01, 05, 07, 09 and 11 was (significantly) higher. This could be explained by interferences caused by high amounts of protein and NA, still present at this stage, before being removed during the consecutive DSP process steps. This was especially true for DSP-07 which is a waste fraction. Sample DSP-02 showed an unusually high standard deviation for the HPSEC analysis. Here, there were only two data points, and they were significantly different. For all other product and waste fractions, acceptable standard deviations were observed (n = 3), as was a good correlation between all three assays. When comparing the orcinol assay with HPAEC-PAD data for all DSP samples, even though it was expected that ethanol and detergents would mostly interfere with the orcinol assay, correlation was good ($R^2 = 0.876$) (see Fig. 5). When comparing the HPSEC and HPAEC-PAD analyses for both USP and DSP fractions, it was concluded that correlation was reasonable considering previously

discussed interference of protein and NA ($R^2 = 0.744$, data not shown). When comparing the HPSEC and orcinol data for DSP fractions alone, correlation was noticeably lower ($R^2 = 0.694$, data not shown). When comparing the total PRP yield between DSP-01 and -17, all methods show a decrease in total Q_{PRP} . The total PRP yield for HPSEC was low (37%), especially when compared to HPAEC-PAD and orcinol for which yields were 56 and 59% respectively (see Table 1). Inevitably these losses were caused by the succession of the various purification steps. As discussed previously, the drawback for correct analysis using HPSEC is the presence of high concentrations of interfering impurities like NA and protein, especially in the start material DSP-01 [6], and also for the waste fractions. Their matrix, being more complex, most certainly caused subsequent overestimation of the Q_{PRP} . The Q_{PRP} of the final purified product was very comparable for all three assays, but with substantial standard deviation (see Table 1). The three final purified PRP batches met all the applicable World Health Organization (WHO) [18] and additional Intravacc quality requirements. The results were comparable to other PRP batches produced under GMP, from which the PRP reference material was derived [5].

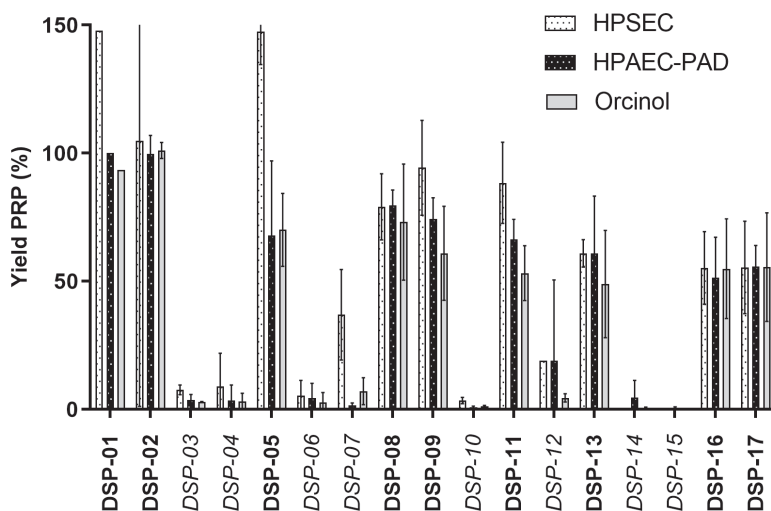


Figure 4: DSP samples analyzed with three different methods ($n = 3$ purifications), except for DSP-01 ($n = 1$). PRP yield has been normalized relative to the DSP-01 sample as analyzed by HPAEC-PAD set to 100%. Product fractions (**bold**) and waste fractions (*italic*) were analyzed by the three different methods.

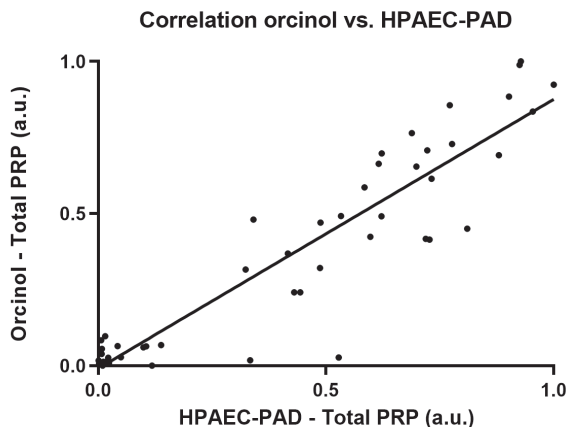


Figure 5: Correlation orcinol vs. HPAEC-PAD for DSP samples from three independent small-scale purifications normalized to arbitrary units (a.u.) ($n = 3$ purifications, 57 data points, $R^2 = 0.8762$).

Orcinol

The orcinol method as used for this investigation (low calibration curve, 0.5–6 nmol), where samples had to be pre-diluted an extra 10 times, yielded good results. This additional dilution most probably had a significant effect on minimizing interferences caused by impurities (*e.g.* protein and NA) and reagents (*e.g.* ethanol and detergents). Nevertheless, for DSP-09 and -11, containing high concentrations of ethanol, and DSP-12 containing both ethanol and deoxycholate (DOC), orcinol underestimated the Q_{PRP} compared to HPAEC-PAD. The LOD for HPAEC-PAD as determined previously is approximately 0.072 nmol [15], suggesting additional dilution (~10 times), would show even less interference. Even though HPAEC-PAD is the preferred method for analysis of samples containing significant amounts of detergents, ethanol and impurities, the orcinol assay is a fast and reliable assay suitable for high through put and rapid analysis of multiple samples.

HPSEC

For USP samples, a peak for PRP could be detected (RI signal), comparable in retention time and shape to that of the PRP reference [5]. The peak area correlated reasonably well with both OD_{590} and HPAEC-PAD data (see Fig. 3). Correlation was observed only up to maximum OD_{590} , after which impurities, as detected by their UV signal overlapping with the main RI peak [6], led to overestimation of the Q_{PRP} . HPSEC analysis showed good reproducibility between the different experiments. Next to RI, which detects all products present, UV signals (215, 260 and 280 nm) generate additional insight in the impurities (*e.g.* protein and NA) [6]. Large amounts of impurities (*e.g.* ~12–200% protein relative to

the Q_{PRP}) could be detected up to DSP-11. Thus, PRP was overestimated, due to large RI peaks accounting for both PRP and co-eluting impurities (especially in DSP-01, -05, -07, -09 and -11), and high variability between experiments could be observed. From DSP-12, less contaminants interfered with the different assays and results became more comparable. The HPSEC analysis is a rapid (30–45 min) and simple detection method informing on both product and impurities, making it fit for real-time monitoring of both USP and DSP fractions.

HPAEC-PAD

HPAEC-PAD analysis did not show any interference by impurities and the different reagents used. Although HPSEC overestimated Q_{PRP} results, for the USP fractions the results correlated reasonably well with the HPAEC-PAD and OD_{590} data. DSP data for HPAEC-PAD was comparable to the orcinol data for all product fractions and most waste fractions and showed a good correlation ($R^2= 0.876$, see Fig. 5). This suggests robustness of the HPAEC-PAD method for analysis of DSP samples and could be extrapolated for USP samples (where orcinol data is lacking). The HPAEC-PAD method has a time-consuming sample preparation, which makes it not fit for real-time analysis of USP and DSP fractions, but nevertheless provides more specific data that is not obtained by the other two methods.

Conclusion

As discussed, the orcinol assay was not suitable for testing Hib USP IPC samples because of the presence of interfering medium components. Pretreatment of the samples using precipitation and/or filtration before the orcinol assay is possible but is too laborious and could introduce bias: PRP losses during the pretreatment vary depending on the fermentation stage and will therefore influence the reliability of the data generated using the orcinol assay. PRP in USP samples was measured accurately with HPAEC-PAD despite the presence of a complex matrix. For HPAEC-PAD analyses, clean chromatograms were observed already early during USP after the lag phase. Here the possibility for diluting samples more, due to higher sensitivity compared to orcinol, led to little or even no interference at all [15]. Likewise, detergents and alcohol caused little interferences in DSP samples. The high correlation obtained with the orcinol test showed that the HPAEC-PAD method does not underestimate, nor overestimates PRP quantities. In addition, a reasonable correlation was found between orcinol and HPSEC for the DSP samples. HPSEC analyses are rapid and are therefore fit for online monitoring. However, interferences from other high mass compounds, such as proteins and NA, occurred frequently. This made HPSEC quantification of PRP less robust due to matrix impurities resulting in frequent

overestimation. Of the three methods, HPAEC-PAD gave the most specific results, since the measured peak can be attributed solely to the PRP monomeric RU [11, 15]. Adding to this, there was little disturbance by matrix effects, for both USP and DSP samples. However, sample preparation is still time-consuming, due to the need for a lengthy alkaline hydrolysis step (~16 h) prior to analysis, and this makes HPAEC-PAD unfit for online monitoring. During PRP fermentation and purification a combination of these three analytical methods has proven to be valuable and was able to provide the data necessary for correct evaluation of both process and final product.

Acknowledgments

The authors would like to thank Prof. Dr. Gideon Kersten (Intravacc) for diligently reviewing and providing expert advice on improving the manuscript.

Conflict of interest

There are no conflicts of interest related to the data presented in this manuscript. Role of funding source: The research and subsequent results presented in this manuscript were funded by Intravacc.

Author contribution statement

R.v.d.P. performed the DSP and analyzed all USP and DSP samples using the 3 methods. A.d.H., participated in the analysis the various USP and DSP samples. J.IJ performed the USP. M.B. participated in setting up and designing the study and contributed to data interpretation. R.v.d.P. drafted the manuscript. All authors have read and approved the final manuscript.

References

- [1] Progress introducing Haemophilus influenzae type b vaccine in low-income countries, 2004–2008. *Wkly Epidemiol Rec* 2008;83:61–8.
- [2] WHO position paper on Haemophilus influenzae type b conjugate vaccines. *WklyEpidemiol Rec* 2006;81:445–52.
- [3] Levine OS, Schwartz B, Pierce N, Kane M. Development, evaluation and implementation of Haemophilus influenzae type b vaccines for young children in developing countries: current status and priority actions. *Pediatr Infect Dis J* 1998;17:S95–113.
- [4] Chu C-Y, Schneerson R, Robbins JB, Rastogi SC. Further studies on the immunogenicity of Haemophilus influenzae type b and pneumococcal type 6A polysaccharide–protein conjugates. *Infect Immun* 1983;40:245–56.
- [5] Hamidi A, Beurret M. Process for producing a capsular polysaccharide for use in conjugate vaccines. United States Patent. The Hague, NL: United States: De Staat der Nederlanden, vert. door de minister van VWS; 2009.
- [6] Beurret M, Hamidi A, Kreeftenberg H. Development and technology transfer of Haemophilus influenzae type b conjugate vaccines for developing countries. *Vaccine* 2012;30:4897–906.
- [7] Hendriks J. Technology transfer in human vaccinology: a retrospective review on public sector contributions in a privatizing science field. *Vaccine* 2012;30:6230–40.
- [8] Branefors-Helander P, Erbing C, Kenne L, Lindberg B. Structural studies of the capsular antigen from Haemophilus influenzae type b. *Acta Chem ScandB* 1976;30:276–7.
- [9] Crisel RM, Baker RS, Dorman DE. Capsular polymer of Haemophilus influenzae, type b. I. Structural characterization of the capsular polymer of strain Eagan. *JBiol Chem* 1975;250:4926–30.
- [10] Lei QP, Lamb DH, Heller R, Pietrobon P. Quantitation of low level unconjugated polysaccharide in tetanus toxoid-conjugate vaccine by HPAEC/PAD following rapid separation by deoxycholate-HCl. *J Pharm Biomed Anal* 2000;21:1087–91.
- [11] Tsai CM, Gu XX, Byrd RA. Quantification of polysaccharide in Haemophilus influenzae type b conjugate and polysaccharide vaccines by high-performance anion-exchange chromatography with pulsed amperometric detection. *Vaccine* 1994;12:700–6.
- [12] Bardotti A, Ravenscroft N, Ricci S, D'Ascenzi S, Guarnieri V, Averani G, et al. Quantitative determination of saccharide in Haemophilus influenzae type b glycoconjugate vaccines, alone and in combination with DPT, by use of high-performance anion-exchange chromatography with pulsed amperometric detection. *Vaccine* 2000;18:1982–93.
- [13] Belfast M, Lu R, Capen R, Zhong J, Nguyen MA, Gimenez J, et al. A practical approach to optimization and validation of a HPLC assay for analysis of polyribosyl–ribitol phosphate in complex combination vaccines. *J ChromatogrB Analyt Technol Biomed Life Sci* 2006;832:208–15.
- [14] Mawas F, Bolgiano B, Rigsby P, Crane D, Belgrave D, Corbel MJ. Evaluation of the saccharide content and stability of the first WHO International Standard for Haemophilus influenzae b capsular polysaccharide. *Biologicals* 2007;35:235–45.
- [15] de Haan A, van der Put RM, Beurret M. HPAEC-PAD method for the analysis of alkaline hydrolyzates of Haemophilus influenzae type b capsular polysaccharide. *Biomed Chromatogr* 2013;27:1137–42.
- [16] Sturgess AW, Rush K, Charbonneau RJ, Lee JI, West DJ, Sitrin RD, et al. Haemophilus influenzae type b conjugate vaccine stability: catalytic depolymerization of PRP in the presence of aluminum hydroxide. *Vaccine* 1999;17:1169–78.
- [17] Ashwell G. Colorimetric analysis of sugars. *Methods Enzymol* 1957;III:73–105.
- [18] WHO Expert Committee on Biological Standardization. Forty-ninth report. Annex 1. Recommendations for the production and control of Haemophilus influenzae type b conjugate vaccines. *WHO Tech Rep Ser* 2000;897:27–60.



Chapter 4

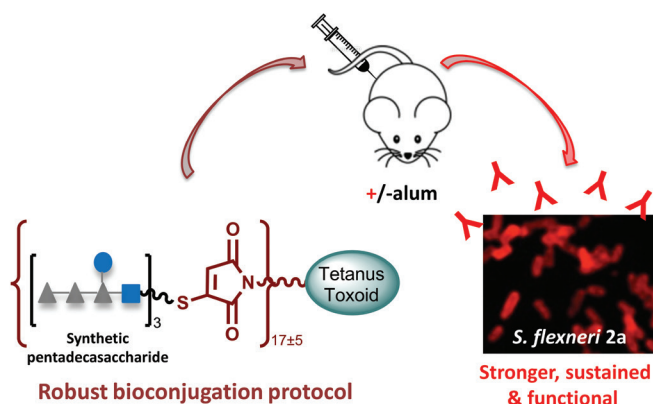
A synthetic carbohydrate conjugate vaccine candidate against shigellosis: improved bioconjugation and impact of alum on immunogenicity

Robert M. F. van der Put,^{a,‡} Tae Hee Kim,^{b,c,‡,†} Catherine Guerreiro,^{b,c} Françoise Thouron,^{d,e} Peter Hoogerhout,^a Philippe J. Sansonetti,^{d,e} Janny Westdijk,^a Michiel Stork,^a Armelle Phalipon,^{d,e} and Laurence A. Mulard^{b,c}

^a Institute for Translational Vaccinology (Intravacc), P.O. Box 450, 3720 AL Bilthoven, the Netherlands, ^b Institut Pasteur, Unité de Chimie des Biomolécules, 28 rue du Dr Roux, 75 724 Paris Cedex 15, France, ^c CNRS UMR 3523, Institut Pasteur, F-75015 Paris, France, ^d Institut Pasteur, Unité de Pathogénie Microbienne Moléculaire, 28 rue du Dr Roux, 75 724 Paris Ce-dex 15, France, ^e INSERM U1202, Institut Pasteur, F75015 Paris, France

Abstract

The conjugation chemistry is amongst the most important parameters governing the efficacy of glycoconjugate vaccines. High robustness is required to ensure high yields and batch to batch reproducibility. Herein, we have established a robust bioconjugation protocol based on the thiol-maleimide addition. Major variables were determined and acceptable margins were investigated for a synthetic pentadecasaccharide-tetanus toxoid conjugate, which is a promising vaccine candidate against *Shigella flexneri* serotype 2a infection. The optimized process is applicable to any thiol-equipped hapten and provides an efficient control of the hapten:carrier ratio. Moreover, comparison of four *S. flexneri* 2a glycoconjugates only differing by their pentadecasaccharide:tetanus toxoid ratio confirmed preliminary findings indicating that hapten loading is critical for immunogenicity with an optimal ratio here in the range of 17 ± 5 . In addition, the powerful influence of alum on the immunogenicity of a *Shigella* synthetic carbohydrate-based conjugate vaccine candidate is demonstrated for the first time, with a strong anti-*S. flexneri* 2a antibody response sustained for more than one year.



Introduction

Diarrheal diseases are a major burden worldwide, and the second cause of death in children under five years of age [1]. Available figures reflect a major improvement in terms of mortality; however incidence rates have declined only slightly over the past decades [2]. Moreover, alerts have emerged, which point to a clear link between diarrhea and lasting disability effects such as growth and cognition stunting, affecting young children, who are the most prone to repeated enteric infections [3, 4]. Noteworthy is also the so-called vicious circle linking diarrhea and malnutrition leading to enteropathy in the targeted population [5]. Shigellosis, an acute rectocolitis otherwise known as bacillary dysentery, remains one of the top diarrheal diseases, especially among children under the age of five in developing

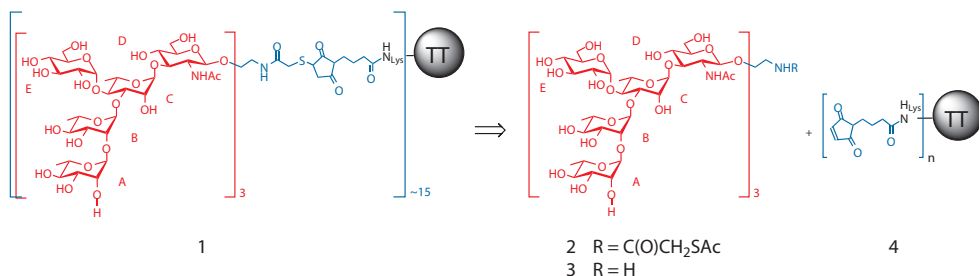
countries [6]. The causative agents of shigellosis are Gram-negative enteroinvasive bacteria named *Shigella* [7]. *Shigella flexneri* is the most prevalent species worldwide, and the major cause of episodes in low-income settings [8]. Despite important efforts directed at their development over the past decades, there are yet no broadly available vaccines against shigellosis [9, 10]. In this context, the renewed awareness of disease burden in the pediatric population, boosted by the growing spread of antibiotic multi-resistant strains [11] and the inadequacy of rehydration therapy, provide strong support for the search for novel vaccine strategies. Conjugates consisting of detoxified lipopolysaccharide (LPS) covalently linked to a protein carrier by use of random chemical conjugation procedures have been investigated extensively, achieving promising results in young adults [12, 13]. However, concern for vaccine immunogenicity in children under age 3 has emerged [14]. The alternative strategy that we have tackled is a two-step process aimed at avoiding the need for antigens of biological origin. Synthetic oligosaccharides of well-defined structure, acting as efficient functional mimics of the O-specific polysaccharide (O-SP) moiety of LPS, and equipped for site-selective conjugation at their reducing end, replace the bacterial polysaccharide. This strategy also provides a convenient process and consistent final conjugates. The use of synthetic oligosaccharides has advanced successfully in the case of *S. flexneri* 2a (SF2a), [15] the most prevalent *Shigella* worldwide. The O-SP from SF2a consists of repeating 2)-[3/4Ac]_{90%}-α-L-Rhap-(1→2)-α-L-Rhap-(1→3)-[α-D-Glcp-(1→4)]-α-L-Rhap-(1→3)-[6Ac]_{60%}-β-D-GlcpNAc-(1→units (AB(E)C_{Ac}D) [16]. From this, panels of well-defined oligosaccharides representing SF2a O-SP substructures were synthesized [17-23]. Molecular investigation of their recognition by sets of protective monoclonal IgG antibodies (mIgGs) enabled the identification of relevant antigenic and structural/conformational O-SP mimics [23-25]. Immunogenicity studies in mice shed light on a promising functional O-SP mimic [24]. A trimer of the non-O-acetylated repeating unit, *i.e.* the pentadecasaccharide [AB(E)CD]₃ [22] is such a mimic. A synthetic pentadecasaccharide-tetanus toxoid (TT) conjugate, with an average molar ratio of [AB(E)CD]₃:TT of 15:1 (SF2a-TT15 (1), Scheme 1), was proposed as the first synthetic carbohydrate-based vaccine candidate against endemic shigellosis [15]. The next step is to get the proof of concept of the immunogenicity of SF2a-TT15 in humans. Toward this aim, we report on an improved synthesis of SF2a-TT15. A robust, two-step site-selective bioconjugation process of the [AB(E)CD]₃ hapten to TT is described. The robust reaction of *N*-γ-(maleimidobutyryl)oxysuccinimide ester (GMBS) and TT and subsequent conjugation of the obtained GMB-modified TT and the linker-equipped [AB(E)CD]₃ synthesized in the form of a masked thiol allows complete control of the average number of oligosaccharides on each TT. Key parameters, the control of which warrants robustness, were identified and optimized. Immunogenicity in mice of the novel conjugates issued from this optimized process confirmed former observations. Additionally, the impact of alum, an adjuvant widely used in humans, was assessed for the first time for a *Shigella* synthetic carbohydrate-

based conjugate vaccine candidate. We show that a higher and sustained anti-LPS IgG response was raised upon immunization with the adjuvanted SF2a-TT15 conjugates, as compared to their non-adjuvanted form. Lastly, we show that the anti-LPS IgGs elicited by the original and second generation SF2a-TT15 conjugates, adjuvanted or not in the latter case, recognize SF2a bacteria and not only purified SF2a LPS, and are protective against SF2a infection in a murine model.

Results and Discussion

Improved bioconjugation toward SF2a pentadecasaccharide-TT conjugates

SF2a-TT15 is obtained according to a two-step route (Scheme 1), involving first the synthesis of pentadecasaccharide **2** [22] equipped with a conjugation-ready linker and second its bioconjugation onto GMB-modified TT (TT_{Mal} **4**) [24]. To fulfill the requirements for site-selective conjugation, pentadecasaccharide **2** is the (*S*-acetylthiomethyl)carbonyl aminoethyl glycoside [AB(E)CD]₃-SAc, originally prepared by chemical synthesis, [22] by means of the key aminoethyl pentadecasaccharide intermediate **3** [22, 26]. Herein, our goal was to proceed through additional validation of the original conjugation chemistry to facilitate scale-up during technical transfer for good manufacturing practice (GMP) production. Having thioacetate **2** in hands, the focus was to secure the covalent attachment of [AB(E)CD]₃ to TT in a robust and scalable process.



Scheme 1. Structures of SF2a-TT15 (**1**), the two precursors [AB(E)CD]₃-SAc (**2**) and GMB-modified TT (**4**), and the key aminoethyl pentadecasaccharide **3**.

The conjugation chemistry is a crucial parameter in glycoconjugate vaccines [27-29] and more generally in the development and use of protein conjugates [30, 31]. In this regard, the well-established thiol-to-maleimide addition, [32] used in the synthesis of SF2a-TT15, is an attractive option owing to chemo selectivity and high-yielding coupling efficacy at controlled pH. Although related maleimide spacers were occasionally found immunogenic in mice [33, 34], this phenomenon was not observed in the case of SF2a-

TT15 [15]. Besides, the fact that the licensed Quimi-Hib® encompasses a maleimide spacer [35], comforted our original choice and encouraged the pursuit of our quest for the proof of concept in human with SF2a-TT15.

Initially, eight batches of TT were compared for protein concentration, aggregation status (entities >150 kDa) and primary amine content, of which the latter two could affect the maleimide grafting on TT and thioacetate **2** coupling to intermediate **4** (Scheme 1). The raw materials showed little variation in aggregates ($28.5 \pm 2.5\%$) whereas the amount of primary amine groups varied considerably 79.0 ± 22.6 mol:mol. After primary buffer exchange, the later declined significantly, which was attributed to the removal of glycine, one of the stabilizing constituents. In contrast, the resulting purified and concentrated batches showed little variation in the amount of both aggregates ($29.4 \pm 2.4\%$) and primary amines (39.0 ± 3.4 mol:mol) (Figure S1). The low batch to batch variation of buffer-exchanged TT with respect to aggregation and primary amine content gave confidence to the sustainable production of future batches complying with the same specifications to be used for GMP manufacturing.

With respect to the grafting of GMBS on TT, *N*-[γ -maleimidobutyryloxy]sulfosuccinimide ester (sulfo-GMBS) was used in the original experiments [15]. However, a screening for both sulfo-GMBS and GMBS using different buffers at different pH's led to the conclusion that using GMBS first dissolved in dimethyl sulfoxide (DMSO) and then diluted in 0.1 M 4-(2-Hydroxyethyl)piperazine-1-ethanesulfonic acid (HEPES) would prevent both hydrolysis of the maleimide moiety and aggregate induction (at least 10% less compared to the use of a 0.1 M Phosphate buffer) during TT modification (Table S1 and Figure S2). Also, different organic solvents in combination with the here fore mentioned buffers were compared, and found not to induce any increase in aggregation (Figure S3). Further characterization of the observed aggregate induction was facilitated through a preparative SEC experiment and subsequent grafting of GMBS on four different pools of eluting fractions, corresponding to oligo-, di-, tri- and monomers of TT (pools 1 to 4, respectively). Data showed that grafting of GMBS was relatively evenly distributed on the different entities of TT (Table S2, Figure S4 – S10). Under these conditions, the GMBS-reaction led to a high modification rate and no unreacted TT was observed (Figure S9). Moreover, aggregation induction was only found for the monomeric TT. To further investigate and optimize the process step of grafting the maleimide group on TT, it was subjected to a design of experiments (DoE) approach to find the best parameters for grafting and prevention of aggregation. Five parameters were chosen that could possibly affect the modification reaction; pH, temperature, TT concentration, GMBS:TT ratio and reaction time (Tables 1 and S3).

Table 1: Investigated factors and ranges in the DoE

Variable	Low	Medium	High
Time (min) ^a	15	45	75
pH	7.0	7.5	8.0
Temperature (°C)	4	20	37
TT concentration (mg/mL)	15	35	55
Ratio GMBS:TT (mol:mol) ^b	10	40	160

^a: Uncontrolled variable, a complete DoE was performed for each time point.

^b: Ratio was 2Log transformed for linearization 10: 3.32, 40: 5.32, 160: 7.32.

Statistical analysis of the DoE, using MODDE, showed acceptable R^2 (> 0.6) for the model applied and the ANOVA analysis showed $p < 0.05$ for the regression and $p > 0.05$ for the lack of fit for all models (Figure S11 and Table S4). Concerning maleimide-grafting on TT, temperature and reaction time had a limited impact. In contrast, the TT concentration and GMBS:TT ratio were the most influencing factors followed by pH. Looking into more detail, we observed that both TT concentration and GMBS:TT ratio had an effect on aggregation induction (Figure 1A), whereas only a direct relationship between the extent of amino group modification and the GMBS:TT proportions was observed (Figure 1B).

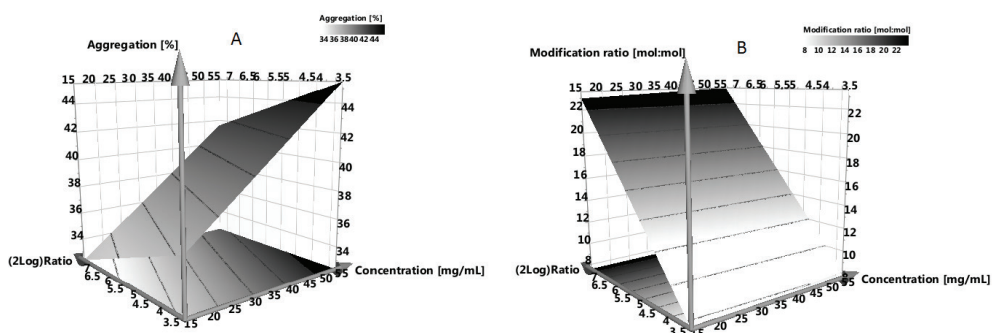


Figure 1: **A:** Response surface plot DoE results for aggregation. X-axis: Protein concentration (mg/mL), Y-axis: applied ratio GMBS:TT 2log transformed for linearization, Z-axis: modification ratio (mol:mol). **B:** Response surface plot DoE results for the modification ratio. X-axis: Protein concentration (mg/mL), Y-axis: applied ratio GMBS:TT 2log transformed for linearization, Z-axis: aggregation (%).

Using the data from the DoE a sweet spot analysis was performed. It was concluded that a TT concentration of 15 mg/mL in combination with a GMBS:TT ratio of 160 and pH between 7.5 - 8.0 was preferred to prevent aggregation induction, less than 7.5%

(Figure S12). Following these results a robustness DoE was conducted using the preferred reaction conditions (protein concentration 15 mg/mL ($\pm 10\%$), GMBS:TT ratio 160 ($\pm 10\%$), pH 7.8 ($\pm 10\%$) and temperature 15 – 25 °C) (Tables S5 and S6). Within these variations, all products complied with the set specifications, therefore facilitating a proper control of the activation step to reach intermediate **4** comprising in average, 25 maleimide groups to each TT. As in the preliminary experiments (Table S2, Figures S9 and S10), the number of covalently linked maleimide groups was calculated from the total protein content as measured by the BCA assays and from the decreased average number of free primary amines before (31 per TT) and after (6 per protein **4**) the modification reaction using TNBS assays. Analogously and critical to our goal, under optimum conditions the outcome of the [2 + 4] coupling demonstrated reproducible kinetics (Figure 2).

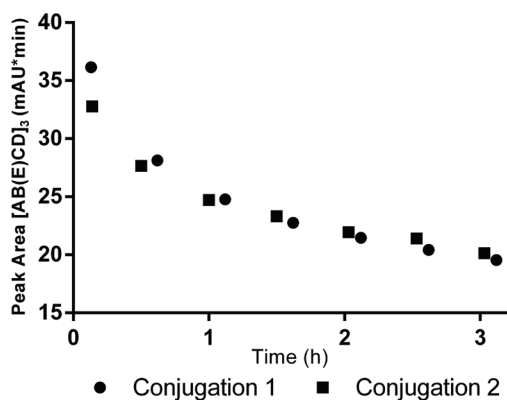


Figure 2: [2 + 4] conjugation kinetics showing the decrease of the peak area of the [AB(E)CD]₃ entities in time. X-axis: time (h), Y-axis: Peak Area of the [AB(E)CD]₃ entities (mAU×min).

The next step consisted in optimizing the purification conditions to ensure the absence of any free pentadecasaccharide in the final preparations (Figure S13). Using the newly established protocol, four conjugates displaying [AB(E)CD]₃:TT average loadings of 4.6 (C1), 8.5 (C2), 17 (C3) and 26 (C4), issued from the use of 5, 10, 25 and 50 molar equivalents of thioacetate **2** per intermediate **4**, respectively, were synthesized. These differences in final conjugated ratio were nicely observed during HPSEC analysis (Figure 3).

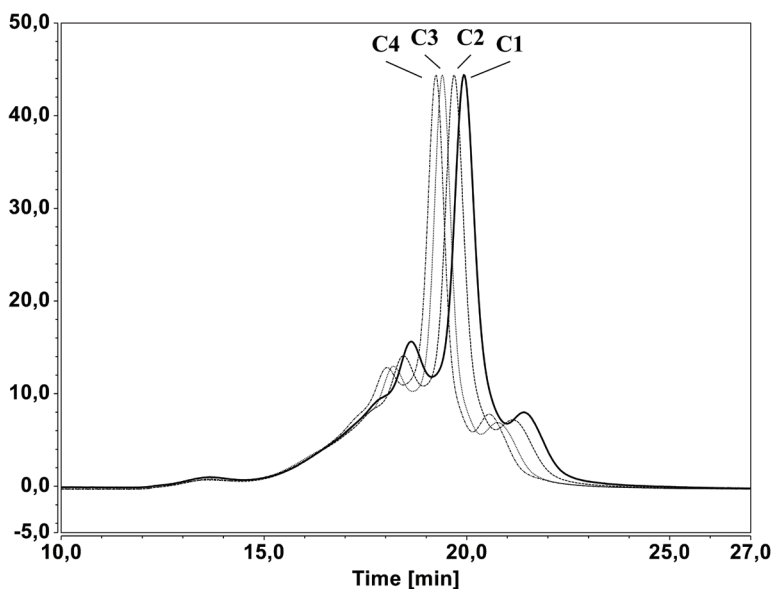


Figure 3: HPSEC analysis of conjugates C1 – C4. X-axis: retention time (min), Y-axis: absorbance (mAU). UV signals were all normalized for the monomer peak (highest peak in chromatogram).

An $[AB(E)CD]_3:TT$ ratio above 20 – in fact 26 based on the Anthrone colorimetric assay – was achieved for the first time, which was indicative of a very powerful process. In fact, it seems that a maximum loading of pentadecasaccharide is achieved, since the average number of modified amino groups coincides with the average number of $[AB(E)CD]_3$ haptens in the final conjugates. The efficiency of the conjugation step relative to thioacetate **2** with escalating molar equivalents of $[AB(E)CD]_3$ per TT was very comparable ($\sim 70\%$) for conjugates C1, C2 and C3, having average loadings of 4.6, 8.5 and 17, respectively. In contrast, the yield of conjugate relative to thioacetate **2** dropped to $\sim 50\%$ in the case of the more heavily loaded C4 ($[AB(E)CD]_3:TT$ molar ratio of 26), which was merely the effect of overshooting the maximum amount of possible conjugated groups available on intermediate **4**. While this observation is in agreement with the accessibility of the lysine residues serving as coupling sites on TT, it is also a relevant parameter, which cannot be left without attention in the selection of a promising vaccine candidate. In this case, up to conjugate C3 with a $[AB(E)CD]_3:TT$ ratio of 17 and possible higher ratios, the yield of the $[2+4]$ conjugation step relative to pentadecasaccharide **2** was 70%, which was considered as acceptable. Noteworthy, the yield of the $[2+4]$ conjugation step relative to intermediate **4** was always in the range of $68 \pm 10\%$, remaining excellent independently of the final composition of the conjugate. The presence of any free unreacted TT at this point is highly unlikely taking the GMBS-modification step into account (Figure S9). Final

capping using cysteamine-HCl did not induce any changes in the composition of the conjugates regarding aggregation (data not shown).

Immunogenicity in mice of the SF2a pentadecasaccharide-TT conjugates

Next, the immunogenicity of the four newly synthesized SF2a pentadecasaccharide-TT conjugates (C1 - C4) differing by their $[AB(E)CD]_3:TT$ ratio was assessed in mice. For each glycoconjugate, a very low level of anti-SF2a LPS Ab response (titer below 1/100) was measured after the two first injections (S1 and S2, data not shown). As previously noticed, [15] a significant increase of the anti-SF2a LPS IgG response was observed after the third injection (S3), using a dose corresponding to 2.5 μg of carbohydrate. Furthermore, the anti-LPS IgG titers rose by a factor 2 after the fourth injection (S4) for all conjugates except C1 (Figure 4) and were sustained for at least 6 months (Figure S14). Conjugate C1 was significantly less immunogenic than the others, substantiating the need for a minimal $[AB(E)CD]_3:TT$ ratio for potency [15]. Although not statistically significant, there was a trend towards a slightly lower immunogenicity for the highly loaded $[AB(E)CD]_{3-26}:TT$ (C4) as compared to C2 and C3 (Figures 4 and S14). Although known for HSA and CRM197 glycoconjugates [36, 37] limitations relevant to hapten loading were to our knowledge never reported in the case of TT conjugated to synthetic carbohydrate haptens. Our data show strong evidence that conjugates encompassing an $[AB(E)CD]_3:TT$ average loading of 17 ± 5 comply with immunogenicity criteria and support the previous selection of the original SF2a-TT15 ($[AB(E)CD]_{3-15}:TT$, **1**) as an investigational vaccine.

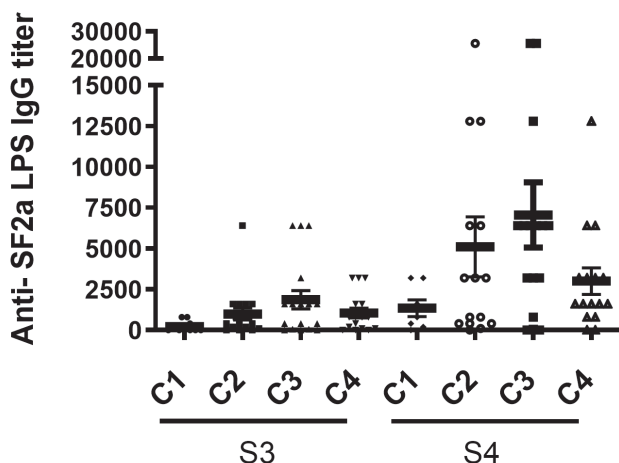


Figure 4: Anti-SF2a LPS IgG titer induced in mice receiving 3 (S3) and 4 (S4) doses of glycoconjugates C1 – C4 containing 2.5 μg of $[AB(E)CD]_3$. X-axis: Glycoconjugate and number of immunizations. Y-axis: Anti-SF2a LPS IgG titer. No statistically significant differences were observed between C2, C3 and C4. The Ab titers induced by these glycoconjugates were significantly higher than that induced by C1. Mean \pm Standard Error of Mean (SEM) are indicated (**bold lines**).

Alum, an adjuvant promoting Ab response, is present in a number of licensed carbohydrate-conjugate vaccines including Prevnar 13® or Synflorix®. So far, it was tested only once in mice for a SF2a glycoconjugate vaccine candidate – in this case, a lattice type conjugate vaccine issued from random conjugation of the detoxified SF2a LPS onto rEPA, a recombinant form of *Pseudomonas aeruginosa* exotoxin A [38]. Therefore, the contribution of alum was assessed next. Undoubtedly, after 3 doses containing 2.5 µg of [AB(E)CD]₃, C2 and C3 adjuvanted with alum gave rise to a significantly higher anti-LPS SF2a IgG titer (S3, 4 and 6 fold increase, respectively) as compared to non-adjuvanted C2 and C3 (Figure 5A and 5B). These novel data support previous findings reported for the only alum-adjuvanted SF2a glycoconjugate vaccine candidate evaluated in mice [38]. Herein, for both alum-adjuvanted conjugates, the induced Ab response was comparable in terms of Ab titer and sustainability, with Ab titer maintained for at least 14 months. At this time point the Ab titers raised with adjuvanted C2 and C3 were still about 20 and 15 times higher than those elicited by non-adjuvanted C2 and C3, respectively (Figure 5B). It is of note that in its alum-adjuvanted form, C2, which has a [AB(E)CD]₃:TT loading half of that of C3, did not give rise to a significantly higher Ab response than non adjuvanted C3 (Figure 5A and 5B). Detailed reports on the role of alum in synthetic carbohydrate-based vaccine formulations can only be interpreted on a case-to-case basis [35, 37, 39-41]. Moreover, data obtained in mice for alum-adjuvanted polysaccharide conjugate vaccine candidates do not necessarily translate to observations in adult volunteers [38]. Nevertheless, this original finding could support further investigation on the systematic introduction of alum in carbohydrate-based vaccine formulations aimed at providing long duration immunity with a minimum number of doses such as that requested, in particular, in young children living in endemic areas.

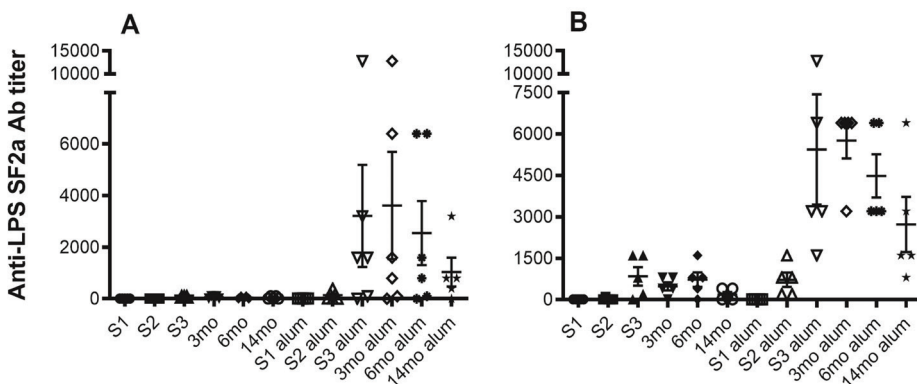


Figure 5: Impact of alum on the immunogenicity of conjugates C2 {[AB(E)CD]₃}-_{8.5}-TT (**A**) and C3 {[AB(E)CD]₃}-₁₇-TT (**B**) administered with or without alum. Ab titers were measured one week after the first, second and third injection (S1, S2 and S3, respectively), and after 3, 6 and 14 months after the 3rd one (3mo, 6mo, 14mo, respectively). X-axis: time of blood sample analysis following immunizations in the absence or presence of alum. Y-axis: anti-SF2a LPS IgG titer. Mean ± SEM are indicated (**bold** line).

Besides binding to purified SF2a LPS [15], Abs induced by C2 and C3 administered in their adjuvanted or non-adjuvanted forms, were shown to recognize virulent SF2a bacteria (Figure 6A), similarly to the recognition observed with sera induced by the original SF2a-TT15 [15] (Figure 6B).

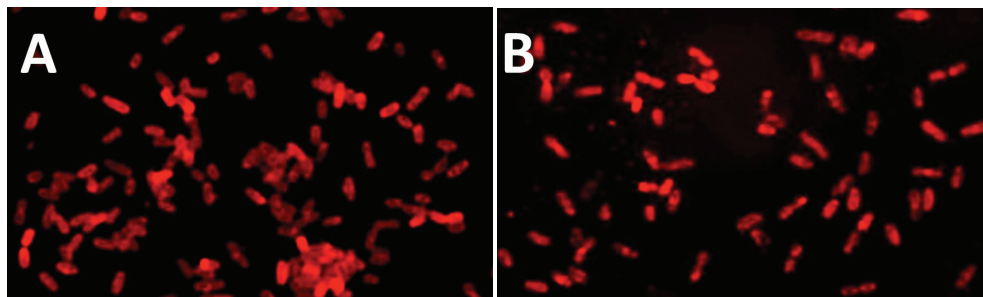


Figure 6: Recognition of SF2a bacteria by mouse sera elicited upon immunization with $\{[AB(E)CD]_3\}_{-8,5}$ -TT (C2) or $\{[AB(E)CD]_3\}_{-17}$ -TT (C3), adjuvanted or not with alum (**A**) and by an original SF2a-TT15 (**B**). *Shigella*-specific Abs in mouse sera were detected upon their binding to bacteria by using anti-mouse IgG Abs coupled to a fluorophore and visualized with a fluorescence microscope. Controls with fluorescent anti-mouse IgG Abs only showed no bacterial recognition (data not shown).

4

In addition, the protective capacity of the induced Abs against SF2a infection was tested *in vivo* in a mouse model of pulmonary infection [42] (Figure 7). As compared to a control group of mice administered intranasally with virulent SF2a bacteria mixed with pre-immune serum, a 10 and 20 fold-reduction in the lung bacterial load was observed in mice administered intranasally with virulent SF2a bacteria mixed with sera displaying the highest raised anti-SF2a IgG titer (1/25,600) from mice immunized with C2 and C3, respectively. Reduction of the bacterial load was shown to be dependent on the anti-SF2a LPS Ab titer. Indeed, by using C2- and C3-induced sera displaying a lower anti-SF2a LPS Ab titer (1/12,800), a 4.9 and 9 fold reduction in the CFU/lung was observed with C2- and C3-induced sera, respectively, as compared to control mice. No significant difference between C2 and C3 was observed. These results confirm our previously published findings [15], showing that SF2a-TT15 incorporating $[AB(E)CD]_3$, a synthetic pentadecasaccharide hapten mimicking the SF2a O-SP, elicits a protective Ab response in mice.

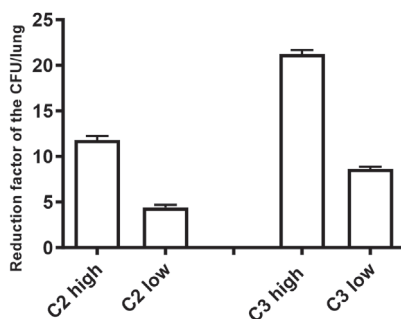


Figure 7: Protective capacity of the anti-SF2a LPS sera induced by C2 ($\{[AB(E)CD]_3\}_{-8.5}$ -TT) and C3 ($\{[AB(E)CD]_3\}_{-17}$ -TT). X-axis: Sera selected for evaluation. Y-axis: Reduction factor of the number of colony-forming units (CFU) per lung in comparison to that in control mice. Sera displaying an anti-SF2a LPS Ab titer of 1/25,600 (high) and 1/12,800 (low) were used. CFU in the lungs were measured 24 h post infection. Mean \pm SEM is indicated.

4 Conclusion

Access to well-defined complex oligosaccharides has for long impaired investigations on their potential as antibacterial vaccine components or therapeutics. This is no longer the case [28, 43, 44]. Yet, Quimi-Hib[®] is still the only licensed synthetic carbohydrate-based vaccine. Paving the way to a phase I clinical trial for SF2a-TT15 (**1**), the first synthetic carbohydrate-based vaccine candidate against endemic shigellosis, this contribution reports an improved synthesis of the selected glycoconjugate ready for GMP scale up. On one hand, the over 40 step chemical synthesis of the conjugation-ready pentadecasaccharide hapten **2** was successfully reproduced as a preliminary step to obtaining the data detailed here. On the other hand, major results reported herein consisted in improving the [**2**+**4**] bioconjugation step, above all ensuring an improved and reproducible process leading to SF2a-TT15. The newly established conjugation process is very robust and allows a substantial margin in terms of applicable variables. The loading of covalently linked $[AB(E)CD]_3$ is efficiently controlled by varying the **2:4** ratio during conjugation, yielding glycoconjugates that comply with the set criteria. The method is applicable to any thiol-equipped hapten. As expected, the finally selected SF2a-TT15 conjugate is immunogenic in mice. It was found superior to the other conjugates described herein, which only differed from the former by their $[AB(E)CD]_3$:TT loading. In addition, in regard to the scarcity of data available in the literature and the case-to-case use of alum in commercialized glycoconjugate vaccines, the novel findings disclosed herein clearly add to the field by demonstrating for the first time the powerful influence of alum on the immunogenicity of a *Shigella* synthetic carbohydrate-based conjugate vaccine candidate, with an increased anti-SF2a LPS IgG Ab titer sustained for more than a year.

Experimental Procedures

BCA assay

Protein concentrations were determined using the Bicinchoninic Acid (BCA) assay (Thermo Fisher Scientific, Pierce) with the following modifications. A calibration curve ranging from 6.25 to 50 μg was constructed using a 0.25 mg/mL BSA standard solution and both sample and standard volumes were 200 μL . The color was detected at 562 nm using a Shimadzu UV 2401-PC double-beam spectrophotometer. From the standard curve, the protein quantities (q , in μg) were calculated.

TNBS assay

Primary amine groups were quantified using an adapted 2,4,6-trinitrobenzenesulfonic acid (TNBS) assay [45, 46]. In short, a calibration curve, ranging from 5 to 60 nmol, was constructed using a 1.0 mM *N*- α -acetyl-L-lysine stock solution. Aliquots of 0.2 M borate buffer (200 μL) and 0.1% TNBS reagent (200 μL) were added, followed by incubation at 37 °C for 120 min. Samples were subsequently cooled to ambient temperature and 10 % SDS (200 μL) was added to prevent protein aggregation followed by 1 M HCl (400 μL) for acidification. The color was detected at 340 nm using a Shimadzu UV 2401-PC double-beam spectrophotometer. From the standard curve, the molar amount of amine groups (q , in nmol) was calculated.

Anthrone assay

The concentrations of [AB(E)CD]₃, in the form of thioacetate **2** or conjugated to TT, were determined using an adapted Anthrone assay [47-49]. In short, a calibration curve, ranging from 10 to 100 nmol, was constructed using a 1:1:1 mixture of 0.2 mM D-glucose, 0.6 mM L-rhamnose and 0.2 mM *N*-acetyl-D-glucosamine as a stock solution. All samples were cooled on ice before the anthrone color reagent (1 mL, 0.2% w/v anthrone in sulfuric acid 95-97%) was added. All samples were equilibrated to ambient temperature and incubated at 90 °C for 15 min. The color was detected at 625 nm using a Shimadzu UV 2401-PC double-beam spectrophotometer. From the standard curve, the molar amount of [AB(E)CD]₃ (q , in nmol) was calculated.

High Performance Size Exclusion Chromatography (HPSEC)

An UltiMate-3000 (Thermo Fisher Scientific) HPLC system was equipped with a SEC Guard column 100 (Wyatt technology), SEC protein column 100 (Wyatt technology), and SEC protein column 30 (Wyatt technology) mounted in series (in this order). The eluent was 0.1 μm sterile filtered phosphate buffered saline (PBS) 10 mM, pH 7.2, and elution was

performed at 1 mL/min (average backpressure 60 bar). All chromatographic parameters were calculated using the Chromeleon software (v. 7.1.2, SP 2, Thermo Fisher Scientific). The percentage of aggregates (*i.e.* all entities larger than the TT monomer) is expressed as (peak area aggregates / total peak area) \times 100%.

NMR analysis

NMR analysis was performed using a JEOL 400MHz spectrometer. Both linkers, *N*- γ -(maleimidobutyl)oxysuccinimide ester (GMBS, Fluka), and *N*- γ -(maleimidobutyl)oxysulfosuccinimide ester (sulfo-GMBS, Sigma) [50-52], were dissolved at 10 mM concentration in 0.1 M phosphate buffer at both pH 7 and 8. To 0.5 mL of the resulting solutions, trimethylsilyl propanoic acid sodium salt (TMSP-2,2,3,3-D4) (0.65 mg/mL D₂O, 0.2 mL) was added as internal standard. ¹H-NMR spectra were acquired at 25 °C with pre-saturation of the water signal at 4.8 ppm using a 30 degree pulse angle. Sequentially, spectra were acquired using a delay of 300 s. Considering the number of scans, acquisition time and relaxation delay, the actual delay between kinetic data points amounted to 434.6 s.

Buffer exchange and concentration

Buffer exchange and concentration was performed using spin filters (Millipore, Amicon ultra 4 and 15) with a 30 kDa MWCO (15 min, 5,000 \times *g*, ambient temperature). For each buffer exchange at least four consecutive cycles were performed, with an exchange ratio of at least 15 per cycle. This led to a final exchange ratio of 15⁴ (\sim 50,000), considered sufficient to replace any buffer or remove any residual constituents like unreacted or hydrolyzed GMBS, remaining [AB(E)CD]₃-SAC (**2**) and derivatives thereof (Figure S13), or DMSO.

Sample preparation and execution of DoE

To this end, aliquots of TT were concentrated and buffer exchanged to their buffers with respective pH and protein concentrations. Samples of 900 μ L concentrated TT were transferred to the individual reaction vessels. After equilibration at the designated temperature for 30 min, the maleimide introduction was initiated by the addition of GMBS dissolved in 60 μ L DMSO at their respective concentrations. After 15, 45 and 75 min, 300 μ L samples were taken from each reaction vessel and directly buffer exchanged (0.1 M Phosphate buffer, pH 6.0, 5 mM Ethylenediaminetetraacetic acid (EDTA)) to stop the reaction and to remove DMSO and any residual or hydrolyzed GMBS. The efficiency of the reaction was evaluated by the decrease in primary amine concentration (BCA and TNBS assay) and total and net induced aggregation (HPSEC analysis). The design of the model and regression analysis was performed using the Umetrics software MODDEV 10.1.1.

TT activation with maleimide followed by conjugation

5.4 mL crude TT (Mw 150 kDa) was buffer exchanged with 0.1 M HEPES pH 7.8 and finally concentrated to 2.0 mL (final concentration of TT: 16 mg/mL). 1.9 mL of the concentrated and buffer exchanged TT (16 mg/mL, 0.107 mM, 0.203 μ mol) was modified using 9.1 mg (32 μ mol) of GMBS dissolved in 127 μ L DMSO (Sigma Aldrich, Fluka, 256 mM, 72 mg/mL) yielding a ratio of 1:160 (TT:GMBS) and a final TT concentration of 15 mg/mL. Modification was performed at ambient temperature for 30 min. After this time, the entire volume of intermediate **4** (4, 2.03 mL) was buffer exchanged with 0.1 M Phosphate buffer pH 6.0, 5 mM EDTA and finally concentrated to 1.62 mL to reach a final concentration of intermediate **4** of 18.75 mg/mL (measured by BCA).

For the conjugation of pentadecasaccharide **2** onto intermediate **4**, 4 individual portions (0.16 mL each) of intermediate **4** (18.75 mg/mL, 3.0 mg, 20 nmol) were used. Conjugation was performed applying **2:4** ratios of 6.25, 12.5, 25 and 50, for which 125 nmol (0.32 mg), 250 nmol (0.65 mg), 500 nmol (1.29 mg) and 1000 nmol (2.59 mg) of pentadecasaccharide **2** were added to each of the vial containing intermediate **4**, respectively, this in a final volume of 20 μ L. For this, thioacetate **2** (5.93 mg) was dissolved in water for injection (WFI, 46 μ L). This stock solution was serial diluted 1/2 (20 μ L stock + 20 μ L WFI etc.) to facilitate the addition of the required amounts for the lower ratios. For all ratios, pentadecasaccharide **2** was added in 20 μ L portions.

Hydroxylamine was added in a 15:1 ratio (NH₂OH:**2**; 1.8, 3.6, 7.5, 15.0 μ mol, respectively) to the intermediate **4** and pentadecasaccharide **2** mixture. Hydroxylamine was treated similarly to the serial dilution for thioacetate **2**. For this, NH₂OH (11.15 mg) was dissolved in WFI (214 μ L). This stock solution was serial diluted 1/2 (20 μ L stock + 20 μ L WFI etc.) to facilitate the addition of NH₂OH quantities needed for the lower conjugation ratios. For all ratios, NH₂OH was added in 20 μ L portions. Conjugation was performed at ambient temperature for 180 min, with final protein concentrations at 15 mg/mL. Conjugation progress was monitored by HPLC (injections at 30 min intervals). Finally, cysteamine-HCl was added to cap any residual reactive maleimide groups. For this, cysteamine-HCl (0.4 mg, 3.0 μ mol, 19 mg/mL) in WFI (20 μ L) was added to all conjugates, facilitating a molar excess of 160 compared to intermediate **4**.

The entire volume of conjugate (0.2 mL) was buffer exchanged with 0.1 M Phosphate buffer pH 6.0 and finally harvested. Volumes of harvest were kept as close as possible to the initial starting volume of 0.2 mL. Final conjugates were analyzed by BCA and Anthrone assay for conjugation yield and carbohydrate:protein ratio.

Conjugation kinetics determination

Conjugation experiments were performed using intermediate **4** prepared from crude TT according to the optimum parameters as found in the DoE. In order to investigate the conjugation dynamics and kinetics, two identical consecutive experiments were performed where different amounts of the pentadecasaccharide **2** were used in a reaction with intermediate **4**. Both conjugation experiments, using a **2:4** molar ratio of 25, were monitored in time by HPSEC analysis. The decrease in peak area for pentadecasaccharide **2** and derivatives thereof was used as a parameter to monitor the progress of the conjugation. Although it was found that the pentadecasaccharide **2** co-eluted with the EDTA present in the conjugation buffer, the peak area of the co-eluting compounds was monitored in time since the EDTA concentration remained constant. It was found that there was a very good correlation for the decrease of the peak area in time, meaning that the conjugations showed good kinetics ($R^2 > 0.99$) and were very comparable.

Mice immunization

Seven week-old Balb/c mice (Janvier Labs, France) were immunized with each of the C1, C2, C3 and C4 conjugates intramuscularly (i.m.) at multiple sites with 2.5 mg equivalent of [AB(E)CD]₃ per dose in 200 μ L of physiological water. Three injections were performed at 3 week-interval, with a fourth injection one month after the third one. Blood samples were recovered one week after each injection (sera S1, S2, S3, and S4) and at 3 and 6 months after the 4th injection (sera S3mo and S6mo, respectively). Fourteen mice were used for glycoconjugates C2, C3 and C4, and only seven mice for glycoconjugate C1 due to limited availability of this conjugate. To test the impact of alum on their immunogenicity, the conjugates C2 and C3 were adsorbed on alum as follows. Alum, also named aluminium hydroxide gel adjuvant (Alhydrogel, Brenntag, Denmark), was used at a concentration of 1.4 mg/mL in Tris pH 7.2 20 mM, and mixed v/v with the conjugates. After overnight incubation at ambient temperature, the adjuvanted C2 and C3 glycoconjugates were then injected in mice i.m. at multiple sites using 500 μ L per mouse/per injection. Three immunizations were performed at 3 week-interval with a dose equivalent to 2.5 μ g of [AB(E)CD]₃, and a dose of 0.35 mg of alum per mouse/per injection. Blood samples were recovered one week after each injection (S1, S2, S3) and 3, 6, and 14 months after the 3rd injection (3mo, 6mo, and 14mo). Five mice were used per group, including groups receiving non adjuvanted C2 and C3 used as a control.

Measurement of the anti-SF2a IgG response

The glycoconjugate-induced anti-LPS IgG response specific for SF2a LPS was measured by ELISA using LPS purified from the SF2a 454 strain as previously described [24]. Briefly, 2.5 μ g of purified SF2a LPS was coated per ELISA plate well in PBS and incubated at 4 $^{\circ}$ C

overnight. After washing the wells with PBS-Tween 20 0.01%, saturation was performed by incubating the plate for 30 min at 37 °C with PBS-BSA 1%. Then, serial dilutions of mouse sera in PBS-BSA 1% were incubated for 1 h at 37 °C. After washing with PBS-Tween 20 0.01%, anti-mouse IgG alkaline phosphatase-labeled conjugate (Sigma-Aldrich) was used as secondary antibody at a dilution of 1/5,000. The IgG titer was defined as the last dilution of serum giving rise to twice the value obtained with pre-immune serum.

Recognition of SF2a bacteria with glycoconjugate-induced sera

SF2a bacteria (strain 454) were grown in TCS (Trypto-Casein-Soy) medium at 37 °C with shaking. When reaching an optical density at 600 nm of 0.5, 1 mL of the bacterial culture was centrifuged at 5000 rpm for 15 min. The bacterial pellet was resuspended in PBS, and the resulting solution centrifuged once again. Then, the PBS-washed bacterial pellet was resuspended in 1 mL PBS, and 100 µL were put on coverslips. After fixation with paraformaldehyde 4% for 20 min at ambient temperature, and saturation with a blocking buffer for 10 min at ambient temperature, bacteria were incubated overnight at 4 °C with 100 µL of immune sera (diluted 1/1,000) from mice immunized with C2 and C3 with or without alum, and a first generation SF2a-TT15 conjugate [15]. After 2 PBS washings, anti-mouse IgG Alexa 594-labeled conjugate (Sigma-Aldrich) was used as secondary antibody at a dilution of 1/5,000 and incubated for 1 h at ambient temperature, while protecting the coverslips from light. After 2 PBS washings, DAPI (4',6'-diamidino-2-phenylindole) staining was performed for 3 s to label bacterial DNA. After 2 washings with distilled water, coverslips were mounted using ProLong-mounting medium (Invitrogen). Fluorescence images were acquired by inverted wide-field (Observer Z1; Carl Zeiss).

Protective capacity of the anti-LPS SF2a IgGs induced by conjugates C2 and C3

The protective capacity of the induced sera was measured in the lung mouse model [42]. Briefly, C2- and C3-induced sera displaying an anti-SF2a LPS IgG antibody titer of 1/25,600 were administered (i.n.) using a volume of 20 µL to mice previously anesthetized via the intramuscular route with 50 µL of a mixture of 12.5% of ketamine (Merial) and 12.5% acepromazine (Vetoquinol). Intranasal challenge was performed using 10⁸ SF2a virulent bacteria in a volume of 20 µL. Measurement of lung-bacterial load was performed 24 h post infection and compared to that in control mice receiving non immune serum. Mice were sacrificed by cervical dislocation and lungs were removed en bloc and ground in 10 mL of sterile PBS (Ultra-turrax T25 apparatus, Janke and Kunkel IKA Labortechnik). Dilutions were plated on trypticase soy broth plates for CFU enumeration. Each experiment was performed using 8 mice per group and repeated 3 times. All of the animal experiments were approved by the Institut Pasteur Animal Use Committee.

Acknowledgments

The authors thank Dr. M. Beurret (Janssen, NL) for initial input, A. de Haan and C. Smitsman (Intravacc) for their role in the DoE study, Bilthoven Biologicals (NL) for the gift of TT, and F. Bonhomme (CNRS UMR3523) for the NMR and HRMS spectra. Lastly, the authors would like to dedicate this manuscript to B. Zomer for his insights and support on this project, they are forever grateful for his contributions.

Funding sources

The research leading to these results has received funding from Institut Pasteur, Agence Nationale pour la Recherche (ANR (France), Grant ANR-06-EMPB-013-02, GLYCOVAX), Korea Science and Engineering Foundation (KOSEF, Post-doctoral fellowship to T.H.K), the French Government's Investissement d'Avenir program, Laboratoire d'Excellence "Integrative Biology of Emerging Infectious Diseases" (grant n°ANR-10-LABX-62-IBEID), and the European Union's Seventh Framework Programme for research, technological development and demonstration under Grant Agreement no 261472-STOPENERICs.

Supporting Information

Experimental protocols for the preliminary investigations, DoE experiments, bioconjugation step and glycoconjugate analysis, including analytical data for glycoconjugates C1 – C4. Complementary immunogenicity data for glycoconjugates C1 – C4. This material is available free of charge via the Internet at <http://pubs.acs.org>.

Abbreviations

AB(E)CD: basic repeating unit of the SF2a O-SP ; CFU: Colony-Forming Unit ; DAPI: 4',6-diamidino-2-phenylindole ; DMSO: dimethyl sulfoxide ; DoE: Design of Experiment ; EDTA: Ethylenediaminetetraacetic acid ; ELISA: Enzyme-Linked ImmunoSorbent Assay ; GMBS: *N*-[γ -maleimidobutyryloxy]succinimide ester ; GMP: Good Manufacturing Practice ; HEPES: 4-(2-Hydroxyethyl)piperazine-1-ethanesulfonic acid ; IgG: Immunoglobulin of isotype G ; LPS: Lipopolysaccharide ; Mal: Maleimide ; mIgG: Monoclonal IgG antibody ; O-SP: O-Specific Polysaccharide ; SF2a: *Shigella flexneri* serotype 2a ; SF2a-TT15: SF2a glycovaccine candidate ; sulfo-GMBS: *N*-[γ -maleimidobutyryloxy]sulfosuccinimide ester ; TT: tetanus toxoid ; WFI: water for injection.

Present Addresses

† Technical Textile & Materials Group, Korea Institute of Industrial Technology, Ansan 15588, Korea

Author Contributions

‡ These authors contributed equally.

Notes

The authors declare no competing financial interests.

References and footnotes

1. World Health Organization. Factsheet No 330: Diarrhoeal disease. WHO. 2013 [cited 2013 Sep 24]. Available from: <http://www.who.int/mediacentre/factsheets/fs330/en/>: p.
2. Fischer Walker, C., et al., Diarrhea incidence in low- and middle-income countries in 1990 and 2010: a systematic review. *BMC Public Health*, 2012. 12(1): p. 220.
3. Fischer Walker, C.L., et al., Does childhood diarrhea influence cognition beyond the diarrhea-stunting pathway? *PLoS ONE*, 2012. 7(10): p. e47908.
4. Scharf, R.J., M.D. Deboer, and R.L. Guerrant, Recent advances in understanding the long-term sequelae of childhood infectious diarrhea. *Curr. Infect. Dis. Rep.*, 2014. 16(6): p. 408.
5. Kolling, G., M. Wu, and R.L. Guerrant, Enteric pathogens through life stages. *Front. Cell. Infect. Microbiol.*, 2012. 2: p. 114.
6. Kotloff, K.L., et al., Burden and aetiology of diarrhoeal disease in infants and young children in developing countries (the Global Enteric Multicenter Study, GEMS): a prospective, case-control study. *Lancet*, 2013. 382(9888): p. 209-222.
7. Niyogi, S.K., Shigellosis. *J. Microbiol.*, 2005. 43(2): p. 133-43.
8. Livio, S., et al., Shigella isolates from the Global Enteric Multicenter Study inform vaccine development. *Clin. Infect. Dis.*, 2014. 59(7): p. 933-941.
9. Levine, M.M., et al., Clinical trials of Shigella vaccines: two steps forward and one step back on a long, hard road. *Nat. Rev. Microbiol.*, 2007. 5(7): p. 540-53.
10. Kaminski, R.W. and E.V. Oaks, Inactivated and subunit vaccines to prevent shigellosis. *Expert Rev. Vaccines*, 2009. 8(12): p. 1693-1704.
11. Klontz, K.C. and N. Singh, Treatment of drug-resistant Shigella infections. *Expert Rev. Anti Infect. Ther.*, 2015. 13: p. 69-80.
12. Barry, E.M., et al., Progress and pitfalls in Shigella vaccine research. *Nat. Rev. Gastroenterol. Hepatol.*, 2013. 10(4): p. 245-255.
13. Ashkenazi, S. and D. Cohen, An update on vaccines against Shigella. *Ther. Adv. Vaccines*, 2013. 1(1): p. 113-123.
14. Passwell, J.H., et al., Age-related efficacy of Shigella O-specific polysaccharide conjugates in 1-4-year-old Israeli children. *Vaccine*, 2010. 28(10): p. 2231-2235.
15. Phalipon, A., et al., A synthetic carbohydrate-protein conjugate vaccine candidate against Shigella flexneri

- 2a infection. *J. Immunol.*, 2009. 182(4): p. 2241-2247.
16. Perepelov, A.V., et al., *Shigella flexneri* O-antigens revisited: final elucidation of the O-acetylation profiles and a survey of the O-antigen structure diversity. *FEMS Immunol. Med. Microbiol.*, 2012. 66(2): p. 201-210.
 17. Mulard, L.A., C. Costachel, and P.J. Sansonetti, Synthesis of the methyl glycosides of a di- and two trisaccharide fragments specific for the *Shigella flexneri* serotype 2a O-antigen. *J. Carbohydr. Chem.*, 2000. 19(7): p. 849-877.
 18. Costachel, C., P.S. Sansonetti, and L.A. Mulard, Linear synthesis of the methyl glycosides of tetra- and pentasaccharide fragments specific for the *Shigella flexneri* serotype 2a O-antigen. *J. Carbohydr. Chem.*, 2000. 19(9): p. 1131-1150.
 19. Segat-Dioury, F. and L.A. Mulard, Convergent synthesis of the methyl glycosides of a tetra- and a pentasaccharide fragment of the *Shigella flexneri* serotype 2a O-specific polysaccharide. *Tetrahedron Asymm.*, 2002. 13: p. 2211-2222.
 20. Bélot, F., et al., Synthesis of the methyl glycoside of a branched octasaccharide fragment specific for the *Shigella flexneri* serotype 2a O-antigen. *Tetrahedron Lett.*, 2002. 43: p. 8215-8218.
 21. Bélot, F., et al., Blockwise approach to fragments of the O-specific polysaccharide of *Shigella flexneri* serotype 2a: Convergent synthesis of a decasaccharide representative of a dimer of the branched repeating unit. *J. Org. Chem.*, 2004. 69(4): p. 1060-1074.
 22. Bélot, F., et al., Synthesis of two linear PADRE conjugates bearing a deca- or pentadecasaccharide B epitope as potential synthetic vaccines against *Shigella flexneri* serotype 2a infection. *Chem. Eur. J.*, 2005. 11(5): p. 1625-1635.
 23. Gauthier, C., et al., Non-stoichiometric O-acetylation of *Shigella flexneri* 2a O-specific polysaccharide: synthesis and antigenicity. *Org. Biomol. Chem.*, 2014. 12(24): p. 4218-32.
 24. Phalipon, A., et al., Characterization of functional oligosaccharide mimics of the *Shigella flexneri* serotype 2a O-antigen: Implications for the development of a chemically defined glycoconjugate vaccine. *J. Immunol.*, 2006. 176(3): p. 1686-1694.
 25. Vulliez-Le Normand, B., et al., Structures of synthetic O-antigen fragments from serotype 2a *Shigella flexneri* in complex with a protective monoclonal antibody. *Proc. Natl. Acad. Sci. U S A*, 2008. 105(29): p. 9976-9981.
 26. Salamone, S., et al., Programmed chemo-enzymatic synthesis of the oligosaccharide component of a carbohydrate-based antibacterial vaccine candidate. *Chem. Commun.*, 2015. 51(13): p. 2581-4.
 27. Hu, Q.-Y., et al., Synthesis of a well-defined glycoconjugate vaccine by a tyrosine-selective conjugation strategy. *Chem. Sci.*, 2013. 4(10): p. 3827-3832.
 28. Adamo, R., et al., Synthetically defined glycoprotein vaccines: current status and future directions. *Chem. Sci.*, 2013. 4(8): p. 2995-3008.
 29. Nilo, A., et al., Exploring the Effect of Conjugation Site and Chemistry on the Immunogenicity of an anti-Group B *Streptococcus* Glycoconjugate Vaccine Based on GBS67 Pilus Protein and Type V Polysaccharide. *Bioconjugate Chemistry*, 2015. 26(8): p. 1839-1849.
 30. Boutureira, O. and G.J.L. Bernardes, Advances in chemical protein modification. *Chem. Rev.*, 2015. 115(5): p. 2174-2195.
 31. Agarwal, P. and C.R. Bertozzi, Site-specific antibody–drug conjugates: the nexus of bioorthogonal chemistry, protein engineering, and drug development. *Bioconj. Chem.*, 2015. 26(2): p. 176-192.
 32. Boeckler, C., et al., Immunogenicity of new heterobifunctional cross-linking reagents used in the conjugation of synthetic peptides to liposomes. *J. Immunol. Methods*, 1996. 191(1): p. 1-10.
 33. Ni, J., et al., Toward a Carbohydrate-Based HIV-1 Vaccine: Synthesis and Immunological Studies of Oligomannose-Containing Glycoconjugates. *Bioconj. Chem.*, 2006. 17(2): p. 493-500.
 34. Grandjean, C., et al., Investigation towards bivalent chemically defined glycoconjugate immunogens prepared from acid-detoxified lipopolysaccharide of *Vibrio cholerae* O1, serotype Inaba. *Glycoconj. J.*, 2009. 26(1): p. 41-55.
 35. Verez-Bencomo, V., et al., A synthetic conjugate polysaccharide vaccine against *Haemophilus influenzae* type b. *Science*, 2004. 305(5683): p. 522-525.

36. Pozsgay, V., et al., Protein conjugates of synthetic saccharides elicit higher levels of serum IgG lipopolysaccharide antibodies in mice than do those of the O-specific polysaccharide from *Shigella dysenteriae* type 1. *Proc. Natl. Acad. Sci. U S A*, 1999. 96(9): p. 5194-5197.
37. Kabanova, A., et al., Evaluation of a Group A *Streptococcus* synthetic oligosaccharide as vaccine candidate. *Vaccine*, 2011. 29(1): p. 104-14.
38. Taylor, D.N., et al., Synthesis, characterization, and clinical evaluation of conjugate vaccines composed of the O-specific polysaccharides of *Shigella dysenteriae* type 1, *Shigella flexneri* type 2a, and *Shigella sonnei* (*Plesiomonas shigelloides*) bound to bacterial toxoids. *Infect. Immun.*, 1993. 61(9): p. 3678-87.
39. Peeters, C.C., et al., Synthetic trimer and tetramer of 3-beta-D-ribose-(1-1)-D-ribitol-5-phosphate conjugated to protein induce antibody responses to *Haemophilus influenzae* type b capsular polysaccharide in mice and monkeys. *Infect. Immun.*, 1992. 60(5): p. 1826-1833.
40. Lefeber, D.J., et al., Th1-directing adjuvants increase the immunogenicity of oligosaccharide-protein conjugate vaccines related to *Streptococcus pneumoniae* type 3. *Infect. Immun.*, 2003. 71(12): p. 6915-20.
41. Safari, D., et al., Antibody- and cell-mediated immune responses to a synthetic oligosaccharide conjugate vaccine after booster immunization. *Vaccine*, 2011. 29(38): p. 6498-504.
42. Mallett, C.P., et al., Evaluation of *Shigella* vaccine safety and efficacy in an intranasally challenged mouse model. *Vaccine*, 1993. 11(2): p. 190-6.
43. Hsu, C.-H., et al., Toward automated oligosaccharide synthesis. *Angew. Chem. Int. Ed.*, 2011. 50(50): p. 11872-11923.
44. Anish, C., et al., Chemical biology approaches to designing defined carbohydrate vaccines. *Chem. Biol.*, 2014. 21(1): p. 38-50.
45. Fields, R., The rapid determination of amino groups with TNBS. *Methods Enzymol.*, 1972. 25C: p. 464-468.
46. Habeeb, A., Determination of free amino groups in proteins by trinitrobenzenesulfonic acid. *Anal. Biochem.*, 1966. 14: p. 328-336.
47. Dische, Z., Color reactions of hexoses. *Adv. Carbohydr. Chem.*, 1962. 1: p. 488-494.
48. Jermyn, M.A., Increasing the sensitivity of the anthrone method for carbohydrate. *Anal. Biochem.*, 1975. 68: p. 332-335.
49. Scott, T.A., Jr. and E.H. Melvin, Determination of dextran with anthrone. *Anal. Chem.*, 1953. 25: p. 1656-1661.
50. Guo, Z. and G.J. Boons, eds. *Carbohydrate based vaccines and immunotherapies*. Wiley series in drug discovery and development. 2009, Wiley.
51. Hermanson, G.T., ed. *Bioconjugate techniques*. 3rd ed. 2008, Elsevier.
52. Scientific, T., ed. *Thermo Scientific Pierce crosslinking technical handbook*. 2009, Thermo Fisher Scientific.

Supplementary material

Bioconjugation step

Comparison of different batches of TT

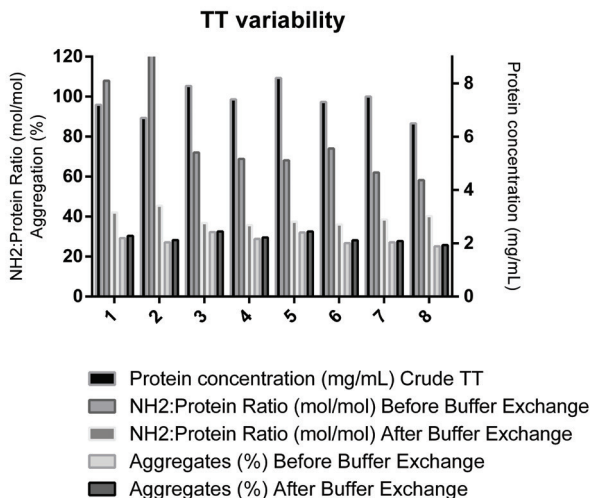


Figure S1: Comparison of different batches of TT before and after buffer exchange. Batch 3 was used for all other experiments due to availability.

Influence of buffers and organic solvents on TT to intermediate 4 conversion

Comparing different buffers for the grafting of GMBS on TT

NMR analysis showed that both GMBS and sulfo-GMBS hydrolyzed at pH 7 and 8 in 0.1 M phosphate buffer. Next to the reaction of the NHS-ester, a reaction of the maleimide group was observed. Considering the degradation of the NHS-ester, a $T^{1/2}$ of 80 and 50 min was observed for GMBS at pH 7 and 8, respectively. For sulfo-GMBS a $T^{1/2}$ of 30 min at pH 7 and a $T^{1/2}$ of 75 min at pH 8 was observed. NMR analysis of both reagents dissolved in 0.1 M HEPES at the here fore mentioned pHs, showed an increase of the $T^{1/2}$ to multiple hours, or even days (data not shown). In the following modification experiments, only GMBS was used because it was dissolved in DMSO and found to be stable for prolonged time (days), whereas sulfo-GMBS was dissolved in the aqueous buffer, and would start to degrade immediately even in 0.1 M HEPES. Four different ratios were compared at two different time points (15 and 60 min) for both phosphate and HEPES buffer (Table S1).

When evaluating the HPSEC profiles, where signals were normalized for the TT peak corresponding to monomeric TT, it was concluded that the modification in 0.1 M

phosphate buffer pH 8 induces significantly higher quantities of aggregates (45-55 %) than modification in 0.1 M HEPES buffer pH 7.5 (35-45 %) (data not shown). The reaction efficiency itself was very similar for both buffers, as was the result after 15 and 60 min for both primary amine group quantity (data not shown) and aggregate content (Figure S2, t = 15 min). These results in combination with the prolonged stability justified the selection of a 0.1 M HEPES buffer and the use of only GMBS for further experiments. Furthermore, DMSO was the solvent of choice due to its European Pharmacopoeia (EP) grade availability, which was beneficial for future GMP production activities.

Table S1: Modification parameters for GMBS using different buffers

	In 0.1 M Phosphate pH 8				In 0.1 M HEPES pH 7.5			
TT:GMBS ratio (mol:mol)	150	80	40	20	150	80	40	20
GMBS amount (μmol)	10.5	5	2.8	1.4	10.5	5.6	2.8	1.4

°: TT: 300 μL , 35 mg/mL, 70 nmol; GMBS solution: 0.5 M, 20 μL

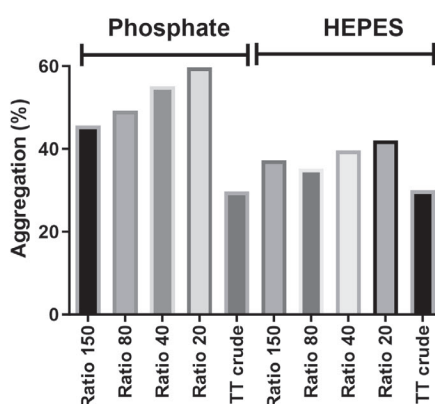


Figure S2: Influence of the buffer on TT aggregation after 15 minutes reaction time. The ratio described for each sample is the GMBS:TT ratio.

Aggregation induction of different organic solvents

Different organic solvents (DMSO, acetonitrile and DMA) were added to TT to investigate aggregation induction. TT was concentrated and buffer exchanged to either 0.1 M phosphate pH 8.0 or 0.1 M HEPES pH 7.5 before adding the organic solvents. When adding 3.5 μL of the respective organic solvents (highest amount of solvent use during experiments) to 50 μL of TT, no effect on aggregation of TT was observed up to 360 min incubation at ambient temperature.

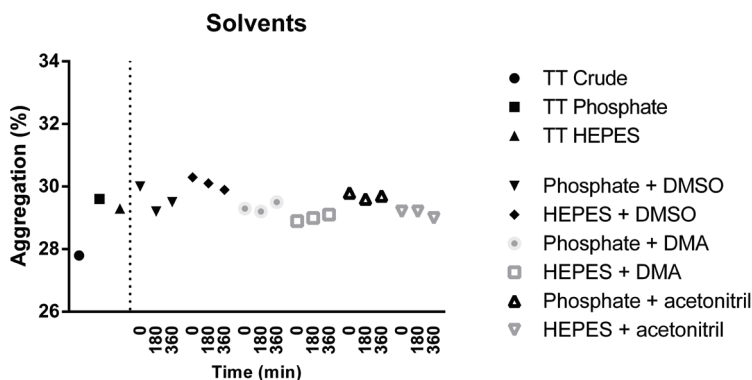


Figure S3: Influence on the aggregation of TT when adding an organic solvent. TT crude: unprocessed TT without both buffer exchange and added solvents; TT Phosphate: buffer exchanged TT without added solvents; TT HEPES: buffer exchanged TT without added solvents

4 Characterization of TT activation

Within this investigation, the final volume of the buffer-exchanged concentrated TT was 3.2 mL, with a final concentration factor of 10. From this concentrate, 3.0 mL was applied on a 11 mm Millipore Vantage L Biochromatography laboratory column (89 cm) with a Sepharose 6FF matrix (GE Lifesciences, 84.55 mL, Plates 1431, Asymmetry 1.45). The applied flow rate was 0.5 mL/min and fraction size was 2.0 mL. A 2 mm UV cell was used for detection, coupled to an AKTA system (GE-Life sciences). The Unicorn software (GE Lifesciences, V 5.11) was used for data acquisition and processing. It was decided to pool several designated fractions to create a pool of interest to be used for the modification experiments. In total four different pools of interest could be assigned (Table S2). Pool one is considered to contain high molecular weight oligomers (fractions 1 – 3), pool two to contain intermediate oligomers (fractions 4 – 8), pool three to contain dimers of TT (fractions 9 – 15) and pool four to contain TT mostly in its monomeric form (fractions 18 – 22). After pooling the fractions, HPSEC analysis confirmed the assumed composition (Figure S4).

Table S2: SEC fraction pools in 0.1 M HEPES pH 7.5

Pool	Fractions (2.0 mL)	BCA (mg/mL)	TNBS (mM)	Ratio (NH ₂ :TT)
1	1 - 3	1.538	0.465	45.4
2	4 - 8	0.823	0.167	30.4
3	9 - 15	8.953	1.649	27.6
4	18 - 22	30.403	6.178	30.5

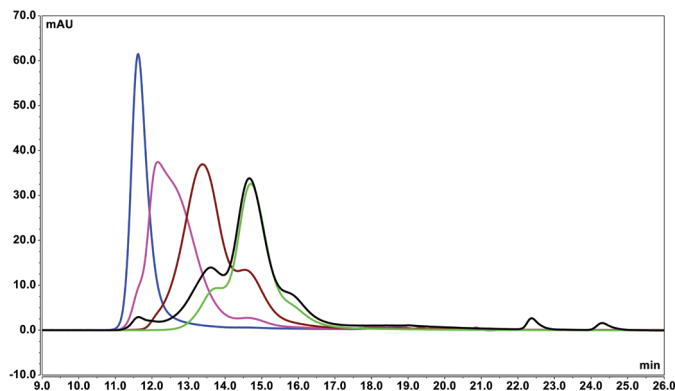


Figure S4: HPSEC profile of TT and pooled fractions. Blue: pool 1, Pink: pool 2, Brown: pool 3, Green: pool 4 and Black: TT. x-axis: retention time (min), y-axis left UV₂₈₀ mAU

All individual pools were modified by applying different GMBS to TT ratios (20, 40, 80 and 150, respectively). The reaction time was 15 minutes at ambient temperature, after which buffer exchange was initiated. When evaluating the HPSEC profiles (signals normalized on peak height, but not retention time), it could be concluded that for pool 1 no difference could be observed between the pool and the modified oligomers (Figure S5). For pools 2 and 3, only a minor shift in retention time is observed, which could suggest an effect of the GMBS-activation reaction (Figures S6 and S7). For pool 4, a minor shift in retention time is also observed. Again, it can be interpreted as a result of the covalent attachment of maleimide groups. In addition, the induction of aggregates for pool 4 is significant (Figure S8). An inverse proportional relationship exists between the GMBS:protein ratio and the induction of aggregation (the higher the ratio the lower the induction of aggregation).

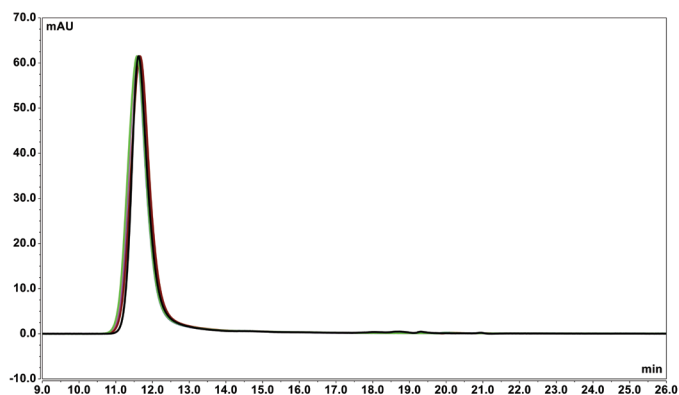


Figure S5: Pool 1 before and after treatment with GMBS at different GMBS:protein ratios, x-axis: retention time (min) y-axis left UV₂₈₀ mAU

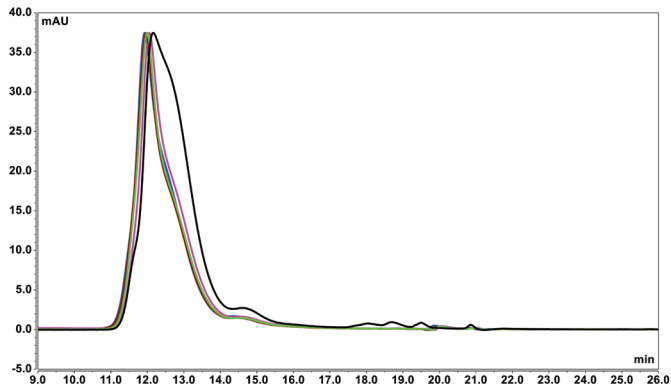


Figure S6: Pool 2 before and after treatment with GMBS at different GMBS:protein ratios, x-axis: retention time (min), mAU y-axis left UV_{280} mAU

4

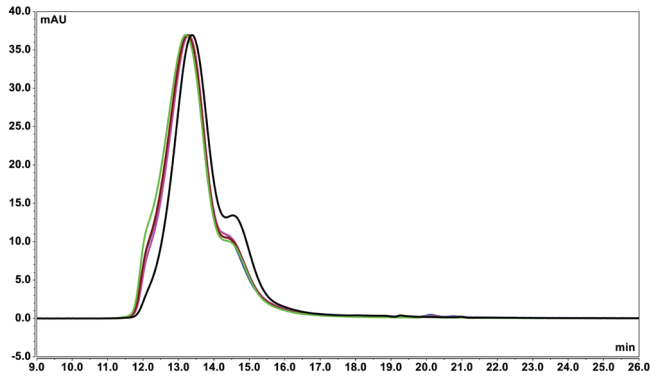


Figure S7: Pool 3 before and after treatment with GMBS at different GMBS:protein ratios, x-axis: retention time (min), y-axis left UV_{280} mAU

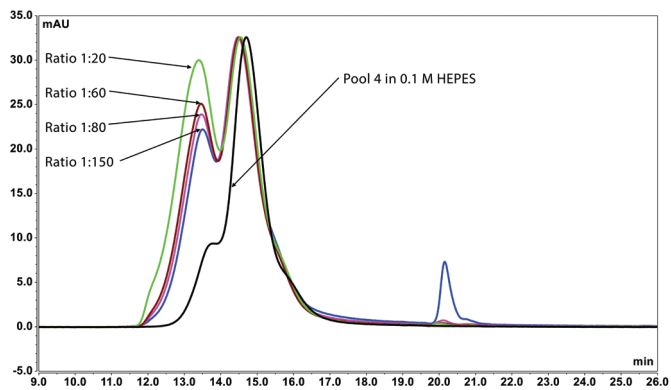


Figure S8: Pool 4 before and after treatment with GMBS at different GMBS:protein ratios, x-axis: retention time (min), y-axis left UV_{280} mAU

The initial quantity of primary amino groups (Figure S9) for pool 1 is significantly different from that of the other pools. This difference remains (although less pronounced) after the GMBS-modification reaction. For all pools, similar dynamics apply; the higher the GMBS:protein ratio the higher the modification ratio (reduction in the amount of primary amino groups per TT).

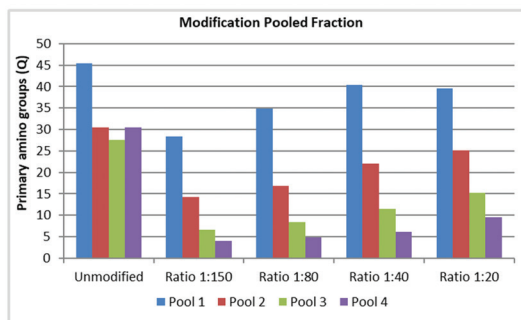


Figure S9: Primary amino group quantities for the pools and the GMBS-modified products

When multiplying the average number of NH_2 groups per protein by the average protein concentration of the original pools, the total contribution of each individual pool is better visualized (Figure S10). Here, it becomes apparent that even though pool 1 has a higher NH_2 mol:mol content, the contribution is marginal when corrected. Pool 4, which is the monomeric TT, has the largest contribution. As a result from this experiment, it was decided that the available original TT batch, with its substantial amount of oligomers, was useable for further process development, since the larger oligomers only contribute marginally to the total amount of reactive NH_2 groups (~2% for pool 1), and therefore to the GMBS-modification reaction. On the other hand, aggregation of monomeric TT, induced by the modification, needs to be minimized.

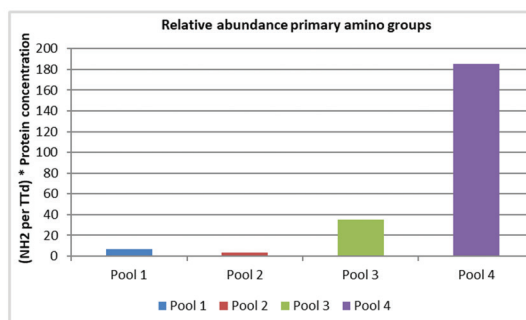


Figure S10: Corrected primary amino group quantities for the pools of the GMBS-modified products

Design of Experiments (DoE) and analysis

Factors investigated in the DoE

In order to find the optimal conditions for introduction of the maleimide linker, several factors were investigated using DoE. A full overview of all the different combinations of factors is given below (Table S3).

Table S3: DoE reaction conditions

Exp	pH	Temperature (°C)	TT concentration (mg/mL) ^a	TT amount (mg)	TT amount (nmol)	TT:GMBS ratio (mol:mol)	GMBS (mM) ^b
1	7	4	15	13.5	96	10	16
2	8	4	15	13.5	96	10	16
3	7	37	15	13.5	96	10	16
4	8	37	15	13.5	96	10	16
5	7	4	55	49.5	352	10	59
6	8	4	55	49.5	352	10	59
7	7	37	55	49.5	352	10	59
8	8	37	55	49.5	352	10	59
9	7	4	15	13.5	96	160	256
10	8	4	15	13.5	96	160	256
11	7	37	15	13.5	96	160	256
12	8	37	15	13.5	96	160	256
13	7	4	55	49.5	352	160	939
14	8	4	55	49.5	352	160	939
15	7	37	55	49.5	352	160	939
16	8	37	55	49.5	352	160	939
17	7.5	20.5	35	31.5	224	40	149
18	7.5	20.5	35	31.5	224	40	149
19	7.5	20.5	35	31.5	224	40	149

^a: initial volume was 300 μ L

^b: initial volume was 20 μ L

Statistical Analysis DoE Modification

The statistical analysis as available in the software module used (MODDE, Umetrics), can address several quality attributes to evaluate the quality and output of the model. Distribution of the response factors and the N-residuals plot showed normal profiles (data not shown). For the coefficients plots, all coefficients, which were non-significant for all three response factors, were removed. This yielded specific coefficients, which were applied to all three output parameters to construct similar models (Figure S11).

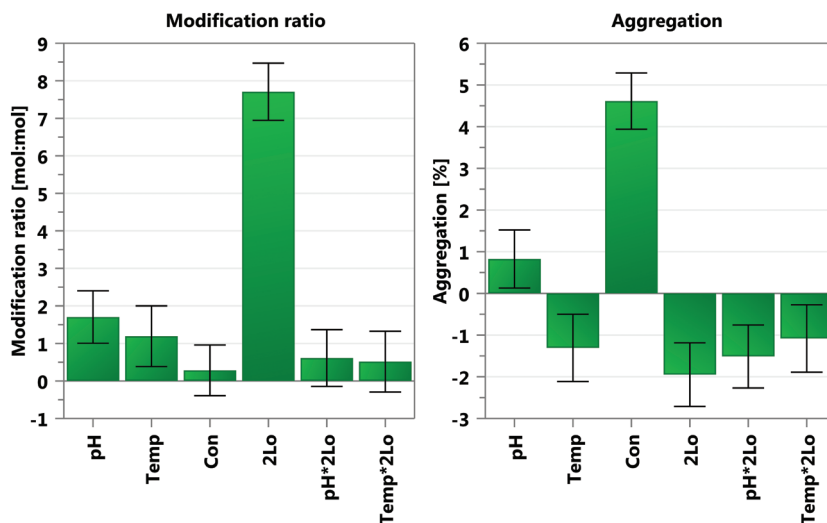


Figure S11: Coefficients plot for modification and aggregation.

Summary of fit results

When evaluating the summary of fit plot; the R², Q² and reproducibility all met specifications (Table S4). The model validity for the modification ratio is low (-0.20), which is a direct effect of the extremely high reproducibility (0.99). For this reason and due to the results for the other performance indicators, the model validity for the modification ratio was ignored. As a final representation of the model performance, the observed versus predicted plots all showed acceptable R² (> 0.6) for the model applied and the analysis of variance (ANOVA) analysis showed $p < 0.05$ for the regression and $p > 0.05$ for the lack of fit for all models (data not shown).

Table S4: Summary of fit results

	Reference values	Total aggregation	Aggregation increase	Modification ratio
R2^a	n.a.	0.80	0.71	0.88
Q2^b	>0.50	0.75	0.62	0.86
R2-Q2^c	< 0.20 - 0.30	0.05	0.09	0.02
Model validity^d	>0.25	0.83	0.52	-0.20
Reproducibility^e	>0.50	0.77	0.76	0.99

^a: goodness of fit, is a measure of how well the regression model can be made to fit the raw data; ^b: goodness of prediction, estimates the predictive power of the model; ^c: for a model to pass this diagnostic test, both R2 and Q2 should be high, and preferably not separated by more than 0.2 – 0.3. A larger difference constitutes a warning of an inappropriate model; ^d: reflects whether a model is appropriate in a general sense, whether the right type of model was chosen; ^e: constitutes the pure error and control of the experimental procedure

Sweet spot analysis

When combining the models for total aggregation, aggregation increase and modification ratio, a sweet spot analysis was created (Figure S12). The chosen set points were a minimum modification ratio of 22.0, a maximum of 7.5% aggregation increase and a maximum of 34.3% total aggregation. The sweet spot analysis ruled out the higher (35 and 55 mg/mL) concentrations of TT and also the lower GMBS:TT ratios (2log 3.32 (1:10) and 2log 5.32 (1:40)). When looking at the upper left graph (TT concentration at 15 mg/mL and GMBS:TT ratios 2log 7.32), the sweet spot is shown in green. There is a broad range for both pH and temperature where the optimal outcome of the modification can be obtained. Sweet spot analysis showed that a process at ambient temperature is feasible for the chosen conditions. This is preferable for ease of the production process design. When applying general temperature conditions (15 – 25 °C) at 15 mg/mL and GMBS:TT ratio of 2log 7.32 (1:160), a range of operations for pH between 7.5 and 8.0 would yield modified TT 4 according to the set specifications.

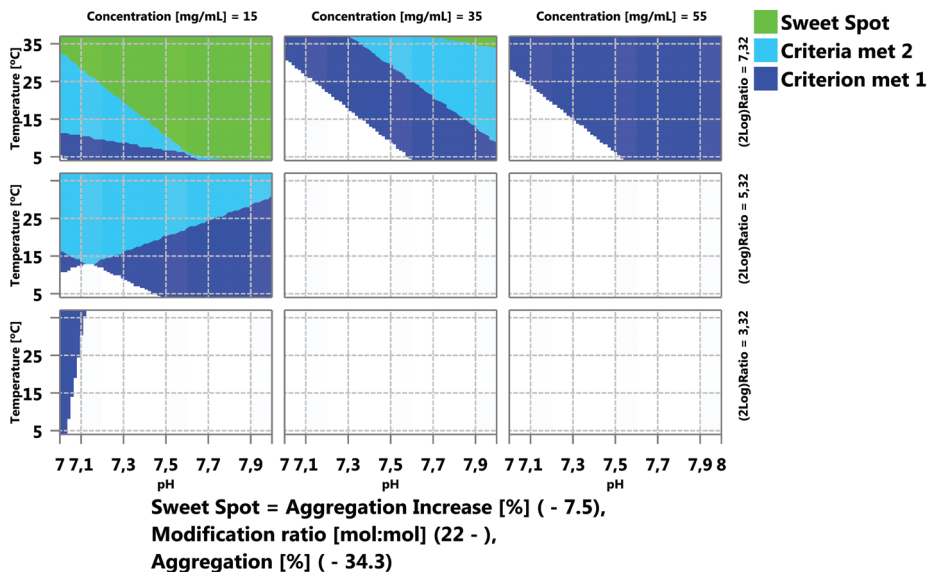


Figure S12: Sweet spot plot analysis

4

Robustness of DoE modification

A robustness investigation was performed, applying the specifications of the sweet spot at which the modification yields optimal results (Table S5). The same factors as for the screening DoE were investigated, this time with respect to the variation that can be readily expected for the individual factors. For the variation in temperature, it was decided to test for robustness over a broader range, which covered the full range for ambient temperature (15 – 25 °C). For the robustness of the DoE, the minimum required response factors as described before would have to apply.

Table S5: Robustness of DoE modification settings

	Expected variation (%)	Low	Mid	high
TT concentration (mg/mL)	10	13.5	15	16.5
2log (ratio) TT:GMBS	10	7.16 (143)	7.32 (160)	7.48 (178)
pH	2.5	7.6	7.8	8.0
Temperature (°C)	12	15	20	25

Compared to the DoE for the GMBS-modification, the exact same statistical parameters were reviewed for the quality of the model. All statistical parameters met the specifications. Again, when assessing the summary of fit, the model validity for the modification ratio was too low (< 0.25), which was again omitted for reasons described before (data not shown). When putting the models for total aggregation, aggregation increase and modification ratio, together a sweet spot analysis was created. The chosen set points, as described, were that a minimum modification ratio of 22.0, a maximum of 7.5% aggregation increase and a maximum of 34.3% total aggregation would be tolerated (Table S6). The sweet spot analysis showed that even when variations were applied to the different parameters, the outcome of the modification still complied with the set requirements (data not shown).

Table S6: Robustness of DoE modification response factors

Responses	Minimum	Maximum
Total aggregation (%)	n.s. ^o	34.3
Aggregation increase (%)	n.s. ^o	7.5
Mal:TT ratio (modified groups)	22.0	n.s. ^o

^o: Not specified

Removal of free pentadecasaccharide after conjugation

After conjugation is completed, the conjugates were purified using buffer exchange. Initial experiments showed that using a 10 kDa MWCO lead to remaining free pentadecasaccharide. However, changing to a 30 kDa MWCO showed complete removal of the free pentadecasaccharide (Figure S13).

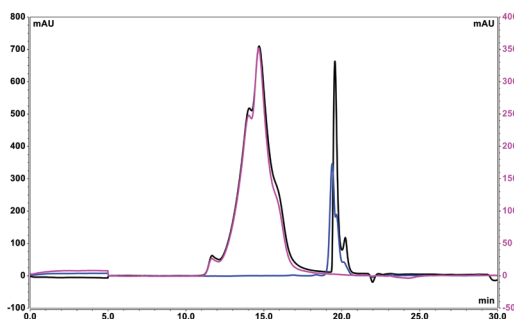


Figure S13: HPLC profiles comparing purification of conjugates using 10 kDa and 30 kDa MWCO filters: Black trace: conjugate processed using a 10 kD cut-off filter with a peak at approximately 19.5 min representing the remaining forms of the pentadecasaccharide; Blue trace: pentadecasaccharide with characteristic elution at approximately 19.5 min; Pink trace: conjugate processed using a 30 kD cut-off filter

Immunogenicity analysis

Statistical analysis: the Mann Whitney test was used for comparing groups of mice.

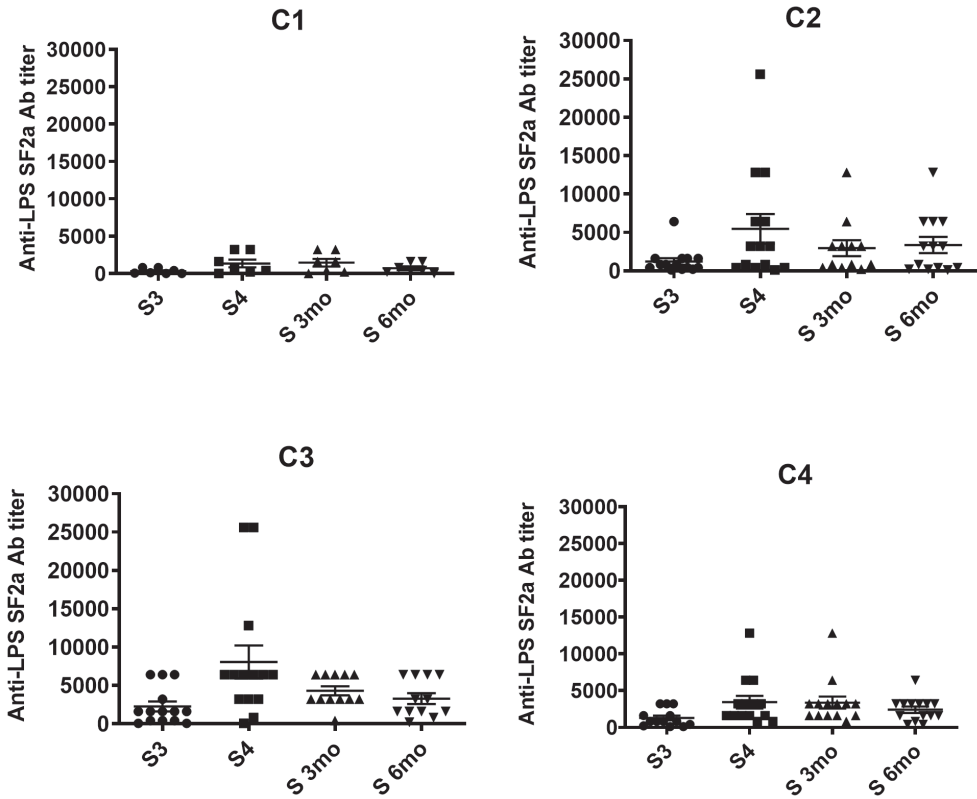


Figure S14: Anti-SF2a LPS IgG titer induced in mice receiving 3 (S3) and 4 (S4) times a dose of glyco-conjugates C1-C4 containing 2.5 μg of $[\text{AB}(\text{E})\text{CD}]_3$ and sustained response after 3 and 6 months (3mo and 6mo, respectively).



Chapter 5

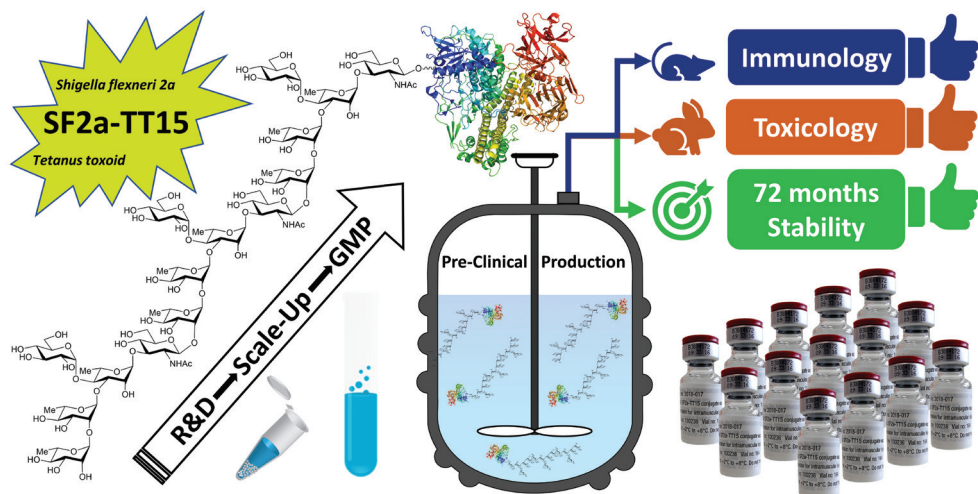
The first-in-human synthetic glycan-based conjugate vaccine candidate against *Shigella*

Robert M.F. van der Put,^a Carolien Smitsman,^{a†} Alex de Haan,^a Martin Hamzink,^a Hans Timmermans,^a Joost Uittenbogaard,^a Janny Westdijk,^a Michiel Stork,^a Olga Ophorst,^a Françoise Thouron,^b Catherine Guerreiro,^c Philippe J. Sansonetti,^{b,d#} Armelle Phalipon,^{b§} and Laurence A. Mulard^c

^a Intravacc, P.O. Box 450, 3720 AL Bilthoven, the Netherlands. ^b Institut Pasteur, U1202 Inserm, Unité de Pathogénie Microbienne Moléculaire, 28 rue du Dr Roux, 75724 Paris Cedex 15, France. ^c Institut Pasteur, Université de Paris, CNRS UMR3523, Unité de Chimie des Biomolécules, 28 rue du Dr Roux, 75724 Paris Cedex 15, France. ^d Collège de France, Chaire de Microbiologie et Maladies Infectieuses, 11, place Marcelin Berthelot, 75005 Paris, France.

Abstract

Shigella, the causative agent of shigellosis, is among the main causes of diarrheal diseases with still a high morbidity in low-income countries. Relying on chemical synthesis, we implemented a multidisciplinary strategy to design SF2a-TT15, an original glycoconjugate vaccine candidate targeting *Shigella flexneri* 2a (SF2a). Whereas the SF2a O-antigen features nonstoichiometric O-acetylation, SF2a-TT15 is made of a synthetic 15-mer oligosaccharide, corresponding to three non-O-acetylated repeats, linked at its reducing end to tetanus toxoid by means of a thiol-maleimide spacer. We report on the scale-up feasibility under GMP conditions of a high yielding bioconjugation process established to ensure a reproducible and controllable glycan/protein ratio. Preclinical and clinical batches complying with specifications from ICH guidelines, WHO recommendations for polysaccharide conjugate vaccines, and (non)compendial tests were produced. The obtained SF2a-TT15 vaccine candidate passed all toxicity-related criteria, was immunogenic in rabbits, and elicited bactericidal antibodies in mice. Remarkably, the induced IgG antibodies recognized a large panel of SF2a circulating strains. These preclinical data have paved the way forward to the first-in-human study for SF2a-TT15, demonstrating safety and immunogenicity. This contribution discloses the yet unreported feasibility of the GMP synthesis of conjugate vaccines featuring a unique homogeneous synthetic glycan hapten fine-tuned to protect against an infectious disease.

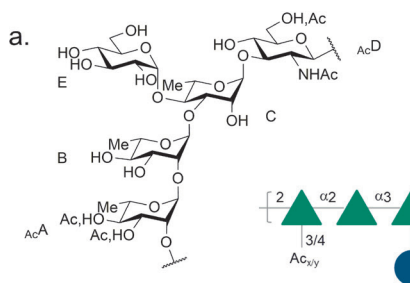


A conjugate vaccine featuring a unique synthetic glycan hapten induces protective antibodies to most *Shigella flexneri* 2a circulating strains: GMP process, successful toxicology data & long-term stability.

Introduction

Bacillary dysentery, or shigellosis, is associated with a significant burden globally. With more than 250 million annual cases estimated to occur in low- and middle-income countries [1], it is one among the four most prevalent diarrheal diseases, affecting in particular children less than five years of age [2, 3]. In this population, frequent diarrheal episodes have been correlated to long-term growth and cognitive impairments [4]. In adults, shigellosis has a higher incidence in the elderly [1] and is a well-established cause of diarrhea in travelers and military personnel [5]. Antimicrobial resistance is growing, which reduces opportunities for efficient treatment [6, 7], and contributes to enhance concern whether from the CDC [8] or the WHO [9]. Improved sanitation and access to clean water represent effective means of preventing shigellosis, but they qualify as a lengthy process. In this context, the development of a *Shigella* vaccine suitable for use in children under the age of five living in low- and middle-income countries is highly desirable [10]. In particular, such a vaccine should provide protection against *Shigella flexneri* and *Shigella sonnei* [11]. *Shigella* lipopolysaccharide (LPS) is an important virulence factor [12], and its O-antigen (O-Ag) component is a major protective antigen [13, 14]. On the basis of the assumption that serum antibodies to the *Shigella* O-Ag could protect against reinfection [15], and pioneered by Drs. J. B. Robbins and R. Schneerson (NIH, MD, USA) [16], several parenterally administered detoxified LPS-protein conjugate vaccine candidates have been developed and tested in clinical trials [17]. Protective efficacy was demonstrated for a *S. sonnei* detoxified LPS-rEPA (recombinant exoprotein from *Pseudomonas aeruginosa*) vaccine prototype in adults and children older than three years of age, although not in the youngest vaccine recipients [18, 19]. Leading the path forward, these prime inspiring achievements prompted further studies on alternatives to this first generation of *Shigella* polysaccharide–protein conjugate vaccines [17]. An increasing interest in vaccines to fight infectious diseases, enhanced in a context of the fast emergence of antibiotic resistance [20–23], and an improved, albeit still limited, understanding of their mechanism of action [24–27] contribute, among other factors, to trigger major developments in the field of glycoconjugate vaccines [28–30]. Otherwise, compelling evidence substantiates the identification of serum IgG antibodies to *Shigella* LPS as a good correlate of protection against shigellosis [31]. In this context, novel families of LPS-based *Shigella* vaccines have successfully passed phase 1 clinical trial and more [32–34]. Synthetic glycans for use as LPS surrogates have been the subject of special interest. They were actively investigated in the search for improved vaccine candidates able to induce anti-LPS serum IgG titers suitable for protecting children under three years of age against shigellosis [17]. In the late 1990s, groundbreaking studies on *S. dysenteriae* 1 showed the superiority in mice of synthetic oligosaccharide-based sun-type conjugates over lattice-type conjugates issued from the random conjugation of the detoxified LPS to rEPA [35]. Aiming at defeating shigellosis, in

particular, *S. flexneri* and *S. sonnei*, which account for some 66% and 24% of the global *Shigella* burden, respectively [11], a related multidisciplinary glycochemistry-based strategy was implemented at Institut Pasteur [36–41]. The most advanced work concerns *S. flexneri* 2a (SF2a), the prevalent *S. flexneri* serotype [11]. The SF2a O-Ag is defined by a branched pentasaccharide repeating unit O-acetylated in a nonstoichiometric manner at two sites (Figure 1a) [42–44]. A chemical biology strategy [45] involving extensive epitope mapping was implemented, which led to the identification of a synthetic pentadecasaccharide [AB(E)CD]₃-NH₂ (**1**) [46] corresponding to three non-O-acetylated O-Ag repeating units as an antigenic [47], conformational [44], structural [48], and functional mimic [49] of the SF2a O-Ag (Figure 1b). Moreover, the well-defined synthetic O-Ag segment **1** was recognized by sera from naturally infected individuals [49]. A glycoconjugate issued from the single-site attachment of [AB(E)CD]₃ to tetanus toxoid (TT), a medically acceptable carrier, by means of a chemoselective conjugation between the thiol-equipped **3** and maleimide-equipped tetanus toxoid (TT_{Mal}), was shown to induce high anti-SF2a O-Ag IgG antibody titers in mice [49]. In addition, an adjuvanted B,T-diepitope glycoliposome displaying the synthetic [AB(E)CD]₃ hapten was shown to induce a proper anti-SF2a immune response [50]. These findings support our original assumption that the well-defined synthetic **1** featured a promising surrogate of the highly heterogeneous natural SF2a O-Ag.



Strains	x / y	z
G1663	~60% / ~25%	~60%
1605	~40% / ~15%	~40%
2457T	30-50% / -	30-60%
454	~20% / ~10%	-

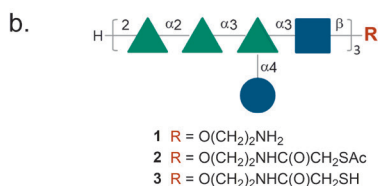
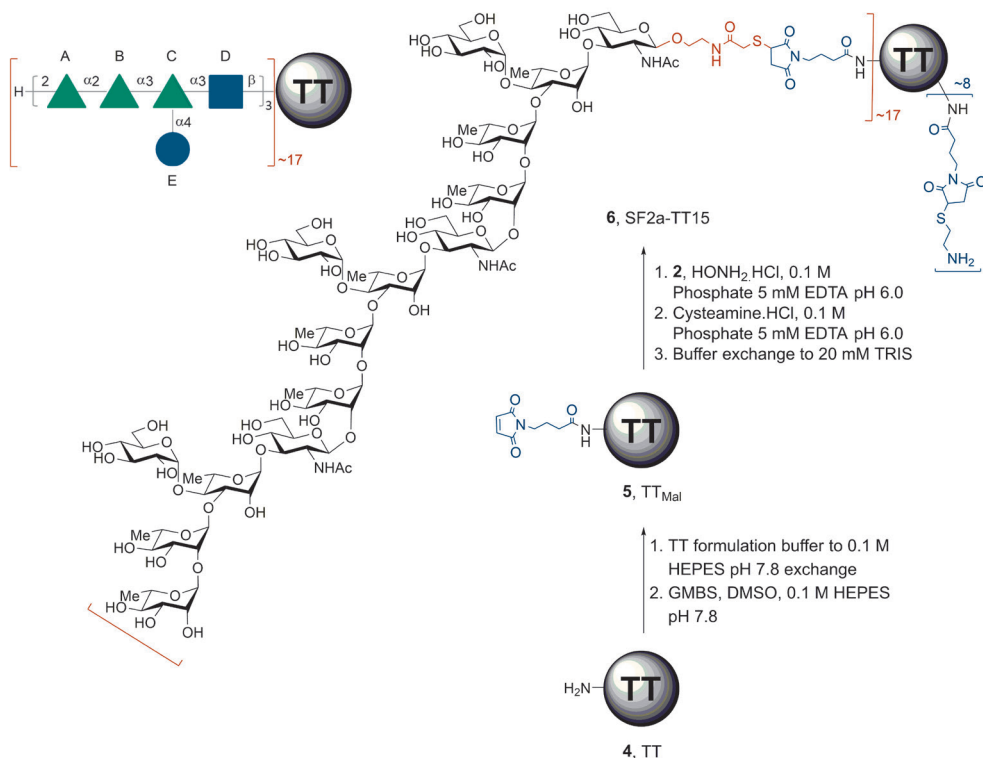


Figure 1. (a) Repeating unit from the SF2a O-Ag showing the sites and ratios of nonstoichiometric O-acetylation [42–44]. (b) Structure of the 15mer oligosaccharide identified as an antigenic, structural, and conformational mimic of the SF2a O-Ag in the form of its aminoethyl glycoside (**1**, [AB(E)CD]₃-NH₂) and equipped with a conjugation-ready linker featuring a masked thiol moiety (**2**, [AB(E)CD]₃-SAC) or a thiol moiety (**3**, [AB(E)CD]₃-SH). Solid green triangles: l-rhamnopyranose; solid blue squares: N-acetyl-d-glucosamine; solid blue circles: d-glucopyranose.

Featuring strong immunogenicity in mice and synthetic manufacturing feasibility, an $[AB(E)CD]_3$ -TT conjugate characterized by an average oligosaccharide:TT molar loading of 17 ± 5 -SF2a-TT15 (**6**, Scheme 1) was subsequently identified as a promising SF2a vaccine candidate to move forward for evaluation in humans [51]. SF2a-TT15 is obtained according to a three-step conjugation process from the chemically synthesized linker-equipped oligosaccharide **2** bearing a masked thiol and commercially available TT (**4**) (Scheme 1). Thus, TT_{Mal} (**5**), resulting from the grafting of 4-maleimidobutyric acid *N*-hydroxysuccinimide ester (GMBS) on TT (step 1), reacts with conjugation-ready **3**, issued from the selective unmasking of the thiol moiety in the more stable precursor **2**, in a precisely controlled **2:5** ratio (mol:mol) of 25 (step 2). Cysteamine-capping of the unreacted maleimide moieties in the conjugation product (step 3) then provides glycoconjugate **6**. Relying on an exhaustive design of experiments (DoE) study aimed at assessing key parameters (temperature, pH, concentration, reaction time, GMBS/TT ratio) to warrant optimal oligosaccharide loading and minimal aggregation, a robust, high yielding chemoselective thiol-maleimide conjugation procedure was established at microscale [51].



Scheme 1. SF2a-TT15 (**6**, $[AB(E)CD]_3$ -TT), a vaccine candidate against SF2a and Synthetic Process to Achieve Its Production from TT (**4**) and the Linker-Equipped Oligosaccharide **2**° GMBS: *N*-[γ -maleimidobutyryloxy]succinimide ester, HEPES: 4-(2-hydroxyethyl) piperazine-1-ethanesulfonic acid, TT: tetanus toxoid, TT_{Mal} : maleimide-modified tetanus toxoid.

Herein, the scale-up and implementation of this microscale conjugation process in a format complying with good manufacturing practice (GMP) conditions, by use of GMP-grade [AB(E)CD]₃-SAC precursor **2** (^{GMP}**2**) and TT (^{GMP}**4**), are reported. A preclinical batch and a clinical batch of SF2a-TT15, each accounting for tens of thousands of doses of the vaccine candidate, were produced to perform the first-in-human clinical trial, including the requested repeated-dose toxicity study. As part of the preclinical requirement for the latter, we also report on the immunogenicity in both mice and rabbits and provide extended stability data in support of the shelf life for the formulated SF2a-TT15 vaccine candidate. Moreover, we demonstrate for the first time that SF2a-specific antibodies elicited upon immunization in mice with a fine-tuned SF2a glycoconjugate vaccine prototype, made of a well-defined chemically synthesized non-O-acetylated O-Ag segment, display *in vitro* bactericidal properties and are able to recognize a large diversity of SF2a strains circulating in different geographical settings. Lastly, the requirements for a broad serotype-coverage *Shigella* vaccine are discussed.

Results and discussion

5 Licensed conjugate vaccines are routinely administered in minute amounts, roughly corresponding to 1–10 µg type- or group-specific glycan per vaccine dose [52]. Available preclinical data supported the assumption that SF2a-TT15 obeys the same rule. This observation had a direct consequence on the GMP process to be developed. It guided the production scale, and therefore the equipment selection, among which were the reactor and filtration device. To fulfill GMP-grade criteria, in particular, relevant to impurity content and scalability, all filtration steps were performed by tangential flow filtration (TFF) instead of spin filtration as originally described [51]. Owing to limitations in terms of the minimal volume compatible with this technology, a 1 L reactor was - at that time - the smallest commercially available vessel found suitable to fulfill the above-mentioned criteria. It was subsequently used specifically during the process development steps regarding scale-up studies and evaluation of process performance with respect to impurity removal in the absence of the thioacetate precursor **2**. It is worth mentioning that irrelevant to the clinical demand, in this case the GMP production scale of both the preclinical batch and clinical batch of SF2a-TT15 had to be adapted to comply with the limitations of the commercially available GMP equipment.

Process development

With our previous achievements serving as a ground basis [46, 51], we engaged in the process development to GMP manufacturing (Figure 2). In the first place, GMP-grade [AB(E)CD]₃-SAC (^{GMP}**2**) was produced on the multigram scale (Figure 2, not described). In

brief, the multistep chemical process was adapted from an established route [46] to reach the known fully protected $[AB(E)CD]_3-N_3$ intermediate, which was then converted in four steps to thioacetate **2** under conditions fulfilling GMP criteria. The GMP-grade material, or drug substance (DS) intermediate, was released based on the evaluation of the certificate of analysis and 1H NMR analysis for identity and purity (Figure S1). The total amount of carbohydrate was assessed by high-performance anion-exchange chromatography with pulsed amperometric detection (HPAEC-PAD). Further process development for the final scaled-up (pre)-clinical DS is described below.

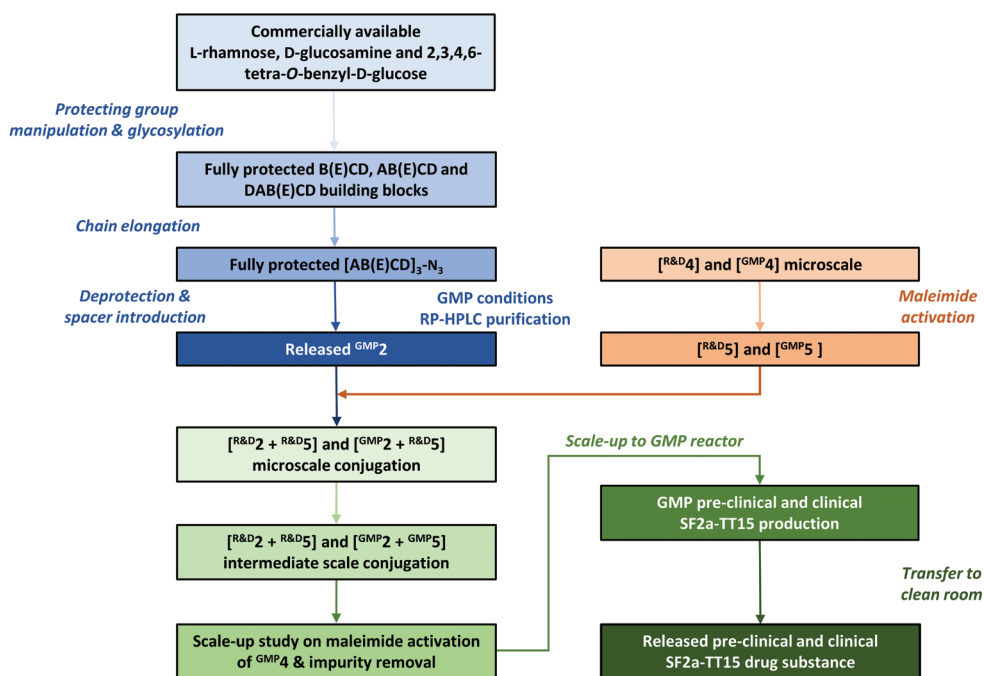


Figure 2: Overview of process development and SF2a-TT15 bulk release. Blue panels: synthesis of GMP grade precursor **2** (^{GMP}**2**) [46]. Orange panels: Maleimide activation of **4** and conjugation reaction with the introduction of **2**. Green panels: process development for GMP manufacturing of SF2a-TT15 from precursor **2**. Release of the (pre)-clinical conjugate vaccine drug substance was based on impurity assessment (NMR), free- and total carbohydrate content (HPAEC-PAD), osmolality, pH, endotoxin, aggregate content (HPSEC). HPAEC-PAD: High-Performance Anion-Exchange Chromatography with Pulsed Amperometric Detection, HPSEC: High Performance Size Exclusion Chromatography.

From microscale to intermediate scale bioconjugation

Having the key oligosaccharide precursor ^{GMP}**2** in hand, the reaction kinetics and the efficiency of the conjugation step at microscale (0.16 mL, 0.02 μmol of TT) were confirmed using research-grade TT (^{R&D}TT) on the one hand and both research-grade and GMP-grade oligosaccharide **2** (^{R&D}**2** and ^{GMP}**2**) on the other hand. As expected, the final [AB(E)CD]₃:TT loading (mol:mol) was fully controlled in a reproducible manner, simply based on the amount of the masked thiol **2** engaged in the reaction (Table S1, Figure S2). The source of the hapten precursor had no detectable influence.

At the intermediate scale (1.0 mL, 0.13 μmol of TT), the modification step performed equally well for ^{R&D}TT as for ^{GMP}TT with respect to aggregate induction (<7.5%) and activation efficiency (>80%). The conjugation step per se was investigated for ^{GMP}TT under the conditions established to achieve an [AB(E)CD]₃:TT loading of 17 ± 5 (mol:mol), as required in the targeted SF2a-TT15. Satisfactorily, the use of 25 mol equiv of ^{GMP}**2** per ^{GMP}**5** resulted in an average [AB(E)CD]₃:TT loading of 17 ± 1 (mol:mol) corresponding to a conjugation efficiency of 68 ± 4% and a yield of 62 ± 5% over two steps from ^{GMP}**2** (Table S1). As expected, the HPSEC profiles were very similar to those of the corresponding microscale experiments. The demonstration that process scale-up had no influence on reaction kinetics (Figure S3) or on the conjugate HPSEC profile supported a deep investigation of impurity removal.

Impurity removal and process performance

As part of this fourth step, a profile was established for each of the impurities present in the bulk vaccine candidate. The fact that the concentrations of impurities were undetectable in the final drug product (DP) led to the rationale for measuring impurities in the DS bulk instead. The maximum allowed concentration of each one of those impurities in the bulk vaccine was calculated from the respective specifications for final products in the ICH guidelines (Table 1). Interestingly, the starting concentrations of DMSO, cysteamine-HCl, and acetohydroxamic acid were already significantly lower than the maximum concentrations allowed according to respective guidelines (Table 1). However, the removal of these impurities was still evaluated to confirm process performance. The latter was primarily investigated by mimicking the large-scale process with only buffers and excipients. Impurity removal was evaluated by comparing the theoretical starting concentrations of excipients and impurities with the actual starting concentrations and decline thereof during each filtration step and compared to specifications set (Table 1). Single-use filters were favored so that a full cleaning validation necessary for GMP production could be omitted. Two filters, selected for their resistance to DMSO (40%) and to hydroxylamine (2 M), were assayed.

Table 1: Impurity considerations during scale-up of the TT modification and conjugation steps in the absence of oligosaccharide **2** and TT.

Impurity	Guideline for GMP	Maximum allowed quantity in the formulated vaccine (µg/dose or µg/0.5 mL unless indicated otherwise)	Maximum allowed quantity in the bulk vaccine ^[a] (mM)	Estimated maximum concentration in the bulk vaccine (mM)
GMBS / GMBA	ICH-M7	12	< 9	15.2 ^[b]
N-Hydroxysuccinimide	ICH-M7	12	< 9	15.2 ^[b]
DMSO	ICH-Q3D	5,000 ppm	< 6,400 ^[c]	761 ^[d]
Hydroxylamine·HCl	ICH-M7 draft status	2	< 12	37.4 ^[e]
Acetohydroxamic acid ^[f]	n.a.	72	< 73	2.5 ^[g]
EDTA ^[h]	ICH-M7	12	< 6	5 ^[h]
Cysteamine·HCl ^[i]	n.a.	200	< 518	14.4 ^[i]

^[a] The bulk SF2a-TT15 is ≥ 100 times more concentrated than the formulated vaccine candidate. ^[b] N-hydroxysuccinimide is a by-product resulting from GMBS coupling to TT or from its hydrolysis into GMBA. Here, we assume 100 % formation of by-product. ^[c] 2019 specification for DMSO is 6,400 mM, which corresponds to 5,000 ppm per vaccine dose. ^[d] $[(\text{volume DMSO mL} / \text{total volume mL}) \times 1,000 = \text{g/L}] / \text{Mw (DMSO) g/mol}$ thus $(6.33 / 106.33) \times 1,000 / 78.13$. ^[e] $(0.26 \text{ g} / 100 \text{ mL}) \times 1,000 \text{ mL} / \text{Mw: } 69.49 \text{ g/mol}$. ^[f] Acetohydroxamic acid is used as a treatment for bladder infections. A normal dose is 12 mg/kg/day, which translates to 720 mg/day for a 60 kg adult. When applying a minimum 1,000-fold decline with respect to process performance and an additional 10-fold safety margin, a maximum amount of 1/10,000 of the starting concentration of thiol **3** is acceptable. ^[g] 6.47 mg/mL: same concentration as thiol **3**. ^[h] The concentration of EDTA in conjugation buffer is 5 mM. ^[i] Cysteamine·HCl is administered as a treatment for nephropathic cystinosis. A daily dose of 2 g/day is accepted. When applying a minimum 1,000 fold decline with respect to process performance and an additional 10 fold safety margin, a maximum amount of 1/10,000 of initial concentration is acceptable or 200 µg/dose ^[i] $(180 \text{ mg} / 110 \text{ ml total}) \times 1000 \text{ mL} / \text{Mw } 113.61$. ICH: International Council for Harmonisation of Technical Requirements for Pharmaceuticals for Human Use, GMBA: 4-maleimidobutyric acid.

Simulating the maleimide activation of **4**, conjugation of the resulting **5**, and capping of the conjugation product **6** has given insight in process performance of the two different filters (see Supporting Information). Both filters performed equally in terms of impurity removal, except for DMSO. Extraction of DMSO during simulation of the conjugation reaction yielded 50% lower concentrations for the LP screen filter (Figure S4). In addition, during final purification, DMSO was removed more efficiently using the LP screen filter, and the full array of impurities was removed to below 0.1% of their respective starting concentrations (see Figure S3 and Table 2). Furthermore, higher filtrate flows and lower transmembrane pressure (TMP), inlet and outlet pressures observed during processing (not discussed) led us to select the LP screen filter for GMP production

Scale-up study on maleimide activation of TT

At production scale (100 mL), the buffer exchange and subsequent concentration of ^{GMP}4 to 1.07 mM, followed by its reaction with GMBS, yielded very similar results as compared to previous microscale experiments. The amine content (mol/mol) of ^{GMP}5 and the amount of modified amines (mol/mol) derived thereof were 3.3 and 20.9, respectively. Likewise, the amount of aggregates fulfills the established threshold of <7.5% (Table 3).

GMP production of preclinical and clinical batches of SF2a-TT15

The GMP production process was defined using the results of the large-scale ^{GMP}4 to ^{GMP}5 conversion, impurity removal investigation, and micro- and intermediate-scale bioconjugation. Reactant ratios for the maleimide introduction, conjugation, and capping steps were kept similar as in the micro- and intermediate-scale experiments. However, two changes in the purification strategy were applied. The amount of buffer exchange volume (BEV) was reduced from 10 to 5 for the purification of ^{GMP}5 and of ^{GMP}6 in order to reduce the process time and buffer usage. Nevertheless, final buffer exchange after capping remained at 10 BEV to ensure that all impurities were removed below the criteria set. This yielded preclinical and clinical batches comprising on average 19 and 17 oligosaccharide chains per TT, respectively, which was well within specifications (17 ± 5). Furthermore, the concentration of all impurities was well below the specifications set (Table 2). The yield of preclinical and clinical bulks was 76% and 80%, respectively, based on the starting amount of oligosaccharide ^{GMP}2, weighted and corrected for water content, and final carbohydrate content in the bulk. This remarkable achievement supports the robustness and scalability of the newly established GMP single-site conjugation process.

Table 2: Impurity removal when using the LP screen filter

Impurity ^[a]	Maximum Q (mM) ^[b]	BEV ^[c]	Removal below specification
GMBS	< 9	6	Yes
GMBA	< 9	6	
N-Hydroxysuccinimide	< 9	6	
DMSO	< 6,400	4	
Hydroxylamine·HCl	< 12	8	
Cysteamine·HCl	< 518	6	

^[a] No data available for acetohydroxamic acid and EDTA. ^[b] Maximum allowed quantity (Q) in the bulk vaccine (mM) See Table 1. ^[c] Amount of buffer exchange volumes needed for 99.9% removal.

Final fill and finish was achieved in 20 mM TRIS-HCl containing 150 mM NaCl, to yield two formulations of the SF2a-TT15 conjugate vaccine candidate corresponding to a 2 µg and 10 µg amount of [AB(E)CD]₃ oligosaccharide per dose (0.5 mL), respectively, based on an HPAEC-PAD quantification assay of saccharide content. Both formulations complied to all set specifications and were subsequently included in a stability study. In addition, the 10 µg formulation was used in a toxicology study and exhaustive immunogenicity study.

Table 3 Scale-up of the maleimide-modification of **4** into **5**

	Microscale ^[a,b]	Production scale ^[b]
Amine:protein molar ratio in 4 post buffer exchange	27.1 ± 1.9	29.5
Amine:protein molar ratio in 5	5.1 ± 2.0	3.3
Total amount of modified amines in 5	22.1 ± 0.6	20.9
Amount of aggregates in concentrated 4 (%)	29.9 ± 3.4	30.1
Amount of aggregates in 5 (%)	36.8 ± 3.8	33.9
Aggregate induction (%) ^[c]	7.0 ± 3.0	3.8

^[a] Microscale experiments results show average and 1 x Standard deviation (SD) (n = 5). ^[b] GMP^{TT} used for both pre-clinical and clinical batches were of the same lot. ^[c] Aggregate induction = Amount of aggregates in **5** (%) - Amount of aggregates in concentrated **4** (%).

Stability of the SF2a-TT15 preclinical and clinical batches

A real time stability study was initiated, where both formulations (8 and 40 µg/mL oligosaccharide, after a two-fold dilution yielded the 2 and 10 µg oligosaccharide equivalent per vaccine dose (0.5 mL)) were stored at 2–8 °C and evaluated at different time points (Figure 3). Stability was assessed by evaluating visual aspects, osmolality, pH and protein content (data not shown), aggregation (molecular size distribution), as well as free and total carbohydrate content.

With respect to aggregation, we observed a downward trend in the first nine months for both formulations in which a root cause analysis was attributed to the analysis and not to a change in the composition of the formulated SF2a-TT15. No significant changes were observed during the remainder of the stability study.

The free carbohydrate content started at 4.1% for the bulk before final fill and finish, for both preclinical and clinical batches. When this parameter was assessed after fill and finish, a significant increase was detected during the first 12 months of conservation, from 4.5% and 6.0% to 16.9% and 14.8% for the vials corresponding to 2 µg and 10 µg oligosaccharide equivalent per vaccine dose, respectively. While existing, this increase

was subsequently much less perceivable to reach 19.8% and 13.7% at 36 months, and 21.7% and 18.1% at 66 months, respectively. All parameters taken into account, the real-time stability data of the preclinical batch demonstrated product stability for a period of at least 66 months, which was exceptional since according to current ICH guidelines (ICH-Q1-A-(R2)) a 12-month period would have sufficed.

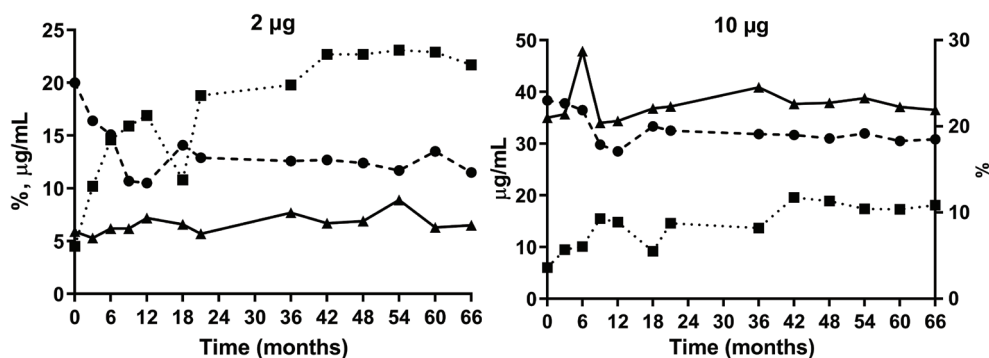


Figure 3 Real-time stability of the SF2a-TT15 clinical batch for two different formulations. **Left panel:** 2 µg carbohydrate equivalent per vaccine dose (amount of SF2a-TT15 corresponding to 8 µg carbohydrate per mL). **Right panel:** 10 µg carbohydrate equivalent per vaccine dose (amount of SF2a-TT15 corresponding to 40 µg carbohydrate per mL). x-axis: Time (months), (●) Aggregation (%), average of two replicates; (■) Free carbohydrate content (% of total carbohydrate, average of three replicates, SD < 0.1%); (▲) Total carbohydrate content (µg/mL, average of three replicates, SD < 0.1%). SD: standard deviation (not shown).

Immunogenicity of the SF2a-TT15 preclinical batch in mice

In the frame of process optimization to achieve SF2a-TT15, we showed that four injections in mice of a conjugate amount equivalent to 2.5 µg of oligosaccharide, as compared to three injections, slightly increased the anti-SF2a LPS IgG titer [51], thereby confirming original observations [49]. Adjuvanting with aluminum hydroxide (alum, Al(OH)₃) significantly increased the immunogenicity of SF2a-TT15, with a sustained anti-SF2a LPS IgG titer still observable at six months after the last injection [51]. The immunogenicity of the preclinical batch was similarly assessed. The previously observed positive impact of a fourth injection and of alum, on the immunogenicity of SF2a-TT15 used at a dose of 2.5 µg of oligosaccharide was confirmed (Figure 4A). Similar results were obtained while using a higher dose, *i.e.*, 10 µg of [AB(E)CD]₃ (Figure 4B). Noticeably, increasing the dose had no significant impact on the anti-SF2a LPS IgG titer. For both doses, formulation with alum overcame the need for a fourth injection. The sustained response at six months post the last injection was confirmed for both doses (data not shown).

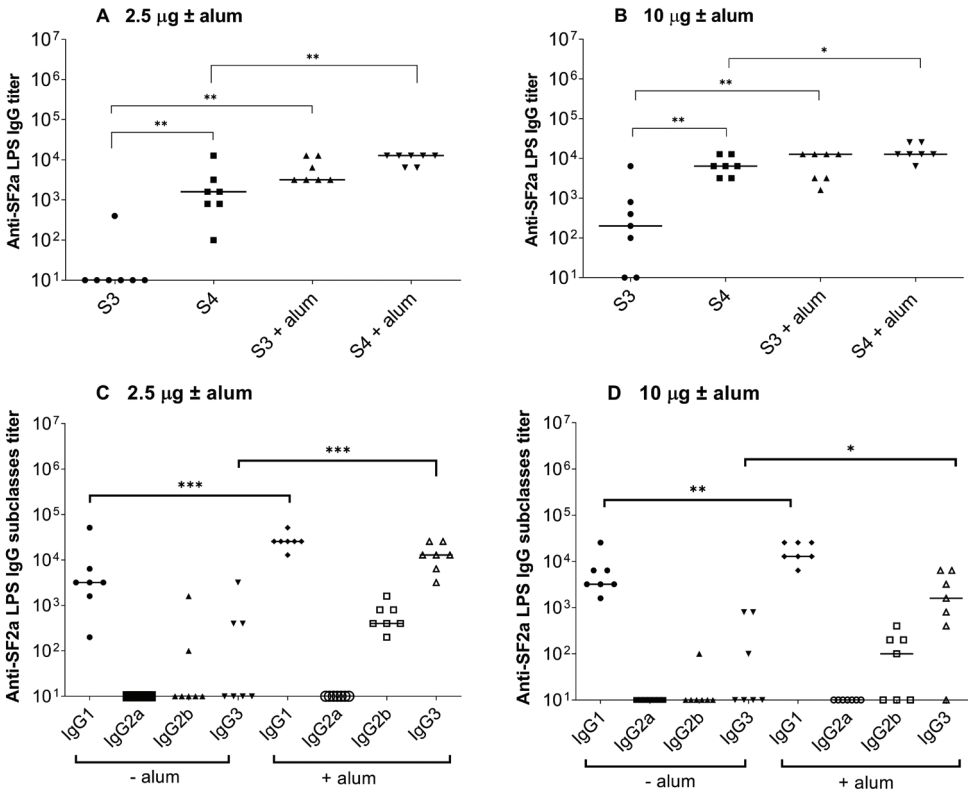


Figure 4: Immunogenicity of the SF2a-TT15 preclinical batch. Mice were immunized i.m. three times at 3 week-interval, followed by a 4th injection one month later with an equivalent of 2.5 µg or 10 µg of carbohydrate per dose adjuvanted or not with alum. Anti-SF2a LPS IgG titers were measured by ELISA seven days after the 3rd (S3) and 4th (S4) injection (panels A and B). Anti-SF2a LPS IgG subclass titers (panels C and D) were determined on the day of the 4th injection. Mann Whitney non parametric t test: * p<0.05; ** p<0.005; *** p<0.0005. The Ab titer median value is indicated with a horizontal bar.

Regarding the IgG subclasses, SF2a-TT15 elicited predominantly an anti-SF2a LPS IgG1 response which significantly increased in the presence of alum for both doses. Of note, the specific IgG3 response that was very low upon immunization with the nonadjuvanted conjugate, was significantly increased with the adjuvanted one for both doses (Figure 4 C, D). These findings show the immunogenicity of the SF2a-TT15 preclinical batch in mice and confirm the role of alum in potentiating the anti-SF2a LPS IgG response. In addition, data indicate that alum favors the induction of both SF2a-specific IgG1- and IgG3-mediated responses.

Cross-reactivity of the antibodies induced by the SF2a-TT15 preclinical batch towards other *S. flexneri* serotypes

Sera from mice immunized twice with the adjuvanted equivalent of 10 µg [AB(E)CD]₃ were tested in ELISA for their binding to LPS purified from SF1b, 2b, 3a, 5a, and 6 as compared to the SF2a LPS. Of note, for SF1b and SF6, two and three different strains, respectively, were used as a source of purified LPS. None of the tested LPSs were recognized (Figure 5), indicating that the murine antibodies induced by the SF2a-TT15 preclinical batch were specific for the homologous SF2a LPS among those tested.

Bactericidal activity of the anti-SF2a LPS IgG Abs induced by the SF2a-TT15 preclinical batch

In previous reports, we used the mouse model of pulmonary infection to report the protective capacity of the anti-SF2a LPS IgG Abs induced by SF2a glycoconjugates [49, 51]. Considering that the serum bactericidal assay (SBA) was recently recognized as the “gold-standard” assay to assess the functionality of antibodies induced by Shigella vaccine candidates [53], the bactericidal antibody titer induced by the SF2a-TT15 preclinical batch was determined. For each tested condition, decomplexed sera pooled from seven immunized mice were used. For the 2.5 µg saccharide dose administered three times without and with alum, the SBA titer (mean value ± SD) was 4600 ± 280 and 16000 ± 500, respectively. The corresponding values for the 10 µg dose administered without and with alum were 10500 ± 500 and 27000 ± 3000, respectively. For both doses, the SBA titer increase observed in the presence of alum was in accordance with the increase of the anti-SF2a LPS IgG titer as compared to the nonadjuvanted conjugate (Figure 4). Similarly, the protective capacity of the SF2a-TT15-induced Abs was shown previously to be dependent on the Ab titer when measured in the murine model of pulmonary infection [51].

Recognition of a panel of clinical SF2a isolates by the anti-SF2a LPS IgG Abs induced by the SF2a-TT15 preclinical batch

The objective of a vaccine being able to protect against the largest diversity of circulating strains, we assessed the recognition of a panel of SF2a clinical isolates characterized at the French National Reference Center for *Enterobacteriaceae* (Institut Pasteur, Paris), upon recovery from stools of individuals with a diarrheal episode when back from traveling to different countries. The clinical isolates were compared to SF2a strain 454, the reference strain used for selecting the oligosaccharide hapten in the SF2a-TT15 conjugate [36, 49].

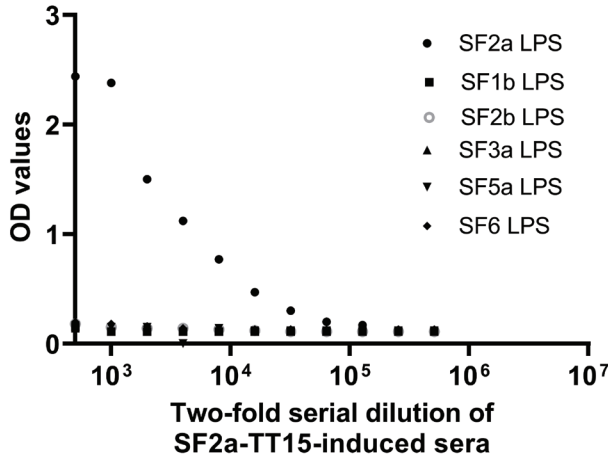


Figure 5: Cross-reactivity of the SF2a-TT15 preclinical batch-induced antibodies. Sera from seven mice immunized with the equivalent of 10 µg [AB(E)CD]₃ per dose were pooled, diluted, and tested in ELISA towards a panel of LPSs purified from different *S. flexneri* serotypes strains. OD: optical density.



Figure 6: Recognition of a panel of 24 SF2a clinical isolates by SF2a-TT15-induced sera. Strain recognition was performed by FACS and arbitrary units defined considering a value of 100 for the reference strain. Data are representative of 3 independent experiments. FACS: Fluorescence-Activated Cell Sorting.

As shown in Figure 6, 18 out of the 24 tested strains were above 50% recognition as compared to SF2a 454, while six were below. The two lowest recognized clinical isolates from Italy and Cambodia were shown to express much less LPS as compared to the other strains (data not shown). These results show that the SF2a-TT15 preclinical batch gives rise to specific SF2a Abs recognizing a large diversity of SF2a circulating strains.

SF2a-TT15 toxicology assessment

To provide data on the local and systemic toxicity and reactogenicity of the formulated preclinical SF2a-TT15 (10 µg carbohydrate per dose), either adjuvanted with Al(OH)₃ or nonadjuvanted, male and female rabbits received four intramuscular (*i.m.*) injections at a 3 week interval. All rabbits were monitored for different parameters: body weight, food intake, body temperature (before, 4 and 24 h after each dose), hematology (red blood cell parameters, coagulation parameters, total or differential white blood cell counts), clinical chemistry, and macro- and microscopic examination of organs. The parameters were either not affected by the treatment or their analysis did not reveal any treatment related effects (not described). The Al(OH)₃-adjuvanted SF2a-TT15 formulation showed mild to moderate widespread mixed inflammation at the injection site. The nonadjuvanted vaccine candidate showed localized mixed inflammation or mild widespread mixed inflammation at the injection site (Tables S2 and S3). For both groups, these effects subsided 17 days after the last injection. It was concluded that the 10 µg carbohydrate-equivalent formulation of the synthetic glycan-based conjugate vaccine candidate, whether alum-adjuvanted or nonadjuvanted, was well tolerated and did not result in any signs of systemic toxicity in vaccine recipients. Additionally, SF2a-TT15 was immunogenic in rabbits (Figure S6) as it was shown to be in mice (Figure 4). Therefore, the evaluation of toxicity as described took into account the presence of the anti-SF2a LPS IgG response.

Conclusions

The Gram-negative bacterium SF2a is the most prevalent *S. flexneri* serotype and the main cause of shigellosis. The need for a vaccine that would protect the youngest living in low-income settings against shigellosis was emphasized recently as *Shigella* was identified as a dominant cause of diarrheal disease in this population. Despite the attractiveness of synthetic glycans as vaccine components [35, 54, 55], limited access to chemically defined complex oligosaccharides has held up investigations on their potential use in the context of antibacterial vaccines. Herein, following up on the successful licensing of Quimi-Hib, we have described the GMP manufacturing of preclinical and clinical batches of SF2a-TT15, a synthetic carbohydrate conjugate vaccine candidate designed against endemic shigellosis. The scale-up of the original 40-step synthetic process [46, 51] was achieved

successfully to reach a 100 mL production scale of the [AB(E)CD]₃-TT conjugate complying with established critical standards, among which glycan loading and aggregation. This corresponded to a volumetric increase by a factor 625 of the microscale conjugation step, further demonstrating the established process robustness. As part of these developments, the use of TFF was proven feasible with conjugation kinetics and efficiency comparable to that seen at the microscale. The final high yielding production of both batches (76% and 80% for the SF2a-TT15 preclinical and clinical batches, respectively, with reference to the oligosaccharide precursor ^{GMP}**2** and buffer exchanged ^{GMP}TT (^{GMP}**4**) provided several tens of thousands of doses of SF2a-TT15 (^{GMP}**6**). The synthetic glycan-TT conjugate designed for vaccination against SF2a infection fulfilled all GMP criteria. The DS was formulated to achieve two vaccine doses (2 µg and 10 µg of glycan per injection, respectively). Whether alum-adjuvanted or nonadjuvanted, SF2a-TT15 passed all toxicology criteria and exhibited strong anti-SF2a immunogenicity in both mice and rabbits. The SF2a-TT15-induced antibodies are specific for the SF2a LPS and functional *in vitro*, exhibiting high anti-SF2a SBA titers. Moreover, they bound to a large diversity of SF2a circulating strains isolated from individuals diagnosed with shigellosis. It is noteworthy that many bacterial polysaccharides are diversely O-acetylated and that O-acetyl groups may compose a meaningful part of the immunodominant epitopes expressed at the surface of pathogenic bacteria [56, 57]. Yet, the extent to which O-acetylation contributes to the immunological properties of polysaccharide antigens is highly variable [58, 59]. Herein, the observed broad SF2a strain recognition substantiated our original observation, (60) also underlined by others [61, 62], that O-Ag O-acetylation does not play a major role in the antibody-mediated immunity to SF2a, despite the fact that SF2a strains are knowingly characterized by O-Ags featuring repeating units di-O-acetylated to various extents. (42–44) These findings support the selection of the non-O-acetylated [AB(E)CD]₃ glycan component in SF2a-TT15, thereby facilitating product manufacturing to a meaningful extent [63, 64]. Not the least, the implementation of a unique homogeneous chemically defined glycan hapten missing the naturally occurring labile substitutions also avoids challenging analytical issues and stability considerations otherwise of concern [65] and therefore cost. The SF2a-TT15 formulations corresponding to both the 2 µg and 10 µg of glycan per vaccine dose were shown to be stable for at least 66 months. In particular, the free carbohydrate content fulfilled typical published specifications both at product release (<10%) and over vaccine shelf life (<25%) [64]. Despite the possible concern arising from reports on the sensitivity of antibody-drug conjugates featuring a thiol-maleimide linker to the chemical and structural dynamics at the conjugation site [66], our data suggest that spacer hydrolysis resulting from the retro-Michael addition of the formed thiosuccinimide [67] remains in an acceptable range under formulation and storage conditions. Besides stability, concern stems from the possibility to generate meaningful levels of anti-spacer antibodies following immunization with glycan conjugates. In the worst case scenario,

immunity diverges toward immunodominant epitopes present on the spacer resulting in poor antibody titers against the glycan component [68, 69]. We have previously stressed the absence of SF2a-TT15-induced detectable anti-linker antibodies in mice [49]. Following up on the licensing of Quimi-Hib, issued from the conjugation of a maleimide-equipped polyribosylribitolphosphate hapten and thiolated TT [70], and adding to a remarkable hapten conjugation yield, far above the readily and consistently achievable 25–40% yield for glycoconjugate vaccine manufacture [64], the significant long-term stability of SF2a-TT15 promotes thiol-maleimide bioconjugation as one of the existing biorthogonal chemistries to explore further in the context of glycoconjugate vaccine development [71, 72].

This original glycoconjugate vaccine candidate was shown to be safe and well tolerated in healthy adults while inducing high titers of anti-SF2a LPS IgGs with bactericidal activity toward SF2a bacteria *in vitro* [33]. The 10 µg saccharide dose, alum-adjuvanted or not, was demonstrated to be highly potent, inducing the highest IgG antibody titer after the first injection. No boosting effect followed the second and third injections. In contrast, for the adjuvanted 2 µg saccharide dose, a boosting effect of the second and third injections was observed in humans. Interestingly, mouse SBA titers might be considered as predictive of what will be induced in humans [31]. In fact, high SBA titers were also measured in the human volunteers. Therefore, it is likely that the diversity of strain recognition shown here with the mouse sera might be extrapolated to human SF2a-TT15-induced sera. Indeed, both assays rely first on the capacity of the vaccine-induced antibodies to bind SF2a bacteria. The successful outcome of this first-in-human study complemented by robust preclinical data as disclosed herein, including long-term stability data demonstrating highly similar quality with the formulated conjugate administered in the phase 1, contributed to prompt further evaluation in humans of SF2a-TT15, a vaccine candidate elaborated from the understanding of the structural basis of the immune recognition of LPS-protective epitopes [47, 48, 60]. Aiming at derisking product development [73], a Control Human Infection Model (CHIM) study [74] will shed light on the protective capacity of SF2a-TT15 in naive adults (NCT0478022). Otherwise, an age-descending study in Kenya will assess the safety and immunogenicity of SF2a-TT15 in the target population, especially infants, in the field (NCT04602975).

This first detailed report on the GMP process of a synthetic carbohydrate–protein conjugate vaccine candidate targeting an infectious disease supports feasibility and strongly encourages further development in a domain, which is the subject of rapidly growing interest.

Author information

Corresponding Authors

Robert M. F. van der Put – Intravacc, P.O. Box 450, 3720 AL Bilthoven, the Netherlands; Email: robert.van.der.put@intravacc.nl, Laurence A. Mulard – Institut Pasteur, Université Paris Cité, CNRS UMR3523, Unité de Chimie des Biomolécules, 28 rue du Dr Roux, 75724 Paris Cedex 15, France; Orcid<https://orcid.org/0000-0002-5622-1422>; Email: laurence.mulard@pasteur.fr

Present Addresses

Present address: Emeritus Professor, Institut Pasteur, 28 rue du Dr Roux, 75 724 Paris Cedex 15, France. Emeritus Professor, Collège de France, 11 Place Marcelin Berthelot, 75005 Paris, France. The Center for Microbes, Development and Health, Institut Pasteur of Shanghai, Shanghai, China. § Present address: Innovation Lab: Vaccines, Institut Pasteur, 28 rue du Dr Roux, 75724 Paris Cedex 15, France

Author Contributions

R. M. F. P.: conceptualization, investigation, supervision and writing; C. S., A. H., M. H. and H. T.: formal analysis, methodology and validation; O. O., J. W., M. S. and J. U.: project administration; F. T. and C. G.: investigation and provision of resources; P. J. S.: Funding; A. P.: Funding, supervision, writing; L. A. M.: Funding, conceptualization, supervision and writing.

Funding

The research leading to these results has received funding from Institut Pasteur (to P.J.S. and L.A.M.), the European Union Seventh Framework Programme for research, technological development and demonstration under Grant Agreement no. 261472-STOPENTERICS (to J.W., P.J.S., and L.A.M.), the French Government Investissement d'Avenir program, the Laboratoire d'Excellence "Integrative Biology of Emerging Infectious Diseases" (Grant No. ANR-10-LABX-62-IBEID to P.J.S. and A.P.), and the Bill & Melinda Gates Foundation (Grant Agreement Investment ID OPP1198140 to A.P. and L.A.M.).

Notes

The findings and conclusions contained within this manuscript are those of the authors and do not necessarily reflect positions or policies of the Bill & Melinda Gates Foundation. The authors declare the following competing financial interest(s): P.J.S., A.P., and L.A.M are coinventors of the patent Nb PCT/IB2004/002657.

Dedication

†This manuscript is dedicated in loving memory of Carolien Smitsman, for her insights and support on this project, we are forever grateful for her contributions.

Acknowledgement

The authors thank Dr. P. Hoogerhout (Intravacc) for his expert advice during experiments and reflection on writing the manuscript, Gerco van Eikenhorst (Intravacc) and Astrid Coolen (Intravacc) for their help in preparing the preclinical lot, Maarten Danial (Intravacc) and Prof. Dr. Roland Pieters (University Utrecht) for their input in reviewing the manuscript and providing guidance during experiments that preceded the scale-up. The authors warmly thank François-Xavier Weill (CNR *Escherichia coli*, *Shigella*, *Salmonella*, Institut Pasteur) for providing the clinical SF2a isolates.

Associated content

Supporting Information

The Supporting Information is available free of charge on the ACS Publications website. Additional information on the conjugation kinetics, impurity removal and immunogenicity data, also including toxicology study results. ¹H-NMR spectrum for oligosaccharide ^{GMP}**2**.

REFERENCES

1. Khalil, I. A.; Troeger, C.; Blacker, B. F.; Rao, P. C.; Brown, A.; Atherly, D. E.; Brewer, T. G.; Engmann, C. M.; Houpt, E. R.; Kang, G. Morbidity and mortality due to *Shigella* and enterotoxigenic *Escherichia coli* diarrhoea: the Global Burden of Disease Study 1990–2016. *Lancet Infect Dis* 2018, 18 (11), 1229– 1240, DOI: 10.1016/S1473-3099(18)30475-4
2. Liu, J.; Platts-Mills, J. A.; Juma, J.; Kabir, F.; Nkeze, J.; Okoi, C.; Operario, D. J.; Uddin, J.; Ahmed, S.; Alonso, P. L. Use of quantitative molecular diagnostic methods to identify causes of diarrhoea in children: a reanalysis of the GEMS case-control study. *Lancet* 2016, 388 (10051), 1291– 1301, DOI: 10.1016/S0140-6736(16)31529-X
3. Platts-Mills, J. A.; Babji, S.; Bodhidatta, L.; Gratz, J.; Haque, R.; Havt, A.; McCormick, B. J.; McGrath, M.; Olortegui, M. P.; Samie, A. Pathogen-specific burdens of community diarrhoea in developing countries: a multisite birth cohort study (MAL-ED). *Lancet Glob*.
4. Troeger, C.; Colombara, D. V.; Rao, P. C.; Khalil, I. A.; Brown, A.; Brewer, T. G.; Guerrant, R. L.; Houpt, E. R.; Kotloff, K. L.; Misra, K. Global disability-adjusted life-year estimates of long-term health burden and undernutrition attributable to diarrhoeal diseases in children younger than 5 years. *Lancet Glob. Health* 2018, 6 (3), e255– e269, DOI: 10.1016/S2214-109X(18)30045-7
5. Porter, C. K.; Olson, S.; Hall, A.; Riddle, M. S. Travelers' Diarrhea: An Update on the Incidence, Etiology, and Risk in Military Deployments and Similar Travel Populations. *Mil Med.* 2017, 182 (S2), 4– 10, DOI: 10.7205/MILMED-D-17-00064
6. Kotloff, K. L.; Riddle, M. S.; Platts-Mills, J. A.; Pavlinac, P.; Zaidi, A. K. M. Shigellosis. *Lancet* 2018, 391 (10122), 801– 812, DOI: 10.1016/S0140-6736(17)33296-8
7. Baker, S.; The, H. C. Recent insights into *Shigella*. *Curr. Opin Infect Dis* 2018, 31 (5), 449– 454, DOI: 10.1097/QCO.0000000000000475
8. Antibiotic Resistance Threats in the United States; CDC, 2019.
9. World Health Organization, Global priority list of antibiotic-resistant bacteria to guide research, discovery, and development of new antibiotics. https://www.who.int/medicines/publications/WHO-PPL-Short_Summary_25Feb-ET_NM_WHO.pdf?ua=1, 2017 (accessed 2021-07-19).
10. Hosangadi, D.; Smith, P. G.; Kaslow, D. C.; Giersing, B. K.; the WHO ETEC & *Shigella* Vaccine Consultation Expert Group. WHO consultation on ETEC and *Shigella* burden of disease, Geneva, 6–7th April 2017: Meeting report. *Vaccine* 2019, 37 (50), 7381– 7390, DOI: 10.1016/j.vaccine.2017.10.011
11. Livio, S.; Strockbine, N. A.; Panchalingam, S.; Tennant, S. M.; Barry, E. M.; Marohn, M. E.; Antonio, M.; Hossain, A.; Mandomando, I.; Ochieng, J. B. *Shigella* isolates from the global enteric multicenter study inform vaccine development. *Clin Infect Dis* 2014, 59 (7), 933– 941, DOI: 10.1093/cid/ciu468
12. Lindberg, A. A.; Karnell, A.; Weintraub, A. The lipopolysaccharide of *Shigella* bacteria as a virulence factor. *Rev. Infect Dis* 1991, 13, S279– S284, DOI: 10.1093/clinids/13.Supplement_4.S279
13. Ferreccio, C.; Prado, V.; Ojeda, A.; Cayyazo, M.; Abrego, P.; Guers, L.; Levine, M. M. Epidemiologic patterns of acute diarrhea and endemic *Shigella* infections in children in a poor periurban setting in Santiago, Chile. *Am. J. Epidemiol* 1991, 134 (6), 614– 627, DOI: 10.1093/oxfordjournals.aje.a116134
14. Cohen, D.; Bassal, R.; Goren, S.; Rouach, T.; Taran, D.; Schemberg, B.; Peled, N.; Keness, Y.; Ken-Dror, S.; Vasilev, V. Recent trends in the epidemiology of shigellosis in Israel. *Epidemiol Infect* 2014, 142 (12), 2583– 2594, DOI: 10.1017/S0950268814000260
15. Robbins, J. B.; Chu, C.; Schneerson, R. Hypothesis for vaccine development: protective immunity to enteric diseases caused by nontyphoidal salmonellae and shigellae may be conferred by serum IgG antibodies to the O-specific polysaccharide of their lipopolysaccharides. *Clin Infect Dis* 1992, 15 (2), 346– 361, DOI: 10.1093/clinids/15.2.346
16. Chu, C. Y.; Liu, B. K.; Watson, D.; Szu, S. S.; Bryla, D.; Shiloach, J.; Schneerson, R.; Robbins, J. B. Preparation, characterization, and immunogenicity of conjugates composed of the O-specific polysaccharide of *Shigella dysenteriae* type 1 (*Shiga's bacillus*) bound to tetanus toxoid. *Infect. Immun.* 1991, 59 (12), 4450– 4458, DOI: 10.1128/iai.59.12.4450-4458.1991

17. Barel, L.-A.; Mulard, L. A. Classical and novel strategies to develop a *Shigella* glycoconjugate vaccine: from concept to efficacy in human. *Hum. Vaccines Immunother.* 2019, 15 (6), 1338– 1356, DOI: 10.1080/21645515.2019.1606972
18. Cohen, D.; Ashkenazi, S.; Green, M. S.; Gdalevich, M.; Robin, G.; Slepon, R.; Yavzori, M.; Orr, N.; Block, C.; Ashkenazi, I. Double-blind vaccine-controlled randomised efficacy trial of an investigational *Shigella sonnei* conjugate vaccine in young adults. *Lancet* 1997, 349 (9046), 155– 159, DOI: 10.1016/S0140-6736(96)06255-1
19. Passwell, J. H.; Ashkenazi, S.; Banet-Levi, Y.; Ramon-Saraf, R.; Farzam, N.; Lerner-Geva, L.; Even-Nir, H.; Yerushalmi, B.; Chu, C.; Shiloach, J.; Robbins, J. B.; Schneerson, R. Age-related efficacy of *Shigella* O-specific polysaccharide conjugates in 1–4-year-old Israeli children. *Vaccine* 2010, 28 (10), 2231– 2235, DOI: 10.1016/j.vaccine.2009.12.050
20. Jansen, K. U.; Knirsch, C.; Anderson, A. S. The role of vaccines in preventing bacterial antimicrobial resistance. *Nat. Med.* 2018, 24 (1), 10– 19, DOI: 10.1038/nm.4465
21. Poolman, J. T. Expanding the role of bacterial vaccines into life-course vaccination strategies and prevention of antimicrobial-resistant infections. *npj Vaccines* 2020, 5, 84, DOI: 10.1038/s41541-020-00232-0
22. Mettu, R.; Chen, C.-Y.; Wu, C.-Y. Synthetic carbohydrate-based vaccines: challenges and opportunities. *J. Biomed Sci.* 2020, 27 (1), 9, DOI: 10.1186/s12929-019-0591-0
23. Micoli, F.; Bagnoli, F.; Rappuoli, R.; Serruto, D. The role of vaccines in combatting antimicrobial resistance. *Nat. Rev. Microbiol* 2021, 19 (5), 287– 302, DOI: 10.1038/s41579-020-00506-3
24. Rappuoli, R. Glycoconjugate vaccines: Principles and mechanisms. *Sci. Transl Med.* 2018, 10 (456), eaat4615 DOI: 10.1126/scitranslmed.aat4615
25. Sun, X.; Stefanetti, G.; Berti, F.; Kasper, D. L. Polysaccharide structure dictates mechanism of adaptive immune response to glycoconjugate vaccines. *Proc. Natl. Acad. Sci. U. S. A.* 2019, 116 (1), 193– 198, DOI: 10.1073/pnas.1816401115
26. Avci, F.; Berti, F.; Dull, P.; Hennessey, J.; Pavliak, V.; Prasad, A. K.; Vann, W.; Wacker, M.; Marcq, O. Glycoconjugates: What It Would Take To Master These Well-Known yet Little-Understood Immunogens for Vaccine Development. *mSphere* 2019, 4 (5), e00520-00519 DOI: 10.1128/mSphere.00520-19
27. Rappuoli, R.; De Gregorio, E.; Costantino, P. On the mechanisms of conjugate vaccines. *Proc. Natl. Acad. Sci. U. S. A.* 2019, 116 (1), 14– 16, DOI: 10.1073/pnas.1819612116
28. Berti, F.; Micoli, F. Improving efficacy of glycoconjugate vaccines: from chemical conjugates to next generation constructs. *Curr. Opin Immunol* 2020, 65, 42– 49, DOI: 10.1016/j.coi.2020.03.015
29. Lang, S.; Huang, X. Carbohydrate Conjugates in Vaccine Developments. *Front. Chem.* 2020, 8, 284, DOI: 10.3389/fchem.2020.00284
30. McGuinness, D.; Kauffhold, R. M.; McHugh, P. M.; Winters, M. A.; Smith, W. J.; Giovarelli, C.; He, J.; Zhang, Y.; Musey, L.; Skinner, J. M. Immunogenicity of PCV24, an expanded pneumococcal conjugate vaccine, in adult monkeys and protection in mice. *Vaccine* 2021, 39 (30), 4231– 4237, DOI: 10.1016/j.vaccine.2021.04.067
31. Cohen, D.; Meron-Sudai, S.; Bialik, A.; Asato, V.; Goren, S.; Ariel-Cohen, O.; Reizis, A.; Hochberg, A.; Ashkenazi, S. Serum IgG antibodies to *Shigella* lipopolysaccharide antigens - a correlate of protection against shigellosis. *Hum. Vaccines Immunother.* 2019, 15 (6), 1401– 1408, DOI: 10.1080/21645515.2019.1606971
32. Obiero, C. W.; Ndiaye, A. G. W.; Scire, A. S.; Kaunyangi, B. M.; Marchetti, E.; Gone, A. M.; Schutte, L. D.; Riccucci, D.; Auerbach, J.; Saul, A. A Phase 2a Randomized Study to Evaluate the Safety and Immunogenicity of the 1790GAHB Generalized Modules for Membrane Antigen Vaccine against *Shigella sonnei* Administered Intramuscularly to Adults from a Shigellosis-Endemic Country. *Front. Immunol.* 2017, 8, 1884, DOI: 10.3389/fimmu.2017.01884
33. Cohen, D.; Atsmon, J.; Artaud, C.; Meron-Sudai, S.; Gougeon, M. L.; Bialik, A.; Goren, S.; Asato, V.; Ariel-Cohen, O.; Reizis, A. Safety and immunogenicity of a synthetic carbohydrate conjugate vaccine against *Shigella flexneri* 2a in healthy adult volunteers: a phase 1, dose-escalating, single-blind, randomised, placebo-controlled study. *Lancet Infect Dis* 2021, 21 (4), 546– 558, DOI: 10.1016/S1473-3099(20)30488-6
34. Talaat, K. R.; Alaimo, C.; Martin, P.; Bourgeois, A. L.; Dreyer, A. M.; Kaminski, R. W.; Porter, C. K.; Chakraborty, S.; Clarkson, K. A.; Brubaker, J. Human challenge study with a *Shigella* bioconjugate vaccine: Analyses of clinical

- efficacy and correlate of protection. *EBioMedicine* 2021, 66, 103310, DOI: 10.1016/j.ebiom.2021.103310
35. Pozsgay, V.; Chu, C.; Pannell, L.; Wolfe, J.; Robbins, J. B.; Schneerson, R. Protein conjugates of synthetic saccharides elicit higher levels of serum IgG lipopolysaccharide antibodies in mice than do those of the O-specific polysaccharide from *Shigella dysenteriae* type 1. *Proc. Natl. Acad. Sci. U. S. A.* 1999, 96 (9), 5194–5197, DOI: 10.1073/pnas.96.9.5194
 36. Phalipon, A.; Costachel, C.; Grandjean, C.; Thuizat, A.; Guerreiro, C.; Tanguy, M.; Nato, F.; Vulliez-Le Normand, B.; Belot, F.; Wright, K. Characterization of functional oligosaccharide mimics of the *Shigella flexneri* serotype 2a O-antigen: implications for the development of a chemically defined glycoconjugate vaccine. *J. Immunol* 2006, 176 (3), 1686–1694, DOI: 10.4049/jimmunol.176.3.1686
 37. Salamone, S.; Guerreiro, C.; Cambon, E.; André, I.; Remaud-Simeon, M.; Mulard, L. A. Programmed chemo-enzymatic synthesis of the oligosaccharide component of a carbohydrate-based antibacterial vaccine candidate. *Chem. Commun.* 2015, 51 (13), 2581–2584, DOI: 10.1039/C4CC08805K
 38. Chassagne, P.; Fontana, C.; Guerreiro, C.; Gauthier, C.; Phalipon, A.; Widmalm, G.; Mulard, L. A. Structural studies of the O-acetyl-containing O-antigen from a *Shigella flexneri* serotype 6 strain and synthesis of oligosaccharide fragments thereof. *Eur. J. Org. Chem.* 2013, 4085–4106, DOI: 10.1002/ejoc.201300180
 39. Hargreaves, J. M.; Le Guen, Y.; Guerreiro, C.; Descroix, K.; Mulard, L. A. Linear synthesis of the branched pentasaccharide repeats of O-antigens from *Shigella flexneri* 1a and 1b demonstrating the major steric hindrance associated with type-specific glucosylation. *Org. Biomol Chem.* 2014, 12 (39), 7728–7749, DOI: 10.1039/C4OB01200C
 40. Hu, Z.; Bongat White, A. F.; Mulard, L. A. Efficient iterative synthesis of O-acetylated tri- to pentadecasaccharides related to the lipopolysaccharide of *Shigella flexneri* type 3 a through di- and trisaccharide glycosyl donors. *Chem. Asian J.* 2017, 12 (4), 419–439, DOI: 10.1002/asia.201600819
 41. Dhara, D.; Mulard, L. A. Exploratory N-Protecting Group Manipulation for the Total Synthesis of Zwitterionic *Shigella sonnei* Oligosaccharides. *Chem.-Eur. J.* 2021, 27 (18), 5694–5711, DOI: 10.1002/chem.202003480
 42. Kubler-Kielb, J.; Vinogradov, E.; Chu, C.; Schneerson, R. O-Acetylation in the O-specific polysaccharide isolated from *Shigella flexneri* serotype 2a. *Carbohydr. Res.* 2007, 342 (3–4), 643–647, DOI: 10.1016/j.carres.2006.09.017
 43. Perepelov, A. V.; L'vov, V. L.; Liu, B.; Senchenkova, S. N.; Shekht, M. E.; Shashkov, A. S.; Feng, L.; Aparin, P. G.; Wang, L.; Knirel, Y. A. A similarity in the O-acetylation pattern of the O-antigens of *Shigella flexneri* types 1a, 1b, and 2a. *Carbohydr. Res.* 2009, 344 (5), 687–692, DOI: 10.1016/j.carres.2009.01.004
 44. Theillet, F. X.; Simenel, C.; Guerreiro, C.; Phalipon, A.; Mulard, L. A.; Delepiere, M. Effects of backbone substitutions on the conformational behavior of *Shigella flexneri* O-antigens: implications for vaccine strategy. *Glycobiology* 2011, 21 (1), 109–121, DOI: 10.1093/glycob/cwq136
 45. Anish, C.; Schumann, B.; Pereira, C. L.; Seeberger, P. H. Chemical biology approaches to designing defined carbohydrate vaccines. *Chem. Biol.* 2014, 21 (1), 38–50, DOI: 10.1016/j.chembiol.2014.01.002
 46. Bélot, F.; Guerreiro, C.; Baleux, F.; Mulard, L. A. Synthesis of two linear PADRE conjugates bearing a deca- or pentadecasaccharide B epitope as potential synthetic vaccines against *Shigella flexneri* serotype 2a infection. *Chem.-Eur. J.* 2005, 11 (5), 1625–1635, DOI: 10.1002/chem.200400903
 47. Theillet, F. X.; Frank, M.; Vulliez-Le Normand, B.; Simenel, C.; Hoos, S.; Chaffotte, A.; Belot, F.; Guerreiro, C.; Nato, F.; Phalipon, A. Dynamic aspects of antibody:oligosaccharide complexes characterized by molecular dynamics simulations and saturation transfer difference nuclear magnetic resonance. *Glycobiology* 2011, 21 (12), 1570–1579, DOI: 10.1093/glycob/cwr059
 48. Vulliez-Le Normand, B.; Saul, F. A.; Phalipon, A.; Belot, F.; Guerreiro, C.; Mulard, L. A.; Bentley, G. A. Structures of synthetic O-antigen fragments from serotype 2a *Shigella flexneri* in complex with a protective monoclonal antibody. *Proc. Natl. Acad. Sci. U. S. A.* 2008, 105 (29), 9976–9981, DOI: 10.1073/pnas.0801711105
 49. Phalipon, A.; Tanguy, M.; Grandjean, C.; Guerreiro, C.; Belot, F.; Cohen, D.; Sansonetti, P. J.; Mulard, L. A. A synthetic carbohydrate-protein conjugate vaccine candidate against *Shigella flexneri* 2a infection. *J. Immunol* 2009, 182 (4), 2241–2247, DOI: 10.4049/jimmunol.0803141
 50. Said Hassane, F.; Phalipon, A.; Tanguy, M.; Guerreiro, C.; Belot, F.; Frisch, B.; Mulard, L. A.; Schuber, F. Rational design and immunogenicity of liposome-based diepitope constructs: application to synthetic

- oligosaccharides mimicking the *Shigella flexneri* 2a O-antigen. *Vaccine* 2009, 27 (39), 5419– 5426, DOI: 10.1016/j.vaccine.2009.06.031
51. van der Put, R. M.; Kim, T. H.; Guerreiro, C.; Thouron, F.; Hoogerhout, P.; Sansonetti, P. J.; Westdijk, J.; Stork, M.; Phalipon, A.; Mulard, L. A. A synthetic carbohydrate conjugate vaccine candidate against shigellosis: Improved bioconjugation and impact of alum on immunogenicity. *Bioconjugate Chem.* 2016, 27 (4), 883–892, DOI: 10.1021/acs.bioconjchem.5b00617
 52. Poolman, J. T.; Peeters, C. C.; van den Dobbelsteen, G. P. The history of pneumococcal conjugate vaccine development: dose selection. *Expert Rev. Vaccines* 2013, 12 (12), 1379– 1394, DOI: 10.1586/14760584.2013.852475
 53. Nahm, M. H.; Yu, J.; Weerts, H. P.; Wenzel, H.; Tamilselvi, C. S.; Chandrasekaran, L.; Pasetti, M. F.; Mani, S.; Kaminski, R. W. Development, Interlaboratory Evaluations, and Application of a Simple, High-Throughput *Shigella* Serum Bactericidal Assay. *mSphere* 2018, 3 (3), e00146-00118 DOI: 10.1128/mSphere.00146-18
 54. Goebel, W. F. Chemo-Immunological Studies on Conjugated Carbohydrate-Proteins: Xii. The Immunological Properties of an Artificial Antigen Containing Cellobiuronic Acid. *J. Exp. Med.* 1938, 68 (4), 469– 484, DOI: 10.1084/jem.68.4.469
 55. Svenson, S. B.; Lindberg, A. A. Artificial Salmonella vaccines: Salmonella typhimurium O-antigen-specific oligosaccharide-protein conjugates elicit protective antibodies in rabbits and mice. *Infect. Immun.* 1981, 32 (2), 490– 496, DOI: 10.1128/iai.32.2.490-496.1981
 56. Boutet, J.; Blasco, P.; Guerreiro, C.; Thouron, F.; Dartevelle, S.; Nato, F.; Canada, F. J.; Arda, A.; Phalipon, A.; Jimenez-Barbero, J.; Mulard, L. A. Detailed Investigation of the Immunodominant Role of O-Antigen Stoichiometric O-Acetylation as Revealed by Chemical Synthesis, Immunochemistry, Solution Conformation and STD-NMR Spectroscopy for *Shigella flexneri* 3a. *Chem.-Eur. J.* 2016, 22 (31), 10892–10911, DOI: 10.1002/chem.201600567
 57. Henriques, P.; Dello Iacono, L.; Gimeno, A.; Biolchi, A.; Romano, M. R.; Arda, A.; Bernardes, G. J. L.; Jimenez-Barbero, J.; Berti, F.; Rappuoli, R. Structure of a protective epitope reveals the importance of acetylation of *Neisseria meningitidis* serogroup A capsular polysaccharide. *Proc. Natl. Acad. Sci. U. S. A.* 2020, 117 (47), 29795– 29802, DOI: 10.1073/pnas.2011385117
 58. Mulard, L. A. Bacterial polysaccharides as major surface antigens: interest in O-acetyl substitutions. *Carbohydr. Chem.* 2017, 43, 71– 103, DOI: 10.1039/9781788010641-00071
 59. Berti, F.; De Ricco, R.; Rappuoli, R. Role of O-Acetylation in the Immunogenicity of Bacterial Polysaccharide Vaccines. *Molecules* 2018, 23 (6), 1340, DOI: 10.3390/molecules23061340
 60. Gauthier, C.; Chassagne, P.; Theillet, F. X.; Guerreiro, C.; Thouron, F.; Delepierre, M.; Sansonetti, P. J.; Phalipon, A.; Mulard, L. A. Non-stoichiometric O-acetylation of *Shigella flexneri* 2a O-specific polysaccharide: synthesis and antigenicity. *Org. Biomol Chem.* 2014, 12 (24), 4218– 4232, DOI: 10.1039/C3OB42586J
 61. Perepelov, A. V.; Shekht, M. E.; Liu, B.; Shevelev, S. D.; Ledov, V. A.; Senchenkova, S. N.; L'vov, V. L.; Shashkov, A. S.; Feng, L.; Aparin, P. G.; Wang, L.; Knirel, Y. A. *Shigella flexneri* O-antigens revisited: final elucidation of the O-acetylation profiles and a survey of the O-antigen structure diversity. *FEMS Immunol Med. Microbiol* 2012, 66 (2), 201– 210, DOI: 10.1111/j.1574-695X.2012.01000.x
 62. Arato, V.; Oldrini, D.; Massai, L.; Gasperini, G.; Necchi, F.; Micoli, F. Impact of O-Acetylation on *S. flexneri* 1b and 2a O-Antigen Immunogenicity in Mice. *Microorganisms* 2021, 9 (11), 2360, DOI: 10.3390/microorganisms9112360
 63. Frasch, C. E. Preparation of bacterial polysaccharide-protein conjugates: Analytical and manufacturing challenges. *Vaccine* 2009, 27 (46), 6468– 6470, DOI: 10.1016/j.vaccine.2009.06.013
 64. Hennessey, J. P., Jr.; Costantino, P.; Talaga, P.; Beurret, M.; Ravenscroft, N.; Alderson, M. R.; Zablacki, E.; Prasad, A. K.; Frasch, C., Lessons learned and future challenges in the design and manufacture of glycoconjugate vaccines. In *Carbohydrate-Based Vaccines: From Concept to Clinic*; Prasad, A. K., Ed.; American Chemical Society, 2018; Vol. 1290, pp 323– 385.
 65. Bazhenova, A.; Gao, F.; Bolgiano, B.; Harding, S. E. Glycoconjugate vaccines against *Salmonella enterica* serovars and *Shigella* species: existing and emerging methods for their analysis. *Biophys Rev.* 2021, 13,

- 221– 246, DOI: 10.1007/s12551-021-00791-z
66. Shen, B. Q.; Xu, K.; Liu, L.; Raab, H.; Bhakta, S.; Kenrick, M.; Parsons-Reponte, K. L.; Tien, J.; Yu, S. F.; Mai, E. Conjugation site modulates the in vivo stability and therapeutic activity of antibody-drug conjugates. *Nat. Biotechnol.* 2012, 30 (2), 184– 189, DOI: 10.1038/nbt.2108
 67. Ravasco, J. M. J. M.; Faustino, H.; Trindade, A.; Gois, P. M. P. Bioconjugation with Maleimides: A Useful Tool for Chemical Biology. *Chem.-Eur. J.* 2019, 25 (1), 43– 59, DOI: 10.1002/chem.201803174
 68. Buskas, T.; Li, Y.; Boons, G.-J. The Immunogenicity of the Tumor-Associated Antigen Lewisy May Be Suppressed by a Bifunctional Cross-Linker Required for Coupling to a Carrier Protein. *Chem.-Eur. J.* 2004, 10 (14), 3517– 3524, DOI: 10.1002/chem.200400074
 69. Ramadhin, J.; Silva-Moraes, V.; Norberg, T.; Harn, D. Monoclonal Antibodies Generated against Glycoconjugates Recognize Chemical Linkers. *Antibodies* 2020, 9 (3), 48, DOI: 10.3390/antib9030048
 70. Verez-Bencomo, V.; Fernandez-Santana, V.; Hardy, E.; Toledo, M. E.; Rodriguez, M. C.; Heynngnezz, L.; Rodriguez, A.; Baly, A.; Herrera, L.; Izquierdo, M.A synthetic conjugate polysaccharide vaccine against *Haemophilus influenzae* type b. *Science* 2004, 305 (5683), 522– 525, DOI: 10.1126/science.1095209
 71. Berti, F.; Adamo, R. Antimicrobial glycoconjugate vaccines: an overview of classic and modern approaches for protein modification. *Chem. Soc. Rev.* 2018, 47 (24), 9015– 9025, DOI: 10.1039/C8CS00495A
 72. Anderluh, M.; Berti, F.; Bzducha-Wróbel, A.; Chiodo, F.; Colombo, C.; Compostella, F.; Durlík, K.; Ferhati, X.; Holmdahl, R.; Jovanovic, D. Recent advances on smart glycoconjugate vaccines in infections and cancer. *FEBS J.* 2021, DOI: 10.1111/febs.15909.
 73. DRAFT WHO Preferred Product Characteristics for Vaccines against *Shigella*; https://www.who.int/immunization/research/ppc-tp/PPC_Shigella_draft_for_review_april2020.pdf; World Health Organization: Geneva, 2020 (accessed 19 July 2021).
 74. MacLennan, C. A.; Riddle, M. S.; Chen, W. H.; Talaat, K. R.; Jain, V.; Bourgeois, A. L.; Frenck, R.; Kotloff, K.; Porter, C. K. Consensus Report on *Shigella* Controlled Human Infection Model: Clinical Endpoints. *Clin Infect Dis* 2019, 69 (Suppl 8), S591– S595, DOI: 10.1093/cid/ciz891

Supporting Information

Supplementary Tables

Table S1. Conjugation efficiency using precursors **2** and **5** of different qualities.

Reagents	Microscale				Intermediate scale	
	R&D 2 + R&D 5		GMP 2 + R&D 5		GMP 2 + GMP 5	
2:5 ratio (mol:mol)	3:4 loading (mol:mol)	Conjugation efficiency (%) ^[a]	3:4 loading (mol:mol)	Conjugation efficiency (%) ^[b]	3:4 loading (mol:mol)	Conjugation efficiency (%) ^[c]
6.25	4.6	71	4.3	72	n.a.	n.a.
12.5	8.5	65	7.1	59	n.a.	n.a.
25	17	63	15	63	17 ± 1	62 ± 5
50	26	49	25	52	n.a.	n.a.

^[a] Average results from two experiments. ^[b] Results from a single experiment. ^[c] Average results from three experiments.

Table S2. Toxicology results summary microscopic observations (subgroup 1, sacrificed 3 days after the last injection) using the pre-clinical batch of SF2a-TT15 (**3:4** loading (mol/mol): 19) versus placebo (20 mM TRIS, 150 mM NaCl).

Vaccine / Placebo		SF2a-TT15	Adjuvanted SF2a-TT15	Placebo	SF2a-TT15	Adjuvanted SF2a-TT15	SF2a-TT15
Animals	Gender	Male			Female		
	Number	5	5	5	5	5	5
Muscle, anterior thigh, right	Inflammation, mixed, localized (minimal/mild)	0	0/2	0	0	1/1	1
	Accumulation of swollen macrophages (mild/moderate)	0	3/1	0	0	5/0	0
Muscle, anterior thigh, left	Necrosis moderate	0	3	0	0	3	0
	Inflammation, mixed, widespread (mild/moderate)	0	1/3	0	4/0	3/2	0

Table S3. Toxicology results summary microscopic observations (subgroup 2, sacrificed after 14 day recovery period) using the pre-clinical batch of SF2 α -TT15 (3:4 loading (mol/mol): 19) versus placebo (20 mM TRIS, 150 mM NaCl).

Vaccine / Placebo		SF2 α -TT15	Adjuvanted SF2 α -TT15	Placebo	SF2 α -TT15	Adjuvanted	SF2 α -TT15
Animals	Gender	Male			Female		
	Number	3	3	3	3	3	3
Muscle, anterior thigh, right	Inflammation, mixed, localized (minimal/mild)	0	1/1	0	0	1/2	0
	Accumulation of swollen macrophages (mild/moderate)	0	3/0	0	0	1/2	0
Muscle, anterior thigh, left	Necrosis moderate	0	1	0	0	1	0
	Inflammation, mixed, wide-spread (mild/moderate)	0	1	0	0	1	0

Supplementary figures

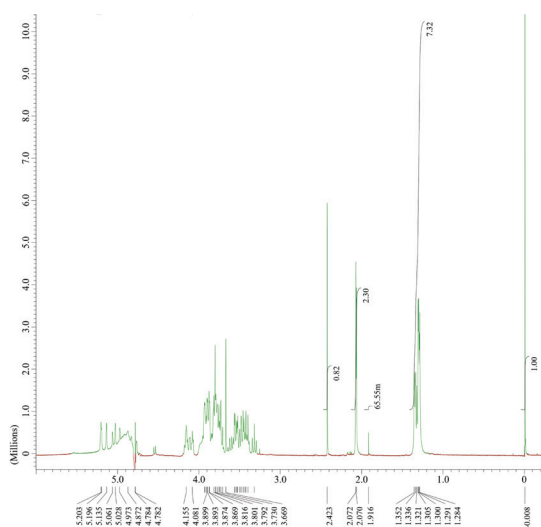


Figure S1. ¹H-NMR spectrum of conjugation-ready 2^{GMP} (D₂O, 400 MHz). x-axis: chemical shift (ppm), y-axis: signal intensity with reference to 3-(trimethylsilyl)propanoic acid (TMSP) as internal standard (δ -0.008 ppm). Extracted: δ 1.35-1.28 (m, 27H, H-6A, H-6B, H-6C), 2.07-1.91 (3s, 9H, H-NAc), 2.42 (s,

3H, H-SAc).

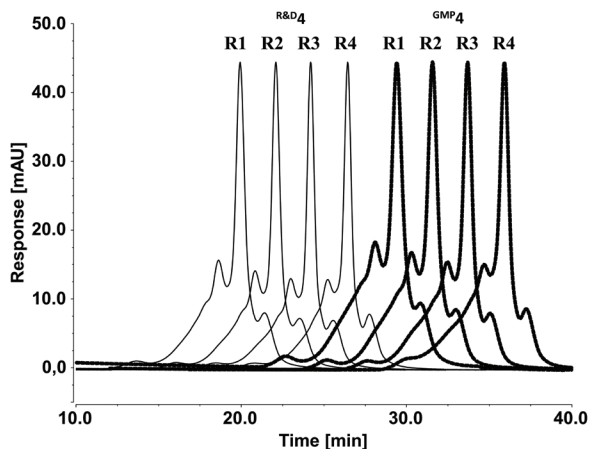


Figure S2. HPSEC analysis of conjugates (microscale experiments). x-axis: retention time (min), y-axis: response (mAU). UV signals were normalized for the monomer peak (highest peak in chromatogram) and an offset was applied to each individual trace to facilitate the overview. Black full trace: using R^{D2} and R^{D5} , black dashed trace: using G^{MP2} and R^{D5} , R: 2:5 input ratio (R1: 6.25, R2: 12.5, R3: 25, R4: 50). **HPSEC method:** An UltiMate-3000 (Thermo Fisher Scientific) HPLC system was equipped with a SEC Guard column 100 (Wyatt Technology), SEC protein column 100 (Wyatt Technology), and SEC protein column 30 (Wyatt Technology) mounted in series (in this order). The eluent was 0.1 μ m sterile filtered phosphate buffered saline (PBS) 10 mM, pH 7.2, and elution was performed at 1 mL/min (average backpressure 60 bar). All chromatographic parameters were calculated using the Chromeleon software (v. 7.1.2, SP 2, Thermo Fisher Scientific).

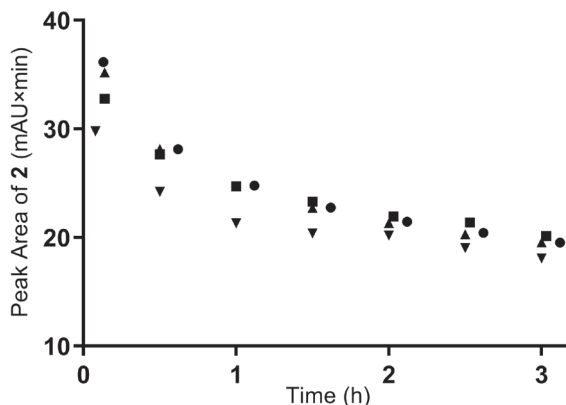


Figure S3. Conjugation kinetics for a 2:5 ratio (mol:mol) of 25 (HPSEC follow up), showing the decrease in peak area of 2 in time. x-axis: time (h), y-axis: Peak Area of R&D2 entity (mAU*min) for microscale conjugation (●) and (■), and of GMP2 at micro (▲) and intermediate (▼) scale. HPSEC: high performance size exclusion chromatography.

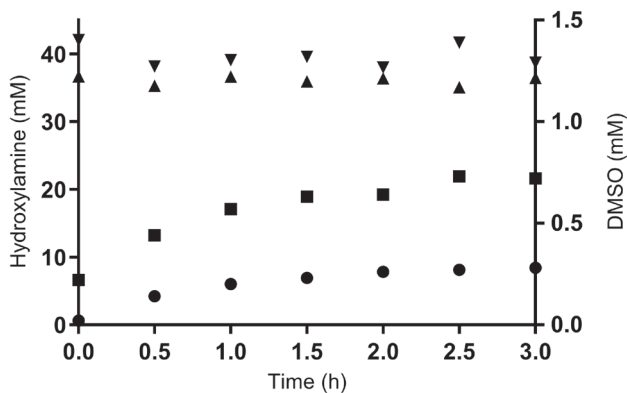


Figure S4. DMSO and hydroxylamine concentration during conjugation. X-axis: Time (h), y-axis: concentration (mM) quantified by NMR. (●) DMSO, LP screen filter; (■) open channel filter; (▲) hydroxylamine, LP screen filter; (▼) hydroxylamine, open channel filter.

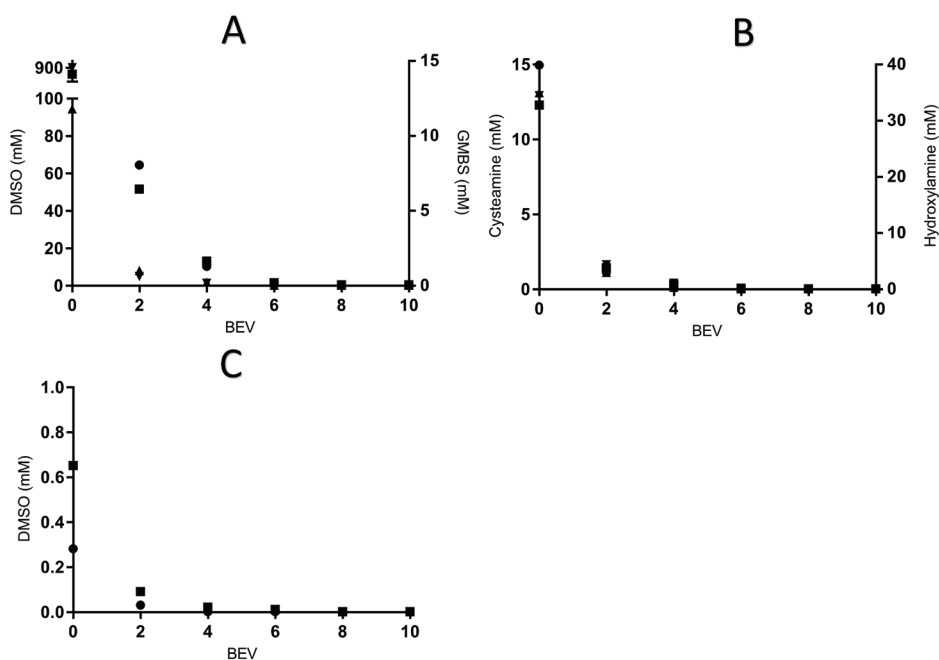


Figure S5. Follow up of impurity concentrations during processing and final buffer exchange at the intermediate scale. (A) DMSO and GMBS/GMBA concentrations during maleimide modification of **4** into **5**, ● DMSO LP screen ■ DMSO open channel ▲ GMBS LP screen ▼ GMBS open channel; (B) Cysteamine and hydroxylamine concentrations during SF2 α -TT15 final buffer exchange, ● cysteamine LP screen ■ cysteamine open channel ▲ hydroxylamine LP screen ▼ hydroxylamine open channel; (C) DMSO concentration during SF2 α -TT15 final buffer exchange ● DMSO LP screen ■ DMSO open chan-

nel; (A, B & C) x-axis: buffer exchange volumes (BEV), y-axis: concentration (mM) quantified by NMR.

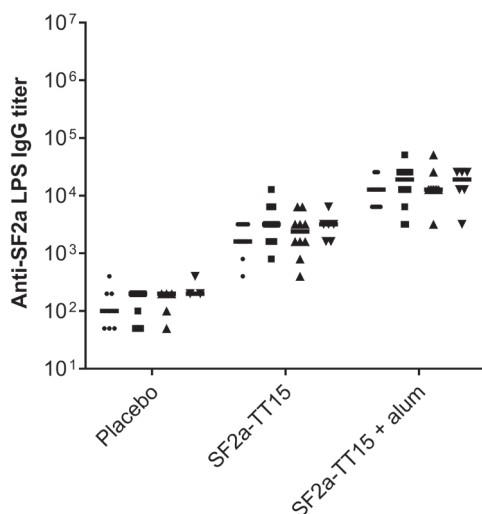


Figure S6. Immunogenicity of SF2a-TT15 preclinical GMP batch in rabbits. Groups of 8 rabbits were immunized i.m. with SF2a-TT15 non adjuvanted or alum-adjuvanted, or with placebo, four times at three weeks interval, i.e. Day 0, 21, 42, and 63. Blood samples were recovered at D42 (3 weeks after the 2nd injection, just before the 3rd injection), Day 63 (3 weeks after the 3rd injection, just before the 4th injection), and D66 (3 days after the 4th injection), and D77, 14 days after the 4th injection. The kinetics of anti-SF2a LPS IgG titers measured by ELISA is presented. Bars indicate the median of the antibody response. ● Day 42 ■ Day 63 ▲ Day 66 ▼ Day 77.

Methods

Safety statement

No unexpected or unusually high safety hazards were encountered during any of the methods, processes or assays.

Chemicals

All chemicals used and presented in this manuscript were of the highest possible available purity and complying with GMP regulations where needed.

General methods

BCA assay, TNBS assay, Anthrone assay, High Performance Size Exclusion Chromatography (HPSEC), buffer exchange, concentration and conjugation kinetics determination were performed as described [1], however with the addition that the methods were validated

for GMP application. NMR analysis was run on a FT-NMR 400 (JEOL) in pre-saturation mode and signal intensity with reference to 3-(trimethylsilyl)propanoic acid (TMS_P, Aldrich). Osmolality was measured using a calibrated Osmomat 3000 (Gonotec). When applicable, samples were prediluted using Milli-Q water (Millipore). The pH was measured using a calibrated FE20 Basic FiveEasyTM pH-meter (Mettler Toledo) and an Inlab Nano pH electrode (Mettler Toledo). ^{GMP}TT was acquired through the open market, from Bilthoven Biologicals (Bilthoven, The Netherlands). It was released for production based on review of the certificate of analysis and compliance to internal specifications in terms of concentration (> 1,500 LF). The ready for conjugation ^{Tox}2 and ^{GMP}2 were acquired through the open market, from Sanofi CEPIA (Antony, France). They were released for production based on review of the certificate of analysis, purity assessment by ¹H-NMR and HPAEC-PAD, and compliance to pre-defined specifications relevant for DS intermediates. Reagents and solvents were from the highest quality compliant with GMP regulations.

Microscale bioconjugation

The microscale bioconjugation assays (0.16 mL each), applying ^{GMP}2:^{R&D}5 ratios of 6.25, 12.5, 25 and 50 were performed as described earlier [1].

Intermediate-scale bioconjugation

The [^{GMP}2 + ^{GMP}5] bioconjugation at intermediate-scale (1.0 mL) was performed essentially according to the protocol used for the microscale conjugation, respecting the reaction conditions [1]. However, in this case ^{GMP}TT was used and only the ^{GMP}2:^{GMP}5 ratio (mol:mol) of 25 was investigated in triplicate. In short, ^{R&D}TT modified with GMBS (Thermo Fisher Scientific, 18.8 mg, 125 nmol) in 0.1 M Phosphate buffer, 5 mM EDTA (in-house), pH 6.0 (18.8 mg/mL, 1.0 mL each) was reacted with ^{GMP}2 (8.1 mg, 3.1 μmol, 25 equiv.) in 0.1 M Phosphate buffer, 5 mM EDTA, pH 6.0 (64.7 mg/mL, 125 μL). Hydroxylamine (Thermo Fisher, 3.3 mg, 46.9 μmol) in 0.1 M Phosphate buffer, 5 mM EDTA, pH 6.0 (125 μL, 26.1 mg/mL) was added in a 15:1 ^{GMP}2 molar ratio. Conjugation was performed at ambient temperature for 180 min, with final protein concentration at 15 mg/mL. Conjugation progress was monitored by HPSEC (injections at 30 min intervals). After 3 h, Cysteamine-HCl (Sigma Aldrich, 2.3 mg, 20.0 μmol, 160 equiv.) in water for injection (WFI, 125 μL, 18.2 mg/mL) was added to all reaction mixtures. Final products were all purified (30 kD Amicon Ultra 15, Merck Millipore, UFC9030) using 20 mM TRIS buffer pH 7 (in-house).

Scale-up study on impurity removal

Both scale-up and impurity removal studies were essentially performed similar to the GMP production of the preclinical batch (see below). However, during these studies only buffers and excipients were used. Additionally, changes relevant to the quantities of BEV

occurred during purification (see main text).

Evaluation of process performance for two different filters

TT maleimide activation was mimicked by 30 minutes of recirculation through the Cogent micro (Merck Millipore), the process time for reaction completion. The filters did not show any apparent interaction with DMSO, GMBS or GMBA. Both DMSO and GMBS/GMBA were removed efficiently ($\geq 99.9\%$) after 8 and 6 buffer exchange volumes (BEV), for the LP screen and open channel filters, respectively (Figure S2A). Filtrate flow, inlet pressure, outlet pressure and trans membrane pressure (TMP) remained constant for both filters during the entire process (data not shown). Similarly, no interaction was observed between hydroxylamine and the filters during the 3h recirculation simulating the conjugation reaction (Figure 4). In contrast, DMSO concentrations increased in time, where the open channel showed twice the amount of DMSO released from the filter compared to the LP screen filter (Figure 4). According to the manufacturer, this phenomenon was not uncommon, since DMSO was held up at the membrane surface during prior process steps in the presence of high concentrations of DMSO (6.3% v/v). This effect could be minimized decreasing the feed volume to membrane area ratio. However, it was decided to evaluate further removal of DMSO during following process steps. During simulation of the capping reaction, cysteamine concentrations remained constant during the 30 min recirculation. At the start of the final buffer exchange, cysteamine was already below the maximum tolerated concentration (518 mM, Table 2), however, more than 99.9 % was removed after 6 BEV (Figure S2B). Hydroxylamine was removed to below the maximum allowed concentration of 12 mM after 2 BEV, and more than 99.9 % after 8 BEV (Figure S2B). As suggested, DMSO extracted from the filter during conjugation, was removed to below detection limit at 4 BEV for the LP screen and 8 BEV for the open channel during final purification (Figure S2C). Final concentration of the TRIS formulation buffer (20 mM) was already acceptable, 18 mM, after 4 BEV for both filters (data not shown).

GMP production of a preclinical batch

The entire production of the preclinical batch was performed in the reaction vessel of the Cogent μ (Millipore) equipped with a Sius-LSn TFF cassette (Repligen, TangenX, LP Screen channel, low binding mPES, 30 kD, 0.01 m²). ^{GMP}TT (^{GMP}4, 1,925 mg, 12.8 μ mol) of the commercial solution (7.7 mg/mL, 250 mL) was concentrated to 100 mL and purified using five BEV (0.1 M HEPES buffer, pH 7.8, in-house) to give ^{GMP}TT (16.0 mg/mL, 1,600 mg, 10.7 μ mol). A solution of GMBS (478.3 mg, 1.7 mmol, 160 equiv., Thermo Fisher Scientific) in DMSO (6.7 mL, 71.7 mg/mL, Sigma Aldrich) was added and the reaction mixture was stirred for 30 min at ambient temperature. The modified ^{GMP}TT was purified using five BEV (0.1 M Phosphate buffer, 5 mM EDTA, pH 6.0, in-house) and concentrated to a final

volume of 80 mL to reach $\text{GMP-TT}_{\text{Mal}}$ ($\text{GMP}^{\mathbf{5}}$, 18.8 mg/mL, 1,500 μmol , 10.0 μmol). $\text{GMP}^{\mathbf{2}}$ [AB(E)CD]₃-SAC ($\text{GMP}^{\mathbf{2}}$, 647 mg, 250.0 μmol , 25 equiv.) in 0.1 M Phosphate buffer, 5 mM EDTA, pH 6.0 (64.7 mg/mL, 10 mL) and Hydroxylamine-HCl ($\text{GMP}^{\mathbf{2}}$ [AB(E)CD]₃-SAC x 15 equiv., 260.6 mg, 3,750 μmol , Thermo Fisher) in 0.1 M Phosphate buffer, 5 mM EDTA, pH 6.0 (26.0 mg/mL, 10 mL) were added. After stirring for 180 min at ambient temperature, Cysteamine-HCl ($\text{GMP}^{\mathbf{2}}$ TT_{Mal} x 160 equiv., 182 mg, 1,600 μmol , Sigma Aldrich) in 0.1 M Phosphate buffer 5 mM EDTA pH 6.0 (18.2 mg/mL, 10 mL) was added and the reaction mixture was stirred for 30 min at ambient temperature. Final purification was performed by 10 BEV (20 mM TRIS-HCl buffer, pH 7.0, in-house), after which the product was 0.22 μm filtered (Pall), analysed, and stored at 2 - 8 °C. Based on the amount of the starting GMP2 (95.5% pure as measured by quantitative ¹H-NMR), the SF2a-TT15 conjugate was obtained in 76% corrected yield. Formulation of the 2 and 10 μg doses was achieved by dilution of the drug substance using 20 mM TRIS-HCl 150 mM NaCl pH 7.0 (in-house) to their respective carbohydrate concentrations – 8 $\mu\text{g}/\text{mL}$ and 40 $\mu\text{g}/\text{mL}$, respectively – before final fill and finish.

GMP production of a clinical batch of SF2a-TT15

The protocol was identical to that described for the preclinical batch, except that the bioconjugation step involved the GMP compliant glycan precursor. Based on the amount of the starting $\text{GMP}^{\mathbf{2}}$ (647 mg, 250.0 μmol , 25 equiv., 94.7% pure as measured by quantitative ¹H-NMR), the SF2a-TT15 conjugate was obtained in 80% corrected yield, which was very similar compared to the preclinical batch. Formulation of the 2 and 10 μg carbohydrate equivalent doses was as described above.

Identity ELISA

Identification of SF2a specificity in SF2a-TT15 vaccine was performed as follows. A high binding microtiter plate (Greiner) was coated overnight at room temperature with horse anti-TT antibodies (Bbio, the Netherlands) in a concentration of 0.6 IU/mL in carbonate buffer pH 9.6. The plate was washed with tap-water containing 0.05% Tween 80 (Merck). Series of negative control (TT; Bbio) and low and high dose vaccine (200 ng/mL carbohydrate each) twofold diluted in assay buffer (0.01 M PBS containing 0.05% Tween 80 and 0.5 % protifar (Nutricia, the Netherlands)) were added to the plate and incubated at 37 °C for 2 h. After washing with tap-water/Tween (0.05%) the plate was incubated at 37 °C for 2 h with an anti-SF2a specific IgG mAb (Institut Pasteur) in a 1/2,000 dilution in assay buffer. The plate was washed as above and 5,000 x diluted Horseradish peroxidase (HRPO)-conjugated goat anti-mouse IgG (Southern Biotech) in assay buffer was added to the plate, followed by incubation at 37 °C for 1.5 h. The plate was washed and 3,3',5,5'-tetramethylbenzidine (TMB) microwell peroxidase substrate (KPL) was added. After 10 min the reaction was stopped by addition of 0.2 M aq. H₂SO₄ (Sigma Aldrich) and

absorbance at 450 nm was measured. Samples were positively identified if the average extinction of the first three dilutions of eleven dilutions of a twofold dilution series of the sample is equal to or higher than three times the average extinction of the first three matching dilutions of the negative control.

HPAEC-PAD-measured carbohydrate total content and free carbohydrate in the SF2a-TT15 conjugate bulks and formulations

All analyses were performed on an ICS-3000 (Thermo Fisher Scientific) HPLC system equipped with an AminoTrap guard (4x50 mm, Thermo Fisher Scientific) and a CarboPac PA10 column (4x250 mm, Thermo Fisher Scientific). A standard curve was constructed (0 – 100 nmol repeating unit) consisting of Rhap, GlcpNAc and Glcp (3:1:1) and fucose (Fucp, 25 nmol) (All, Sigma Aldrich), which was used as an internal standard. The method was validated for GMP applications. The total carbohydrate content was measured as follows. SF2a-TT15 conjugate formulations (0.5 mL) containing carbohydrates (8 and 40 µg/mL corresponding to the 2 and 10 µg carbohydrate content per vaccine dose, respectively), whether in their free form or conjugated, were hydrolyzed to their respective monosaccharides using 0.5 mL 4 M aq. TFA (121 °C, 60 min, Biosolve). Free carbohydrate content was measured as follows. SF2a-TT15 conjugate formulations containing carbohydrates (8 and 40 µg/mL corresponding to the 2 and 10 µg carbohydrate content per vaccine dose, respectively) were passed through 30 kD-filters. Sample filtrates were hydrolyzed as above. The hydrolyzed samples and standards were pre-diluted using 20 mM TRIS-HCl pH 7.0 (in-house) and eluted using 18 mM aq. NaOH (in-house) isocratic conditions. All chromatographic parameters were calculated using the Chromeleon software (v. 7.1.2, SP 2, Thermo Fisher Scientific).

Toxicology study in rabbit

The study design comprised six groups of 8 animals (SPF quality New Zealand White albino rabbits, app. 13 weeks old, equal number of male to female). Group 1 received the conjugate vaccine (10 µg dose, 0.5 mL), group 3 received the vehicle control treatment (20 mM TRIS-HCl, 150 mM NaCl buffer, pH 7.0, 0.5 mL) and group 2 received the adjuvanted conjugate vaccine (10 µg dose, 0.5 mL containing Al(OH)₃ (alum, 1.36 mg/mL, Brenntag Biosector, Alhydrogel 2% Ph.Eur.)). The placebo or vaccine formulations were administered within 1 hour after preparation. Each animal received four i.m. injections each at a different site at three week intervals (on day 0, 21, 42 and 63). Blood samples were recovered at day 42, 63, 66 and 77 and kept at -20 °C. Each group was subsequently divided into two subgroups. Rabbits in the first groups (5 males and 5 females) were sacrificed three days after the last immunization (day 66). Members of the second groups (3 males and 3 females) were sacrificed after a 14 day recovery period post the last injection (day 80). The welfare

of the animals was maintained in accordance with the general principles governing the use of animals in experiments of the European Communities (Directive 2010/63/EU) and Dutch legislation (The revised Experiments on Animals Act, 2014).

Immunogenicity study in rabbits

The glycoconjugate-induced anti-LPS IgG response specific for SF2a LPS was measured by ELISA using LPS purified from the SF2a 454 strain as previously described [2]. Briefly, purified SF2a LPS in 0.04 M car-bonate buffer pH 9.6 (2.5 µg/mL, 100 µL) was added per ELISA plate well and the plates were incubated overnight at 2-8 °C. After washing the wells with Tween 80 0.05%, blocking was performed by incubating the plates for 30 min at 37 °C with PBS-BSA 1% (100 µL) followed by washing with Tween 80 0.05%. Then, rabbit sera (originating from the toxicology study, see above) in PBS-BSA 1% was added in a two-fold dilution series and the plates were incubated for 1 h at 37 °C. After washing with Tween 80 0.05%, anti-rabbit IgG alkaline phosphatase-labeled conjugate (Sigma-Aldrich) was added to each well at a dilution of 1/20,000 in PBS-BSA 1% (100 µL). The plate was covered with aluminum foil and incubated at rt for 1 h. The reaction was stopped by adding 1.5 M aq. NaOH (50 µL) to each well. The IgG Ab titer was defined as the last dilution of serum giving an OD value ($\lambda = 405$ nm) twice that of the OD value obtained with the pre-immune serum.

Immunogenicity study in mice

SF2a-TT15, adjuvanted or not with alum, was administered to seven week-old Balb/c mice (Janvier Labs, France) i.m. at multiple sites with 2.5 or 10 µg equivalent of [AB(E)CD]₃ per dose in 0.5 mL of TRIS-HCl 20 mM pH 7.2. Alum-adjuvanted SF2a-TT15 was obtained by mixing v/v the conjugate with aluminum hydroxide (Alhydrogel, Brenntag, Denmark) at a concentration of aluminum of 1.4 mg/mL (corresponding to a dose of 0.35 mg of aluminum (Al³⁺) per mouse/per injection) in TRIS-HCl 20 mM pH 7.2 for 30 min at ambient temperature with rotor shaking. Three injections were performed at three-week interval, and a fourth one, one month later. Blood samples were recovered one week after each injection and at six months after the 4th injection. Seven mice were used per group. All of the mice experiments were approved by the Institut Pasteur Animal Use Committee.

Measurement of the anti-SF2a IgG antibody response

The glycoconjugate-induced anti-LPS IgG response specific for SF2a LPS was measured by ELISA using LPS purified from the SF2a 454 strain as previously described [2]. Briefly, 2.5 µg of purified SF2a LPS was coated per ELISA plate well in PBS and incubated at 4 °C

overnight. After washing the wells with PBS-Tween 20 0.01%, saturation was performed by incubating the plate for 30 min at 37 °C with PBS-BSA 1%. Then, serial dilutions of mouse sera in PBS-BSA 1% were incubated for 1 h at 37 °C. After washing with PBS-Tween 20 0.01%, anti-mouse IgG alkaline phosphatase-labeled conjugate (Sigma-Aldrich) was used as secondary antibody at a dilution of 1/5,000. The IgG titer was defined as the last dilution of serum giving rise to twice the OD value ($\lambda = 405$ nm) obtained with pre-immune serum.

SBA assay

Sera from mice collected after the 3rd or the 4th immunization with either 2.5 or 10 μg [AB(E)CD]₃ equivalent, adjuvanted or not with alum, were pooled per group and heat-inactivated. The SF2a 454 strain, used as reference strain, was grown in Trypto-Casein-Soy (TCS) medium to log-phase ($\text{OD}_{600 \text{ nm}}$: 0.2), diluted 1/30,000 in SBA buffer (50 mM phosphate buffer, 0.5% BSA) to 3×10^3 colony forming units (CFU)/mL and distributed into sterile polystyrene U bottom 96-well microliter plates (20 μL /well). Heat-inactivated sera were serially diluted 2-fold, and added to each well (75 μL /well). Baby Rabbit Complement (BRC, Cederlane) diluted twice in SBA buffer was then added to each plate (50 μL /well), completed to a final volume of 150 μL per well with SBA buffer. Incubation of bacteria with complement (in the absence of serum sample) was used as control. After 2 h at 37 °C, for each well, 100 μL out of the 150 μL were plated on TCS-agar plates. CFU counting was performed after 24 h of incubation at 37 °C. SBA titer was determined as the serum dilution required to obtain 50% CFU reduction as compared to control. Both samples and control were tested in duplicates and two independent experiments were performed.

Recognition of a set of SF2a clinical isolates by SF2a-TT15-induced murine sera

The SF2a clinical isolates were obtained from the French National Reference Center for *Escherichia coli*, *Shigella* and *Salmonella* (Institut Pasteur, Paris, France). They were isolated and characterized from stools of individuals developing diarrhea when back from travelling to the indicated country. After isolation on Congo red plates, one single colony for each clinical isolate and the SF2a 454 strain, used as the reference strain to identify [AB(E)CD]₃ as the SF2a-TT15 hapten were grown overnight in TCS (Trypto-Casein-Soy) medium at 37 °C with shaking. Then, 5 mL of each bacterial culture was centrifuged at 5,000 rpm for 5 min and the pellet was suspended in PBS/BSA 0.5% to a concentration of 107 CFU/mL. After a washing step using PBS/BSA 0.5%, bacteria resuspended in 1 mL of PBS/BSA 0.5% were incubated with 200 μL of mouse serum samples diluted 1:20. After 30 min incubation at 37 °C, two PBS/BSA 0.5%-washings were performed, and the bacterial pellet resuspended in 1 mL of the same buffer was incubated with anti-mouse IgG Alexa Fluor 488-labeled secondary antibody (Thermo Fisher) at a dilution of 1:2,000. After 30 min

incubation at 37 °C in the dark, and two PBS-washings, bacteria resuspended in PBS (1.0 mL) were analyzed by flow cytometry (Attune, Thermo Fisher). Controls using AF 488-only labelled bacteria, and bacteria incubated with pre-immune sera, were used to account for background fluorescence and non-specific binding of mouse IgG, respectively. Results were analyzed using FlowJo 10.3.

Statistical analysis

For statistical significance while comparing groups of mice, an unpaired t test was performed. *, **, and *** indicate a p value < 0.05, < 0.005, and < 0.0005, respectively.

REFERENCES

1. van der Put, R.M., et al., A synthetic carbohydrate conjugate vaccine candidate against shigellosis: Improved bioconjugation and impact of alum on immunogenicity. *Bioconjugate Chem.*, 2016. 27(4): p. 883-892.
2. Phalipon, A., et al., Characterization of functional oligosaccharide mimics of the *Shigella flexneri* serotype 2a O-antigen: implications for the development of a chemically defined glycoconjugate vaccine. *J Immunol*, 2006. 176(3): p. 1686-94.



Chapter 6

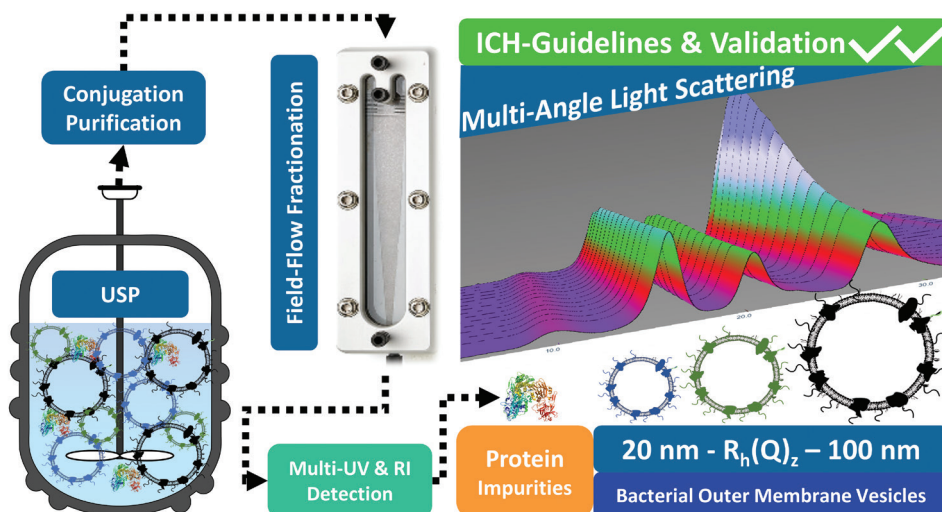
Validation of an FFF-MALS method to characterize the production and functionalization of outer membrane vesicles for conjugate vaccines

Robert M. F. van der Put,^{a,b} Arnoud Spies,^b Bernard Metz,^b Daniel Some,^c Roger Scherrers,^d Roland Pieters,^a and Maarten Danial^b

^a Department of Chemical Biology & Drug Discovery, Utrecht Institute for Pharmaceutical Sciences, Utrecht University, P.O. Box 80082, NL-3508 TB Utrecht, The Netherlands, ^b Intravacc, P.O. Box 450, 3720 AL Bilthoven, the Netherlands, ^c Wyatt Technology Corp., Santa Barbara, CA 93117, USA, ^d Wyatt Technology Europe, Dernbach, Germany.

Abstract

With the ongoing development of conjugate vaccines battling infectious diseases, there is a need for novel carriers. Although tetanus toxoid and CRM197 belong to the traditional carrier proteins, outer-membrane vesicles (OMVs) are an excellent alternative: in addition to their size, OMVs have self-adjuvanting properties due to the presence of genetically detoxified lipopolysaccharide (LPS) and are therefore ideal as a vaccine component or antigen carrier. An essential aspect of their development for vaccine products is characterization of OMVs with respect to size and purity. We report on the development of a field-flow fractionation multiangle light-scattering (FFF-MALS) method for such characterization. Here, we introduced NIST-traceable particle-size standards and BSA as a model protein to verify the precision of the size and purity analysis of the OMVs. We executed a validation program according to the principles provided in the ICH Guidelines Q2 (R1) to assess the quality attributes of the results obtained by FFF-MALS analysis. All validation characteristics showed excellent results with coefficients of variation between 0.4 and 7.32%. Estimation of limits of detection for hydrodynamic radius and particle concentration revealed that as little as 1 μg OMV still yielded accurate results. With the validated method, we further characterized a full downstream purification process of our proprietary OMV. This was followed by the evaluation of other purified OMVs from different bacterial origin. Finally, functionalizing OMVs with *N*- γ -(maleimidobutyryl)-oxysuccinimide-ester (GMBS), generating ready-to-conjugate OMVs, did not affect the structural integrity of the OMVs and as such, they could be evaluated with the validated FFF-MALS method.



Introduction

The development of conjugate vaccines against a variety of pathogens has been a cornerstone in disease prevention. This has been of particular importance for infants and children since the introduction of conjugate vaccines in the 1990s against pathogenic bacteria, such as *meningococcus*, *Haemophilus influenzae* type b, and *pneumococcus*, resulting in a significant reduction in morbidity in Europe [1]. These conjugate vaccines utilize carrier proteins [2] like tetanus toxoid [3], diphtheria toxoid [4], the genetically modified cross-reacting material of diphtheria toxin (CRM197) [5], meningococcal outer-membrane protein complex [6], or *H. influenzae* protein D [7]. With the ongoing development of new conjugate vaccines targeting a large array of infectious diseases, there is a growing need to find alternatives for these traditional carriers. Outer membrane vesicles (OMVs), spherical lipid bilayer membranes extracted from bacteria, would be an excellent option as these carriers are larger and thus bear more potential covalent linking sites relative to the smaller protein carriers. In addition, the size of OMVs offers a favorable trade-off between accumulation in draining lymph nodes on one hand and a high level of opsonization activity leading to an enhanced Th1 response on the other [8, 9]. OMVs are stable and permit ample opportunity for covalent conjugation of pathogen-specific antigens to membrane-associated proteins using water-compatible chemistries. Furthermore, OMVs are self-adjuvanting due to the presence of LPS within the membrane [10]. While LPS is known to cause severe inflammation and can result in septic shock [11], efforts in the past 20 years have established detergent-enabled purification processes or genetic detoxification methods [12]. These methods reduce the adverse effects of LPS, while preserving an adequate response to pathogen-associated molecular patterns, such as those recognized by the toll-like receptors TLR2 and TLR4 [13, 14]. In particular, OMVs equipped with genetically detoxified LPS enable effective vaccine formulations without aluminum-based adjuvants [15, 16], as opposed to many of the traditional conjugate vaccines. Other major advantages of OMVs are (1) they are highly amenable to genetic alteration or enhancement, so that unwanted proteins can be deleted or edited, creating a more favorable immunological profile toward the antigen of choice and (2) heterologous proteins originating from other high-risk or hard-to-produce pathogens (e.g. bacteria, viruses, or parasites) can be expressed. Both properties aid in the versatility and broad application of such OMVs as potential carriers for conjugate vaccines. This combination of characteristics indicates the versatility of OMVs for use either in stand-alone drug products or as novel carriers for the next generation of conjugate vaccines consisting of pathogen-derived antigens such as extracted polysaccharides, synthetic oligosaccharides, peptides, or proteins. En route to developing OMV-based conjugate vaccines, it is imperative to evaluate and characterize both purified and GMBS functionalized OMVs. Such an evaluation should confirm, on the one hand, the purity of OMV at the end of the production process,

and on the other that functionalization using GMBS - enabling conjugation to any thiol-bearing immunogenic moiety - does not affect the integrity and size distribution of the OMV. Furthermore, such methods could be used to evaluate the progression of purification or downstream processing (DSP) in terms of purity and yield. Purified OMVs are generally characterized by dynamic light scattering (DLS) or nanoparticle tracking analysis (NTA). DLS is predominantly used to assess the hydrodynamic radius of particles, but in most cases does not determine particle concentration and suffers from low resolution with respect to size distributions in mixed populations. NTA has the advantage that it can count particles and quantify particle-size distributions more accurately; however, the need for extremely large dilutions and the interference of impurities make it potentially unreliable [17]. Additionally, the cutoff radius for NTA lies in the order of 30 nm, which makes it unsuitable for the OMVs we want to evaluate, which start at ~25 nm. Finally, neither NTA nor DLS apply any separation to the sample, making both suboptimal for fully characterizing DSP samples with respect to purity in the presence of potential protein impurities. Recent advances in particle characterization using field-flow fractionation (FFF) suggest that it is applicable both to characterizing the purification process of these OMVs and to determining the integrity of the intermediate and final conjugate vaccines. FFF is very productive for nanoparticle characterization when combined with multiangle light scattering (MALS) and additional detectors. Validation of an FFF-MALS method for characterizing liposomal drug formulations has been described by Parot et al [18]. A fully optimized separation method makes FFF-MALS suitable not only for the characterization of purified and functionalized OMVs but also for DSP samples containing complex mixtures of impurities and OMVs. In addition, the method can quantify particle concentration more accurately than NTA because it separates the OMVs from the impurities, eliminating any potential cross-interference during detection. In this study, we present optimization of the FFF separation and characterization of purified OMVs, a model impurity and particle standards by simulating their elution under different flow conditions. This initial method development was followed by a full validation of the FFF method according to current ICH guidelines (Q2 R1) [19]. Using the validated method, we evaluated the DSP of OMVs and several other purified OMV products. Finally, we evaluated GMBS-functionalized OMVs as a carrier for conjugate vaccines.

Experimental section

FFF-MALS

The separation method used to characterize OMVs was a type of FFF known as asymmetric-flow field-flow fractionation, or AF4. The principle of AF4 is described in detail by Giddings [20]. Given that AF4 is the most widespread and useful method of FFF, we commonly refer to it as FFF for simplicity. In brief, it is based on the application of two

flow streams (crossflow and channel flow) in an open separation channel consisting of a solid plate parallel to a frit-supported membrane. The channel flow transports the sample through the channel, whereas the crossflow pushes the particles toward the membrane. Brownian motion counteracts the crossflow, causing the particles to diffuse away from the membrane in a size-dependent manner. As a result, smaller particles are on average higher above the membrane than larger particles. Since the channel flow is laminar and thus the flow velocity varies with the height above the membrane, the smaller particles encounter higher flow velocities due to their higher average height and are flushed out faster than larger particles, which remain closer to the membrane. FFF is typically followed by multiple online detection modalities, including UV/vis, MALS, DLS, refractive index (RI), and/or fluorescence. These provide rich, high-resolution information on each size fraction generated during FFF.

Field flow fractionation modeling

One means for modifying the separation properties of an FFF channel is the variation of the overall height of the channel using spacers of differing thickness. Another means is variation of the ratio of channel flow to crossflow, which may be done during the elution according to a preprogrammed method. The impact of varying the channel height, crossflow, and channel flow on the elution of particles of a given size may be predicted through numerical modeling and testing these effects *in silico* is very useful in developing an optimal FFF separation method. Such predictive modeling was performed using the SCOUT software (v R1705, Wyatt Technology currently marketed under the product name VISION DESIGN), which applies first principles FFF theory to calculate and display a predicted fractogram. The prediction includes possible band-broadening effects and the dilution of the sample in the FFF channel during separation. Iterating through a series of simulated conditions enables optimization of a method, and as a final optimization step, the results of a separation run may be fed back into SCOUT to adjust estimated physical parameters and come up with a final flow program [21]. For modeling, we used assumed particle sizes between 50 and 100 nm. We adjusted the channel height and flow conditions to achieve elution of the OMV during the applied crossflow period to facilitate separation. FFF Methods A–D described below were developed in this way.

FFF separation methods

For all of the described methods (A–D), a focus flow of 1.5 mL/min and an inject flow of 0.2 mL/min were applied to the short separation channel (Wyatt Technology). A Millipore 10 kDa molecular weight cutoff (MWCO), regenerated cellulose membrane was installed in the channel along with spacers (both provided by Wyatt Technology). All crossflows were programmed using a linear decay.

Method A (OMV)

For Method A, a 350 μm wide-format spacer was installed in the channel. The carrier solvent was PBS (10 mM phosphate, 150 mM NaCl, pH 7.2) running at a detector flow rate of 1 mL/min. The elution method consisted of the following steps: Elution (0–3 min, 3 mL/min crossflow), Focus (3–4 min), Focus + inject (4–9 min), Focus (9–10 min), Elution (10–25 min, 3–0.1 mL/min crossflow), Elution (25–40 min, 0.0 mL/min crossflow), and Elution + Inject (40–45 min, 0.0 mL/min crossflow). The first two steps, though labeled here and in other methods as “Elution” and “Focus” in correspondence to the terms used in the FFF software, serve as channel flushes prior to sample injection.

Method B (OMV)

Method B was identical to Method A, apart from replacing the 350 μm spacer with a 250 μm wide format spacer.

Method C (OMV-BSA)

For Method C, a 250 μm , wide format spacer was used with 10 mM phosphate buffer, pH 7.2 as the eluent and a detector flow of 0.5 mL/min. The elution method consisted of the following steps: Elution (0–1 min, 3 mL/min crossflow), Focus (1–2 min), Focus + inject (2–4 min), Focus (4–6 min), Elution (6–11 min, 3 mL/min crossflow), Elution (11–16 min, 3–0.5 mL/min crossflow), Elution (16–34 min, 0.5–0.05 mL/min crossflow), Elution (34–40 min, 0.05 mL/min crossflow), and Elution + Inject (40–45 min, 0.0 mL/min crossflow).

Method D (Particle standards)

For Method D, a 250 μm spacer wide format was used with 10 mM phosphate buffer, pH 7.2 as the eluent and a detector flow of 0.5 mL/min. The elution method consisted of the following steps: Elution (0–1 min, 1 mL/min crossflow), Focus (1–2 min), Focus + inject (2–4 min), Focus (4–6 min), Elution (6–11 min, 1 mL/min crossflow), Elution (11–16 min, 1–0.5 mL/min crossflow), Elution (16–34 min, 0.5–0.05 mL/min crossflow), Elution (34–40 min, 0.05 mL/min crossflow), and Elution + Inject (40–45 min, 0.0 mL/min crossflow).

DLS and NTA

The description of these methods is available in the supporting information (Method S3 and S4).

ASTRA data processing

All light scattering results described below were calculated using ASTRA software v.

7.3.2.19 (system 1) and/or 8.0.2.5 (system 2), both from Wyatt Technology.

Hydrodynamic size

The online DLS module detects fluctuations in light scattered by particles in the MALS flow cell and provides autocorrelation functions (ACF) periodically, with a minimum ACF acquisition time of 2s, to measure hydrodynamic radii across the fractogram. ASTRA determines diffusion coefficients from dynamic light scattering by employing the method of cumulants and then applies the Stokes–Einstein equation to determine the hydrodynamic radius $R_h(Q)$ [22]. The average radius across a peak or segment of the fractogram is calculated as the z-average of instantaneous radii $R_h(Q)$ values, $R_h(Q)_z$.

Geometric radius

The MALS detector quantifies the intensity of light, scattered by the sample in the flow cell, at 18 angles relative to the direction of propagation of the illuminating laser beam, at intervals of typically 0.5 or 1 s during the elution. The geometric radius R_{geom} is calculated from the angular dependence of the scattered light using a model that assumes a uniform sphere, and the average R_{geom} across a peak or segment of the fractogram is calculated as the z-average of the instantaneous values, $R_{geom,z}$ [23].

Particle concentration

Particle concentration N is calculated from MALS data [24]. The refractive index of OMV used for determining N was initially set to 1.485 on knowledge that the OMV consists mostly of protein, and a spherical particle shape was assumed. The total number of particles in a peak or segment of the fractogram is calculated by integrating the product of the instantaneous particle concentration, the data collection interval, and the flow rate through the detector.

Molecular weight

Calculation of molecular weight, used to validate BSA (Thermo Scientific, Pierce BSA, 23209) as an impurity, requires MALS and concentration data [23]. Concentration was obtained from the refractive index detector, applying dn/dc of 0.185 mL/g for BSA and other proteins. The same dn/dc value was used in the MALS analysis.

Chromatographic parameters

All chromatographic parameters for the purity assessment of DSP fractions, only using FFF system 1, were calculated using Chromeleon software (v.7.2. SR 6 7553, Thermo Scientific),

which was also used to control the instrument. Purity was calculated for different DSP fractions by comparing the UV₂₈₀ peak area of the impurity compared to the total peak area of all eluting species. Considering the heterogeneity of the OMV population and inherent differences in the molar extinction coefficient, the purity assessment was taken as a qualitative parameter.

OMV production process

The OMVs were produced as described previously [25, 26] and stored in a 10 mM TRIS buffer at pH 7.4 with 3% sucrose. For a concise overview of all DSP fractions, see Table 1.

Table 1: Overview of DSP fractions for purification of OMVs

Fraction	Description
1	Biomass after diafiltration
2	EDTA extracted biomass
3	After centrifugation of the extracted biomass
4	OMV after digestion
5	OMV after centrifugation
6	OMV after clarification/filtration
7	OMV after size exclusion chromatography
8	OMV after sterile filtration

Validation strategy

Accuracy

The accuracy of an analytical procedure expresses the closeness of agreement between the measured value and a value that is either the conventional “true” value or is otherwise an accepted reference value. For OMVs, there is no biological particle-size reference standard available (e.g. provided by National Institute of Standards and Technology (NIST) or another standards agency). However, polystyrene NIST-traceable nanospheres, available in a size range comparable to the OMV, were used for confirmation of the analytical FFF-MALS method. In addition, DLS and NTA measurements of the OMVs were used as a reference.

Particle size

Rh of the OMV was first assessed six times (three times by two technicians) by both DLS and NTA. The z-average Rh from DLS, the number-average Rh from NTA, and CV (n = 6) from both assays were used for reference. This was followed by FFF-MALS analysis of the

OMV six times (three times by two technicians), and z-average Rh and CV were calculated. Using the polystyrene size standards to show the accuracy for determining Rh(Q)z in the range of the radii expected for the OMV (20–200 nm), these were assessed six times by FFF-MALS, and the average Rh and CV were calculated. A similar approach was applied to determine the value and CV of Rgeom,z.

Particle concentration

For the assessment of particle concentration, the OMV was measured six times (three times by two technicians) by NTA to determine average and CV. FFF-MALS was performed six times (three times by two technicians) and average particle concentration and CV were calculated and compared to the NTA reference.

Impurity profile

Evaluation of impurity profiles involved spiking different amounts of a model impurity, BSA, into an OMV sample, performing FFF separation, and quantifying the OMV size, OMV concentration, BSA molar mass, and eluted BSA mass. For the OMV, both DLS and NTA data served as a reference to verify the particle size (radius in nm) and concentration (particles/mL). Each measurement was performed over six repeats (three times by two technicians).

Precision

Repeatability An OMV sample was analyzed at three different dilutions (undiluted, 2× and 4× diluted) in triplicate. Average Rh and particle concentration were determined, and from these the average and CV were calculated.

Intermediate precision The same experiment as for repeatability was performed by a second technician on a different day. New membranes were installed in the FFF channels and freshly prepared buffer applied. From these results, the average and CV between the two technicians were calculated.

Reproducibility Reproducibility expresses the precision between the measurement results obtained at different laboratories. This interlaboratory variation was evaluated by comparing the particle standard analyses performed on FFF-MALS systems 1 and 2, both using Method D particle standards elution profile. From these results, the average and CV between the two laboratories were calculated.

Specificity

To ensure the identity of the analyte, three different batches of OMV were analyzed in triplicate. Additionally, particle standards in the size range of the OMV (20, 50, 100, and

200 nm) were analyzed 6-fold. Three blank runs were performed to demonstrate that no detector signal is observed in the elution range of the OMV and SSTs. Finally, BSA (67 kg/mol) was spiked into the OMV solution to show that free proteins do not coelute with OMV and that it was possible to separate free proteins from OMV (same run as purity assessment in the following section).

Purity assessment

The OMV solution was spiked with BSA as a model protein to mimic the protein impurity and evaluated for recovery (Table S10). BSA did not interfere with OMV characterization since it did not elute in the range of protein impurities and was subsequently evaluated to the extent the spiked-in BSA could still be detected.

Linearity and range

An effective dilution series was performed for OMV by decreasing the injected volume of the sample to a point that Rh or particle concentration could no longer be calculated. This assay was performed in triplicate. Five points were included to evaluate linearity. This determined the minimum quantity of OMV that could be injected while the analysis still yielded an accurate and precise result for hydrodynamic radius. Additionally, analysis of the particle concentration (particles/mL) over the dilution series should yield a calibration curve with the coefficient of determination $R^2 > 0.95$.

Quantification and Detection limit

Using the data from the linearity and range experiments, the limit of quantification and limit of detection were calculated.

GMBS functionalization of OMVs

OMVs ~1.4 mg/mL were buffer-exchanged to 10 mM HEPES pH 7.8 using manual hollow-fiber tangential-flow filtration (HF TFF, Repligen, C02-E100-05-S, 100 kDa MWCO). The OMV suspension was diluted to an effective protein concentration of 1.1 mg/mL, of which 2.25 mL was used for functionalization with GMBS (Mw 280.23 kDa) dissolved in DMSO. To facilitate GMBS reactions 1, 2, and 3, we dissolved 0.8, 1.2, and 1.8 mg GMBS, respectively, in 0.25 mL of DMSO and was subsequently added to the OMV. The reaction lasted for 30 min on a continuous roller bench at ambient temperature. The GMBS-modified OMVs were again buffer-exchanged to 10 mM HEPES pH 7.8 using manual HF TFF (Repligen, C02-E100-05-S, 100 kDa MWCO) before analysis.

Results and discussion

FFF method development and modeling

SCOUT software uses FFF theory to create *in silico*, “virtual” experiments that predict the fractogram resulting from a given set of conditions. The approximate particle sizes (e.g. obtained by offline DLS) are entered and the operator sets the channel-flow rate, crossflow profile (i.e., variation of crossflow with time, which may involve a crossflow gradient), spacer height, and channel type. To validate the FFF method, an initial method was developed using the modeling software to provide good separation conditions. This was followed by an optimization step. An initial method assessment was performed using a standard default screening method (Method A). This was known to be a nonoptimal method, wherein the OMV might elute, in part, past the end of the crossflow gradient (Figure S1), where crossflow was set to zero, resulting in reduced resolution. Nevertheless, it was decided to evaluate the OMV elution behavior with this method, and we did in fact observe a pronounced delay in elution compared to the predicted elution according to the model developed in SCOUT: the OMV eluted fully past the end of the crossflow gradient (Figure S2). At that point, there is no longer size-dependent separation, and the eluting material consists of unseparated mixtures, which result in unreliable and unusable data. The first iteration of the separation method involved changing the spacer height to 250 μm , per Method B. The benefit to changing spacer height was predicted by the *in silico* model, yielding earlier elution of the OMV, in the range where there would still be crossflow and subsequent separation (Figure S3). In practice, OMV elution was delayed once again beyond the crossflow gradient (Figure S4). It was hypothesized that the elution buffer (PBS), containing 150 mM NaCl, led to an interaction between the OMVs or of the OMV with the membrane. For a second iteration of the separation procedure, it was decided to continue using Method B but change the elution buffer to 10 mM phosphate, which now led to the OMV eluting well within the crossflow gradient. Several further iterations on the crossflow gradient and the detector flow were made that facilitated elution of the individual particle-size standards, BSA and OMV (Figures S5 and S6). To facilitate the separation of BSA from OMV, an initial crossflow of 3 mL/min was found necessary for retaining the BSA so that it elutes after the void peak (which appears at ~ 7.5 min). Ensuring that BSA elutes after the void peak was highly desirable when considering that the envisioned application is evaluation of DSP samples containing primarily free-protein impurities. This method was observed to work well for separating OMV and BSA. However, the particle-size standards could not be separated efficiently when an initial crossflow of 3 mL/min was applied. A method that separates these particle-size standards is required not only during the validation study but also as a system suitability test for a GMP-grade quality-control regime. After careful consideration, we ended up with two methods that differed only in the early elution program for retaining BSA but were the same for the region in which the

OMV and particle-size standards eluted. Hence, we adopted two final elution profiles: one to separate BSA and OMV (Method C OMV-BSA, Figure 1a) and the other for particle-size standards (Method D Particle standards, Figure 1b). With these, we were able to separate the different entities and apply them to validating this FFF-MALS method (Figure 1).

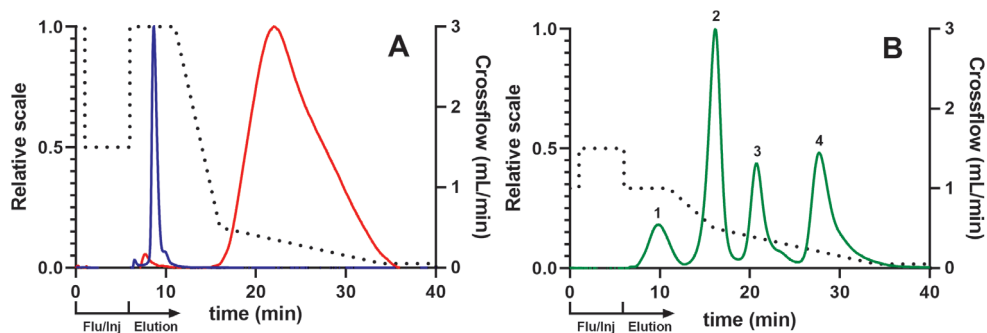


Figure 1: Elution profiles for the separation of BSA, OMV, and particle-size standards. The left-side y axes pertain to the relative signal from the 90° light-scattering detector. **(A)** Method C for the elution of BSA (blue) and OMV (red) and **(B)** Method D for the elution of particle-size standards (green) with radii of (1) 11.5 nm, (2) 25.5 nm, (3) 50.0 nm, and (4) 101.5 nm. The crossflow for both figures is plotted as the black dotted line, of which the first 6 min represent the steps to flush the channel and inject the sample (Flu/Inj).

Validation of the FFF-MALS method

With the goal of utilizing the FFF method for the characterization of OMV, it was decided to perform a full validation of the assay. Validation ensures that the assay and the results thereof may be relied upon in the analysis of drug substance following the production purification process, other purified OMV drug substances, GMBS-functionalized OMV, and possibly future conjugate vaccines employing OMV as a carrier. Furthermore, a validated FFF-MALS assay could be employed as a quality control release assay and for stability studies of the OMV drug substance (concentrated bulk product) and drug product (final formulated vaccine, not part of this investigation). ICH guidelines Q2 (R1) [19] were evaluated and used in developing the validation plan. These guidelines state that particle-size determination for drug substances has not been addressed in the initial text on the validation of analytical procedures. In the absence of specific guidelines for particle size determination, it was decided to validate according to the “testing for impurities” regime that includes all relevant characteristics: accuracy, precision, specificity, limit of quantitation, limit of detection, linearity, and range. Since the ICH guidelines do not state any limits and no known references were available in the field toward validation of a similar method, we did not set any predefined limits prior to validation of the analytical procedure. With respect to particle-size standards, it was somewhat surprising that no biological standard, preferably NIST-traceable, was available. Therefore, nanosphere size

standards, a polystyrene equivalent to OMV, were used instead to validate separation and analysis of particles in the size range of our OMVs. Additionally, we confirmed that the FFF method elutes particles of a known size at the elution time designated according to *in silico* modeling. With this, we were able to validate the method despite the absence of such a biological standard. With NIST-traceable particle-size standards and BSA defined as a model impurity, both Method C (OMV-BSA) and Method D (particle standards) were applied to the validation strategy outlined above.

Accuracy

For the validation of accuracy in particle size, the hydrodynamic radius of OMV was assessed by FFF-MALS, DLS, and NTA (Table S1). It was noted that there were inherent differences in the outcome of the individual methods, for example, batch DLS provides a harmonic z-average, NTA provides a number average, and FFF-MALS provides a z-average (though the latter can also provide number and mass averages). Particle-size standards, in the range of the radii expected for the OMV, were also evaluated by FFF-MALS, DLS, and NTA (Tables S2–S4). For both DLS and NTA, individual particle standards were analyzed, but measurements of the mixture of sizes resulted in non-distinguishable individual peaks and very high polydispersity index and were hence not usable. Here, the advantage of the FFF really stood out as it produced useful data for each individual size after separation of the mix of particle standards. The 51 nm standard showed a slight offset in the final MALS result of around 60 nm confirmed by DLS and NTA. The NTA instrument was not able to determine the size of the 23 nm size standard, as expected, since the low cutoff for this analysis is around 30 nm. Accuracy of particle concentration measurements for OMV was assessed with FFF-MALS and NTA (see Table S5). The measurement is not supported by the DLS instrument used in this investigation. There was a striking difference between the results from NTA (average 5.67×10^{11} particles/mL) and FFF-MALS (average 1.45×10^{12} particles/mL), where 2.6 times more particles were determined by FFF-MALS. This discrepancy could be ascribed to two factors: (1) the OMV distribution contains particles smaller than 30 nm, which are not detected by NTA but are included in the FFF-MALS analysis and (2) the RI value used for calculating the particle concentration in FFF-MALS (1.485) was estimated and is still under investigation. Accuracy assessment for Rh(Q)z and molecular weight of eluting BSA, envisioned as both a system suitability test and model impurity, showed excellent CV for both the molecular weight (CV 0.89%) and Rh(Q)z (CV 2.50%) (see Table S6).

Precision

With regard to intermediate precision, the CV for both Rh(Q)z (1.65%) and particle concentration (15.93%) was highest for the 4-fold diluted sample (see Tables S7 and S8).

The intermediate precision (difference between technician 1 and technician 2) over three different dilutions was also calculated and resulted in a CV of 1.1% (see Tables S7 and S8).

Specificity

ICH guidelines prescribe that for assessing specificity, we are to ensure the identity of the analyte. In the absence of a biological reference standard, we chose to evaluate three batches of OMVs, analyzed in triplicate. Here, different elution profiles were observed for each OMV batch, but all eluted in the expected range (Figure S7 and Table S9). To further confirm that the method was specific for a particular range, particle standards in the size range of the OMV (20, 50, 100, and 200 nm) were assessed 6-fold (Figure S8). Blank runs performed in triplicate did not show any eluting particles (data not shown).

Purity assessment

Purity was assessed by spiking BSA into OMV (Table S10). Baseline separation between OMV and BSA was observed for all spiked samples, excluding any potential matrix effects or interactions between the OMV and spiked BSA (Figure S9). Disregarding the differences in the molar extinction coefficient between BSA and OMV (UV_{280}), this test shows that protein impurities were detected to a level of at least 1% w/w, when injecting 54 μg OMV or more. Furthermore, no specification was set for R^2 , but we could appreciate the excellent coefficient of 0.999 (Table S11 and Figure S10).

Linearity and range

For the evaluation of linearity and range, a dilution series was performed on the OMV, in triplicate. The minimum quantity of OMV (μg) was evaluated by determining the point that Rh or particle concentration could no longer be quantified accurately. With respect to Rh(Q)z, the minimum injected quantity that enabled determining Rh was as low as 1 μg (protein content of OMV). At 0.5 μg , the chromatograms became inconsistent, with subsequent CV going up to 15% (Table S12). While this test was not carried out, in principle, MALS is $\sim 100\times$ more sensitive than online DLS and the limit of quantification for Rgeom is expected to be about 0.01 μg (protein content of OMV). Using the same dilution series, the particle concentration was determined, yielding a calibration curve with $R^2 > 0.980$ (Figure S11). However, upon reviewing individual data points, it was observed that the CV % increased significantly and particle concentration became unreliable for injections containing 5 μg and less (Table S13).

Quantification and Detection limit

Using the data from the linearity and range experiments, the LoQ and LoD for size and

particle concentration were determined by visual evaluation. Both system 1 and system 2 showed comparable results. Here, it was concluded that both the LoQ and LoD for particle size should be set at 1 μg OMV protein content, and LoQ and LoD for particle concentration were set at 10 and 1 μg OMV protein content, respectively.

Reproducibility

Interlaboratory variation was evaluated by comparing the results of particle standard analysis using the method. Here, it was observed that the two different laboratories, using two different FFF set-ups, produced comparable results in equivalence tests that fell within 10.5% (Tables S14 and S15).

Recovery

For both BSA and OMV, the recovery was evaluated and were 92.8 and 90.8%, respectively (Table S16).

Summary

We were able to successfully execute all experiments necessary to test the individual validation criteria. The size particle standards aided greatly, considering that a NIST-traceable biological standard representing OMV was not available. The successful repeated elution of a mixture of these standards gave a lot of confidence in the abilities of the method. BSA was successfully introduced as a model protein to mimic impurities and was separated from OMV as demonstrated by FFF-MALS analysis. Before starting the validation, we had experience running and analyzing samples to a certain extent, not knowing how accurate the results could be. In conclusion, we were able to evaluate all validation criteria and were able to report the individual results. FFF-MALS analysis performed exceptionally well and showed very low CV % at all stages of the validation (see Table 2).

Table 2: Validation results

Validation parameter	Determined limits (%CV)
Accuracy - OMV Rh(Q)z Table S1	0.40
Accuracy - Particle standard SST geometric radius Table S2-4	5.06 *
Accuracy - Particle concentration Table S5	7.32
Accuracy - BSA SST (Mw) Table S6	2.50
Intermediate precision - Particle size Rh(Q)z Table S7	1.10
Intermediate precision - Particle concentration Table S8	1.10
Repeatability - Particle size Rh(Q)z Table S7	1.65
Repeatability - Particle concentration Table S8	4.03
Purity Table S10-11 **	n.a.
LoD/LoQ - Particle size Rh(Q)z Table S12 **	n.a.
LoD/LoQ - Particle concentration Table S13 **	n.a.
Reproducibility Table S14 & S15 ***	10.5 ***

* highest CV found for 51 nm particle, ** not based on CV, *** highest value for the 51 nm particle

Evaluation of the OMV downstream purification process

As stated in the ICH Q6B guidelines [27], knowledge of the physicochemical properties of the drug substance and drug product is desired when filing for approval. Product characterization and determining the size of the product as well as of the impurities (if present) are of essence to ensure product safety. In addition, ensuring product quality and consistency are of high importance within the downstream production process as well as at the drug substance and drug formulation stages. With the validated FFF-MALS method in hand, we now wanted to see if it was possible to evaluate the OMV DSP production process. To this end, fractions were collected at critical stages of the downstream production process and subjected to the validated FFF-MALS analysis. The spike experiments using BSA as a model impurity were particularly informative and it was of interest to see if the FFF-MALS method could be applied to complex matrices containing mixtures of impurities and OMVs. All fractions specified in Table 1 were analyzed in triplicate (Figures 2 and S12). For fraction 2, we did observe a slightly different elution pattern on one of the repeats, possibly attributed to the difficult matrix or the nonoptimal elution method for this fraction. However, it was well appreciated that other early fractions, from 1 to 6, also contain complex matrices, yet showed excellent comparability across repeats. Purity was evaluated over the entire downstream process by separating and quantifying impurities relative to OMV. This valuation is not without challenges. In cases where baseline separation between impurities and OMV did not occur in the UV fractogram, overlapping peaks were split at the bottom of the valley between them. Also, differences in molar extinction coefficients of the earlier eluting impurities can lead to either an over- or

underestimation of the degree of purity. In early purification stages, some of the successive fractions did not show the expected increasing degree of purity, which we attribute to the difficult matrices and differing concentrations and volumes between those stages (Figures 2 and S12). Nevertheless, we were able to fully track all intermediate fractions and show that, after the final SEC purification step, the OMV product was 99.2% pure.

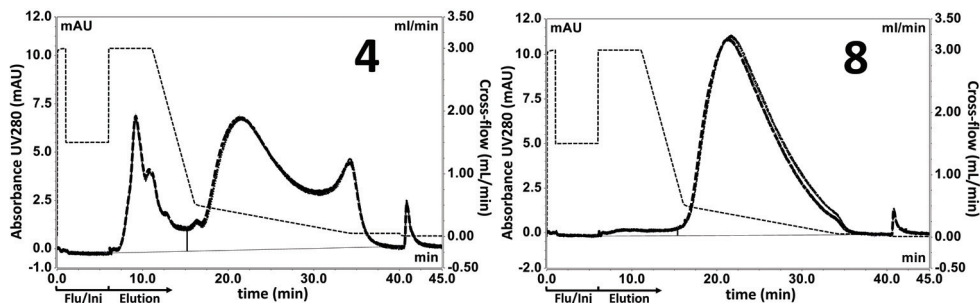


Figure 2: FFF-MALS results ($n = 3$): fractions 4 and 8 collected from DSP steps as described in Table 1 (for fractions 1–3 and 5–7), see Figure S12. Crossflow for both figures is shown as the black dotted line, of which the first 6 min represent the steps to flush the channel and inject the sample (Flu/Inj).

Analysis of different purified OMV's

With a validated method in hand for characterizing OMV, we turned to investigating whether other types of purified OMVs could be evaluated by the same FFF-MALS method, Method C. This would be extremely helpful for the evaluation of new OMVs and conjugate vaccine carriers that are either extracted directly from the bacteria or are genetically constructed. The different purified OMVs consisted of *Neisseria meningitidis* type-B, *N. meningitidis* type-B containing two heterologous *Gonococcus* antigens, *Bordetella pertussis*, and *Escherichia coli*. These were produced using the same process as for the standard OMV product.

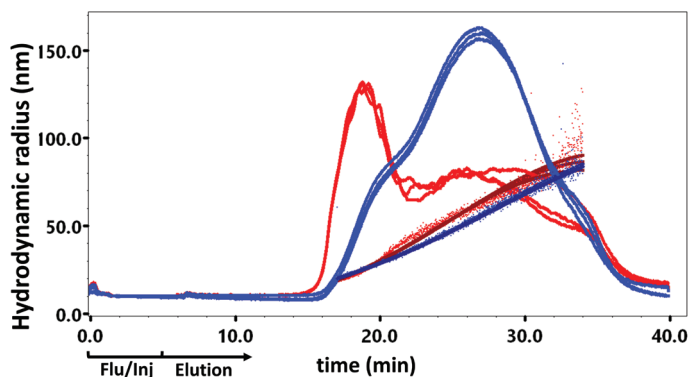


Figure 3: Different OMVs analyzed with FFF-MALS method C (OMV-BSA, $n = 3$). Blue: *B. pertussis* - $R_h(Q)_z = 55.0 \pm 0.4$ nm; red: *E. coli* - $R_h(Q)_z = 58.2 \pm 0.7$ nm.

GMBS functionalization of OMVs

The use of GMBS for conjugating vaccine antigens to a carrier is a proven technology [28, 29]. The succinimide ester of GMBS targets primary amines, which are available as lysine residues on membrane proteins, phosphoethanolamine as part of LPS, or phosphatidylethanolamine as part of phospholipids, all of which are part of the OMV. Here, we investigated whether functionalization of OMVs using GMBS was possible without affecting the structure of the OMV. This functionalization would be a first step in preparation for any thiol-bearing antigen used in a succeeding conjugation step, suggesting a very broad range of applications. Other than some minor differences in the fractograms (differing peak areas due to different overall concentrations), functionalization with OMV/GMBS ratios of 3:1, 2:1, and 1.3:1 (w/w) did not affect the OMV size distribution (Figure 4). This information is highly beneficial for future conjugation chemistry approaches targeting a free thiol on an antigen.

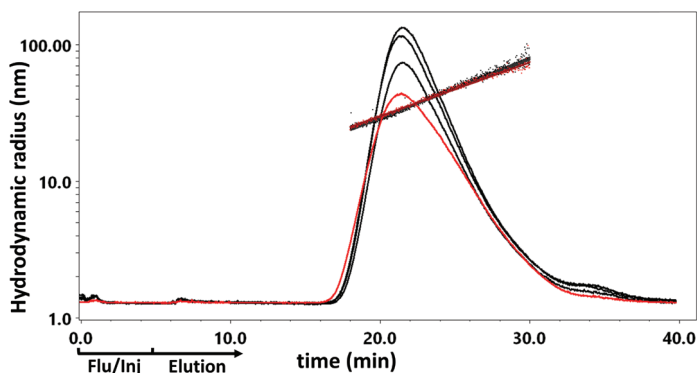


Figure 4: FFF-MALS analysis: OMV, OMV buffer-exchanged, and OMV-GMBS-modified; no differences in size distributions were found for OMV/GMBS ratios of 3:1, 2:1, or 1.3:1.

Conclusions

FFF-MALS methods were successfully developed to separate a model impurity, BSA, from OMVs and to separate a mixture of particle-size standards. Both these separation methods aided in the validation of FFF-MALS analysis of OMV. Where the ICH guidelines predominantly prescribed expected the result to fall within a CV of <30%, we observed surprisingly lower CVs for all evaluated parameters (see Table 2). This led to applying much lower CV requirements and, consequently, a higher quality level to the FFF-MALS analysis (Table 3). Recovery for both the model impurity BSA and OMV as target analyte was >90%, confirming the excellent quantitative performance of the analysis. Finally, it stood out that it was possible to evaluate the size and particle concentration of an OMV with as little as 1 µg of sample. This will be especially usable for evaluation of future down-scaled nonoptimized production processes during early process development. With the validated method in hand, it was used to successfully evaluate the DSP process for the production and purification of OMVs. Even though the early fractions contain highly complex matrices, it was appreciated that all fractions could be evaluated for purity. Subsequently, different purified OMVs were successfully analyzed. Finally, the FFF-MALS method was used to evaluate the OMVs functionalized with GMBS in preparation for conjugation of any thiol-bearing vaccine antigen. Functionalization with different concentrations of GMBS yielded similar particle-size distributions. The OMVs held their integrity without decomposing or aggregating, which is essential for successful conjugate vaccine development. Further studies following the work presented in this paper will include the conjugation of synthetic oligosaccharides, synthetic peptides, and proteins. The application could potentially include antigens for a wide variety of infectious diseases (prophylactic), but therapeutic targets would also be of interest.

Table 3: Validation results

Validation parameter	Set limits (%CV)
Accuracy - OMV Rh(Q)z	< 10
Accuracy - Particle standard SST geometric radius	< 10
Accuracy - Particle concentration	< 10
Accuracy - BSA SST (Mw)	< 10
Repeatability - Particle size Rh(Q)z	< 10
Repeatability - Particle concentration	< 20
Purity	> 1%*
Intermediate - Precision Particle size Rh(Q)z	< 10
Intermediate - Precision Particle concentration	< 20

Validation parameter	Set limits (%CV)
Reproducibility	< 10
LOD - Particle size Rh(Q)z	1 µg*
LOQ - Particle size Rh(Q)z	1 µg*
LOD - Particle concentration	1 µg*
LOQ - Particle concentration	10 µg*

* not based on CV

Associated content

Supporting information

The Supporting Information is available free of charge at <https://pubs.acs.org/doi/10.1021/acs.analchem.2c01590>. Results for all of the FFF-MALS validation criteria, SCOUT prediction models, and FFF-MALS fractograms, recovery measurements, method description for NTA, DLS, particle standards, FFF configurations, and safety statement.

Author information

Corresponding author

* Robert M. F. van der Put – Department of Chemical Biology & Drug Discovery, Utrecht Institute for Pharmaceutical Sciences, Utrecht University, NL-3508 TB Utrecht, The Netherlands; Intravacc, 3720 AL Bilthoven, The Netherlands; orcid.org/0000-0001-7686-9632; Email: r.m.f.vanderput@uu.nl

Author contributions

Robert M.F. van der Put: conceptualization, supervision, visualization, writing - review and editing; Arnoud Spies: methodology, validation, investigation, formal analysis; Bernard Metz: supervision, recourses; Roger Scherrers: validation, writing original draft; Daniel Some: writing - review & editing; Roland Pieters: supervision; and Maarten Danial: supervision, writing - original draft.

Acknowledgements

The authors thank Dr. Zaskia Eksteen (Intravacc) for her input on the validation plan, Tess van den Bergen for the input on the validation plan and data processing, Eelke Bouma (Intravacc) for statistical analysis, and Louisa Eyl (Wyatt Technologies Europe) for performing the measurements at the Wyatt Europe laboratory.

References

1. Peltola, H., Worldwide Haemophilus influenzae type b disease at the beginning of the 21st century: global analysis of the disease burden 25 years after the use of the polysaccharide vaccine and a decade after the advent of conjugates. *Clin Microbiol Rev* 2000, 13 (2), 302-17.
2. Pichichero, M. E., Protein carriers of conjugate vaccines: characteristics, development, and clinical trials. *Hum Vaccin Immunother* 2013, 9 (12), 2505-23.
3. Croxtall, J. D.; Dhillon, S., Meningococcal quadrivalent (serogroups A, C, W135 and Y) tetanus toxoid conjugate vaccine (Nimenrix). *Drugs* 2012, 72 (18), 2407-30.
4. Bilukha, O.; Messonnier, N.; Fischer, M., Use of meningococcal vaccines in the United States. *Pediatr Infect Dis J* 2007, 26 (5), 371-6.
5. Ilyina, N.; Kharit, S.; Namazova-Baranova, L.; Asatryan, A.; Benashvili, M.; Tkhostova, E.; Bhusal, C.; Arora, A. K., Safety and immunogenicity of meningococcal ACWY CRM197-conjugate vaccine in children, adolescents and adults in Russia. *Hum Vaccin Immunother* 2014, 10 (8), 2471-81.
6. Scaria, P. V.; Rowe, C. G.; Chen, B. B.; Muratova, O. V.; Fischer, E. R.; Barnafo, E. K.; Anderson, C. F.; Zaidi, I. U.; Lambert, L. E.; Lucas, B. J.; Nahas, D. D.; Narum, D. L.; Duffy, P. E., Outer membrane protein complex as a carrier for malaria transmission blocking antigen Pfs230. *NPJ Vaccines* 2019, 4, 24.
7. Vesikari, T.; Wysocki, J.; Chevallier, B.; Karvonen, A.; Czajka, H.; Arsene, J. P.; Lommel, P.; Dieussaert, I.; Schuerman, L., Immunogenicity of the 10-valent pneumococcal non-typeable Haemophilus influenzae protein D conjugate vaccine (PHiD-CV) compared to the licensed 7vCRM vaccine. *Pediatr Infect Dis J* 2009, 28 (4 Suppl), S66-76.
8. Lehmann, A. K.; Halstensen, A.; Aaberge, I. S.; Holst, J.; Michaelsen, T. E.; Sornes, S.; Wetzler, L. M.; Guttormsen, H., Human opsonins induced during meningococcal disease recognize outer membrane proteins PorA and PorB. *Infect Immun* 1999, 67 (5), 2552-60.
9. Liu, Y.; Hammer, L. A.; Liu, W.; Hobbs, M. M.; Zielke, R. A.; Sikora, A. E.; Jerse, A. E.; Egilmez, N. K.; Russell, M. W., Experimental vaccine induces Th1-driven immune responses and resistance to Neisseria gonorrhoeae infection in a murine model. *Mucosal Immunol* 2017, 10 (6), 1594-1608.
10. Skidmore, B. J.; Chiller, J. M.; Morrison, D. C.; Weigle, W. O., Immunologic properties of bacterial lipopolysaccharide (LPS): correlation between the mitogenic, adjuvant, and immunogenic activities. *J Immunol* 1975, 114 (2 pt 2), 770-5.
11. Raetz, C. R.; Whitfield, C., Lipopolysaccharide endotoxins. *Annu Rev Biochem* 2002, 71, 635-700.
12. Zariri, A.; Pupo, E.; van Riet, E.; van Putten, J. P.; van der Ley, P., Modulating endotoxin activity by combinatorial bio-engineering of meningococcal lipopolysaccharide. *Sci Rep* 2016, 6, 36575.
13. Kawasaki, T.; Kawai, T., Toll-like receptor signaling pathways. *Front Immunol* 2014, 5, 461.
14. Takeuchi, O.; Hoshino, K.; Kawai, T.; Sanjo, H.; Takada, H.; Ogawa, T.; Takeda, K.; Akira, S., Differential roles of TLR2 and TLR4 in recognition of gram-negative and gram-positive bacterial cell wall components. *Immunity* 1999, 11 (4), 443-51.
15. Tan, K.; Li, R.; Huang, X.; Liu, Q., Outer Membrane Vesicles: Current Status and Future Direction of These Novel Vaccine Adjuvants. *Front Microbiol* 2018, 9, 783.
16. Gnopo, Y. M. D.; Watkins, H. C.; Stevenson, T. C.; DeLisa, M. P.; Putnam, D., Designer outer membrane vesicles as immunomodulatory systems - Reprogramming bacteria for vaccine delivery. *Adv Drug Deliv Rev* 2017, 114, 132-142.
17. Filipe, V.; Hawe, A.; Jiskoot, W., Critical evaluation of Nanoparticle Tracking Analysis (NTA) by NanoSight for the measurement of nanoparticles and protein aggregates. *Pharm Res* 2010, 27 (5), 796-810.
18. Parot, J.; Caputo, F.; Mehn, D.; Hackley, V. A.; Calzolari, L., Physical characterization of liposomal drug formulations using multi-detector asymmetrical-flow field flow fractionation. *J Control Release* 2020, 320, 495-510.
19. ICH ICHQ2R1. <https://www.ema.europa.eu/.../scientific-guidelines/ich-guidelines>.
20. Giddings, J. C., Field-flow fractionation: analysis of macromolecular, colloidal, and particulate materials. *Science* 1993, 260 (5113), 1456-65.

21. Johann, C. Field-Flow Fractionation: Virtual Optimization for Versatile Separation Methods. <https://www.chromatographyonline.com/view/field-flow-fractionation-virtual-optimization-versatile-separation-methods-0> (accessed 03-03-2022).
22. Stetefeld, J.; McKenna, S. A.; Patel, T. R., Dynamic light scattering: a practical guide and applications in biomedical sciences. *Biophys Rev* 2016, 8 (4), 409-427.
23. Wyatt, P. J., Differential light scattering and the measurement of molecules and nanoparticles: A review. *Anal Chim Acta X* 2021, 7-8, 100070.
24. Van Holde, K. E. Physical biochemistry, Chapter 7. [http://www.fisica.uniud.it/~deangeli/test/Principles%20of%20Physical%20Biochemistry%20\(Prentice%20Hall,%202005\).pdf](http://www.fisica.uniud.it/~deangeli/test/Principles%20of%20Physical%20Biochemistry%20(Prentice%20Hall,%202005).pdf).
25. van der Ley, P. A.; Zariri, A.; van Riet, E.; Oosterhoff, D.; Kruiswijk, C. P., An Intranasal OMV-Based Vaccine Induces High Mucosal and Systemic Protecting Immunity Against a SARS-CoV-2 Infection. *Front Immunol* 2021, 12, 781280.
26. Gerritzen, M. J. H.; Salverda, M. L. M.; Martens, D. E.; Wijffels, R. H.; Stork, M., Spontaneously released Neisseria meningitidis outer membrane vesicles as vaccine platform: production and purification. *Vaccine* 2019, 37 (47), 6978-6986.
27. ICH ICH Q6B. <https://www.ema.europa.eu/en/ich-q6b-specifications-test-procedures-acceptance-criteria-biotechnologicalbiological-products>.
28. Cohen, D.; Atsmon, J.; Artaud, C.; Meron-Sudai, S.; Gougeon, M. L.; Bialik, A.; Goren, S.; Asato, V.; Ariel-Cohen, O.; Reizis, A.; Dorman, A.; Hoitink, C. W. G.; Westdijk, J.; Ashkenazi, S.; Sansonetti, P.; Mulard, L. A.; Phalipon, A., Safety and immunogenicity of a synthetic carbohydrate conjugate vaccine against Shigella flexneri 2a in healthy adult volunteers: a phase 1, dose-escalating, single-blind, randomised, placebo-controlled study. *Lancet Infect Dis* 2021, 21 (4), 546-558.
29. Verez-Bencomo, V. e. a.; Fernandez-Santana, V.; Hardy, E.; Toledo, M. E.; Rodriguez, M. C.; Heynngnezz, L.; Rodriguez, A.; Baly, A.; Herrera, L.; Izquierdo, M.; Villar, A.; Valdes, Y.; Cosme, K.; Deler, M. L.; Montane, M.; Garcia, E.; Ramos, A.; Aguilar, A.; Medina, E.; Torano, G., A synthetic conjugate polysaccharide vaccine against Haemophilus influenzae type b. *Science* 2004, 305 (5683), 522-5.

Supporting Information

Table of contents

Table S1	Validation results for accuracy OMV
Table S2	Validation results for accuracy particle size standards FFF-MALS
Table S3	Validation results for accuracy particle size standards NTA
Table S4	Validation results for accuracy particle size standards DLS
Table S5	Validation results for accuracy particle count OMV FFF-MALS NTA
Table S6	Validation results for accuracy
Table S7	Validation results for intermediate precision OMV Rh FFF-MALS
Table S8	Validation results for intermediate precision OMV particle count FFF-MALS
Table S9	Validation results for specificity OMV FFF-MALS
Table S10	Validation set-up for OMV spiked with BSA FFF-MALS
Table S11	Validation results for OMV spiked with BSA FFF-MALS
Table S12	LOD LOQ Rh(Q) _z OMV FFF-MALS
Table S13	LOD LOQ particle count OMV FFF-MALS
Table S14	Particle size standards evaluated at Wyatt technologies Dernbach
Table S15	Equivalence TOST-test
Table S16	Recovery
Figure S1	Scout prediction method A
Figure S2	Separation OMV using method A
Figure S3	Scout prediction method B
Figure S4	Separation OMV using method B
Figure S5	Scout prediction method C OMV-BSA
Figure S6	Separation OMV using method C OMV-BSA
Figure S7	Validation results for specificity OMV FFF-MALS
Figure S8	Elution of particle size standards elution using method D particle standards
Figure S9	Validation results for OMV spiked with BSA FFF-MALS
Figure S10	Validation results for OMV spiked with BSA FFF-MALS
Figure S11	LOD LOQ particle count OMV FFF-MALS
Figure S12	Fraction 2, 5, 6 and 7 from the downstream purification process
Method S1	FFF-MALS configurations
Method S2	BSA and particle standards
Method S3	Nanoparticle tracking analysis
Method S4	Batch dynamic light scattering
General	Safety statement

I. Supporting information Tables

Table S1. Accuracy: OMV average radius, measured by DLS, NTA and FFF-MALS

Repetition	Rh from DLS (harmonic z-average radius, nm)	Mean size from NTA (number-average radius, nm)	Rh(Q) _z from FFF-MALS (z-average hydrodynamic radius, nm)
1 (Technician 1)	49.0	65.7	54.0
2 (Technician 1)	49.0	62.4	53.8
3 (Technician 1)	48.4	60.5	54.1
4 (Technician 2)	48.6	60.2	53.6
5 (Technician 2)	48.4	60.6	54.0
6 (Technician 2)	48.7	61.4	53.6
Average	48.7	61.8	53.9
Std. deviation	0.3	2.1	0.2
CV (%)	0.56	3.32	0.40

Table S2. Accuracy: Z-average geometric radius R_{geom,z} of a mixture of particle size standards, separated and measured by FFF-MALS

Repetition	Peak 1 (nominal size: 11.0 nm) R _{geom,z} (nm)	Peak 2 (nominal size: 25.5 nm) R _{geom,z} (nm)	Peak 3 (nominal size: 51.0 nm) R _{geom,z} (nm)	Peak 4 (nominal size: 101.5 nm) R _{geom,z} (nm)
1 (Technician 1)	11.0	29.0	51.1	101.1
2 (Technician 1)	11.0	30.2	51.5	101.6
3 (Technician 1)	11.0	27.8	50.5	101.0
4 (Technician 2)	10.2	32.1	52.7	102.0
5 (Technician 2)	11.0	28.7	50.9	101.0
6 (Technician 2)	10.8	29.2	51.0	100.8
Average	10.8	29.5	51.3	101.3
Std. deviation	0.3	1.5	0.8	0.5
CV (%)	2.96	5.06	1.49	0.45

Table S3. Accuracy: Mean radius of mixtures of individual particle size standards, measured by NTA

Repetition	Mean size nominal: 11.5 nm)	Mean size nominal: 25.5 nm)	Mean size nominal: 51.0 nm)	Mean size nominal: 101.5 nm)
1 (Technician 1)	n.d.	29.7	46.9	95.8
2 (Technician 1)	n.d.	32.2	46.9	96.8
3 (Technician 1)	n.d.	29.5	47.0	96.1
4 (Technician 2)	n.d.	29.5	47.2	96.0
5 (Technician 2)	n.d.	32.3	46.2	97.3
6 (Technician 2)	n.d.	36.9	46.8	93.6
Average	n.d.	31.67	46.83	95.92
Std. deviation	n.d.	2.9	0.3	1.3
CV (%)	n.d.	9.10	0.72	1.34

n.d.: particle standards of 23 nm could not be measured by NTA.

Table S4. Accuracy: Harmonic z-average radius of individual particle size standards, measured by DLS

Repetition	Mean size (11.5 nm)	Mean size (25.5 nm)	Mean size (51.0 nm)	Mean size (101.5 nm)
1 (Technician 1)	11.9	31.6	56.8	109.8
2 (Technician 1)	11.8	31.3	56.9	111.4
3 (Technician 1)	11.7	30.9	55.4	110.4
4 (Technician 2)	11.6	30.9	55.9	109.8
5 (Technician 2)	11.8	31.0	56.0	111.4
6 (Technician 2)	11.8	30.8	56.0	111.4
Average	11.8	31.1	56.1	110.7
Std. deviation	0.1	0.3	0.6	0.8
CV (%)	0.79	0.99	1.02	0.73

Table S5. Accuracy: Overall particle concentration of OMV, measured by FFF-MALS and NTA

Repetition	Particles per mL (NTA)	Particles per mL (FFF-MALS) ^[1]
1 (Technician 1)	3.85×10^{11}	1.37×10^{11}
2 (Technician 1)	5.87×10^{11}	1.33×10^{12}
3 (Technician 1)	5.70×10^{11}	1.60×10^{12}
4 (Technician 2)	6.20×10^{11}	1.47×10^{12}
5 (Technician 2)	6.18×10^{11}	1.55×10^{12}
6 (Technician 2)	6.21×10^{11}	1.38×10^{12}
Average	5.7×10^{11}	1.45×10^{12}
Std. deviation	9×10^{10}	1.1×10^{11}
CV (%)	16	7

^[1] Particles n/mL = Particles (n) / 30 * 1000

Table S6. Accuracy: Weight-average molar mass Mw and z-average hydrodynamic radius Rh(Q)z of BSA, measured by FFF-MALS

Repetition	Mw (kDa)	Rh(Q)z (nm)
1 (Technician 1)	65.2	3.3
2 (Technician 1)	66.6	3.3
3 (Technician 1)	66.0	3.1
4 (Technician 2)	65.1	3.3
5 (Technician 2)	65.7	3.3
6 (Technician 2)	66.2	3.3
Average	65.8	3.3
Std. deviation	0.6	0.1
CV %	0.9	2.5

Table S7. Intermediate precision: z-average hydrodynamic radius Rh(Q)z of OMV, measured over 3 dilutions by FFF-MALS

Repetition	Undiluted Rh(Q)z (nm)	2-fold diluted Rh(Q)z (nm)	4-fold diluted Rh(Q)z (nm)
1 (Technician 1)	54.0	53.4	54.7
2 (Technician 1)	53.8	53.5	53.4
3 (Technician 1)	54.1	53.6	55.0
4 (Technician 2)	53.6	53.5	52.8
5 (Technician 2)	54.0	53.8	54.3
6 (Technician 2)	53.6	53.8	53.2
Average	53.9	53.6	53.9
Std. deviation	0.2	0.2	0.9
CV %	0.4	0.3	1.7

Table S8. Intermediate precision: Particle concentration of OMV, measured over 3 dilutions by FFF-MALS

Repetition	Undiluted Particles/mL	2-fold diluted Particles/mL	4-fold diluted Particles/mL
1 (Technician 1)	1.37×10^{12}	5.77×10^{11}	1.76×10^{11}
2 (Technician 1)	1.33×10^{12}	6.93×10^{11}	2.40×10^{11}
3 (Technician 1)	1.47×10^{12}	5.87×10^{11}	1.91×10^{11}
4 (Technician 2)	1.60×10^{12}	6.03×10^{11}	2.57×10^{11}
5 (Technician 2)	1.55×10^{12}	5.33×10^{11}	2.52×10^{11}
6 (Technician 2)	1.38×10^{12}	5.63×10^{11}	1.98×10^{11}
Average	1.45×10^{12}	5.9×10^{11}	2.2×10^{11}
Std. deviation	1.1×10^{11}	5×10^{10}	3×10^{10}
CV %	7	9	16

Table S9. Specificity: z-average hydrodynamic radius Rh(Q)z for 3 individual batches of OMV, measured by FFF-MALS

Repetition	Batch-1 Rh(Q)z	Batch-2 Rh(Q)z	Batch-3 Rh(Q)z
1 (Technician 1)	57.0	53.6	50.5
2 (Technician 1)	57.1	54.0	50.2
3 (Technician 1)	56.8	53.6	50.8
Average	57.0	53.7	50.5
Std. deviation	0.2	0.2	0.3
%RSD	0.3	0.4	0.6

Table S10. Purity: Validation set-up for OMV spiked with BSA FFF-MALS

Spiked BSA (%)	OMV (µg) ^[1]	BSA (µg)	OMV (µL)	OMV (µg)	BSA (µg)	µL BSA	WFI (µL)
1	54.3	0.54	239	216	2.16	1.08	54.3
2.5	54.3	1.36	240	217	5.43	2.71	54.3
5	54.3	2.72	240	217	10.86	5.43	54.3
10	54.3	5.43	240	217	21.71	10.86	54.3
15	54.3	8.15	240	217	32.57	16.28	54.3
20	54.3	10.86	240	217	43.43	21.71	54.3
25	54.3	13.58	240	217	54.28	27.14	54.3
50	54.3	27.15	240	217	108.56	54.28	54.3

^[1] Based on OMV at 0.9047 mg/mL total protein concentration (Peterson), injection volume 75 µL, yielding 54.3 µg OMV per injection

Table S11. Purity: Validation results for OMV spiked with BSA FFF-MALS

Spiked BSA + OMV (%)	1	2.5	5	10	15	20	25	50
Peak Area (mAU*min) 1	0.95	1.67	3.73	6.72	10.17	13.26	16.91	32.26
Peak Area (mAU*min) 2	0.96	1.68	3.80	7.01	10.78	13.91	17.40	33.55
Peak Area (mAU*min) 3	0.88	1.67	3.46	7.32	10.57	14.08	17.28	33.71
Average	0.93	1.67	3.66	7.0	10.51	13.8	17.2	33.2
Std. deviation	0.04	0.01	0.18	0.3	0.31	0.4	0.3	0.8
%RSD	4.4	0.4	5	4	3	3	1.5	2.4

Table S12. Data for determining LOD and LOQ of z-average hydrodynamic radius Rh(Q)z of OMV by FFF-MALS

Q OMV (μg)	0.5	1	2.5	5	10	15	20	25	50	75
Size Rh(Q)z 1	60.3	41.4	41.3	40.9	41.6	41.5	41.9	41.9	41.8	40.8
Size Rh(Q)z 2	54.1	41.7	40.6	41.4	41.6	41.6	41.8	41.5	41.9	40.6
Size Rh(Q)z 3	44.2	40.8	41.4	40.9	41.3	41.7	41.7	41.6	41.6	40.3
Average	53	41.3	41.1	41.1	41.5	41.6	41.8	41.7	41.8	40.6
Std. deviation	8	0.5	0.4	0.3	0.2	0.1	0.1	0.2	0.2	0.3
CV %	15	1.1	1.1	0.7	0.4	0.2	0.2	0.5	0.4	0.6

Table S13. Data for determining LOD and LOQ of particle concentration of OMV by FFF-MALS

Q OMV (μg)	0	1	2	5	10	15	20	25	50	75
Particle (n/mL) 1	2.7×10^8	3.7×10^9	1.4×10^{10}	5.1×10^{10}	4.3×10^{10}	6.7×10^{10}	8.1×10^{10}	1.12×10^{11}	1.83×10^{11}	2.28×10^{11}
Particle (n/mL) 2	1×10^7	3.2×10^9	1.0×10^{10}	3.4×10^{10}	4.6×10^{10}	6.8×10^{10}	8.3×10^{10}	1.03×10^{11}	1.87×10^{11}	2.39×10^{11}
Particle (n/mL) 3	6.1×10^8	2.3×10^9	1.6×10^{10}	2.8×10^{10}	4.6×10^{10}	6.9×10^{10}	9.0×10^{10}	1.12×10^{11}	1.92×10^{11}	2.45×10^{11}
Average	3×10^8	3.1×10^9	1.3×10^{10}	3.8×10^{10}	4.5×10^{10}	6.80×10^{10}	8.5×10^{10}	1.09×10^{11}	1.87×10^{11}	2.37×10^{11}
Std. Dev.	23×10^8	7×10^8	3×10^9	1.2×10^{10}	1.8×10^9	6×10^8	5×10^9	5×10^9	5×10^9	9×10^9
CV %	100	22	24	31	4	0.9	5.7	4.7	2.4	3.6

Table S14. Reproducibility: Z-average geometric radius $R_{geom,z}$ of mixed particle size standards evaluated by FFF-MALS at Wyatt Technology

	Peak 1 (nominal – 11.0 nm) $R_{geom,z}$ (nm)	Peak 2 (nominal – 25.5 nm) $R_{geom,z}$ (nm)	Peak 3 (nominal – 51.0 nm) $R_{geom,z}$ (nm)	Peak 4 (nominal – 101.5 nm) $R_{geom,z}$ (nm)
1	12.1	27.9	54.7	100.0
2	12.6	28.3	56.0	99.5
3	10.5	27.5	55.7	99.3
4	11.5	28.8	57.0	99.2
5	10.3	28.7	56.0	98.6
6	10.3	30.3	55.7	98.7
Average	11.2	28.6	55.9	99.2
Standard deviation	1.0	1.0	0.7	0.5
CV%	8.89	3.40	1.32	0.52

Table S15. Reproducibility: Equivalence TOST-test

Equivalent (TOST-test) *	
Peak 1 (11.0 nm)	Yes ($p=0.047$)
Peak 2 (25.5 nm)	Yes ($p=0.008$)
Peak 3 (51.0 nm)	Yes ($p=0.018$)
Peak 4 (101.5 nm)	Yes ($p<0.0001$)

* Threshold: 10.5%

Table S16. Recovery calculations for BSA and OMV

	BSA AS (mAU/min)	BSA AD (mAU/min)	OMV AS (mAU/min)	OMV AD (mAU/min)
Measurement 1	48.8	52.2	73.7	48.8
Measurement 2	46.1	52.4	71.4	46.1
Measurement 3	49.4	51.1	71.5	49.4
Average	48.1	51.9	72.2	48.1
Recovery (%)	92.6		90.8	

AS is the peak area of the eluted sample, AD is the peak area of sample directly injected into the detector. Analyte recovery (%): $AS/AD \times 100$.

II. Supporting information Figures

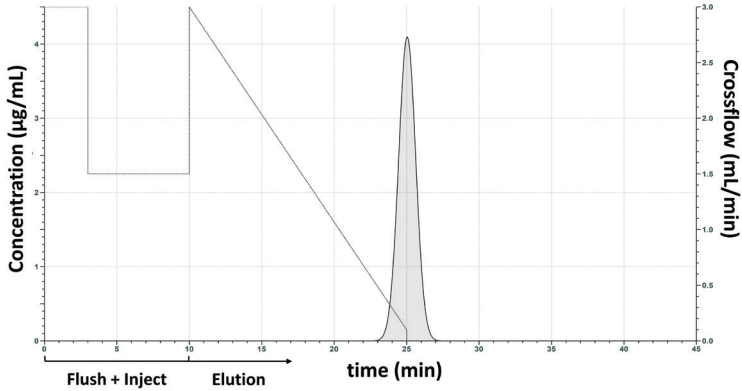


Figure S1. Fractogram predicted by SCOUT FFF method development software, for Method A, assuming a wide format, 350 μm spacer and 1 mL/min detector flow. The elution method consisted of the following steps: Elution (0 - 3 min, 3 mL/min cross flow), Focus (3 - 4 min), Focus + inject (4 - 9 min), Focus (9 - 10 min), Elution (10 - 25 min, 3 - 0.1 mL/min crossflow gradient), Elution (25 - 40 min, 0.0 mL/min cross flow), Elution + Inject (40 - 45 min, 0.0 mL/min cross flow).

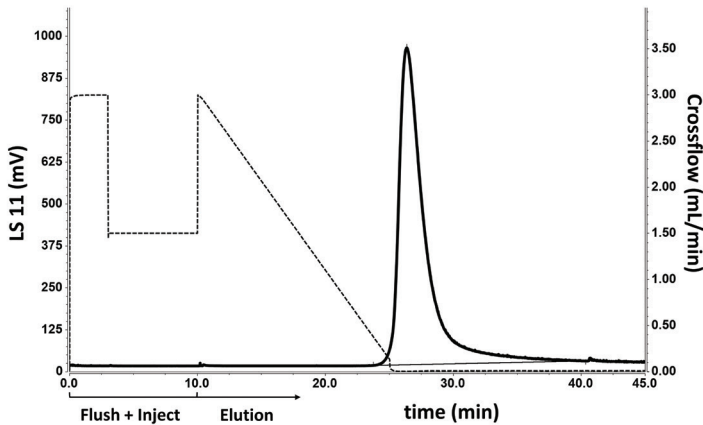


Figure S2. UV fractogram from Chromleon for OMV eluting with Method A: x-axis: time (min), y-axis left: LS 11 signal (mV), Y-axis right: Cross flow (mL/min).

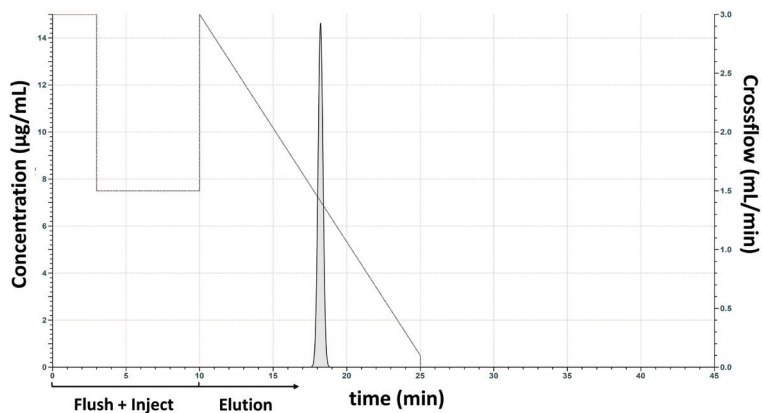


Figure S3. Fractogram predicted by SCOUT FFF method development software, for Method B, assuming a wide format, 250 µm spacer and 1 mL/min detector flow. The elution method consisted of the following steps: Elution (0 - 3 min, 3 mL/min cross flow), Focus (3 - 4 min), Focus + inject (4 - 9 min), Focus (9 - 10 min), Elution (10 - 25 min, 3 - 0.1 mL/min crossflow gradient), Elution (25 - 40 min, 0.0 mL/min cross flow), Elution + Inject (40 - 45 min, 0.0 mL/min cross flow).

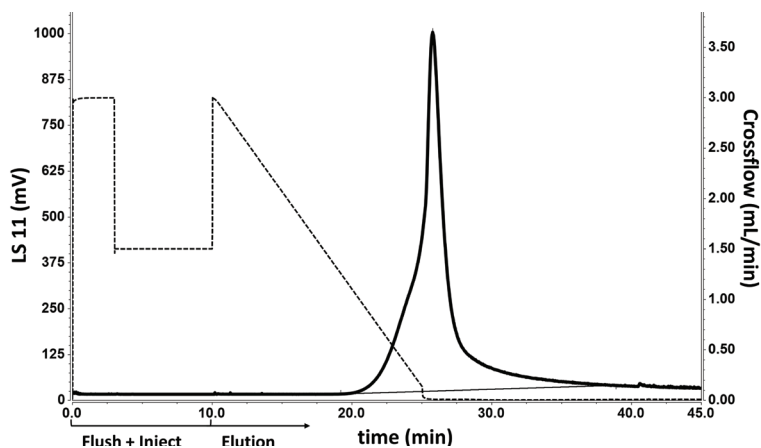


Figure S4. UV fractogram from Chromleon for OMV eluting with method B: x-axis: time (min), y-axis left: LS 11 signal (mV), Y-axis right: Crossflow (mL/min).

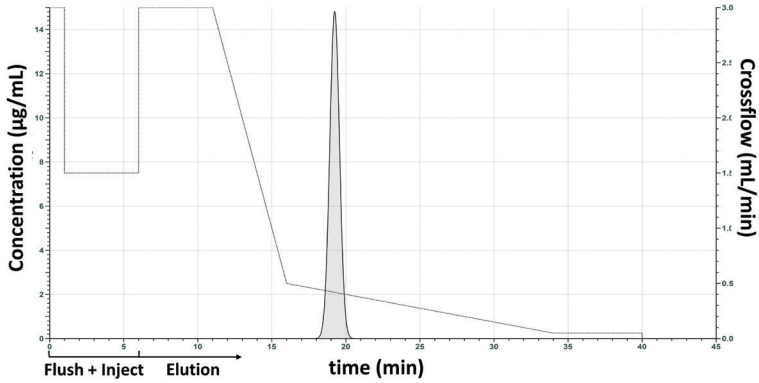


Figure S5. Fractogram predicted by SCOUT FFF method development software, for Method C, assuming a wide format, 250 μm spacer and 1 mL/min detector flow. The elution method consisted of the following steps: Elution (0 - 1 min, 3 mL/min cross flow), Focus (1 - 2 min), Focus + inject (2 - 4 min), Focus (4 - 6 min), Elution (6 - 11 min, 3 mL/min cross flow), Elution (11 - 16 min, 3 - 0.5 mL/min cross-flow gradient), Elution (16 - 34 min, 0.5 - 0.05 mL/min cross-flow gradient), Elution (34 - 40 min, 0.05 mL/min cross flow), Elution + Inject (40 - 45 min, 0.0 mL/min cross flow).

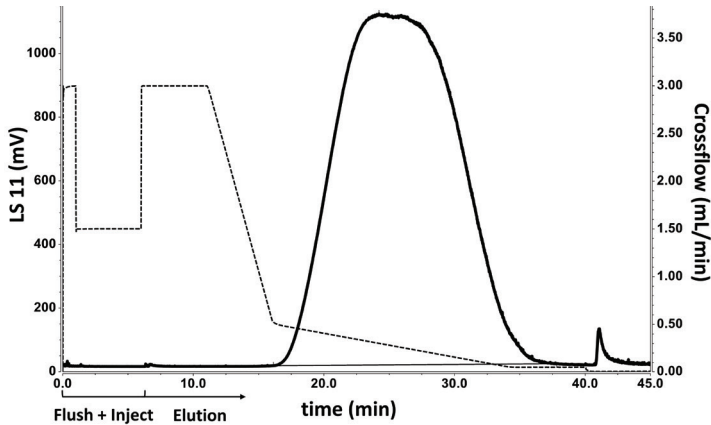


Figure S6. UV fractogram from Chromeleon for OMV eluting with Method C OMV-BSA: x-axis: time (min), y-axis left: LS 11 signal (mV), Y-axis right: Crossflow (mL/min).

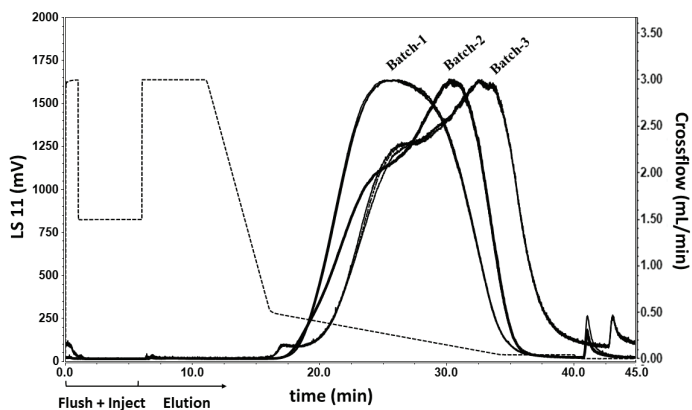


Figure S7. Overlay of light scattering fractograms for repeats of different OMV Batches 1-3; X-axis time (min); Y-axis signal from the 90° light scattering detector.

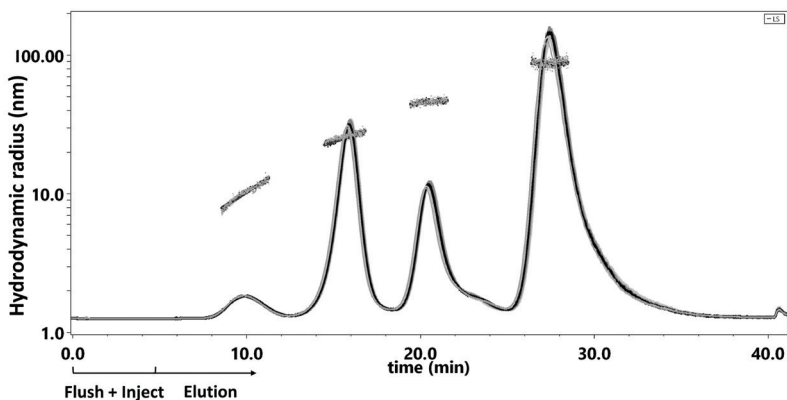


Figure S8. Elution of particle size standards elution using method D particle standards (n=6). Thermo Fisher polystyrene particle size standard mixture, 22 nm, 51 nm, 100 nm, and 203 nm (diluted 1X, 5X, 40X, 100X respectively prior to mixing); X-axis Time (min), Y-axis Hydrodynamic radius (nm).

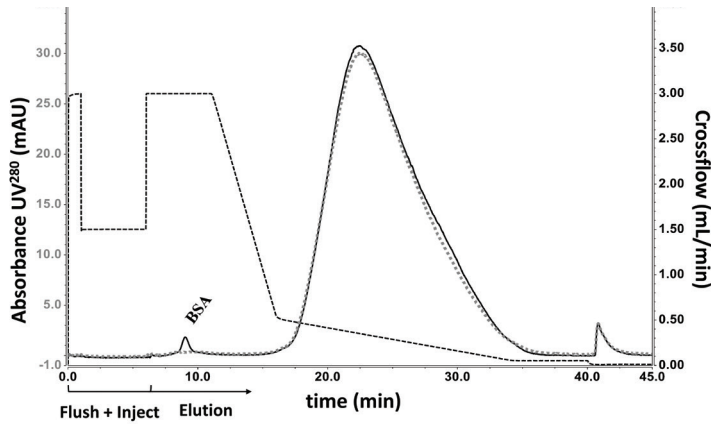


Figure S9: Lowest BSA injection (1% or 054 μg); X-axis time (min); Y-axis left Absorbance UV280, Y-axis right Crossflow (mL/min).

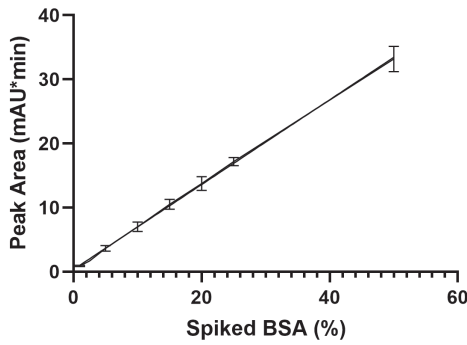


Figure S10: Triplicate overlay of correlation Spiked BSA (%) to response (Area). X-axis BSA Spiked (%); Y-axis Peak Area (mAU*min). Mean with 95% CI, R2: 0.999.

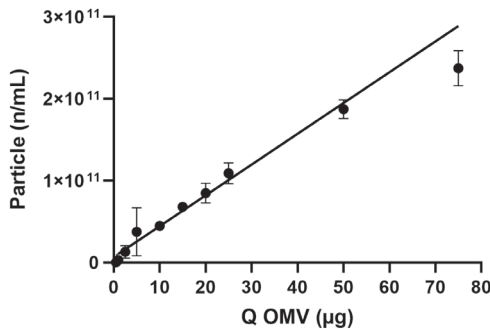


Figure S11: Triplicate overlay of correlation particle count OMV. X-axis QOMV (μg); Y-axis Particle count (n). Mean with 95% CI, R2: 0.980. The last point in the graph was considered an outlier and as such excluded from the calculations.

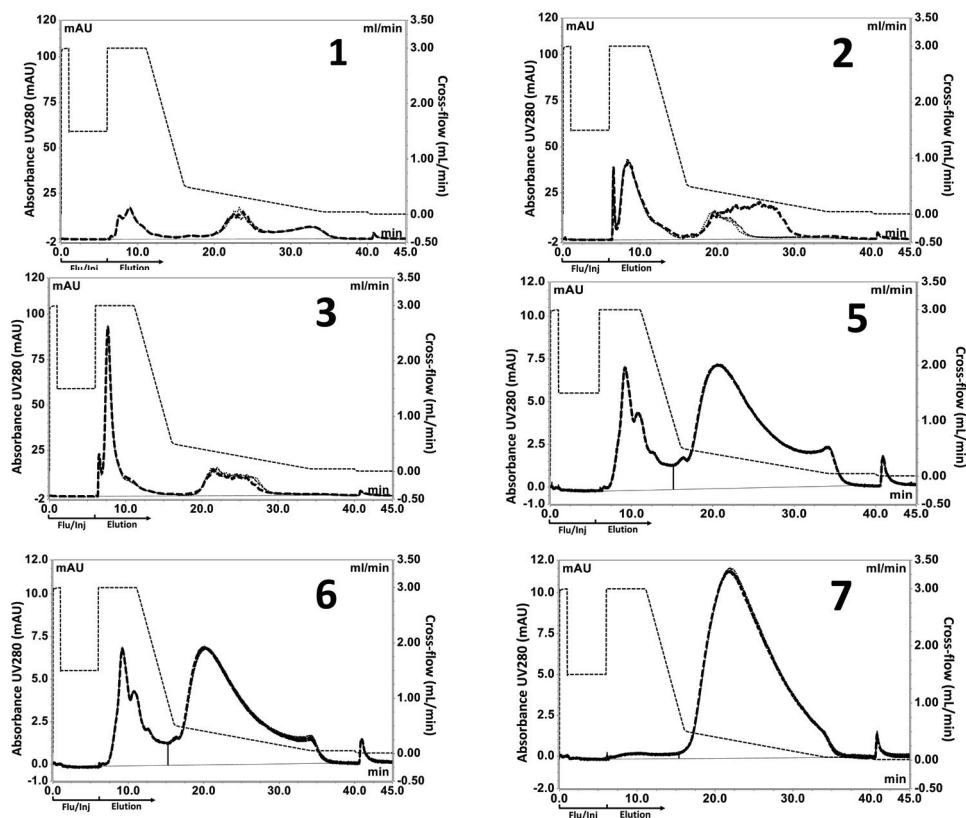


Figure S12: FFF-MALS results ($n=3$) for fraction 1, 2, 3, 5, 6 and 7 from the downstream purification process as described in Table 1. X-axis: time (min). Crossflow is shown as the black dotted line, of which the first 6 minutes represent the steps to flush the channel and inject the sample (Flu/Inj). Typically smaller, protein like impurities, elute in the range between 6 and 12 minutes.

III. Supporting information Methods

Method S1 FFF-MALS configurations

FFF system 1 consisted of an Eclipse AF4 FFF controller (Wyatt Technology) and an Ultimate 3000 HPLC pump equipped with a UHPLC⁺ temperature-controlled autosampler (Thermo Fisher Scientific). FFF separation was performed at 20 °C in a thermostatic column oven (Shimadzu CTO-20AC) using the SC short FFF channel (Wyatt Technology). For online characterization we employed a DAWN HELEOS II 18-angle light scattering detector (Wyatt Technology) equipped with an embedded Wyatt QELS DLS module replacing the photodiode at MALS angle 17, an Optilab T-REX RI detector (Wyatt Technology) for determination of concentration, and a VWD-3400 variable-wavelength UV absorption detector (Thermo Fisher Scientific) set at 280 nm. The system was controlled by

Chromeleon software (Thermo Fisher Scientific) with Eclipse (Wyatt FFF module) plug-in and data were analyzed in ASTRA software 7.1.0 (Wyatt Technology).

FFF system 2, operated at Wyatt Technology, Dernbach, Germany, comprised an Eclipse NEON FFF controller (Wyatt Technology) with DCM dilution control module to increase eluting sample concentration, a 1260 Infinity II quaternary pump and a 1260 Infinity II temperature-controlled vial sampler (both from Agilent Technologies). Separation took place in a stainless-steel SC short FFF channel (Wyatt Technology). Online characterization employed a DAWN NEON 18-angle light scattering detector and an Optilab NEON RI detector (both from Wyatt Technology), and an Infinity II multi-wavelength UV detector (Agilent Technologies). The system was controlled by VISION software 3.1.0.33 and data were analyzed in ASTRA software 8.0.2.5 (both from Wyatt Technology).

The readiness or cleanliness to operate for both systems was visually confirmed on the LS-11 signal on the MALS-detector showing a minimum of 5 decimals. When 5 decimals were not obtained the system was extensively purged using a 0.5 % sodium dodecyl sulfate solution applying the night rinse option for at least 48 hours.

Method S2 BSA and particle standards

Pierce bovine serum albumin (BSA), delivered in standard ampoules at 2 mg/mL, was obtained from Thermo Fisher Scientific. Nanosphere particle size standards (Thermo Fisher Scientific) included the following sizes: 20 nm (mean diameter 23 nm \pm 2 nm, or radius 11.5 \pm 1 nm), 3020A; 50 nm (mean diameter 51 nm \pm 3 nm, or radius 25.5 \pm 1.5 nm), 3050A; 100 nm (mean diameter 100 nm \pm 4 nm, or radius 50 nm \pm 4 nm), 3100A; 200 nm (mean diameter 203 nm \pm 5 nm, or radius 101.5 nm \pm 2.5 nm), 3200A. Both the BSA and particle standards are envisioned as the system suitability test (SST) within the method after validation.

Method S3 Nanoparticle tracking analysis

A NanoSight NS500 (Malvern Instruments) equipped with an sCMOS camera module and a 488 nm laser module was used for all NTA measurements to determine particle size distributions and particle counts. With a sample loaded in the chamber, static measurements were obtained by capturing 10 measurements of 30 seconds each. In flow mode, data were acquired with a flow rate of \sim 2.6 μ L/min, yielding a y-drift of 4.0 pixels per frame. Like the static measurements, the flow measurements consisted of 10 measurements of 60 seconds each, with an additional 5-second delay between measurements. Temperature control was set to 25 $^{\circ}$ C. Data from both static and flow

measurements were analyzed using NTA 3.2 software build 3.2.16. The capture settings of the NTA software were: Camera shutter 1300; Camera gain 512; Camera level 16; Camera hi-limit 3294; Camera lo-limit 0; Stage -57; Focus -16546. The analysis settings were: Detector threshold variable; Auto blur and Auto min track length both 'on'. The machine was calibrated by the NanoSight NTA concentration measurement upgrade. All results are reported as the mean radius (nm), which is the number-average hydrodynamic radius.

Method S4 Batch dynamic light scattering

Off-line DLS measurements were performed using a Zetasizer Nano ZS (Malvern Instruments) to determine particle size. Measurements were made in disposable polystyrene semi-micro cuvettes (Greiner Bio-one, 613101) and analyzed with the Zetasizer software version 7.11. A standard operating procedure (SOP) was defined for the measurements wherein the sample was set as 'protein' (refractive index of 1.450, absorption of 0.001) and the dispersant set as 'water' (viscosity of 0.8872 cP, refractive index of 1.330). Each sample was measured three times using the measurement angle of 173° (backscatter), automatic measurement duration and "seek for optimal position" as positioning setting. Data processing was performed with the general purpose (normal resolution) analysis model. All results are reported as the harmonic 'z-average' radius R_h in units of nanometers.

Safety statement

No unexpected or unusually high safety hazards were encountered during any of the methods, processes, or assays.



Chapter 7

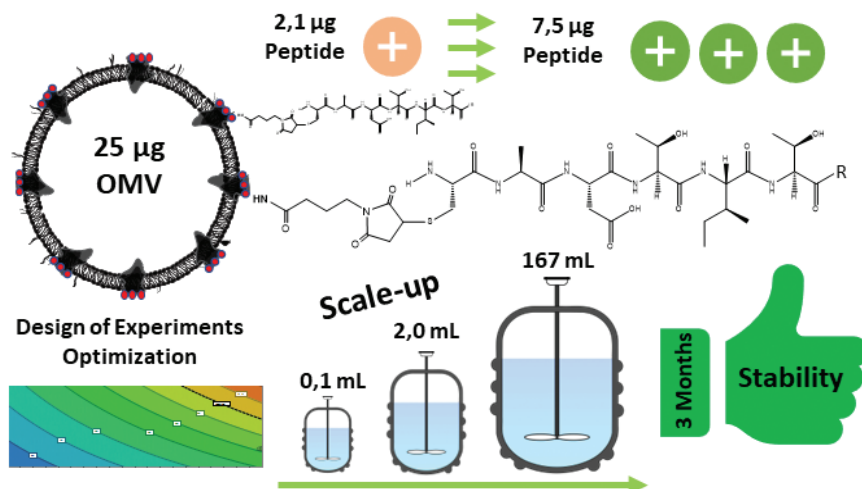
A modular vaccine platform for prophylactic and therapeutic vaccines: exogeneous decoration of bacterial outer membrane vesicles with synthetic peptide antigens

Robert M. F. van der Put,^{*,a} Thomas J.M. Michiels,^a Zaskia Eksteen,^a Arnoud Spies,^a Hugo D. Meiring,^a Ronald Maas,^a Roland Pieters,^b Bernard Metz,^a and Corine Kruiswijk^a

^a Intravacc, P.O. Box 450, 3720 AL Bilthoven, the Netherlands. ^b Department of Chemical Biology & Drug Discovery, Utrecht Institute for Pharmaceutical Sciences, Utrecht University, P.O. Box 80082, NL-3508 TB Utrecht, The Netherlands

Bioconjugate chemistry. To be submitted

Graphical abstract



Abstract

Pandemics cause significant social instability and millions of deaths. It is necessary to be prepared for such events in the future. Accelerating vaccine development is one means of addressing pandemic preparedness. Vaccines have a valuable role in the protection against infectious diseases. Accelerated vaccine development based on well-established platforms is an approach that could be useful. For example, conjugate vaccines can be tailored towards highly specific antigens and can be developed quickly. In this study, we determined the feasibility of using outer membrane vesicles (OMVs) as carriers of a conjugated vaccine antigen and we developed an upscaled GMP production process. A SARS-CoV-2 peptide that was designed and synthetically produced was used as the antigen. This report provides information on the characterization of OMVs before and after antigen conjugation and on approaches that improve the conjugation to the OMVs. While initially 2.1 µg of peptides was conjugated to OMVs, after a design of experiments (DoE) 7.5 µg of peptides was conjugated to 25 µg OMV. Furthermore, the process was successfully upscaled 2000-fold using a GMP-qualified reactor. Finally, the OMV-conjugated peptide product was evaluated in a stability study. This production platform is likely to be a valuable tool for rapid development of new vaccines.

Keywords

Conjugate Vaccine, Outer Membrane Vesicles, Peptide antigen, Platform Technology, Scale-up, Thiol-maleimide Chemistry

Introduction

The Antonine Plague (165 to 180 AD) is one of the first known pandemics which had a major impact on society [1], affecting numerous individuals worldwide. Throughout human history, many pandemics occurred *e.g.*, Black Death (1346–1353), Smallpox (1520), Spanish flu (1918-1919), HIV/AIDS (1981 - present) [1, 2] and most recently SARS-CoV-2 [3]. New pandemics will emerge in the future for which society must be prepared. Therefore, the capacity to rapidly develop vaccines is required [4]. A platform-based approach would enable fast-track development of such vaccines. In the last decades, conjugate vaccines have displayed their potential towards providing such a platform. Most conjugate vaccines rely on traditional protein carriers like tetanus toxoid [5], diphtheria toxoid [6] and CRM197 [7]. As highlighted before, due to observed carrier-induced epitope suppression (CIES) related to these carriers, new conjugate vaccine carriers are highly desirable [8, 9]. Outer membrane vesicles (OMVs), spherical lipid bi-layer membranes extracted from bacteria, could be an excellent carrier. OMVs have a proven track-record and safety profile and have demonstrated efficacy in clinical studies against meningococcal disease [10, 11]. Furthermore, they can be obtained in high yield using a reliable and scalable production process [12, 13]. Other advantages are that OMVs can be equipped with heterologous antigens [14, 15] aiding in multivalency and that OMVs have self-adjuvanting properties governed by the presence of pathogen-associated molecular patterns (PAMPS) such as lipooligosaccharide (LOS) and lipoproteins [16-18]. The size of OMVs (50-200 nm) has a significant positive impact on the immune response by improving uptake by antigen presenting cells and providing a large surface area bearing a variety of properties like hydrophobicity, charge, and the potential for B-cell-receptor interaction [19]. These aspects make OMVs excellent carriers for the conjugation of less immunogenic antigens like peptides or polysaccharides. Contrary to protein and carbohydrate-based antigens, synthetic peptides targeting emerging diseases can be more rapidly designed, tailored towards specific pathogens, and produced in large quantities. Here we introduce a synthetically produced linear SARS-CoV-2 peptide consisting of 47 amino acids (Mw 5448 Da). The peptide contains three T cell epitope clusters that were previously identified [20, 21]. The peptide includes a thiol bearing cysteine at the C-terminus, which enables covalent binding to maleimide-activated OMVs via a Michael addition reaction (Figure 1).

The aim of this study is to develop an upscaled production process for conjugation of peptides to OMVs. The strategy of the conjugation process is summarized in Figure 1. OMVs derived from *Neisseria meningitidis* type B were used as a carrier for the conjugation of the peptide. *N*- γ -(maleimidobutyl)oxysuccinimide ester (GMBS) was used as a linker targeting primary amines of the OMV and the thiol group at the C-terminus of the peptide. GMBS is a well-known and safe linker that has been used in prior applications

of human vaccines [22-24]. The conjugation efficiency was optimized by using design of experiments (DoE). Subsequently, the production process was scaled up towards a high yielding GMP-ready production process. Finally, we characterized the composition and the stability of the final product. In this paper, we thus describe the successful development of a production process for the conjugation of peptides to OMVs. This platform can be exploited for rapid development of new vaccines in the prophylactic and therapeutic domain.

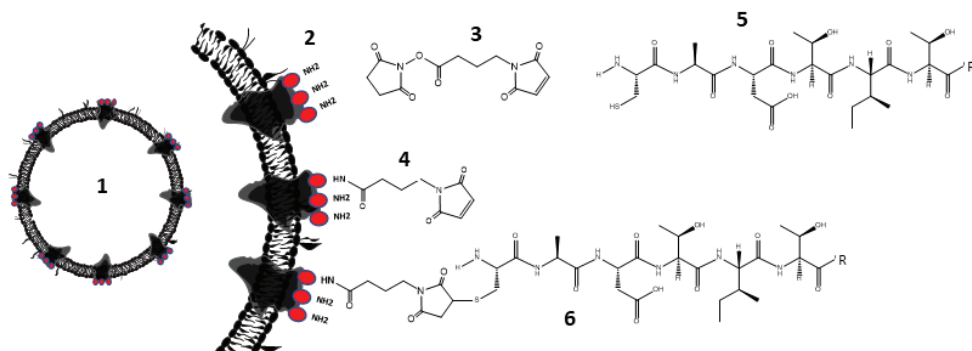


Figure 1: Conjugation strategy for an OMV-Peptide conjugate vaccine. Two step reaction; **Modification Step 1**) OMVs (**1**) containing primary amines (**2**) are reacted with NHS-bearing GMBS (**3**) forming OMVMAL (**4**); **Conjugation Step 2**) Thiol-Maleimide coupling to the thiol (SH-) on the C-terminus of the peptide (**5**) yielding the final conjugate (**6**). Note: Peptide shows only the last 6 of a total of 47 amino acids of the complete peptide structure.

Results

Characterization of OMVs including GMBS reaction

The first step of the conjugation process is the coupling of the NHS ester of the GMBS linker to the primary amines of the OMVs. The location distribution of the primary amines on the OMVs was determined by LC-MS analysis, based on the detection of GMBS adducts. The major locations of primary amines in OMVs were conserved in the porB protein (42%) and phosphatidylethanolamine (PE: 42%), whereas the LOS and other proteins were functionalized to a lesser extent and contributed only 14 and 2% respectively (Figure S1). For phosphatidylserine (PS) no GMBS modified primary amines were detected. Ideally, GMBS only functionalizes proteins in OMVs and no phospholipids, as modified phospholipids can potentially destabilize OMVs and interfere with its adjuvanting properties. Therefore, reaction conditions were investigated aiming to selectively modify proteins. By keeping the number of GMBS molar equivalents below 16 relative to ~1 nmol of peptide, it was possible to prevent the unwanted lipid modification, as indicated by LC-MS (Table 1).

Table 1: Degree of conversion of OMV-PE at different GMBS to peptide ratios.

Equiv. GMBS ^[a]	PE C32:1 (counts)	PE C32:1 maleimide (counts)	Conversion (%)
256	4.1×10^6	2.5×10^5	6.1
64	3.6×10^6	2.8×10^4	0.8
16	3.5×10^6	< LOD ^[b]	0
4	4.7×10^6	< LOD	0
1	5.5×10^6	< LOD	0
0	6.6×10^6	< LOD	0

^[a] Molar equivalents to 5 μ g peptide (~ 1 nmol) per 25 μ g OMV protein. ^[b] limit of detection (LOD).

LC-MS analysis showed that with a GMBS to peptide ratio of 16 (mol:mol), 2.1 μ g peptide could be conjugated to 25 μ g OMV which represents a 42% efficiency. SDS-PAGE analyses of this conjugate (Figure 2) showed that up to three peptides were attached to the most abundant protein in the OMVs, PorB (~ 35 kDa), indicating that every PorB protein contains at least three lysine residues susceptible to conjugation. Furthermore, DLS distribution plots demonstrated that the average size and particle heterogeneity slightly increased, and no aggregates were formed (Figure S2). This finding indicates that under these conditions both the GMBS-modification and conjugation of the peptide to OMVs did not result in immediate particle instability, or crosslinking due to the bifunctional GMBS linker.

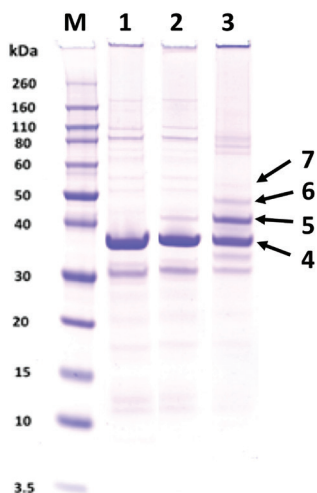


Figure 2. SDS-PAGE of (1) OMVs, (2) OMVs mixed with peptide (the purification process has removed any remaining free peptide) and (3) OMV-peptide conjugate. In the final conjugate we observed the PorB protein (4) and the PorB protein with three peptides conjugated (5 peptide 1, 6 peptide 2 & 7 peptide 3).

Design of Experiments rationale

A design of experiments (DoE) was initiated to define the process parameters at which the quantity of conjugated peptide could be maximized without inducing colloidal instability. Four process parameters (factors) were chosen that could potentially affect the conjugation reaction: GMBS to peptide ratio, OMV protein concentration, peptide to OMV ratio, and reaction time (Table 2). For the DoE, a screening interactions design in combination with a full factorial model at 2 levels without any constraints was applied. This led to 19 individual batch experiments including 3 center points (Table S1).

Table 2: Investigated factors and ranges for the DoE.

	Low	Center point	High
Ratio GMBS to peptide (mol:mol)	8	16	24
OMV protein concentration ($\mu\text{g}/\text{mL}$)	150	250	350
Peptide to OMV ratio (w/w) ^[a]	5	10	15
Time (hrs.)	1	3	5

^[a] quantity of peptide reacted for every 25 μg of OMV

Design of Experiments results

LC-MS analysis showed that between 2 (experiments 1 and 9) and 12 (experiment 8 and 18) μg of peptide was conjugated when applying different process parameters (Figure 3 and Table S2). Colloidal stability was inferred from the shift in particle size distribution (PSD) measured by FFF-MALS analysis. While most conjugates showed a shift in PSD $\leq 10\%$, batches produced with a 24-molar excess of GMBS and the highest peptide to OMV ratio (N6, 8, 14 and 16) showed a shift in PSD of up to 25% (Figure 3 and Table S2). The center points (N17 – N19) showed low variance for both conjugated peptide and shift in PSD. The DoE was statistically evaluated using this dataset.

The evaluation of the histograms (R2) did not show any need for transformation and Variability (Q2) of the replicates was low (Table 3). This was followed by evaluation of the coefficients plot where all the non-significant coefficients or factors were excluded (Figure S4). Interactions were observed, where the combination of 2 factors together influenced the outcome of the conjugation reaction. Three such combinations were identified; for conjugated peptide (GMBS to peptide ratio x OMV concentration, GMBS to peptide ratio x peptide to OMV ratio, and OMV concentration x peptide to OMV ratio, Figure S4) and two combinations for shift in PSD (GMBS to peptide ratio x peptide to OMV ratio, and OMV concentration x peptide to OMV ratio, Figure S4). All statistical values were well above the minimum requirements to have an acceptable model (Table 3, [25]). The degrees of freedom were well above five, which was indicative of a strong model.

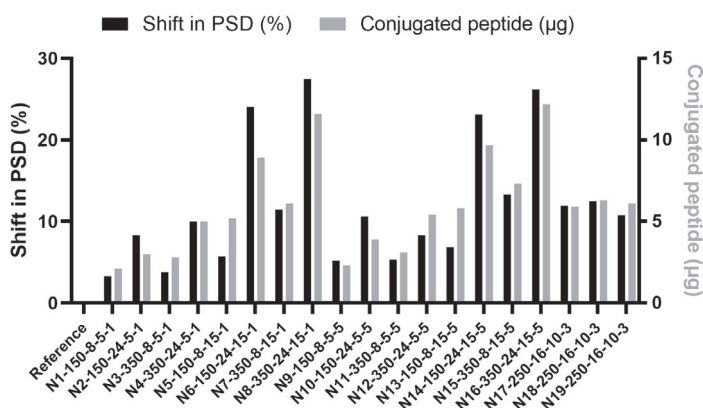


Figure 3: DoE results for 19 individual batches produced with different process parameters. Shift in PSD (black, FFF-MALS), Conjugated peptide to 25 µg of OMV (grey, LC-MS). Sample code consist of N(X) – OMV concentration (µg/mL) – GMBS to peptide ratio (mol:mol) – peptide to OMV ratio (w/w) – incubation time (hrs.).

Table 3: Summary of fit.

	Minimum requirement	Peptide conjugated	Shift in particle size distribution
Regression analysis R2 ^[a]	> 0.50	0.996	0.984
Goodness of prediction Q2 ^[b]	> 0.50	0.988	0.963
R2-Q2 ^[c]	< 0.20 – 0.30	0.008	0.021
Model validity ^[d]	> 0.25	0.811	0.770
Regression analysis reproducibility ^[e]	> 0.50	0.995	0.987
Degrees of freedom	5	11	13

^[a] goodness of fit is a measure of how well the regression model can be made to fit the raw data; ^[b] goodness of prediction, estimates the predictive power of the model; ^[c] for a model to pass this diagnostic test, both R2 and Q2 should be high, and preferably not separated by more than 0.2 – 0.3. A larger difference constitutes a warning of an inappropriate model; ^[d] With a model validity of 0.25 or lower, the p-value for the lack of fit test will exceed 0.05; ^[e] constitutes the pure error and control of the experimental procedure

Further statistical analysis shows that for the residuals plots there are no outliers outside of the 4SD area within the response versus the normal probability of the distribution for both the conjugated peptide and shift in PSD (Figure S5). The observed versus predicted plot shows that both models have a good correlation (Figure S6). With both models for conjugated peptide and the shift in PSD in place, two response contour plots were created (Figure 4). Both the highest quantity of conjugated peptide and the highest shift in particle size are in the top right area of the contour plots. This indicates that a trade-off had to be made between the highest amount of peptide conjugated, preventing a substantial shift in PSD.

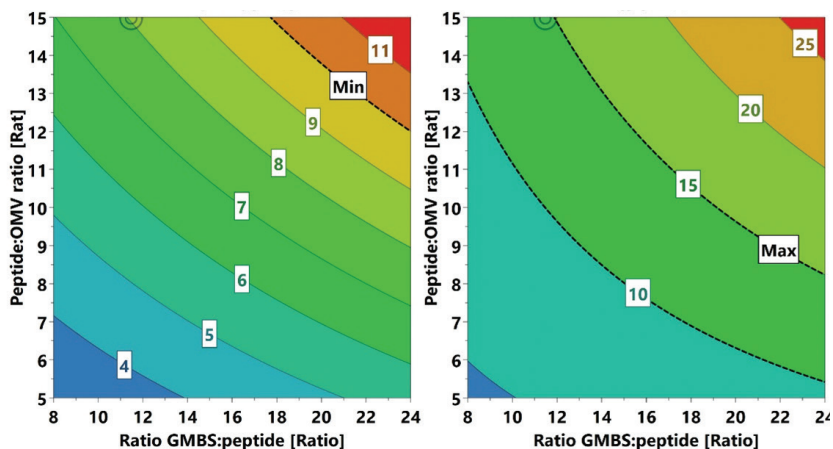


Figure 4: The quantity of conjugated peptide (left) and shift in PSD (right). Both graphs showing GMBS to peptide ratio (X-axis) vs the peptide to OMV ratio (Y-axis) at 350 $\mu\text{g}/\text{mL}$ protein OMV and 5 hours conjugation time.

Confirmation of optimized conditions

With the observed constraints a prediction was generated for conjugates resulting in the highest quantity peptide conjugated and the smallest shift in PSD. With settings to conjugate more than 10 μg peptide with a maximum of 15% shift in PSD, based on the DoE data, optimized reaction conditions were defined (Table S3). Two experiments were performed to confirm the process parameters, of which experiment B had a higher peptide to OMV ratio as an attempt to conjugate more peptide (Table 4). Both experiments yielded products in the range of the set specifications. Experiment A and B yielded an average of 7.5 and 8.4 μg of conjugated peptide with an efficiency of 50.3 and 41.8% respectively (Table 4). However, the increase from peptide to OMV ratio of 15 to 20 (33% increase), only yielded an increase in conjugated peptide of 12%, which was deemed inefficient. When evaluating the FFF-MALS results, it became apparent that for both experiments the shift in particle size distribution was well below the predicted 15% with 10.6% for experiment A and 12.1% for experiment B (Table 4). Based on the DoE we optimized the quantity of peptide conjugated without inducing significant changes to the OMVs colloidal stability. After optimization, 7.5 μg of peptide was conjugated to 25 μg of OMVs (protein).

Table 4: Model confirmation reactions

Peptide:OMV ratio for every 25 μg OMV	Peptide for every 25 μg OMV	Efficiency (%) ^[c]	Shift in particle size distribution (%)
Prediction ^[a]	8.1	54.0	14.9
Experiment 1: 15 ^[b] (n=3)	7.5 \pm 0.2	50.3 \pm 1.0	10.6 \pm 1.0
Experiment 2: 20 ^[b] (n=3)	8.4 \pm 0.1	41.8 \pm 0.7	12.1 \pm 0.2

^[a] predicted outcome (Table S3) ^[b] protein OMV concentration 350 $\mu\text{g}/\text{mL}$, 5 hours conjugation time, GMBS:peptide ratio 11.5. ^[c] efficiency is calculated by comparing the quantity of peptide conjugated to the initial quantity of peptide added in the reaction.

Scale-up study

The optimized conditions (Table 4, experiment A) were used to scale up the production in a GMP ready reactor (Cogent μ , Merck Millipore). All tangential flow filtration (TFF) steps were within operating specifications, where none of the maximum pressure limits (1 bar) were exceeded at any point during processing. Additionally, the conversion (Filtrate flow rate / Feed flow rate) never exceeded 30% warranting TFF and not normal flow filtration (Table S4). During the first TFF process step TRIS (interfering with the NHS-based chemistry) and sucrose were removed completely after 6 buffer exchange volumes (BEV). DMSO was used twice in the process, both for the dissolution of GMBS and the peptide prior to their respective reactions. The type of filters used during this experiment were known to retain DMSO which was confirmed by the fact that after 10 BEV, DMSO was not completely removed (Table S4). However, the DMSO concentration was within safety levels (6400 mmol/L, ICH-Q3D) when only 0.2 mmol/L DMSO was demonstrated in the final product. During final exchange to formulation buffer, both TRIS and sucrose were at their required levels, 10 and 233 mM respectively, after 5 BEV. Performing the conjugation strategy at this scale, we were able to successfully produce an OMV-peptide vaccine bearing 8.3 μg of peptide with only 13.0 % shift in PSD.

Stability study

A stability study was conducted with the conjugated OMV (drug substance, DS). Before storing the DS at 2-8°C, we created 4 batches at different concentrations: 0.6, 1.0, 2.0 and 3.0 mg/mL protein. With respect to a shift in PSD, there were some minor differences between the different DS concentrations beforehand, while no real significant increase in PSD was detected for the duration of the study (Figure 5). SDS-PAGE analysis did not show any dissociation of peptide, which would be visible by a reduction of the ladder intensity (Figure 6). LC-MS analysis performed on samples that were stored for 3 months

showed that the DS at 0.6, 2.0 and 3.0-mg/mL still contained 7.8, 7.3 and 7.8 μg peptide conjugated, respectively, which was between 88% and 95% recovery compared to the original sample (8.3 μg peptide). For the 1.00-mg/mL sample we found 5.3 μg peptide or 65% recovery.

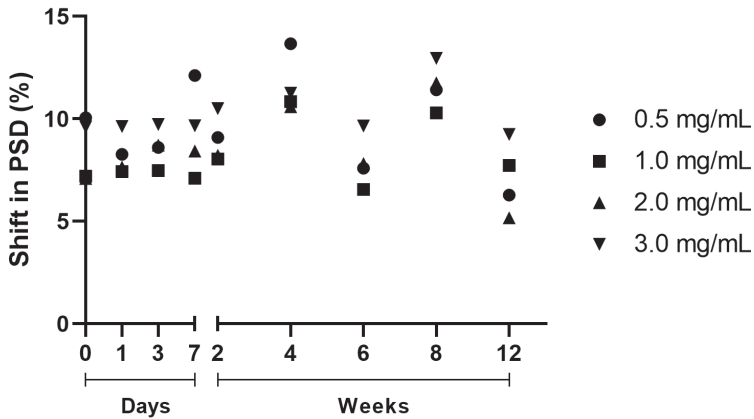


Figure 5: Stability of the DS stored at 2-8 C for 3 months expressed in Shift in PSD (%).

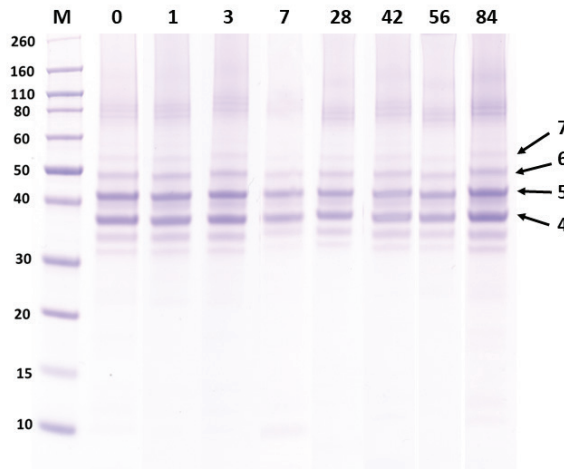


Figure 6: Stability of the conjugate protein fingerprint evaluated by SDS-PAGE. Example of 2-8°C, 0.556 mg/mL, up to 84 days (other protein concentrations showed similar results, data not shown). In the final conjugate we observed the PorB protein (**4**) and the PorB protein with three peptides conjugated (**5** peptide 1, **6** peptide 2 & **7** peptide 3).

Discussion

In this study, we have developed a production process for a broadly applicable OMV-synthetic peptide conjugate vaccine. Initial characterization for the controlled site-specific conjugation reaction, grafting GMBS onto OMVs, included the evaluation of primary amine distribution over the different membrane components by LC-MS analysis.

Here it was concluded that the porB protein and PE were the two major contributors to the total primary amine content. While looking for maximum conjugation of peptides to the carrier OMV, we wanted to prevent potential colloidal instability by grafting GMBS onto PE. For this we were able to identify conditions for GMBS to react predominantly with the primary amine groups of proteins, especially with the most abundant PorB protein.

In an effort to further optimize the quantity of conjugated peptide, a DoE (a full factorial design) in a down scaled conjugation process was used to screen all important factors which influence the conjugation reaction. The study revealed that the quantity of conjugated peptide could be increased to as much as 12 μg , however not without affecting the colloidal stability. Additionally, no solubility issues were observed for both the peptide during the conjugation reaction itself and for the final OMV-peptide conjugate. Applying process conditions as defined using the optimized conditions, supported by the DoE model, it was possible to produce a conjugate with 7.5 μg conjugated peptide with only 10.6% shift in PSD.

From the optimized setting in the down-scaled model, we opted for an approximate 2000-fold scale-up from the first experiments at 100 μL scale. First confirming that all process related impurities were removed, we produced 8.3 μg conjugated peptide for every 25- μg protein OMV (33% w/w), which exceeded the 7.5 μg obtained from the small-scale experiment.

The stability of the conjugate, or unintentional release of the peptide, is highly dependent on potential transfer of any exogeneous thiol nucleophile towards the maleimide moiety [26]. This is especially true directly after conjugation, where the maleimide is not yet fully hydrolyzed. In an exploratory stability study, we did not find any unexpected major increase in free-peptide, confirming that the product was stable for at least 3 months at 2-8°C. With successful OMV-based clinical studies, employing a dose between 50 – 100 μg protein OMV [27], in this case extrapolated to an approximate peptide dose between 15 and 30 μg based on 8.3 μg conjugated peptide for every 25- μg protein OMV. With this

scalable production platform, able to easily facilitate increased process volumes of up to 100 liters, one could produce between 650.000 – 1.3000.000 doses in a single one-day production cycle considering a ready to use of the shelf OMV.

With this study we have shown that production of an OMV-peptide conjugate vaccine is feasible. It will be of interest to tailor synthetic-peptides towards specific diseases and therapeutic targets. The peptide design can include a range of different epitopes like B-cell epitopes that have the capacity to elicit protective antibodies and also T-cell epitopes that can induce protective immunity in the context of infectious diseases but can also be directed towards immuno-oncology targets [28-31]. However, limitations in synthetic peptide chemistry restrict these to a maximum of approximately 50 amino acids. Peptide lengths for MHC-restricted T cells ranging between 8–9 amino acids for class I and 12–15 amino acids for class II [32], and therefore a single long peptide of 50 amino acids can only contain 3-5 epitopes. This platform technology can be possibly expanded towards the conjugation of other antigens, which could include not only multi-epitope synthetic peptides (50 amino acids), but also protein domains or small proteins (200-300 amino acids), or oligosaccharides. A key consideration would be solubility and compatibility with, in this case, the NHS-maleimide chemistry and that the peptide or protein itself does not interfere with the colloidal stability of the OMV.

While making significant advances in the ability and optimization of conjugating peptides to OMVs, these final conjugates will need further assessment based on their immunological performance. While higher peptide:OMV ratios are desirable from a process efficiency perspective, there could be unwanted immunological consequences. During prior research it was shown that there is a maximum of antigen loading with respect to the highest antibody titer to be obtained [33]. While, in this case it was specifically observed for a tetanus toxoid-oligosaccharide conjugate, it will be of high interest to investigate if there is also such optimum for OMV-peptide conjugates.

Within this study OMVs have shown to be highly amenable and we made significant advancement in the platform-based concept of an OMV-peptide conjugate vaccine. OMVs can be easily produced and have an outstanding stability record enabling stockpiling. Their self-adjuvanting properties make them excellent candidates as a carrier for peptide-based conjugate vaccines. While this study employed a SARS-CoV-2 peptide, other peptides can be easily designed towards new and existing diseases and can be produced swiftly and at high purity. These characteristics make them the prime candidates for new potential vaccines and emergency use.

Experimental procedures

OMVs

The PorA deficient *N. meningitidis* meningococcal strain was constructed using marker free mutagenesis as described before [15, 30]. The OMVs, suspended in 10 mM TRIS, 3% sucrose pH 7.4, were produced using the downscaled production platform as describe before [12, 31].

Peptide

The SARS-CoV-2 epitope clusters were identified as previously described [20]. Using VaccineCAD [32], three of those epitope clusters were linked together in a “string-of-beads”. The synthetic peptide was produced by Pepscan (Lelystad, The Netherlands) at >95% purity and consisted of a 47 amino-acid sequence (Mw 5448) with a thiol bearing cysteine on the C-terminus for thiol-maleimide addition (conjugation). Absolute quantification by LC-MS analysis was performed using the stable isotopically labeled signature peptide GVYYP[¹³C₆, ¹⁵N₄-R].

Peterson

The total protein concentration determination was based on the Lowry protein assay with Peterson adaptation (Sigma Aldrich, TP0300) for the precipitation of soluble proteins by DOC and TCA and micro plate-based adaptations.

SDS-PAGE

5 µg total protein for each sample was diluted to 20 µL using Milli-Q and a 4 times concentrated bromophenol blue reduced loading buffer. After dilution, the samples were incubated at 100°C for 10 minutes. 20 µL of samples and 5 µL of the marker (Invitrogen, Novex® Sharp pre stained marker, LC5800, P/N 57318) were loaded on the gel. The voltage was set to 200V, and gels were run for 38 minutes. Afterwards the casting was removed, and the gel was rinsed with demi water and subsequently stained for 1 hour (Invitrogen, Imperial Protein Stain, 24615). Finally, the gels were de-stained using demi water overnight before image acquisition was performed using a scanner.

TNBS

Primary amine groups were quantified using a 2,4,6-trinitrobenzenesulfonic acid (TNBS) assay. The assay was performed as described before [29], however with a micro plate-based adaptation.

DLS/ELS

Hydrodynamic sizing or DLS analysis was performed on a Malvern Instruments Zetasizer Nano-ZS ZEN3600 equipped with an Avalanche Photodiode QE He-Ne 633 nm applying the NIBS method (non-invasive backscattering). Software: Malvern Zetasizer Software version 7.13. Electrophoretic mobility was assessed using the same Zetasizer as for DLS however now applying M3-PALS (Mixed Mode Measurement – phase analysis light scattering) with the Avalanche Photodiode QE.

LC-MS

LC-MS (phospholipids)

The relative quantification of phospholipids and their maleimide containing derivatives was performed as described by an application note from Agilent. The sample extraction was performed on a 1:1 mixture of D0:D6 2-mercaptoethanol-labeled OMVs at a 0.25 mg/mL OMV protein concentration. Measurements were performed using an LTQ Orbitrap XL (Thermo Scientific) in negative ESI mode, with an Orbitrap readout at 15k resolution (FWHM). A selection of interesting phospholipids was quantified (relative, label free, without the addition of stable isotopically labeled analogues). This selection included: PG C32:1, PG C34:1, PE C28:0, PE C30:1, PE C30:0, PE C32:2, PE C32:1 and PE C32:0.

LC-MS (proteomics)

Analyte stability: Model peptides Ac-GLFGRKTG and SPAEPSVYATL were used to verify the stability of the conjugate product towards the required denaturation step for bottom-up LC-MS-based proteomics protein analysis. To the peptide mixture, a 64-fold-molar excess of either sulfo-NHS-acetate (Thermo 26777, serves as a stable control), Azido acetic acid NHS ester (Thermo 900919-1G) or GMBS (Sigma Aldrich 63175) was added and incubated for 1 hour at room temperature. The GMBS-treated sample was incubated for an additional hour in the presence of a 640-fold-molar excess of either beta-mercaptoethanol or deuterated beta-mercaptoethanol. LC-MS analysis revealed that both the acetylation and the reaction with the maleimide resulted in full conversion to the expected products. The reaction with the azido acetic acid NHS ester resulted in various (unidentified) side products and poor overall conversion. Subjecting the original peptide reaction mixture to the denaturation step (*i.e.*, 30 min incubation at 100°C in the presence of 0.1% Rapigest SF) and subsequent LC-MS-based proteomics analysis, revealed an increased amount of hydrolyzed maleimide for peptide Ac-GLFGRKTG, but no degradation of the maleimide-thiol bond.

Gas Chromatography (lipooligosaccharide)

GC analysis was essentially performed as described previously [33]. The analysis determined the quantity of the most dominant LOS species from which the quantity of primary amines were deducted.

Enzymatic fluorescent detection of phosphatidylethanolamines

Phospholipids that contain primary amines can function as a nucleophile and react with NHS-based chemicals such as GMBS. To determine the fraction of primary amines on OMVs originating from phosphatidylethanolamine (PE) and phosphatidylserine (PS), both phospholipids were assessed using the MAK361 and MAK371 kits (Sigma Aldrich), respectively. These assays were conducted in accordance with the manufacturer's instructions.

FFF-MALS

The FFF-MALS analysis was performed as described earlier [34]. Samples were analyzed by injecting 20 µg total protein as determined by the Peterson protein assay. For shift in particle size distribution, after separation, the UV₂₈₀ trace was divided by a split peak at ~30 min, this is where the OMVs alone elution ended in the chromatogram, which was compared to the total peak area (Figure S3).

Conjugation of peptide to PorB vesicles using spin filtration

To 100 µL 1.1 mg/mL (protein) OMV in 10 mM HEPES buffer pH 7.4, 3.6 µL GMBS solution (5.0 mg/mL in DMSO, 58.8 nmol) and 6.4 µL buffer were added followed by 60 min incubation at ambient temperature. Remaining GMBS and DMSO were removed using 0.5 mL 100kDa Amicon spin filters for 5 cycles with 10 mM HEPES buffer pH 7.4 with sample volumes corrected to 100 µL using 10 mM HEPES buffer pH 7.4. To 25 µL sample 75 µL HEPES buffer pH 7.4 to obtain a 0.25 mg/mL OMV solution. Conjugation was initiated by adding 10 µL of a 1.0 mg/mL peptide solution (0.91 nmol) dissolved in DMSO and lasted for 60 min. at ambient temperature. Final purification of the conjugate, removing any free peptide, was done by the same spin filtration method as described above, only now using 10 mM Tris pH 7.4 with 3% sucrose.

Manual hollow fiber tangential flow filtration operation

All manual TFF HF operations were performed according to the supplier's specification using a MicroKros 20 cm 100 kDa MPES 0.5mm ML hollow fiber (Repligen, C02-E100-05-S).

Design of experiments

As described in the main text, the design and statistical analysis of the DoE was performed using the MODDE Pro software (Sartorius, V13.0.0.24874, Feb 10, 2021). With respect to the 19 experiments, we described experiment 1 as an example on which all other 18 reaction conditions are based (Table S1). OMVs at 1.44 mg/mL protein in 10 mM TRIS 3% sucrose pH 7.4 were buffer exchanged using manual TFF HF to 10 mM HEPES pH 7.8. 2.25 mL OMV was reacted with 0.206 mg GMBS (Mw 280.23) dissolved in 0.25 mL DMSO, at a final OMV concentration of 1.00 mg/mL for 30 minutes at ambient temperature. DMSO and residual GMBS/GMB were removed by manual TFF HF using 10 mM HEPES pH 7.8. For conjugation, 1.8 mL of the GMB modified OMV (OMV^{MAL}) was reacted with 0.06 mg peptide (Mw 5448) dissolved in 200 μ L DMSO, at a final OMVMAL concentration of 0.15 mg/mL for 1 hour at ambient temperature. DMSO and residual peptide were removed by manual TFF HF using 10 mM HEPES pH 7.8.

Confirmation of optimized conditions

The execution for the optimized conjugation A was performed essentially the same as for the DoE using the reaction conditions as described in Table S3 (Row 1).

Large scale conjugation

A Cogent μ (Merck Millipore, CUP0300) was equipped with a disposable flow-path including 4 0.01 m² TFF filters (Repligen, PP100MP1L), chemically sterilized using 0.1 M NaOH and operated as described before [22]. Reaction conditions were scaled-up from the optimized experiment A and intermediate and final purification was extended to 10 buffer exchange volumes using the respective buffers. In short, GMBS modification reaction was performed at 100 mL scale at 1 mg/mL protein concentration reacting 35.5 mg of GMBS facilitating the 11.5 GMBS:peptide ratio. 41.6 mL of the OMV^{MAL} was removed and replaced with 91.6 mL of 10 mM HEPES pH 7.8 to a final volume of 150 mL. Conjugation was initiated by adding 35 mg peptide dissolved in 17 mL DMSO facilitating the 25:15 ratio. The final volume of conjugate was 150 mL at a 0.56 mg/mL protein concentration.

Stability study on concentrated conjugate

The DS (0.56 mg/mL total protein) was stored for 1 week at 2-8° before the initiation of the stability study. From the conjugate at 0.56 mg/mL 8.0, 14.4, 28.8 and 43.2-mL aliquots were concentrated to a final volume of 8 mL each, to obtain 0.56, 1.00, 2.00 and 3.00 mg/mL, respectively. Concentration was accomplished by using manual TFF HF MicroKros 20 cm 100 kDa MPES 0.5mm ML hollow fiber (Repligen, C02-E100-05-S). From each of the different concentrations 2 mL was stored at 2-8 °C for the duration of the study.

Associated content

Supporting Information

Additional information on primary amines distribution on OMVs, DLS plots, DoE shift in particle size distribution, DoE coefficients plot, DoE residuals and observed vs predicted plot, DoE LC-MS results, DoE MODDE optimizer run results and NMR analysis of filtrate fractions and TFF conversion rates from scale-up study.

Author information

Corresponding author

Robert M.F. van der Put, Intravacc, P.O. Box 450, 3720 AL Bilthoven, the Netherlands, email: r.m.f.vanderput@uu.nl

Author contributions

R.M.F.P: Conceptualization, Formal analysis, Methodology, Investigation, Writing - Original Draft, Writing - Review & Editing; T.J.M.M: Conceptualization, Methodology, Investigation, Writing - Review & Editing; Z.E: Conceptualization, Methodology, Investigation, Writing - Original Draft; A.S.: Formal analysis, Investigation; H.D.M.: Conceptualization, Methodology, Investigation, Writing - Original Draft; R.H.W.M.: Supervision; R.J.P.: Supervision; B.M.: Supervision; C.K.: Supervision, Project administration

Notes

The authors declare no competing interests.

Acknowledgments

The authors thank Maarten Danial for his input in the scientific discussions; Lilli Stangowez for her help during the large-scale experiments; Jari Verbunt for performing all the SDS-PAGEs and Ramon Ramlal for assisting on the LC-MS analyses.

References

1. Clemens, S.A.C. and R. Clemens, The need and challenges for development of vaccines against emerging infectious diseases. *J Pediatr* (Rio J), 2022.
2. WHO. HIV fact sheet. 18-January-2023]; Available from: <https://www.who.int/news-room/fact-sheets/detail/hiv-aids>.
3. Zhu, N., et al., A Novel Coronavirus from Patients with Pneumonia in China, 2019. *N Engl J Med*, 2020. 382(8): p. 727-733.
4. Shang, W., et al., The outbreak of SARS-CoV-2 pneumonia calls for viral vaccines. *NPJ Vaccines*, 2020. 5(1): p. 18.
5. Croxtall, J.D. and S. Dhillon, Meningococcal quadrivalent (serogroups A, C, W135 and Y) tetanus toxoid conjugate vaccine (Nimenrix). *Drugs*, 2012. 72(18): p. 2407-30.
6. Bilukha, O., N. Messonnier, and M. Fischer, Use of meningococcal vaccines in the United States. *Pediatr Infect Dis J*, 2007. 26(5): p. 371-6.
7. Ilyina, N., et al., Safety and immunogenicity of meningococcal ACWY CRM197-conjugate vaccine in children, adolescents and adults in Russia. *Hum Vaccin Immunother*, 2014. 10(8): p. 2471-81.
8. Pichichero, M.E., Protein carriers of conjugate vaccines: characteristics, development, and clinical trials. *Hum Vaccin Immunother*, 2013. 9(12): p. 2505-23.
9. Broker, M., et al., Polysaccharide conjugate vaccine protein carriers as a "neglected valency" - Potential and limitations. *Vaccine*, 2017. 35(25): p. 3286-3294.
10. Cartwright, K., et al., Immunogenicity and reactogenicity in UK infants of a novel meningococcal vesicle vaccine containing multiple class 1 (PorA) outer membrane proteins. *Vaccine*, 1999. 17(20-21): p. 2612-9.
11. de Kleijn, E.D., et al., Immunogenicity and safety of a hexavalent meningococcal outer-membrane-vesicle vaccine in children of 2-3 and 7-8 years of age. *Vaccine*, 2000. 18(15): p. 1456-66.
12. Gerritzen, M.J.H., et al., Spontaneously released *Neisseria meningitidis* outer membrane vesicles as vaccine platform: production and purification. *Vaccine*, 2019. 37(47): p. 6978-6986.
13. van der Pol, L., M. Stork, and P. van der Ley, Outer membrane vesicles as platform vaccine technology. *Biotechnol J*, 2015. 10(11): p. 1689-706.
14. Klouwens, M.J., et al., Vaccination with meningococcal outer membrane vesicles carrying *Borrelia OspA* protects against experimental Lyme borreliosis. *Vaccine*, 2021. 39(18): p. 2561-2567.
15. van der Ley, P.A., et al., An Intranasal OMV-Based Vaccine Induces High Mucosal and Systemic Protecting Immunity Against a SARS-CoV-2 Infection. *Front Immunol*, 2021. 12: p. 781280.
16. Skidmore, B.J., et al., Immunologic properties of bacterial lipopolysaccharide (LPS): correlation between the mitogenic, adjuvant, and immunogenic activities. *J Immunol*, 1975. 114(2 pt 2): p. 770-5.
17. Liu, Y., et al., Experimental vaccine induces Th1-driven immune responses and resistance to *Neisseria gonorrhoeae* infection in a murine model. *Mucosal Immunol*, 2017. 10(6): p. 1594-1608.
18. Lehmann, A.K., et al., Human opsonins induced during meningococcal disease recognize outer membrane proteins PorA and PorB. *Infect Immun*, 1999. 67(5): p. 2552-60.
19. Bachmann, M.F. and G.T. Jennings, Vaccine delivery: a matter of size, geometry, kinetics and molecular patterns. *Nat Rev Immunol*, 2010. 10(11): p. 787-96.
20. De Groot, A.S., et al., Better Epitope Discovery, Precision Immune Engineering, and Accelerated Vaccine Design Using Immunoinformatics Tools. *Front Immunol*, 2020. 11: p. 442.
21. Meyers, L.M., et al., Highly conserved, non-human-like, and cross-reactive SARS-CoV-2 T cell epitopes for COVID-19 vaccine design and validation. *NPJ Vaccines*, 2021. 6(1): p. 71.
22. van der Put, R.M.F., et al., The First-in-Human Synthetic Glycan-Based Conjugate Vaccine Candidate against *Shigella*. *ACS Central Science*, 2022. 8(4): p. 449-460.
23. Verez-Bencomo, V., et al., A synthetic conjugate polysaccharide vaccine against *Haemophilus influenzae* type b. *Science*, 2004. 305(5683): p. 522-5.
24. Cohen, D., et al., Safety and immunogenicity of a synthetic carbohydrate conjugate vaccine against *Shigella flexneri* 2a in healthy adult volunteers: a phase 1, dose-escalating, single-blind, randomised,

- placebo-controlled study. *Lancet Infect Dis*, 2021. 21(4): p. 546-558.
25. Sartorius. MODDE 12 user guide. 15-Jan-2023]; Available from: <https://www.sartorius.com/download/544636/modde-12-user-guide-en-b-00090-sartorius-data.pdf>.
 26. Tumey, L.N., et al., Mild method for succinimide hydrolysis on ADCs: impact on ADC potency, stability, exposure, and efficacy. *Bioconjug Chem*, 2014. 25(10): p. 1871-80.
 27. Peeters, C.C., et al., Phase I clinical trial with a hexavalent PorA containing meningococcal outer membrane vesicle vaccine. *Vaccine*, 1996. 14(10): p. 1009-15.
 28. Basu, R., et al., Immunization with phage virus-like particles displaying Zika virus potential B-cell epitopes neutralizes Zika virus infection of monkey kidney cells. *Vaccine*, 2018. 36(10): p. 1256-1264.
 29. Jin, M., et al., Enhancing immune responses of ESC-based TAA cancer vaccines with a novel OMV delivery system. *J Nanobiotechnology*, 2024. 22(1): p. 15.
 30. Sungsuwan, S., et al., Structure Guided Design of Bacteriophage Qbeta Mutants as Next Generation Carriers for Conjugate Vaccines. *ACS Chem Biol*, 2022.
 31. Warner, N.L. and K.M. Fietze, Development of Bacteriophage Virus-Like Particle Vaccines Displaying Conserved Epitopes of Dengue Virus Non-Structural Protein 1. *Vaccines (Basel)*, 2021. 9(7).
 32. Hemmer, B., et al., Minimal peptide length requirements for CD4(+) T cell clones—implications for molecular mimicry and T cell survival. *Int Immunol*, 2000. 12(3): p. 375-83.
 33. van der Put, R.M., et al., A Synthetic Carbohydrate Conjugate Vaccine Candidate against Shigellosis: Improved Bioconjugation and Impact of Alum on Immunogenicity. *Bioconjug Chem*, 2016. 27(4): p. 883-92.
 34. Johnston, D.M. and J.G. Cannon, Construction of mutant strains of *Neisseria gonorrhoeae* lacking new antibiotic resistance markers using a two gene cassette with positive and negative selection. *Gene*, 1999. 236(1): p. 179-84.
 35. van de Waterbeemd, B., et al., Identification and optimization of critical process parameters for the production of NOMV vaccine against *Neisseria meningitidis*. *Vaccine*, 2012. 30(24): p. 3683-90.
 36. Moise, L., et al., iVAX: An integrated toolkit for the selection and optimization of antigens and the design of epitope-driven vaccines. *Hum Vaccin Immunother*, 2015. 11(9): p. 2312-21.
 37. Baart, G.J., et al., Modeling *Neisseria meningitidis* metabolism: from genome to metabolic fluxes. *Genome Biol*, 2007. 8(7): p. R136.
 38. van der Put, R.M.F., et al., Validation of an FFF-MALS Method to Characterize the Production and Functionalization of Outer-Membrane Vesicles for Conjugate Vaccines. *Anal Chem*, 2022. 94(35): p. 12033-12041.

Supplementary Information

Table of contents

Figure S1	Primary amines on OMV
Figure S2	DLS plot OMV and OMV-peptide conjugate
Figure S3	Shift in particle size distribution
Figure S4	DoE coefficients plot
Figure S5	DoE Residuals normal probability plot
Figure S6	DoE observed versus predicted
Table S1	DoE factors evaluated
Table S2	LC-MS results for the individual DoE experiments
Table S3	Optimizer run in MODDE
Table S4	Scale-up conjugation reaction results
	Safety statement
	Chemicals statement

Supplementary Figures

Primary Amines on OMV

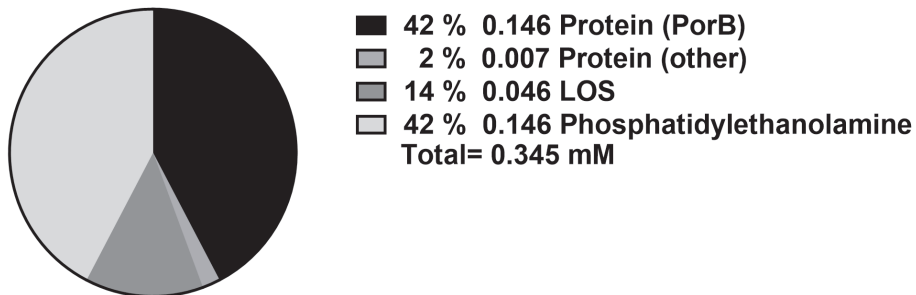


Figure S1. Pie-chart comparing the molar ratios of OMV components that contribute to the total primary amine content

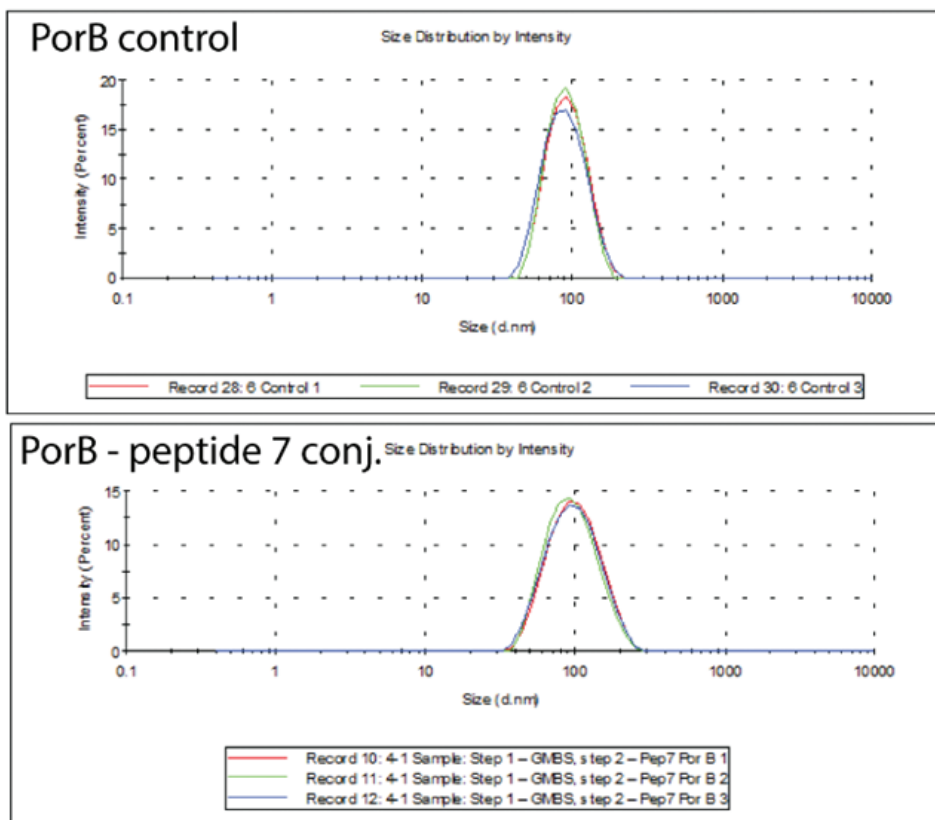


Figure S2. DLS plots of the OMV (top) and OMV-peptide conjugate (bottom).

7

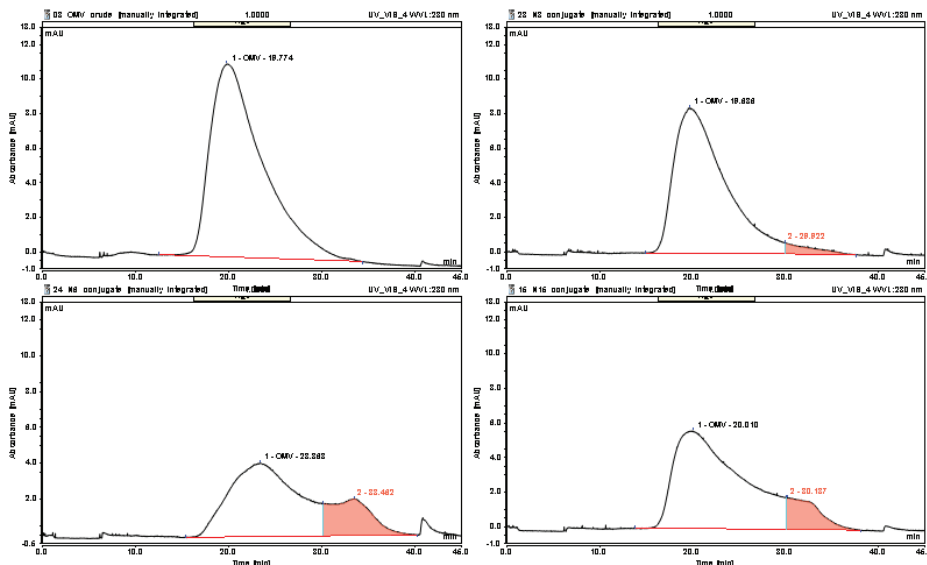


Figure S3: 4 examples for the FFF-MALS analysis, Top left OMV crude, Top right N3-350-8-5-1, Bottom left N6-150-24-15-1, Bottom right N15-350-8-15-5, shift in particle size distribution is calculated by comparing the peak area of the pink area to the total peak area expressed in %.

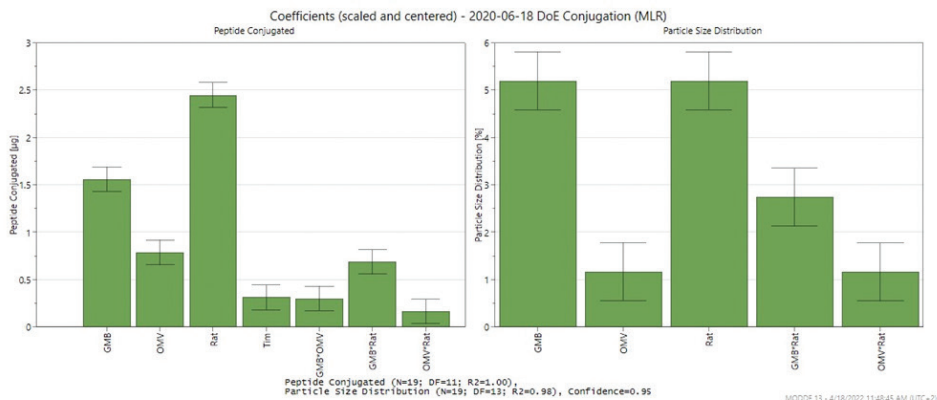


Figure S4: Coefficients plot for conjugated peptide (left) and shift in particle size distribution (right).

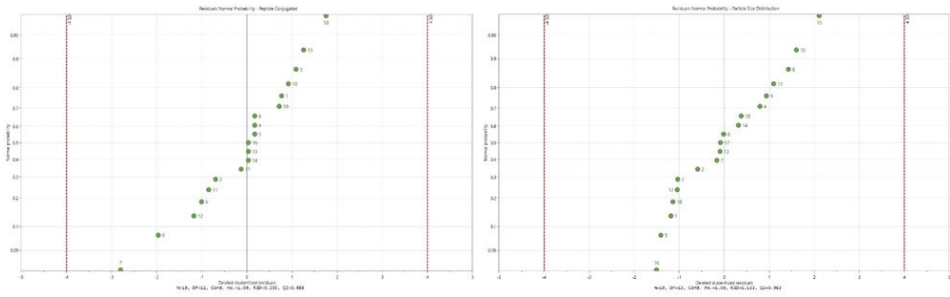


Figure S5: Residuals normal probability plot for conjugated peptide (left) and shift in particle size distribution (right).

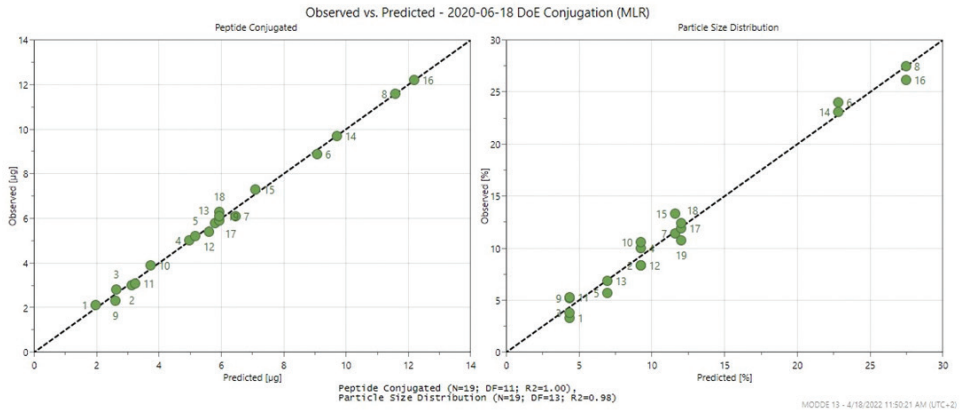


Figure S6: Observed versus predicted for conjugated peptide (left) and shift in particle size distribution (right).

Supplementary Tables

Table S1: The evaluated factors for the DoE.

Exp No	Ratio GMBS: peptide	Protein concentration OMV (mg/mL)	Peptide: OMV ratio	Time (hr)	Q GMBS (mg)	Q peptide (mg)
1	8	150	5	1	0.206	0.06
2	24	150	5	1	0.617	0.06
3	8	350	5	1	0.206	0.14
4	24	350	5	1	0.617	0.14
5	8	150	15	1	0.617	0.18
6	24	150	15	1	1.852	0.18
7	8	350	15	1	0.617	0.42
8	24	350	15	1	1.852	0.42
9	8	150	5	5	0.206	0.06
10	24	150	5	5	0.617	0.06
11	8	350	5	5	0.206	0.14
12	24	350	5	5	0.617	0.14
13	8	150	15	5	0.617	0.18
14	24	150	15	5	1.852	0.18
15	8	350	15	5	0.617	0.42
16	24	350	15	5	1.852	0.42
17	16	250	10	3	0.823	0.20
18	16	250	10	3	0.823	0.20
19	16	250	10	3	0.823	0.20

Table S2: LC-MS results for the individual DoE experiments

Description	Targeted Peptide (µg/mL)	Targeted PorB Protein (µg/mL)	Total protein based on PorB/70% (µg/mL)	µg Peptide for every 25 µg OMV	Shift in PSD (%)
N1 conjugate	12	99	141	2.1	3.3
N2 conjugate	8	45	64	3.0	8.3
N3 conjugate	23	143	204	2.8	3.8
N4 conjugate	12	42	60	5.0	10.0
N5 conjugate	36	121	173	5.2	5.7
N6 conjugate	28	55	79	8.9	24.0
N7 conjugate	57	164	234	6.1	11.4
N8 conjugate	88	133	190	11.6	27.5
N9 conjugate	6.8	51	73	2.3	5.2
N10 conjugate	18	80	2	3.9	10.6
N11 conjugate	25	142	203	3.1	5.3
N12 conjugate	20	65	93	5.4	8.3
N13 conjugate	51	155	221	5.8	6.8
N14 conjugate	30	54	77	9.7	23.1
N15 conjugate	105	252	360	7.3	13.3
N16 conjugate	116	167	239	12.2	26.2
N17 conjugate	45	134	134	5.9	11.9
N18 conjugate	47	131	131	6.3	12.4
N19 conjugate	46	133	133	6.1	10.8

LC-MS analysis yielded two sets of quantitative data. On the one hand the concentration PorB and the peptide concentration on the other. From the PorB concentration the total protein concentration was extrapolated by the fact that it made up 70% of the total protein content.

Table S3: Optimizer run in MODDE

Ratio GMBs:pep- tide	Protein concentration OMV ($\mu\text{g}/\text{mL}$)	Pep- tide:OMV ratio	Time (hr)	MS Pep- tide conju- gated	Shift in particle size dis- tribution (%)	log(D)
11.47	344.10	14.97	4.90	8.13	14.87	0.081
11.46	350.00	14.92	4.88	8.14	14.94	0.085
11.58	344.00	15.00	5.00	8.19	14.99	0.087
12.37	310.30	15.00	5.00	8.16	15.00	0.088
11.81	334.20	15.00	4.87	8.16	15.00	0.088
12.67	297.60	15.00	5.00	8.15	15.00	0.089
11.73	337.80	15.00	4.68	8.13	15.00	0.089
13.57	258.30	15.00	5.00	8.08	14.98	0.090
14.12	235.60	15.00	5.00	8.04	14.99	0.094
14.12	235.60	15.00	5.00	8.04	14.99	0.094
13.62	257.00	15.00	4.75	8.05	15.00	0.094
11.79	343.70	14.90	4.95	8.20	15.10	0.094
14.77	209.60	14.96	5.00	7.97	15.00	0.097
14.87	204.10	15.00	4.99	7.96	15.00	0.098
15.11	194.00	14.99	5.00	7.93	15.00	0.099
15.21	189.20	15.00	5.00	7.91	15.00	0.100
11.53	345.60	15.00	2.83	7.85	14.99	0.102
12.88	343.80	13.95	4.88	8.09	15.19	0.105
22.37	349.90	8.65	4.99	7.66	15.00	0.112
23.95	345.00	8.17	3.21	7.40	15.00	0.124

Table S4: Scale-up conjugation filtrate fractions NMR analysis of constituents and TFF conversion rates

	DMSO (mM)	Tris (mM)	Sucrose (mM)	TFF Conversion (%)^[1]
OMV in TRIS sucrose	n.a.	9.94	85.60	n.a.
OMV buffer exchange filtrate 0	n.a.	2.37	39.42	0
OMV buffer exchange filtrate 1	n.a.	1.34	23.73	22
OMV buffer exchange filtrate 2	n.a.	0.51	9.68	22
OMV buffer exchange filtrate 3	n.a.	0.24	4.46	20
OMV buffer exchange filtrate 4	n.a.	0.07	1.55	20
OMV buffer exchange filtrate 5	n.a.	0.03	0.63	20
OMV buffer exchange filtrate 6	n.a.	<LOQ	<LOQ	22
OMV buffer exchange filtrate 7	n.a.	<LOQ	<LOQ	19
OMV buffer exchange filtrate 8	n.a.	<LOQ	<LOQ	23
OMV buffer exchange filtrate 9	n.a.	<LOQ	<LOQ	24
OMV buffer exchange filtrate 10	n.a.	<LOQ	<LOQ	24
OMV in modification buffer	n.a.	<LOQ	<LOQ	n.a.
OMV:GMBS modification reaction 30 min at ambient temperature				
OMV ^{MAL} buffer exchange 0	879.79	n.a.	n.a.	12
OMV ^{MAL} buffer exchange 1	527.80	n.a.	n.a.	24
OMV ^{MAL} buffer exchange 2	186.74	n.a.	n.a.	23
OMV ^{MAL} buffer exchange 3	60.47	n.a.	n.a.	23
OMV ^{MAL} buffer exchange 4	23.51	n.a.	n.a.	22
OMV ^{MAL} buffer exchange 5	7.65	n.a.	n.a.	21
OMV ^{MAL} buffer exchange 6	2.88	n.a.	n.a.	24
OMV ^{MAL} buffer exchange 7	1.20	n.a.	n.a.	23
OMV ^{MAL} buffer exchange 8	0.51	n.a.	n.a.	23
OMV ^{MAL} buffer exchange 9	0.31	n.a.	n.a.	25
OMV ^{MAL} buffer exchange 10	0.19	n.a.	n.a.	25
OMV ^{MAL} in conjugation buffer	0.06	n.a.	n.a.	n.a.
OMV:peptide conjugation reaction 180 min at ambient temperature				
Conjugate buffer exchange 0	n.a.	n.a.	n.a.	31
Conjugate buffer exchange 1	562.18	5.71	123.64	32
Conjugate buffer exchange 2	214.81	8.71	186.88	28
Conjugate buffer exchange 3	92.91	10.00	217.38	27
Conjugate buffer exchange 4	34.93	10.60	225.10	27
Conjugate buffer exchange 5	13.42	11.71	233.49	25
Conjugate buffer exchange 6	5.48	11.62	229.98	24

	DMSO (mM)	Tris (mM)	Sucrose (mM)	TFF Conversion (%) ^[1]
Conjugate buffer exchange 7	2.34	11.57	233.75	23
Conjugate buffer exchange 8	0.83	11.57	231.27	25
Conjugate buffer exchange 9	0.49	11.65	232.72	24
Conjugate buffer exchange 10	0.29	11.11	231.87	24
Conjugate in formulation buffer	0.20	12.37	272.99	n.a.

^[1] Conversion: Filtrate flow rate (mL/min) / Feed flow rate (mL/min)

Safety statement

No unexpected or unusually high safety hazards were encountered during any of the methods, processes or assays.

Chemicals

All chemicals used and presented in this manuscript were of the highest possible available purity and complying with GMP regulations where needed.





Chapter 8

Summary and Perspectives



Summary

New conjugate vaccines are under development targeting different diseases. This is directly related to the introduction of new synthetically designed and manufactured antigens that are becoming more and more available. This has substantial advantages with respect to the conventional extraction processes as historically applied to polysaccharides. Additionally, new protein carriers are being investigated and used in the field as well. Here we do see trends towards the introduction of nanoparticles and proteins replacing the traditional carriers. The combination of nanoparticle carriers and synthetic antigens require new, sophisticated methods to characterize and evaluate their quality both physicochemically and immunologically. In this thesis we provide a stepwise progression from an extracted polysaccharide conjugated through random coupling to tetanus toxoid towards site-specific conjugation of an intricate synthetically produced oligosaccharide. This conjugation method is then further evaluated for the development of an OMV-based synthetic peptide vaccine. For all three vaccines described in this thesis (*Haemophilus influenzae* type b (Hib), *Shigella flexneri* 2a and OMV-peptide), we used and developed an indispensable set of quality control tests for physicochemical characterization. Also Design of Experiments (DoE) was utilized for the optimization of conjugation processes. This approach provided a pivotal tool to reduce time and costs during small-scale development and optimization of several individual production process.

In **Chapter 2** a comprehensive overview is given of recent developments regarding glycoconjugate vaccines. In a two-tiered approach, the introduction of new carriers and the advancements of target antigens are discussed, focusing on conjugate vaccines directed against the ESKAPE pathogens. New carriers are essential to overcome potential pitfalls of carrier-induced epitope suppression (CIES) as observed for some of the traditional carriers. These new carriers consisted of 1) outer membrane vesicles (OMVs) and generalized modules for membrane antigens, 2) glycoengineered proteins and OMVs, 3) carrier proteins, 4) virus like particles, 5) protein nanocages and 6) peptides. Multiple examples of new developments regarding carriers, published over the past five years, are discussed.

In addition, the focus was put on anti-microbial resistance (AMR), classified as the new silent pandemic. While AMR is attributed to a broad range of pathogens, here we focused on the so called ESKAPE pathogens (*Enterococcus faecium*, *Staphylococcus aureus*, *Klebsiella pneumoniae*, *Acinetobacter baumannii*, *Pseudomonas aeruginosa* and *Enterobacter spp.*) which are all on the top of both the WHO and CDC priority lists. We summarized attempts to develop glycoconjugate vaccines, targeting ESKAPE pathogens, that are still in the early

development or pre-clinical stage. While abundant efforts are made in the field of new carriers, this is less obvious for glycoconjugate vaccines targeting ESKAPE pathogens. While one could attribute the lack in development of new AMR targeted vaccines as a direct effect of the COVID-19 pandemic, new vaccine candidates can be expected soon.

In **Chapter 3**, the analysis of samples, generated during the production and purification of the capsular polysaccharide (CPS) polyribosyl-ribitol-phosphate (PRP) of Hib is presented. Traditionally, PRP was quantified using either immunochemical or colorimetric methods. Both methods lack accuracy due to interference from either fermentation components and or reagents used during purification. The introduction of an improved and highly specific high-performance anion exchange chromatography pulsed-Amperometric detection (HPAEC-PAD) method eliminated these interferences. The HPAEC-PAD method really excelled in terms of specificity and accuracy compared to the traditionally used colorimetric assay and HPSEC method. The introduction of the HPAEC-PAD method accelerated the process development of the Hib vaccine. It can also be applied to the quality control of new production lots.

In **Chapter 4** the development and characterization of a conjugate vaccine candidate against Shigellosis is presented. Two key advances are introduced: 1) synthetic oligosaccharides (sOS) acting as functional copy of the O-specific polysaccharide moiety of *Shigella* LPS and 2) site-specific GMBS conjugation chemistry for a highly controlled and predictive production process. Before conjugation of the sOS, the maleimide addition on primary amines available on the tetanus toxoid was first evaluated and optimized using a design of experiments (DoE) approach. Optimum reaction conditions were defined at which the highest portion of the primary amines were functionalized, and the least amount of aggregates were formed. Four conjugates were prepared with different conjugated sOS to tetanus toxoid ratios (4.6, 8.5, 17 and 26 mol/mol). A maximum conjugation number of twenty-six sOS per toxoid molecule was achieved. However, immunogenic evaluation revealed seventeen sOS per toxoid molecule induced the highest antibody titers compared to other ratios. The addition of alum as an adjuvant had a very positive influence on immunogenicity. These results confirmed that a synthetic pentadecasaccharide hapten mimicking the SF2a O-SP, elicited a protective Ab response in mice that was retained for more than a year.

Chapter 5 describes the development of a *Shigella* conjugate vaccine equipped with a synthetic carbohydrate towards a commercial-scaled GMP manufacturing process. The starting point was the data as presented in **chapter 4**. A 1000-fold scale-up was achieved successfully and the introduction of tangential flow filtration provided comparable

products with respect to conjugation kinetics and efficiency as obtained by the small-scale process. The GMP production of two batches resulted in materials for a toxicology study in rabbits, and a clinical study in humans. Both batches were produced at a 76 and 80% conjugation efficiency, respectively. The first batch passed all toxicology-related criteria and exhibited a strong anti-SF2a immune response in both mice and rabbits. The antibodies were specific for SF2a LPS and functional in vitro revealing high anti-SF2a SBA titers. Furthermore, they recognized a large pool of Sf2a circulating strains isolated from individuals diagnosed with shigellosis. The final vaccine lots were stable for at least 66 months. The free carbohydrate content fulfilled the specifications for product release (<10%) and vaccine shelf life (<25%). This glycoconjugate vaccine candidate was shown to be safe and well tolerated in healthy adults while inducing high anti-SF2a LPS titers [1]. No additional effect of the adjuvant (alum) or the repeated immunization (booster) was observed when 10 µg of glycan per vaccine was administered. On the other hand, an improved immune response was apparent for the 2-µg dose. This vaccine candidate was further evaluated in two consecutive phase-II trials. Firstly, a controlled human infection model (CHIM) study evaluating the protective capacity of SF2a-TT15 in naive adults (NCT0478022) and secondly an age-descending study in Kenya assessing the safety and immunogenicity of SF2a-TT15 in the target population, especially infants, in the field (NCT04602975).

In **Chapter 6** we introduce field-flow fractionation coupled to multiangle light-scattering (FFF-MALS) for the characterization of OMVs as a new carrier for conjugate vaccines. In **chapter 2** we presented OMVs as one of the new carriers for conjugate vaccines. OMVs are an attractive alternative for the traditional carriers due to their stable composition, self-adjuvanting properties, and their ability to express heterologous antigens of specific pathogens. Functionalization of OMVs using *N*-γ-(maleimidobutryl)-oxysuccinimide-ester (GMBS), enabling conjugation to any thiol-bearing immunogenic moiety, yields OMVs ready for conjugation. The FFF-MALS method was developed for separating OMVs from protein impurities. Several iterations led to an improved method. The final method was successfully subjected to a full validation study according to ICH guidelines (Q2 R1). The validated assay was then applied for the evaluation of the OMV production and purification processes. It was possible to evaluate the purity and OMV size distribution in all different fractions obtained during the purification process. It was a challenging task with respect to solvents and other matrix constituents used. OMVs originating from other bacterial origins were also successfully analyzed. Finally, GMBS-modified OMVs were successfully analyzed using the validated FFF-MALS method. Here, we found that the GMBS reaction did not have any effect on the colloidal stability of the OMV. By applying the FFF-MALS method it is now possible to evaluate the production, purification, and functionalization of OMVs with GMBS. These ready-to-conjugate OMVs can be used as a

carrier for virtually any oligosaccharide, peptide, and or protein antigen for prophylactic or therapeutic application.

In **Chapter 7** OMVs are further investigated in their ability to serve as a carrier for a synthetic model peptide. Here we first subjected the OMVs to an investigation with respect to primary amine distribution and GMBS-modification. Primary amines are available on porB proteins, phosphatidylethanolamine (PE), lipooligosaccharide, and other proteins. To prevent possible colloidal instability by modifying OMVs too much, the maximum molar equivalents of GMBS were confirmed. Under these non-optimized conditions, it was possible to conjugate up to 2.1 μg of peptide to 25 μg of OMV. From these initial reaction conditions, a DoE was applied to optimize the conjugation reaction, to increase the quantity of conjugated peptide (assessed by LC-MS) and minimize changes in size distribution (assessed by FFF-MALS, expressed as shift in particle size distribution, PSD). The full-factorial design, including four factors, resulted in nineteen experiments yielding conjugates with up to 12.1 μg peptide conjugated, however at these conditions we also observed the largest shift in PSD (25%). With conditions provided by the optimizer function from MODDE, we were able to conjugate 7.5 μg of peptide with only 10.6% shift in PSD. The same conditions were applied in a scale-up study where 8.3 μg peptide was conjugated at 13.0% shift in PSD. This conjugate was then subjected to a real-time stability study at 0.6, 1.0, 2.0 and 3.0 mg/mL for the duration of three months. The shift in PSD and protein profile (SDS-PAGE) remained stable in time. The peptide content at the end of the study was similar, except for one product, which showed a decrease to 5.3 $\mu\text{g}/\text{mL}$. In this study, we made significant advancements with the platform-based concept using an OMV as a carrier. With both the OMVs production and conjugation platforms developed, it will be of interest to design peptide-based antigens eliciting protective immune responses to particular diseases, both the prophylactic and therapeutic domain. Since this is a scalable set-up, increased process volumes of up to 10 or 100 liters are easily achievable. Assuming a human vaccine dose is 5 μg peptide, we can produce up to 230.000 – 2.3000.000 doses in a single production cycle of just one day.

Perspectives

It is without a doubt that the most effective application for society to rely on to prevent and protect against infectious diseases are vaccines. This has been clearly highlighted once more with the SARS-Cov-2 pandemic. Vaccines were one of the first strategies implemented more than five hundred years ago in the fight against infectious diseases [2]. It was not until the late 18th century for Jenner to come forward with his live-attenuated smallpox vaccination [2], followed by Pasteur with a live-attenuated rabies vaccine in the 19th century. It took the development of new methods, like cell-culture and culture media, to propagate viruses and bacteria before vaccines, such as polio and tetanus were introduced. In the mid 1980's, the first glycoconjugate vaccine was developed with the use of extracted polysaccharides from *Haemophilus influenzae* type b [3, 4]. Since then, conjugate vaccines have expanded toward other infectious diseases and have had significant impact on reducing the burden of disease and saving lives.

Within this thesis we have shown that by applying diligent process development in combination with design of experiments and state-of-the-art analytical techniques it is possible to develop conjugate vaccines relatively quickly and have them complying to the highest quality standards. As such, there is a bright future for applications past the traditional conjugate vaccines. The development of new and improved conjugate vaccines is moving quickly in multi-faceted directions but is not without its challenges (Fig 1), of which several perspectives are further discussed.

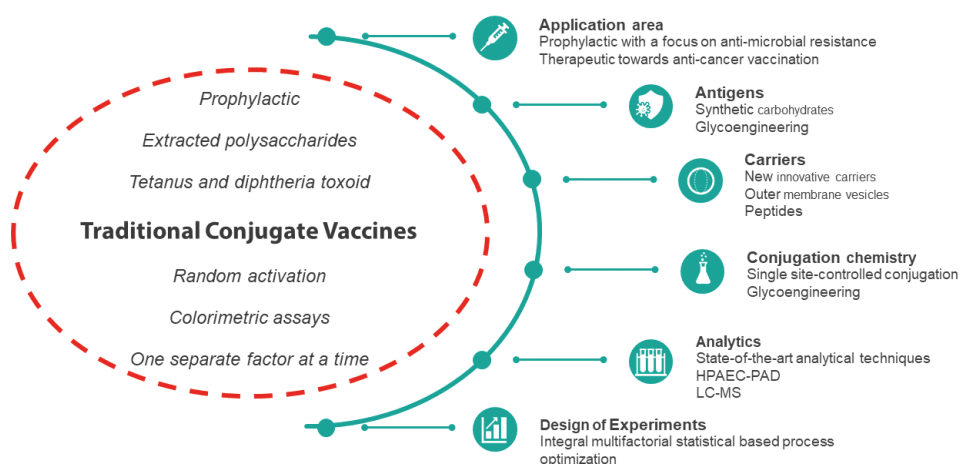


Figure 1: Advances from traditional towards future proof and innovative conjugate vaccines.

Conjugate vaccine carriers

The introduction of conjugate vaccines has had its challenges, especially when looking at the carrier proteins applied and subsequent interference of immunogenicity [5, 6]. Two major known underlying mechanisms are antigen competition and carrier-induced epitope suppression (CIES), both of which result in a reduced immune response towards the conjugated polysaccharide antigen [7-10]. The introduction of new carriers from the same species as the polysaccharide antigen could hypothetically avoid this reduced immunogenicity and simultaneously find a broader application in targeting several serotypes [8]. While the first safe and efficacious carrier proteins were toxoids produced from diphtheria and tetanus toxin, potential unwanted effects could come from chemical detoxification leading to unwanted modifications and heterogeneity.

Important selection criteria for new conjugate vaccine carriers would be 1) ease of reproducible production at large scale under GMP conditions, 2) solubility and stability, 3) sufficient exposure of conjugation-receptive reactive amino acids, 4) assessment and acceptance by regulatory bodies, like WHO, EMA and FDA, and 5) immunogenicity after conjugation, especially when the carrier is also used as an antigen itself. Current efforts on the evaluation of new carriers include liposomes, polymers, inorganic gold particles, dendrimers, nanodiscs, outer membrane vesicles (OMV) and generalized modules for membrane antigens (GMMA), glycoengineered proteins and OMVs, (recombinant) proteins, virus-like particles (VLP), protein nanocages and peptides. While many carriers are assessed with different rates of success, two carriers have the most potential to progress and provide a platform for the development of future conjugate vaccines.

Outer Membrane Vesicles

OMVs are an extremely attractive carrier for conjugate vaccines (**Chapter 2, 6 & 7**) that can be produced from many different bacteria. The presence of pathogen-associated molecular patterns (PAMPS), like lipooligosaccharide (LOS) and lipoproteins give them self-adjuvanting properties [11-13]. Additionally, their size (50-200 nm) and large surface area aid in the uptake by APCs [14]. They can be genetically modified to include both homologous and heterologous proteins for broader strain coverage and produced efficiently at large scale [15, 16]. Furthermore, they can also be used as a platform for glycoengineered conjugates by the *in vivo* protein glycan coupling technology (PGCT) enabling the construction of a glycoconjugate directly in bacteria [17]. These characteristics make them one of the most versatile platform to improve current vaccine strategies and to future proof society for upcoming diseases.

Synthetic peptides

Peptide-based vaccines are based on synthetically produced short (single-epitope) sequences with the potential to be combined into multiple single epitopes (long-peptides, **Chapter 7**) or recombinant overlapping peptides to broaden their applications and effectiveness [18, 19]. The main advantages are that they have an excellent safety profile and can be produced rapidly using simple processes at high yield and purity including conjugation-ready reactive groups [20]. Vaccine-oriented peptides can be effectively used both as carrier and antigen and even as an adjuvant (*e.g.*, universal T-cell epitope PADRE). Another major advantage is that peptides can be designed towards providing a specific B-cell or T-cell-mediated immune response. Peptides can be considered one of the most promising platforms utilizing their capabilities in fast and tailored vaccine development both in the prophylactic and therapeutic domain.

Conjugate vaccine design

Traditionally the first conjugate vaccines were made using polysaccharides extracted from pathogens. Their empirical design, the use of broadly distributed extracted polysaccharides and random activation chemistries are still very effective but seem somewhat outdated in light of current capabilities. Not only the introduction of new synthesis strategies will improve the manufacturing of carbohydrate antigens, but also advance conjugation opportunities.

Synthetic carbohydrate strategies

There has been made enormous progress in the approaches for the manufacturing of complex carbohydrates, including synthetic, chemoenzymatic and glycoengineering methods [21]. The techniques in synthetic carbohydrate chemistry take away from the somewhat ill-defined extracted carbohydrates towards their well-defined and characterized synthetic counterparts with unparalleled purity. With these synthetic carbohydrates being significantly smaller than their extracted and purified counterparts, it is critical to identify the minimal epitopes size of the oligosaccharide needed for an adequate immune response. There is currently only one registered vaccine making use of a synthetic carbohydrate moiety, the Cuban Hib vaccine [22]. Another example of a more elaborate carbohydrate structure mimicking the LPS O-antigen of *Shigella* (**Chapter 4 & 5**), has made great progress towards phase-II clinical trials [23]. Future developments in elucidating and designing synthetic pathways of new synthetic carbohydrate chemistry approaches will be aided by state-of-the-art techniques, like X-ray crystallography, glycan arrays, NMR, and surface plasmon resonance. This will result in the ability to produce more complex bacterial glycans faster and more efficiently. Finally, the introduction of automated synthesis techniques will provide a platform to increase reproducibility [24].

Single site conjugation strategies

Traditional conjugate vaccines make use of extracted polysaccharides combined with random activation conjugation strategies, *e.g.*, CDAP or NaIO_4 oxidation. While these methods have proven to be very efficacious, they end up in rather heterogeneous, high molecular weight entities [25]. The introduction of synthetically manufactured well-defined oligosaccharides in combination with single site conjugation strategies will drastically improve homogeneity of conjugate vaccines. This will simplify the control of the number of conjugated glycans per carrier [26]. Moreover, the use of oligosaccharides increases vaccine manufacturability. Traditionally, conjugation chemistries are directed towards the abundant most surface exposed lysine residues. Several approaches to improve site selective conjugation from the carrier perspective are the introduction of non-natural amino acids, enzyme catalyzed conjugation, chemical modification of amino acid residues or bioconjugation. With more chemistry approaches available, future single site conjugation strategies will not only include different chemistries targeting the same carrier, but also multivalent antigens improving coverage for specific or multivalency for infectious diseases.

Glycoengineering

In vivo protein glycan coupling technology (PGCT) is realized through recombinant enzymatic assembly of a glycoconjugate directly in bacteria [17] (**Chapter 2**). This glycoengineering conjugation technique can be applied to either generate OMVs or proteins expressing the glycan of interest. Currently there are some disadvantages in the manufacturing of bioconjugates. In general, these glycoproteins are heterogeneously expressed, and the polysaccharides show polydispersity. Additionally, the conjugation rate is not very well controlled, with inherent differences of polysaccharide to protein ratios. Finally, not for all bacterial O-SP there are fully compatible OTases available, resulting in more heterogeneous bioconjugates. While these disadvantages should not be ignored, there are substantial advantages, like the redundancy for glycan synthesis, purification, conjugation, and related process controls. Additionally, the potential of exploiting dual carrier/antigen roles increases applicability towards polyvalent vaccine candidates. As such, the field of glycoengineering feels like an early-stage development. However, this promising technique will expand fast and overcome the current challenges and become a major player for the development of conjugate vaccines.

Conjugate vaccines targets

Current developments in conjugate vaccines show incredible potential for a wide range of pathogens related to antimicrobial resistance (AMR) [27, 28] and therapeutic targets in the cancer and neurodegenerative space [29-34].

Antimicrobial resistance

AMR can be considered as the next pandemic, and including carbohydrates in vaccine designs targeting AMR seems crucial. Next to the efforts in developing vaccines to battle the ESKAPE pathogens (**Chapter 2**), other emerging pathogens designated by the WHO and FDA include *Clostridium difficile*, *Enterococcus faecium*, *Neisseria gonorrhoea*, non-typhoidal *Salmonella*, *Candida aureus* and group A and B *Streptococci*. It is without question that future developments and progress in the synthetic and chemoenzymatic synthesis of these complex carbohydrates will improve towards new and able vaccine candidates. With current and future analytical and predictive techniques, like artificial intelligence, synthesis strategies can be derived swiftly and made more efficient.

Anti-cancer

Anti-cancer vaccines can be classified into prophylactic and therapeutic vaccines. Examples of prophylactic anti-cancer vaccines are HPV and Hepatitis B. Therapeutic anti-cancer vaccines can be considered as an immunotherapy, which is training and activating the own immune system to eliminate cancer cells. The major advantage of vaccination in cancer treatment is the invasiveness and side-effects of current radio- and chemotherapy treatments. Anti-cancer vaccines are based on synthetic moieties representing tumor-associated carbohydrate antigens (TACAs) [30] which can be classified into 4 groups: (1) glycolipids like Globo-H, SSEA4 and SSEA3 associated with breast, ovary, colon, prostate and lung cancer; (2) glycolipid-based gangliosides GM2, GD2, GD3, fucosyl-GM1 associated with neuroblastoma, sarcoma, B-cell lymphoma and melanoma; (3) Lewis^x, Lewis^y, sialyl Lewis^x and sialyl Lewis^a associated with breast, ovary, colon, prostate and lung cancer; (4) protein-linked Tn, Sialyl-Tn (STn) and TF (conjugated to the -OH group of serine) associated with breast, ovary and prostate cancer. The development of anti-cancer prevention and treatments has made significant progress in the field of carbohydrate-based vaccines. There are still many challenges also towards fully synthetic anti-cancer vaccines and even more related to differences between animal models and clinical trials. Also, the expression of TACAs on normal cells could induce tolerance. While challenging and more efforts are needed to solve anti-cancer vaccine related issues, such as breaking the immune-tolerance, carbohydrate-based anti-cancer vaccines will provide viable options in the near future to either replace or be co-administered with traditional radio- and chemotherapy. With the current developments of glyco-marker identification,

personalized glycan based anti-cancer vaccines could be envisioned providing expedited development.

Conclusion

Conjugate vaccines have proven their value and will contribute to protecting society against disease in the future. They will find their application in the prophylactic and therapeutic area. Current and future techniques will make conjugate vaccines evolve. Improvements can be found in their immunogenicity through better design or the addition of specific adjuvants. Antigen design will be more rapid and expand towards multivalent presentations. New synthetic and glycoengineering routes will be made more scalable and cost-effective towards global access reducing the current vaccine inequity gap. The combination of the current plethora of new carriers, conjugation chemistries, antigens and adjuvants make them the most versatile vaccine platform of the future.

References

1. Cohen, D., et al., Safety and immunogenicity of a synthetic carbohydrate conjugate vaccine against *Shigella flexneri* 2a in healthy adult volunteers: a phase 1, dose-escalating, single-blind, randomised, placebo-controlled study. *Lancet Infect Dis*, 2021. 21(4): p. 546-558.
2. CDC. History of Smallpox. September 29th 2022]; Available from: <https://www.cdc.gov/smallpox/history/history.html>.
3. Schneerson, R., et al., Quantitative and qualitative analyses of serum antibodies elicited in adults by *Haemophilus influenzae* type b and pneumococcus type 6A capsular polysaccharide-tetanus toxoid conjugates. *Infect Immun*, 1986. 52(2): p. 519-28.
4. Schneerson, R., et al., *Haemophilus influenzae* type B polysaccharide-protein conjugates: model for a new generation of capsular polysaccharide vaccines. *Prog Clin Biol Res*, 1980. 47: p. 77-94.
5. Broker, M., et al., Polysaccharide conjugate vaccine protein carriers as a "neglected valency" - Potential and limitations. *Vaccine*, 2017. 35(25): p. 3286-3294.
6. Pichichero, M.E., Protein carriers of conjugate vaccines: characteristics, development, and clinical trials. *Hum Vaccin Immunother*, 2013. 9(12): p. 2505-23.
7. Barington, T., et al., Influence of prevaccination immunity on the human B-lymphocyte response to a *Haemophilus influenzae* type b conjugate vaccine. *Infect Immun*, 1991. 59(3): p. 1057-64.
8. Dagan, R., J. Poolman, and C.A. Siegrist, Glycoconjugate vaccines and immune interference: A review. *Vaccine*, 2010. 28(34): p. 5513-23.
9. Herzenberg, L.A., T. Tokuhisa, and L.A. Herzenberg, Carrier-priming leads to hapten-specific suppression. *Nature*, 1980. 285(5767): p. 664-7.
10. Schutze, M.P., et al., Epitopic suppression in synthetic vaccine models: analysis of the effector mechanisms. *Cell Immunol*, 1987. 104(1): p. 79-90.
11. Lehmann, A.K., et al., Human opsonins induced during meningococcal disease recognize outer membrane proteins PorA and PorB. *Infect Immun*, 1999. 67(5): p. 2552-60.
12. Liu, Y., et al., Experimental vaccine induces Th1-driven immune responses and resistance to *Neisseria gonorrhoeae* infection in a murine model. *Mucosal Immunol*, 2017. 10(6): p. 1594-1608.
13. Skidmore, B.J., et al., Immunologic properties of bacterial lipopolysaccharide (LPS): correlation between the mitogenic, adjuvant, and immunogenic activities. *J Immunol*, 1975. 114(2 pt 2): p. 770-5.
14. Bachmann, M.F. and G.T. Jennings, Vaccine delivery: a matter of size, geometry, kinetics and molecular patterns. *Nat Rev Immunol*, 2010. 10(11): p. 787-96.
15. Gerritzen, M.J.H., et al., Spontaneously released *Neisseria meningitidis* outer membrane vesicles as vaccine platform: production and purification. *Vaccine*, 2019. 37(47): p. 6978-6986.
16. van der Pol, L., M. Stork, and P. van der Ley, Outer membrane vesicles as platform vaccine technology. *Biotechnol J*, 2015. 10(11): p. 1689-706.
17. Langdon, R.H., J. Cuccui, and B.W. Wren, N-linked glycosylation in bacteria: an unexpected application. *Future Microbiol*, 2009. 4(4): p. 401-12.
18. Jiang, L., et al., A bacterial extracellular vesicle-based intranasal vaccine against SARS-CoV-2 protects against disease and elicits neutralizing antibodies to wild-type and Delta variants. *J Extracell Vesicles*, 2022. 11(3): p. e12192.
19. Zhang, H., et al., Comparing pooled peptides with intact protein for accessing cross-presentation pathways for protective CD8+ and CD4+ T cells. *J Biol Chem*, 2009. 284(14): p. 9184-91.
20. Skwarczynski, M. and I. Toth, Peptide-based synthetic vaccines. *Chem Sci*, 2016. 7(2): p. 842-854.
21. Micoli, F., et al., Glycoconjugate vaccines: current approaches towards faster vaccine design. *Expert Rev Vaccines*, 2019. 18(9): p. 881-895.
22. Verez-Bencomo, V., et al., A synthetic conjugate polysaccharide vaccine against *Haemophilus influenzae* type b. *Science*, 2004. 305(5683): p. 522-5.
23. van der Put, R.M.F., et al., The First-in-Human Synthetic Glycan-Based Conjugate Vaccine Candidate against *Shigella*. *ACS Cent Sci*, 2022. 8(4): p. 449-460.
24. Panza, M., et al., Automated Chemical Oligosaccharide Synthesis: Novel Approach to Traditional Challenges. *Chem Rev*, 2018. 118(17): p. 8105-8150.
25. Khatun, F., R.J. Stephenson, and I. Toth, An Overview of Structural Features of Antibacterial Glycoconjugate Vaccines That Influence Their Immunogenicity. *Chemistry*, 2017. 23(18): p. 4233-4254.
26. Schneerson, R., et al., (CNBr !!) Preparation, characterization, and immunogenicity of *Haemophilus*

- influenzae type b polysaccharide-protein conjugates. *J Exp Med*, 1980. 152(2): p. 361-76.
27. Del Bino, L., et al., Synthetic Glycans to Improve Current Glycoconjugate Vaccines and Fight Antimicrobial Resistance. *Chem Rev*, 2022. 122(20): p. 15672-15716.
 28. Micoli, F., P. Costantino, and R. Adamo, Potential targets for next generation antimicrobial glycoconjugate vaccines. *FEMS Microbiol Rev*, 2018. 42(3): p. 388-423.
 29. Bajad, N.G., et al., A systematic review of carbohydrate-based bioactive molecules for Alzheimer's disease. *Future Med Chem*, 2021. 13(19): p. 1695-1711.
 30. Feng, D., A.S. Shaikh, and F. Wang, Recent Advance in Tumor-associated Carbohydrate Antigens (TACAs)-based Antitumor Vaccines. *ACS Chem Biol*, 2016. 11(4): p. 850-63.
 31. Guo, C., et al., Therapeutic cancer vaccines: past, present, and future. *Adv Cancer Res*, 2013. 119: p. 421-75.
 32. Hossain, F. and P.R. Andreana, Developments in Carbohydrate-Based Cancer Therapeutics. *Pharmaceuticals (Basel)*, 2019. 12(2).
 33. Shivatare, S.S., V.S. Shivatare, and C.H. Wong, Glycoconjugates: Synthesis, Functional Studies, and Therapeutic Developments. *Chem Rev*, 2022. 122(20): p. 15603-15671.
 34. Sorieul, C., et al., Recent advances and future perspectives on carbohydrate-based cancer vaccines and therapeutics. *Pharmacol Ther*, 2022. 235: p. 108158.





Appendices

Nederlandse samenvatting

Curriculum vitae

List of publications

Dankwoord



Nederlandse samenvatting

Nieuwe conjugaat vaccins in ontwikkeling richten zich op verschillende ziektes. Dit is direct gekoppeld aan de beschikbaarheid van nieuwe synthetisch antigenen welke ontwikkeld worden. Synthetisch geproduceerde antigenen hebben substantiële voordelen vergeleken met de conventionele extractie processen van polysachariden. Daarnaast is er ook veel onderzoek naar nieuwe andere drager eiwitten en nano deeltjes welke de traditionele eiwitten (tetanus, difterie) vervangen. Voor de combinaties van nano deeltjes en synthetische antigenen zijn ook nieuwe analysemethodes nodig om deze zowel fysicochemisch als immunologisch te kunnen karakteriseren.

In deze thesis laten we de stapsgewijze aanpak zien van traditioneel geëxtraheerd polysachariden gekoppeld via willekeurige activatie aan tetanus toxoïde naar gecontroleerde single-site conjugatie van een volledig synthetisch oligosacharide. Deze conjugatie methode passen we verder toe op de ontwikkeling en karakterisatie van een OMV synthetisch peptide vaccin. Voor alle drie de vaccins die worden beschreven in deze thesis (*Haemophilus influenzae* type b (Hib), *Shigella flexneri* 2a en OMV-peptide), beschrijven we ook toepassing en ontwikkeling van de benodigde kwaliteit controle testen welke nodig zijn voor de fysicochemische karakterisatie. Verder is ook design of experiments (DoE) gebruikt voor de optimalisatie van conjugatieprocessen. Deze aanpak bood een cruciaal hulpmiddel om tijd en kosten te verminderen tijdens de ontwikkeling en optimalisatie van de productieprocessen.

In **hoofdstuk 2** wordt een uitgebreid overzicht gegeven van recente ontwikkelingen met betrekking tot glycoconjugaatvaccins. In een tweeledige aanpak worden de introductie van nieuwe carriers en de vooruitgang in ontwikkelingen voor specifieke antigenen besproken. De nadruk ligt hier op conjugaat vaccins gericht tegen ESKAPE-pathogenen. Nieuwe carriers zijn essentieel om potentiële problemen gerelateerd aan carrier-induced epitope suppression (CIES) te voorkomen, zoals waargenomen voor sommige van de traditionele conjugaat vaccin eiwit carriers. De nieuwe carriers welke besproken worden bestaan uit 1) OMV's en GMMAs, 2) glycoengineered eiwitten en OMV's, 3) drager eiwitten, 4) virus like particles, 5) protein-nanocages en 6) peptiden. Meerdere voorbeelden van nieuwe ontwikkelingen welke in de afgelopen vijf jaar gepubliceerd zijn, met betrekking tot de genoemde dragers, worden besproken.

Daarnaast werd de focus gelegd op antimicrobiële resistentie (AMR), ook wel benoemd als de nieuwe stille pandemie. Terwijl AMR wordt toegeschreven aan een breed scala aan pathogenen, hebben we ons hier gericht op de zogenaamde ESKAPE-pathogenen (*Enterococcus faecium*, *Staphylococcus aureus*, *Klebsiella pneumoniae*, *Acinetobacter*

baumannii, *Pseudomonas aeruginosa* en *Enterobacter* spp.), welke allemaal bovenaan de prioriteitenlijst van zowel de WHO als de CDC staan. Hier hebben we de huidige ontwikkelingen samengevat om glycoconjugaatvaccins te ontwikkelen, gericht op ESKAPE-pathogenen die zich nog in de vroege ontwikkeling of preklinische fase bevinden. Hoewel er veel voorbeelden zijn waar nieuwe carriers worden gebruikt voor conjugaat vaccins, is dit niet evident voor glycoconjugaatvaccins gericht op ESKAPE-pathogenen. Waar het lijkt dat nieuwe vaccinontwikkelingen gericht op AMR achterblijven en dat mogelijk is toe te schrijven aan de COVID-19-pandemie, kan het niet anders dan dat er op korte termijn nieuwe vaccinkandidaten richting de markt komen.

In **hoofdstuk 3** wordt de analyse van in-process control (IPC) monsters beschreven, welke gegenereerd zijn tijdens de productie en zuivering van het capsulaire polysaccharide (CPS) polyribosyl-ribitol-fosfaat (PRP) van Hib. Traditioneel werd PRP gekwantificeerd met behulp van immunochemische of colorimetrische methoden. Beide methoden zijn niet nauwkeurig als gevolg van storende fermentatiecomponenten en of reagentia die tijdens de zuivering worden gebruikt. De introductie van een verbeterde en zeer specifieke high-performance anion exchange chromatography pulsed-Amperometric detection (HPAEC-PAD) methode elimineerde de effecten van storende componenten. De HPAEC-PAD-methode was significant beter wat betreft specificiteit en nauwkeurigheid in vergelijking met de traditioneel gebruikte colorimetrische assay en HPSEC-methode. Met de introductie van de HPAEC-PAD-methode werd niet allen de procesontwikkeling van het Hib-vaccin versneld, maar kon deze ook worden toegepast voor de kwaliteitscontrole van nieuwe productiepartijen.

In **hoofdstuk 4** wordt de ontwikkeling en karakterisatie van een conjugaat vaccin kandidaat tegen Shigellose gepresenteerd. Twee belangrijke verbeteringen worden geïntroduceerd: 1) synthetische oligosacchariden (sOS) die fungeren als functionele kopie van het O-specifieke polysaccharide gedeelte van *Shigella* LPS en 2) single-site GMBS-conjugatiechemie voor een zeer gecontroleerd en voorspelbaar productieproces. Vóór conjugatie van het sOS werd de maleimide-toevoeging op primaire amines die beschikbaar zijn op het tetanustoxoïde eerst geëvalueerd en geoptimaliseerd met behulp van design of experiments (DoE). Optimale reactiecondities werden gedefinieerd waarbij de hoogste hoeveelheid primaire aminen werd gefunctionaliseerd en de minste hoeveelheid aggregatie werd geïnduceerd. Vier conjugaten met verschillende geconjugeerde sOS:tetanus toxoïde verhoudingen (4,6, 8,5, 17 en 26 mol:mol) werden bereid. Er werd een maximum aantal van 26 sOS moleculen per toxoïde geconjugueerd. Tijdens de evaluatie in een immunogeniciteits-studie werd duidelijk dat 17 sOS per toxoïde molecuul de hoogste antilichaam titers induceerde in vergelijking met de conjugaten

met andere sOS:tetanus toxoïde verhouding. De toevoeging van aluminium als adjuvans had een zeer positieve invloed op de immunogeniciteit. Deze resultaten bevestigden dat een synthetische pentadecasaccharide haptent welke het SF2a O-SP nabootst, een beschermende antilichaam respons kon opwekken bij muizen welk langer dan een jaar kon worden aangetoond.

Hoofdstuk 5 beschrijft de ontwikkeling van een *Shigella*-conjugaat vaccin uitgerust met een synthetisch oligosaccharide voor welke een GMP-productieproces op commerciële schaal is ontwikkeld. Uitgangspunt waren de resultaten zoals gepresenteerd in Hoofdstuk 4. Een 1000-voudige opschaling werd met succes bereikt en de introductie van TFF leverde vergelijkbare producten op met betrekking tot conjugatiekinetiek en efficiëntie zoals eerder bevestigd in het kleinschalige proces. De GMP-productie van twee batches resulteerde in materialen voor een toxicologisch onderzoek in konijnen en een klinische studie in mensen. Beide batches werden geproduceerd met een conjugatie-efficiëntie van respectievelijk 76 en 80%. De eerste batch voldeed aan alle toxicologische criteria en vertoonde een sterke anti-SF2a immuunrespons bij zowel muizen als konijnen. De antilichamen waren specifiek voor SF2a LPS en functioneel in vitro waarbij hoge anti-SF2a SBA-titers werden gevonden. Bovendien herkenden ze een grote pool van Sf2a-circulerende stammen geïsoleerd van personen met de diagnose shigellose. De uiteindelijke vaccinpartijen waren minstens 66 maanden stabiel. Het gehalte aan vrije oligosaccharide voldeed aan de specificaties voor productvrijgave (<10%) en houdbaarheid van conjugaat vaccins (<25%). Dit kandidaat-glycoconjugaatvaccin bleek veilig te zijn en goed te worden verdragen bij gezonde volwassenen, terwijl het hoge anti-SF2a LPS-titers induceerde. Er werd geen additioneel effect van het adjuvans (aluminium) of de herhaalde immunisatie (booster) waargenomen wanneer 10 µg oligosaccharide werd toegediend. Aan de andere kant was een verbeterde immuunrespons zichtbaar voor de dosis van 2 µg. Dit kandidaat-vaccin werd verder geëvalueerd in twee opeenvolgende fase-II-onderzoeken. Ten eerste in een gecontroleerd humaan infectiemodel (CHIM) dat de beschermende capaciteit van SF2a-TT15 bij naïeve volwassenen evalueert (NCT0478022) en ten tweede een leeftijd aflopende studie in Kenia die de veiligheid en immunogeniciteit van SF2a-TT15 beoordeelt in de doelpopulatie, met name zuigelingen, in het veld (NCT04602975).

A In **hoofdstuk 6** introduceren we field flow fractionation gekoppeld aan multi-angle lichtscattering (FFF-MALS) voor de karakterisering van OMV's als een nieuwe carrier voor conjugaat vaccins. In hoofdstuk 2 presenteerden we OMV's als een van de nieuwe carriers voor conjugaat vaccins. OMV's zijn een aantrekkelijk alternatief voor de traditionele carriers vanwege hun stabiele samenstelling, zelf adjuverende eigenschappen en hun vermogen om heterologe antigenen van specifieke pathogenen tot expressie te brengen.

Functionalisatie van OMV's met behulp van *N*- γ -(maleimidobutyryl)-oxysuccinimide-ester (GMBS), waardoor conjugatie aan elk thiol-dragend immunogeen mogelijk is, levert OMV's op die klaar zijn voor conjugatie. De FFF-MALS-methode is ontwikkeld voor het scheiden van OMV's van eiwitonzuiverheden. Verschillende iteraties leidden tot een verbeterde methode. De uiteindelijke methode werd met succes onderworpen aan een volledige validatiestudie volgens de ICH-richtlijnen (Q2 R1). De gevalideerde test werd vervolgens toegepast voor de evaluatie van de OMV-productie- en zuiveringsprocessen. Het was mogelijk om de zuiverheid en OMV-grootteverdeling te evalueren in alle verschillende fracties die tijdens het zuiveringsproces werden verkregen. Het was een uitdagende taak met betrekking tot gebruikte oplosmiddelen en andere matrixbestanddelen. OMV's afkomstig van andere bacteriële oorsprong werden ook met succes geanalyseerd. Ten slotte werden GMBS-gemodificeerde OMV's met succes geanalyseerd met behulp van de gevalideerde FFF-MALS-methode. Hier vonden we dat de GMBS-reactie geen effect had op de colloïdale stabiliteit van de OMV. Door toepassing van de FFF-MALS methode is het nu mogelijk om de productie, zuivering en functionalisatie van OMV's met GMBS te evalueren. Deze ready-to-conjugate OMV's kunnen worden gebruikt als carrier voor vrijwel elk oligosaccharide-, peptide- en of eiwitantigeen voor profylactische of therapeutische toepassing.

In **hoofdstuk 7** worden OMV's verder onderzocht als toepassing om te dienen als carrier voor een synthetisch modelpeptide. Hier hebben we eerst de OMV's onderworpen aan een onderzoek met betrekking tot primaire aminedistributie en GMBS-modificatie. Primaire amines zijn beschikbaar op porB-eiwitten, fosfatidylethanolamine (PE), lipooligosaccharide en andere eiwitten. Om mogelijke colloïdale instabiliteit te voorkomen door OMV's te veel te modificeren, werden de maximale toe te passen molaire GMBS equivalenten onderzocht. Onder deze niet-geoptimaliseerde omstandigheden was het mogelijk om tot 2,1 μg peptide te conjugeren aan 25 μg OMV.

Van deze initiële reactieomstandigheden werd een DoE toegepast om de conjugatiereactie te optimaliseren, om de hoeveelheid geconjugerd peptide te verhogen (geanalyseerd door LC-MS) en om veranderingen in grootteverdeling te minimaliseren (geanalyseerd door FFF-MALS). Een full-factorial ontwerp, inclusief vier factoren, resulteerde in 19 experimenten die conjugaten opleverden met maximaal 12,1 μg peptide geconjugerd. Echter zagen we onder deze omstandigheden ook de grootste verschuiving in deeltjesgrootte (25%). Met de reactiecondities gespecificeerd in de optimizer-functie van MODDE konden we 7,5 μg peptide conjugeren met slechts 10,6% verschuiving in deeltjesgrootte. Dezelfde reactiecondities werden toegepast in een scale-up studie waarbij 8,3 μg peptide werd geconjugerd en 13,0% verschuiving in deeltjesgrootte. Dit conjugaat vaccin werd vervolgens onderworpen aan een real-time stabiliteitsstudie bij concentraties van 0,6, 1,0, 2,0 en 3,0 mg/ml voor de duur van drie maanden. De

verschuiving in deeltjesgrootte en eiwitprofiel (SDS-PAGE) bleef stabiel in de tijd. Het peptidegehalte aan het einde van de studie was vergelijkbaar, behalve voor één product, dat een afname tot 5,3 µg/ml vertoonde.

In deze studie hebben we aanzienlijke vooruitgang geboekt met het platform concept waar een OMV als carrier diende. Nu zowel de productie- als conjugatieplatforms van OMV's zijn ontwikkeld, zal het van belang zijn om op peptiden gebaseerde antigenen te ontwerpen die een beschermende immuunrespons opwekt voor bepaalde ziekten, zowel in het profylactische als het therapeutische domein. Omdat dit een schaalbare proces is, zijn grotere procesvolumes tot 10 of 100 liter gemakkelijk haalbaar. Ervan uitgaande dat een humane vaccindosis 5 µg peptide bevat, kunnen we tussen de 230.000 - 2.3000.000 doses produceren in een enkele productiecycclus van slechts één dag.

Curriculum vitae

Robert van der Put was born on the 26th of December 1975 in Etten-Leur, The Netherlands. He attended secondary school at Katholieke Scholengemeenschap Etten-Leur, from which he graduated in 1992, which was followed directly with his secondary school laboratory education, from which he graduated in 1997. At that time not sure yet of his scientific endeavor to come, he held several positions as a restaurant manager and as a microbiological technician in the professional field. It wasn't until late 2002 that he found back his passion working at the Netherlands Vaccine Institute, Bilthoven. At the unit quality control and support he was responsible for the production and development of monoclonal antibodies used for the characterization of vaccines. In that period he finished his part-time professional education (HLO) at the Institute of Life sciences and Chemistry Utrecht in 2009 while also transitioning towards the process development department. Between 2010 - 2013 he successfully finished his masters education in drug innovation at the faculty of pharmaceutical sciences at the university of Utrecht. Combining his master study with his day-to-day work he studied several topics like the assessment of the biochemical characteristics of Rotavirus; implications for process development, the cell biology and infection kinetics for RSV in a Vero cell-culture model and the design and development of a synthetic Shigella flexneri 2a conjugate vaccine production process using design of experiments. While working in the field of vaccine development at Intravacc, Robert already managed to write several publications on the development of conjugate vaccines. However it wasn't until 2021 that this was formalized in the objective towards obtaining a PhD. Under the guidance of Prof. Roland Pieters, Dr. Maarten Danial and Dr. Bernard Metz he managed to further develop his scientific skills working on the process development of several conjugate vaccines and the development of high-end quality control tests, which all concluded to the work presented in this thesis. After defending his thesis Robert will continue to work within Intravacc at the business development department.

List of publications

Alex de Haan, **Robert M. F. van der Put** and Michel Beurret. (2013). "HPAEC-PAD method for the analysis of alkaline hydrolyzates of *Haemophilus influenzae* type b capsular polysaccharide", Biomedical Chromatography, DOI: 10.1002/bmc.2918.

Bernard Metz, Wichard Tilstra, **Robert M.F. van der Put**, Nanda Spruit, Jan van den IJssel, Jolanda Robert, Coenraad Hendriksen and Gideon Kersten (2013). "Physicochemical and immunochemical assays for monitoring consistent production of tetanus toxoid." Biologicals 41(4): 231-237.

Robert M.F. van der Put, Alex de Haan, Jan G.M. van den IJssel, Ahd Hamidi and Michel Beurret (2014) "HPAEC-PAD quantification of *Haemophilus influenzae* type b polysaccharide in upstream and downstream samples", Vaccine, DOI: 10.1016/j.vaccine.2014.07.028,

Robert M. F. van der Put, Tae Hee Kim, Catherine Guerreiro, Françoise Thouron, Peter Hoogerhout, Philippe J. Sansonetti, Janny Westdijk, Michiel Stork, Armelle Phalipon, and Laurence A. Mulard (2016) "A synthetic carbohydrate conjugate vaccine candidate against shigellosis: improved bioconjugation and impact of alum on immunogenicity", ACS Bioconjugate Chemistry, DOI:10.1021/acs.bioconjchem.5b00617

Janny Westdijk, Amy Kogelman, **Robert M.F. van der Put**, Zaskia Eksteen, Diego Suarez, Gideon F.A. Kersten, Bernard Metz and Maarten Danial (2022) "Immunochemical and biophysical characterization of inactivated Sabin poliovirus products: Insights into rapid quality assessment tools", Journal of Pharmaceutical Sciences, DOI: 10.1016/j.xphs.2022.01.031

Robert M. F. van der Put, Carolien Smitsman, Alex de Haan, Martin Hamzink, Hans Timmermans, Joost Uittenbogaard, Janny Westdijk, Michiel Stork, Olga Ophorst, Françoise Thouron, Catherine Guerreiro, Philippe J. Sansonetti, Armelle Phalipon and Laurence A. Mulard (2022) "The First-in-Human Synthetic Glycan-Based Conjugate Vaccine Candidate against *Shigella*", ACS Central Science, DOI: 10.1021/acscentsci.1c01479

Robert M. F. van der Put, Arnoud Spies, Bernard Metz, Daniel Some, Roger Scherrers, Roland J. Pieters, and Maarten Danial (2022) "Validation of an FFF-MALS method to characterize the production and functionalization of outer-Membrane Vesicles for conjugate vaccines", ACS Analytical Chemistry, DOI: 10.1021/acs.analchem.2c01590

Robert M.F. van der Put, Bernard Metz and Roland J. Pieters (2023) "Carriers and Antigens: New Developments in Glycoconjugate Vaccines", MDPI Vaccines Special Issue "State-of-the-Art Vaccine Researches", DOI: 10.3390/vaccines11020219

Robert M.F. van der Put, Thomas J.M. Michiels, Zaskia Eksteen, Arnoud Spies, Hugo D. Meiring, Ronald H.W. Maas, Roland J. Pieters, Bernard Metz and Corine Kruiswijk (2023) "A modular vaccine platform for prophylactic and therapeutic vaccines: exogeneous decoration of bacterial outer membrane vesicles with synthetic peptide antigens", ACS Bioconjugate Chemistry, to be submitted

Dankwoord

En dan is het ineens zover, dit boekwerk is bijna af. Dan zit er nog veel tijd en moeite in en tussen voor het daadwerkelijk naar de drukker gaat. Dan is het tijd om nog eens het hele proces door te gaan en herinneringen op te halen van wat er allemaal voor nodig is geweest om dit voor elkaar te krijgen. Inmiddels zit ik 21 jaar in vaccin ontwikkeling waar ik verschillende posities heb bekleed. Waar ik vaak de verbindende factor probeer te zijn, is het niet gek dat conjugaat vaccins dan mijn grote liefde zijn. Mijn traject als buitenpromovendus heeft er voor gezorgd dat ik op een andere manier dan gewoonlijk mijn PhD heb doorlopen. Als ik dan alleen kijk naar die redelijk korte periode zou ik veel mensen tekort doen om te bedanken. Dus dan maar wat verder terug in de tijd.

Mijn start bij PD zorgde ervoor dat ik mijn HBO en Master heb mogen behalen, dat had niet gekund zonder Leo van der Pol en Danielle Lankveld. Eerder al bij QCO, maar zeker bij PD kwam ik meer en meer in contact met conjugaat vaccins. Michel Beurret, I really take my hat off for you. You have really taken me in and have inspired me to be a better scientist. Your attention to detail is something that still helps me today. It still shows in the labs. We should go for loempias more often. Hans Kreeftenberg, Ahd Hamidi, Jan Hendriks, Jan van den Ijssel, Peter Hoogerhout en Alex de Haan Hib Hib hoera! Wat een succes in tech transfer en samenwerking. En ja Jan, af en toe spelen we nog best een infantiel spelletje; en Nee Alex (mijn lab maatje), ik gebruik gelukkig de laatste tijd niet meer de verkeerde PRP-ADH.

A special thanks goes to Institut Pasteur Paris (Armelle Phalipon and team). The whole Shigella project has had a significant impact on both my personal development and the content of my PhD. Laurence Mulard, deserves a special mention. The way we have connected on both a scientific and personal level cannot be underestimated. The countless times we were online at night and in the weekend fixing things and managing deadlines was impressive. Thank you very much for all your invaluable support.

A Het Intravacc team wat het Shigella project al die tijd voort heeft getrokken Juli ten Velde, Wilma Meis, Joost Uitenbogaard, Alex de Haan (zonder iemand te vergeten). Janny Westdijk, Carla Hoitink, Olga Ophorst onze reisjes zijn niet te vergeten. Rome was mooi, maar Parijs blijft toch altijd nog beter. Zeker met de minimaal geklede dame in de flat tegenover de vergader ruimte bij Pasteur. Ik bloos er nog van als ik er aan denk.

Als het dan over een project gaat wat met piepen en kraken begonnen is: ons OMV-peptide project. Qua persoonlijke ontwikkeling heb ik hier wel de grootste stap gezet. Het ging niet zo makkelijk in het begin, werkelijk een project met een lach en een traan, misschien omdat ik toch wel soms eigenwijs ben? Corine Kruiswijk, Bernard Metz, Zaskia Eksteen, Thomas Michiels en Hugo Meiring we hebben er toch een succes van gemaakt. Wat zijn we naar elkaar toe gegroeid en daar plukken we nog steeds de vruchten van; dank jullie wel.

PD afdeling, wat een prachtige club mensen. Er is wat gevraagd van ons in de laatste jaren. Het niveau van flexibiliteit, creativiteit en kwaliteitsbewustzijn overstijgt alles. Dat is wat ik ook mee neem voor de rest van mijn carrière; wat je ook over de heg gegooit krijgt, het is (bijna) altijd op te lossen. Dank voor jullie inspiratie, motivatie en ondersteuning.

Arnoud Spies, wat een berg werk heb jij verzet. Tomeloze inzet om alle metingen af te hebben als er weer eens een deadline was. En dan nu sta je zelf middenin het conjugatiewerk, dat gaat je zeker lukken! Dank je wel voor al je bijdragen en effort.

Michiel Stork door jouw inzet binnen Intravacc is dit uiteindelijk allemaal gestart. In soms onzekere tijden waar we niet wisten of we maanden later er nog zouden zijn als bedrijf, hebben we dit er maar even tussendoor gefikst. Dank je wel voor jouw vertrouwen en aanzet tot dit mooie resultaat.

Ronald Maas onze persoonlijke gesprekken hebben veel bijgedragen aan dit succes. Jouw visie, mening en perspectief hebben mij veelal doen nadenken en hebben er voor gezorgd dat ik een betere wetenschapper en persoon ben geworden. Jouw support is van onschatbare waarde geweest, dank je wel daarvoor.

Maarten Danial: probeer het maar eens, mij een beetje sturen en begeleiden. Het is je toch zeker gelukt. Helaas hebben wij het niet samen kunnen afmaken. Ik wil bedanken voor alle tijd en moeite die je er in hebt gestoken om mij te begeleiden en helpen met deze mijlpaal.

Bernard Metz, dank je wel voor het helpen finishen. Al onze gesprekken en interacties zijn van onschatbare waarde. Je kritische blik heeft mij veel geholpen om verder te komen als wetenschapper. Jouw deur stond altijd open wanneer ik weer eens voorbij kwam met een idee of probleem. Je had er altijd even tijd voor, ik hoop dat je deur nog lang open staat.

Roland Pieters tijdens mijn Master stage gaf je al aan “als je ooit een PhD wil doen”. Hoe bijzonder dat wij hier dan nu zijn. Dank je wel voor de mogelijkheid, het vertrouwen en alle wetenschappelijke input.

Carolien Smitsman, mijn maatje, na al onze tijd samen op kantoor kun je dit helaas niet meer mee maken. Jouw tomeloze inzet tijdens veel van onze experimenten en het vervangen van mij toen ik er even niet was, wat een respect heb ik voor jou. Wat mis ikje, maar ik weet dat je altijd dichtbij bent. Tot de tijd dat we elkaar weer zien !

Mijn paranimfen, Hans en Arno. Eigenlijk meer mijn ski-maatjes. Dank dat jullie deze taak op je hebben willen nemen. Door jullie is het laatste stukje meer een blauwe dan een zwarte piste, minder slalom en meer een super-G. Dank voor jullie inzet en toewijding.

Lotte en Luuk al die weekenden en avonden dat ik op mijn kantoor thuis zat. Jullie hebben je (soms) keurig gedragen. Ik weet dat jullie trots op mij zijn, maar niet zo trots als ik op jullie. Papa belooft dat dit het laatste kunst stukje was en dat er nu meer tijd moet zijn voor leuke dingen en niet publicaties schrijven in de avonden en weekenden. Blijf dicht bij jezelf en zorg ervoor dat je dingen doet in het leven waar je blij van wordt!

Sandra mijn vrouw, mijn rots, mijn steun en toeverlaat. Zonder jou had dit allemaal nooit kunnen gebeuren. De manier hoe jij altijd alles voor elkaar hebt heeft ervoor gezorgd dat ik tijd had voor dit avontuur. Ja, ik was veel gefocust op andere dingen dan thuis. Maar dat ben ik, ik doe het goed met volle overtuiging of niet. Nu is het dan klaar. Tijd om te vieren waar wij zo hard aan gewerkt hebben. Dank je wel voor je tomeloze liefde en steun.